

**Structural Characterization and Non-linear Optical
Properties of Metal Complexes of Some Donor-Acceptor
Substituted *N*-salicylidene-*N'*-aroylhydrazine Ligands**

**Thesis submitted to
Cochin University of Science and Technology**

**In partial fulfillment of the
requirements for the degree of**

DOCTOR OF PHILOSOPHY

Under the Faculty of Science

By

Bessy Raj. B.N.



**Department of Applied Chemistry
Cochin University of Science and Technology
Kochi - 682 022**

February 2009



***Structural Characterization and Non-linear Optical Properties of
Metal Complexes of Some Donor-Acceptor Substituted N-
salicylidene-N'-aroylhydrazine Ligands***
Ph. D. Thesis under the Faculty of Science

Author:

Bessy Raj. B. N.

Research Fellow, Department of Applied Chemistry

Cochin University of Science and Technology

Kochi, India 682 022

E mail: bessyraj@yahoo.co.in

Research Advisor:

Dr. M. R. Prathapachandra Kurup

Professor

Department of Applied Chemistry

Cochin University of Science and Technology

Kochi, India 682 022

Email: mrp@cusat.ac.in

Department of Applied Chemistry,
Cochin University of Science and Technology
Kochi, India 682 022

February 2009

Front cover: Crystal structure of a polymeric copper(II) complex of *N*-4-diethylamino-2-hydroxybenzaldehyde- *N'*-4-nitrobenzoylhydrazone.

.... to my

Achan and Amma



Phone Off. 0484-2575804
Phone Res. 0484-2576904
Telex: 885-5019 CUIIN
Fax: 0484-2577595
Email: mrp@cusat.ac.in
mrp_k@yahoo.com


**DEPARTMENT OF APPLIED CHEMISTRY
COCHIN UNIVERSITY OF SCIENCE AND TECHNOLOGY
KOCHI - 682 022, INDIA**

Prof. M.R. Prathapachandra Kurup

26th February 2009

CERTIFICATE

This is to certify that the thesis entitled “**Structural Characterization and Non-linear Optical Properties of Metal Complexes of Some Donor-Acceptor Substituted *N*-salicylidene-*N'*-aroylhydrazine Ligands**” submitted by Ms. Bessy Raj B.N, in partial fulfillment of the requirements for the degree of Doctor of Philosophy, to the Cochin University of Science and Technology, Kochi-22, is an authentic record of the original research work carried out by her under my guidance and supervision. The results embodied in this thesis, in full or in part, have not been submitted for the award of any other degree.


M. R. Prathapachandra Kurup
(Supervisor)

DECLARATION

I hereby declare that the work presented in this thesis entitled **“Structural Characterization and Non-linear Optical Properties of Metal Complexes of Some Donor-Acceptor Substituted *N*-salicylidene-*N'*-aroylhydrazine Ligands”** is entirely original and was carried out independently under the supervision of Professor M. R. Prathapachandra Kurup, Department of Applied Chemistry, Cochin University of Science and Technology and has not been included in any other thesis submitted previously for the award of any other degree.

26-02-2009

Kochi-22



Bessy Raj B.N.

PREFACE

The interaction of transition metal ions with ligands having long π -delocalized system provides one of the most fascinating areas of coordination chemistry and non-linear optics. Transition metal complexes nowadays comprise a great interest in medicine and chemical investigations.

Recent years witnessed an intensive investigation of the coordination chemistry of Schiff bases due to their interesting coordination properties and diverse applications. The present work deals with the complexation of Schiff bases of aroylhydrazines with various transition metal ions. The hydrazone systems selected for study have long π -delocalized chain in the ligand molecule itself, which get intensified due to metal-to-ligand or ligand-to-metal charge transfer excitations upon coordination. Complexation with metal ions like copper, nickel, cobalt, manganese, iron, zinc and cadmium are tried. Various spectral techniques are employed for characterization. The structures of some complexes have been well established by single crystal X-ray diffraction studies. The non-linear optical studies of the ligands and complexes synthesized have been studied by hyper-Rayleigh scattering technique.

The work is presented in seven chapters and the last one deals with summary and conclusion. One of the hydrazone system selected for study proved that it could give rise to polymeric metal complexes. Some of the copper, nickel, zinc and cadmium complexes showed non-linear optical activity. The NLO studies of manganese and iron showed negative result, may be due to the inversion centre of symmetry within the molecular lattice.

Acknowledgement

At the outset, it is a pleasure to remember those individuals whose thoughts, words and deeds helped in the successful culmination of this doctoral studies. Here are a few words to express my sincere gratitude.

In the first place I would like to record my heartfelt gratitude to my supervising guide, Dr. M. R. Prathapachandra Kurup, for his supervision, advice, and guidance from the very early stage of this research as well as giving me whole hearted support throughout the work. I am indebted to him more than he knows.

I wish to express my warm and sincere thanks to Dr. Girish Kumar, Head of the Department and Dr. S. Sugunan, former Head of the department for their support and encouragement.

I am extremely thankful to Dr. K. K. Muhammed Yusuff too for supporting me as my doctoral committee member. I also remember with gratitude, the moral support and help received from all the teaching and non-teaching staff of the Department of Applied Chemistry, CUSAT.

This research has been supported and funded by the Department of Science and Technology, Govt. of India. The financial support received for the research work is gratefully acknowledged.

My thanks are due to Dr. E. Suresh, CSMCRI, Gujarat for single crystal X-ray diffraction studies and Dr. P. K. Das, IISc Bangalore for non-linear optical activity studies.

I am thankful to the head of the institutions of SAIF Kochi, IISc Bangalore, IIT Roorkee, IIT Bombay and CDRI Lucknow for the services rendered in sample analyses.

I acknowledge Dr. Rohit. P. John, Dr. Chandini. R. Nayar, Dr. Varughese Philip, Dr. Marthakutty Joseph and Dr. Sreekanth during the initial stages of my research tenure. I express my sincere gratitude to Dr. Sreeja. P. B. for her help and support during my lab work. I consider myself extremely lucky to have the friendship and guidance of my dearest senior Sunichechi. The timely suggestions and constant support I gained from her shall always be cherished. Many thanks go in particular to Daly for her warm friendship and assistance in literature collection. I am deeply obliged to Mini whose enthusiasm and

companionship made life in CUSAT memorable for me. I also remember my friendship with Roshini and Suja and the cheerful days we spent in the hostel. The friendly and inspiring working atmosphere provided by my labmates Raphael Sir, Laly miss, Seena, Manoj, Prem, Sreeshia, Leji, Binu, Sheeja, Nancy and others.

Collective and individual acknowledgments are also owed to all my colleagues at CUSAT especially, Radhu, Maya, Kochurani, Ambili, Rekha, John, Arun, Rajesh, Ramanathan, Ashly and Manju, whose presence somehow perpetually refreshed, helpful, and memorable.

I am indebted to the teachers of Sree Narayana College, Chempazhanthy, TVPM, for making me realize that chemistry is my field of study. I am thankful to all my B.Sc classmates, especially, Sangeetha, Sreekanth and Sivaprasad.

I extend my deep-felt gratitude to the teachers of the Department of Chemistry of Kerala University Campus, who taught me how to study chemistry and to all my M.Sc classmates.

I also acknowledge all my teachers during my school education, for installing a scientific spirit in me and for teaching the basics of the subject.

I am thankful to all my colleagues at Central Polytechnic College, TVPM, especially the general staff for their constant help and encouragement.

Much gratitude is due to my dear parents and beloved little sister for their love, understanding and constant encouragement, which made what I am today.

I also realize the love and support I received from my in-laws. Lastly I feel honoured by the whole-hearted support, patience and understanding rendered by my husband, without which, this thesis could not have been completed.

Above all, my heart goes out to god, in gratitude, for the little forms of blessings showered upon me throughout my life and carrier.

Bessy Raj. B. N.

CONTENTS

Page No.

CHAPTER 1

A brief prologue on structure and applications of acylhydrazones and non-linear optics

| | | |
|------|---|----|
| 1.1. | Importance of hydrazones | 3 |
| 1.2. | Applications of hydrazones | 8 |
| 1.3. | Non-linear optics | 11 |
| 1.4. | Materials for second order non-linear optics | 13 |
| 1.5. | Metal complexes and non-linear optics | 14 |
| 1.6. | Objectives of the present work | 15 |
| 1.7. | Physical measurements | 16 |
| 1.8. | Crystallographic data collection and structure analyses | 17 |
| | References | 18 |

CHAPTER 2

Syntheses, spectral characterization, crystal structures and non-linear optical properties of the *N*-salicylidine-*N'*-aroylhydrazone ligands

| | | |
|---------|---|----|
| 2.1. | <i>N</i> -4-Diethylamino-2-hydroxybenzaldehyde- <i>N'</i> -4-nitrobenzoylhydrazone, H ₂ L ¹ | 26 |
| 2.1.1. | Experimental | 26 |
| 2.1.1a. | Materials | 26 |
| 2.1.1b. | Synthesis | 26 |
| 2.1.2. | Crystal structure | 27 |
| 2.1.3. | Spectral studies | 29 |
| 2.1.3a. | NMR spectra | 29 |
| 2.1.3b. | IR spectrum | 34 |
| 2.1.3c. | Electronic spectrum | 35 |
| 2.2. | <i>N</i> -2-hydroxy-4-methoxybenzaldehyde- <i>N'</i> -4-nitrobenzoylhydrazone, H ₂ L ² | 36 |

| | | |
|---------|---|----|
| 2.2.1. | Experimental | 36 |
| 2.2.1a. | Materials | 36 |
| 2.2.1b. | Synthesis | 36 |
| 2.2.2. | Crystal structure | 37 |
| 2.2.3. | Spectral studies | 40 |
| 2.2.3a. | NMR spectra | 40 |
| 2.2.3b. | IR spectrum | 44 |
| 2.2.3c. | Electronic spectrum | 45 |
| 2.3. | <i>N</i> -2-hydroxy-4-methoxyacetophenone - <i>N'</i> -4-nitrobenzoylhydrazone, H ₂ L ³ | 45 |
| 2.3.1. | Experimental | 45 |
| 2.3.1a. | Materials | 45 |
| 2.3.1b. | Synthesis | 45 |
| 2.3.2. | Crystal structure | 46 |
| 2.3.3. | Spectral studies | 47 |
| 2.3.3a. | NMR spectra | 47 |
| 2.3.3b. | IR spectrum | 53 |
| 2.3.3c. | Electronic spectrum | 53 |
| 2.4. | Non-linear optical properties of <i>N</i> -salicylidine- <i>N'</i> -aroylhydrazone ligands | 54 |
| 2.4.1. | Materials for second order non-linear optics | 55 |
| | References | 58 |

CHAPTER 3

Syntheses, characterization and non-linear optical properties of copper(II) complexes of the aroylhydrazone ligands

| | | |
|--------|-------------------------------------|----|
| 3.1. | Stereochemistry | 65 |
| 3.2. | Experimental | 66 |
| 3.2.1. | Materials | 66 |
| 3.2.2. | Syntheses of ligands | 66 |
| 3.2.3. | Preparation of copper(II) complexes | 66 |

| | | |
|---------|---|-----|
| 3.3. | Results and discussion | 69 |
| 3.3.1. | Crystal structure of complexes | 69 |
| 3.3.1a. | Crystal structures of $[\text{CuL}^1]_2$ | 69 |
| 3.3.1b. | Crystal structures of $[\text{CuL}^1\text{pi}]$ | 72 |
| 3.3.1c. | Crystal structures of $[\text{CuL}^2\text{py}]$ | 74 |
| 3.3.2 | Spectral characteristics of Cu(II) complexes | 77 |
| 3.3.2a | Infrared spectral studies | 77 |
| 3.3.2b | Electronic spectral studies | 79 |
| 3.3.2c | EPR spectral studies | 83 |
| 3.4. | Non-linear optical properties of Cu(II) complexes | 102 |
| | References | 105 |

CHAPTER 4

Syntheses, characterization and non-linear optical properties of nickel(II) and cobalt(II) complexes of the aroylhydrazone ligands

| | | |
|---------|---|-----|
| 4.1. | Stereochemistry of Ni complexes | 115 |
| 4.2. | Stereochemistry of Co complexes | 115 |
| 4.3. | Experimental | 117 |
| 4.3.1. | Materials | 117 |
| 4.3.2. | Syntheses of ligands | 117 |
| 4.3.3. | Preparation of nickel(II) complexes | 117 |
| 4.3.4. | Preparation of cobalt(II) complexes | 119 |
| 4.4. | Results and discussion | 121 |
| 4.4.1. | Crystal structure of complexes | 122 |
| 4.4.1a. | Crystal structure of $[\text{NiL}^1\text{py}_3]\text{py}$ | 122 |
| 4.4.1b. | Crystal structure of $[\text{NiL}^1\text{pi}]$ | 125 |
| 4.4.2. | Spectral characteristics of Ni(II) complexes | 127 |
| 4.4.2a. | Electronic spectral studies | 127 |
| 4.4.2b. | Infrared spectral studies | 130 |
| 4.4.3. | Spectral characteristics of Co(II) complexes | 131 |
| 4.4.3a. | Electronic spectral studies | 131 |

| | | |
|---------|--|-----|
| 4.4.3b. | Infrared spectral studies | 133 |
| 4.4.3c. | EPR spectral studies | 134 |
| 4.5. | Non-linear optical properties of Ni(II) and Co(II) complexes | 140 |
| | References | 142 |

CHAPTER 5

Syntheses, characterization and non-linear optical properties of manganese(II) and iron(III) complexes of the aroylhydrazone ligands

| | | |
|---------|---|-----|
| 5.1. | Stereochemistry of Mn(II) complexes | 150 |
| 5.2. | Stereochemistry of Fe(III) complexes | 151 |
| 5.3. | Experimental | 151 |
| 5.3.1. | Materials | 151 |
| 5.3.2. | Syntheses of ligands | 151 |
| 5.3.3. | Preparation of Mn(II) complexes | 151 |
| 5.3.4. | Preparation of Fe(III) complexes | 152 |
| 5.4. | Results and discussion | 153 |
| 5.4.1. | Spectral characteristics of Mn(II) complexes | 153 |
| 5.4.1a. | Electronic spectral studies | 153 |
| 5.4.1b. | Infrared spectral studies | 154 |
| 5.4.1c. | EPR spectral studies | 156 |
| 5.4.2. | Spectral characteristics of Fe(III) complexes | 160 |
| 5.4.2a. | Electronic spectral studies | 160 |
| 5.4.2b. | Infrared spectral studies | 162 |
| 5.4.2c. | EPR spectral studies | 163 |
| 5.5. | Non-linear optical properties of Mn(II) and Fe(III) complexes | 168 |
| | References | 169 |

CHAPTER 6

Syntheses, characterization and non-linear optical properties of zinc(II) and cadmium(II) complexes of the aroylhydrazone ligands

| | | |
|---------|--|-----|
| 6.1. | Stereochemistry of Zn(II) complexes | 174 |
| 6.2. | Stereochemistry of Cd(II) complexes | 174 |
| 6.3. | Experimental | 174 |
| 6.3.1. | Materials | 174 |
| 6.3.2. | Syntheses of ligands | 175 |
| 6.3.3. | Preparation of Zn(II) complexes | 175 |
| 6.3.4. | Preparation of Cd(II) complexes | 177 |
| 6.4. | Results and discussion | 180 |
| 6.4.1. | Spectral characteristics of Zn(II) complexes | 180 |
| 6.4.1a. | Electronic spectral studies | 180 |
| 6.4.1b. | Infrared spectral studies | 181 |
| 6.4.1c. | ¹ H NMR spectral studies | 184 |
| 6.4.2. | Spectral characteristics of Cd(II) complexes | 185 |
| 6.4.2a. | Electronic spectral studies | 185 |
| 6.4.2b. | Infrared spectral studies | 186 |
| 6.5. | Non-linear optical properties of Zn(II) and Cd(II) complexes | 192 |
| | References | 194 |

CHAPTER 7

| | |
|------------------------|-----|
| Summary and conclusion | 196 |
|------------------------|-----|

CHAPTER ONE

A brief prologue on structure and applications of acylhydrazones and non-linear optics

Coordination complexes were known - although not understood in any sense - since the beginning of chemistry, e.g. Prussian blue and copper vitriol. Coordination chemistry was pioneered by Nobel Prize winner Alfred Werner. He received the Nobel Prize in 1913 for his coordination theory of transition metal-amine complexes. At the start of 20th century, inorganic chemistry was not a prominent field until Werner studied metal-amine complexes such as $[\text{Co}(\text{NH}_3)_6\text{Cl}_3]$. When coordination theory was enunciated, the electron had not been discovered. Electron later became the basic of all theories of chemical bonding. The elucidation of geometry and bonding which were based mainly on preparative procedures received a theoretical foundation from electronic theory of valency. This was followed by the concept of valence bond theory and electron pair repulsion given by Sidgwick – Powell, which are still used extensively, though the ideas have undergone a significant change. Since then the field of coordination chemistry has been widely explored. The number, variety and complexity of coordination compounds still continue to grow. A survey of literature in inorganic chemistry reveals that at least 70% of the published articles deal with coordination compounds. They provide stimulated problems to be resolved particularly in the context of their stereochemistries.

The importance of coordination complexes in our day to day life is increasing due to their complex structures and interesting magnetic, electronic and optical properties. The diversity in structures exhibited by coordination complexes of multidentate ligands have led to their usage as sensors, models for enzyme mimetic

centers, medicines etc. Ligands chosen are of prime importance in determining the properties of coordination compounds. The presence of nitrogen, oxygen and sulfur atoms attached to ligands increases their denticity and thereby enhancing coordinating possibilities. Moreover, presence of these atoms in the coordination sphere leads to their biological activity.

Hydrazones, azomethines characterized by the grouping $R_2-C=N-N-R_2$ belonging to this class are of special mention. They are distinguished from other members of this class by the presence of two interlinked nitrogen atoms and are generally prepared by the condensation of appropriate hydrazine and an aldehyde or ketone. Attaching groups with potential donor sites increases the denticity of these hydrazones as a ligand in coordination chemistry. One such group is $-C=O$, which marked the coordination again stable by proper electron delocalization and these ligands are called acylhydrazones. These are prepared by the condensation of suitable aldehydes or ketones with acylhydrazines. The resultant hydrazones can function as chelating agents complexing with transition or main group metals producing complexes having versatile stereochemistries, applications and enhanced bioactivity compared to the parental ligands. Moreover, these compounds contain the basic unit of peptide linkage $[-C(=O)-NH-]$ group which is a part of primary structure of proteins and is of crucial importance in biological systems. In enzyme systems, metal ions play an important role in terms of both structure and function. These metal cations are not only involved in the structural properties of proteins, but also show catalytic activity. Over the past few decades, metal Schiff-base complexes have been widely investigated with regard to their function as model compounds for biological enzymes [1, 2]. Some N–O containing metal-Schiff base complexes possessing high catalytic activity shows potential application in the field of catalysis [3, 4]. The presently studied coordination compounds consist of ONO donor acylhydrazones.

1.1. Importance of hydrazones

Hydrazones are compounds containing the characteristic –N–N– linkage, which are derived by the condensation of substituted hydrazides with carbonyl compounds namely aldehydes and ketones. According to the needs of a polydentate ligand, the group functionalities are increased by condensation and substitution. The general formula for a substituted acylhydrazone is given in Fig. 1.1.

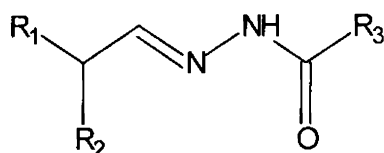


Fig. 1.1. General formula of a substituted acylhydrazone.

An attractive aspect of the hydrazones is that they are capable of exhibiting tautomerism (Fig. 1.2). In the solid state, the compound predominantly exists in keto form (I), whereas in the solution state enol form (II) predominates.

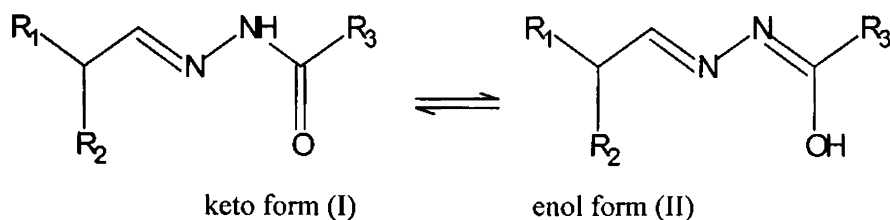


Fig. 1.2. Keto-enol tautomerism of a substituted hydrazone.

By attaining enolic form, the effective conjugation along hydrazone skeleton is increased thereby giving rise to an efficient electron delocalization. The presence of aromatic substituents on the skeleton can further enhance the delocalization of

electron charge density. In the present work, we have chosen 4-diethylamino-2-hydroxybenzaldehyde, 4-methoxy-2-hydroxybenzaldehyde and 4-methoxy-2-hydroxyacetophenone as the carbonyl components of our ligands.

The reaction of aroylhydrazones with transition metal ions can proceed according to two pathways attaining the keto (I) or enol (II) forms for the hydrazide part of the molecule. Thus coordination compounds with the existence of the ligands in the neutral form and also in the anionic form via deprotonation at the enolate oxygen are possible.

The keto form itself exists in *cis* or *trans* form depending on the substituents resulting in a more stable structure (Fig. 1.3). Existence of the acylhydrazones in these geometrical forms in the solid state is well established by crystallographic studies. Stereochemistry of the hydrazone is much decided by the steric effects of the various substituents in the hydrazone moiety and also favored by additional interactions such as intramolecular hydrogen bonding. It is observed that the *cis* nature of the bond usually transforms to *trans* geometry, while coordinating to metal ions. This phenomenon is assumed to be due to chelate effect, which results in an increased stability due to better electron delocalization in chelated ring system consisting of metal ions. The enol form of the ligand could exist in four possible forms (Fig. 1.4) thus acting as monodentate or bidentate. Upon complexation, the enol form usually adopts a suitable geometry, with maximum number of coordination sites leading to chelation.

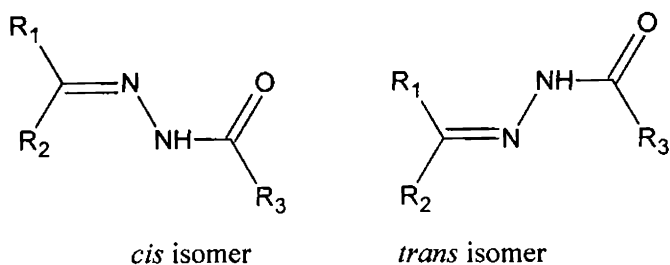


Fig. 1.3. Geometrical isomers of the keto form.

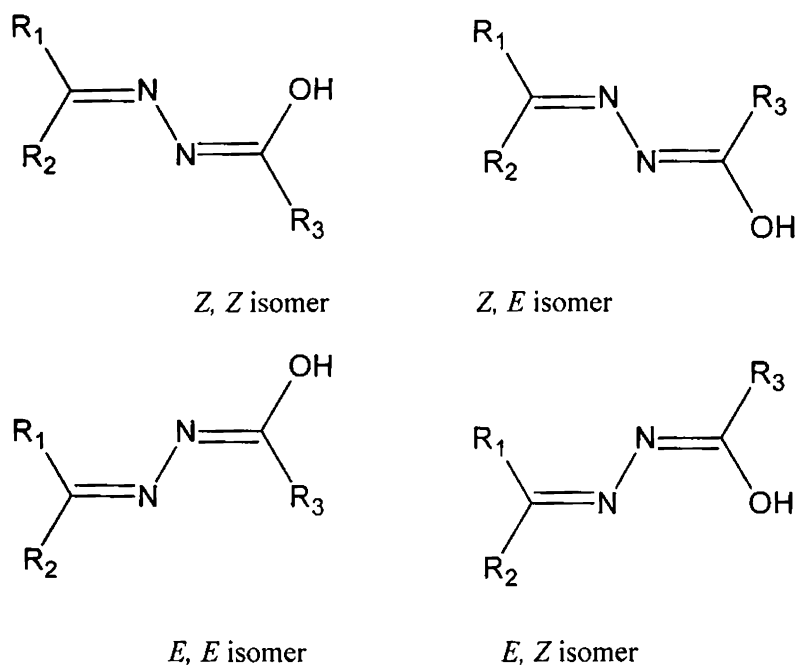
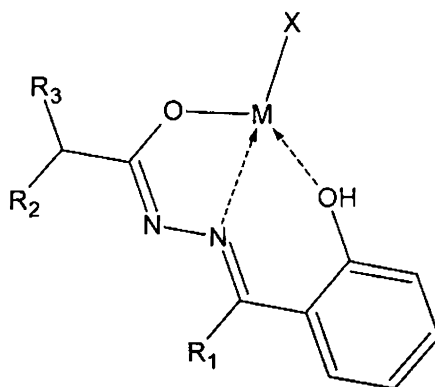


Fig. 1.4. The possible configurations of the enolic form of the ligand.

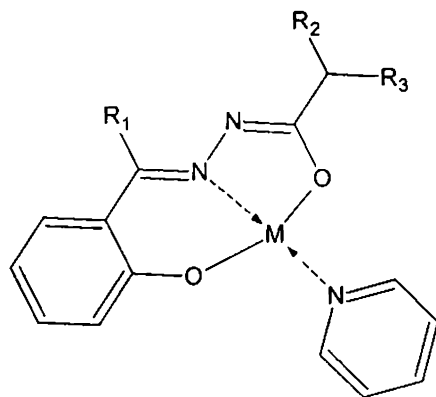
Substituents with potential donor sites increase the denticity of the ligand. Depending on the reaction conditions and the stability of the metal complex formed, hydrazones show a variety of coordination modes with transition metal, adopting any

one of the above four possible forms. Number and type of the substituents influence the coordination mode. All the three carbonyl compounds presently selected provide additional oxygen as a donor due to the deprotonation of the phenolic group at the time of complexation. Other two coordinating sites are the azomethine nitrogen and the enolate oxygen. A depiction of a four coordinate metal complex (Structure I) with the tridentate ligand together with the anionic coligand 'X' is given below.

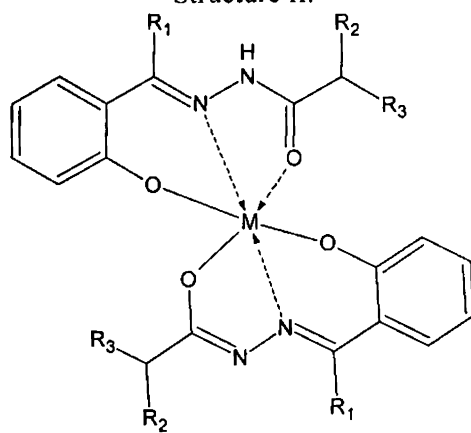


Structure I.

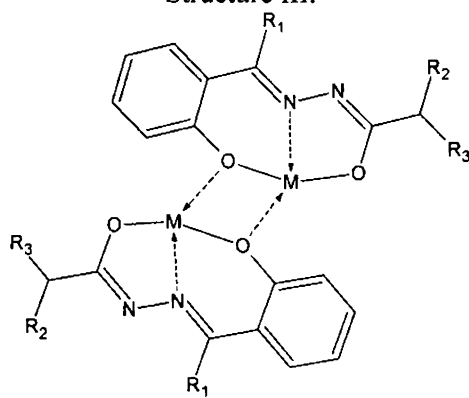
It should be mentioned here that it is not necessary that the ligand should undergo deprotonation and coordinate. Thus the ligand can also coordinate with the metal, in the neutral form. The various possible coordination modes of hydrazone ligands under study are shown below (Structures II-IV).



Structure II.



Structure III.



Structure IV.

1.2. Applications of hydrazones

Many of the physiologically active hydrazones find applications [5] in the treatment of diseases such as tuberculosis, leprosy and mental disorder and aroylhydrazones are also reported to possess tuberculostatic activity [6,7]. This is attributed to the formation of stable chelates with transition metals present in the cell. Thus many vital enzymatic reactions catalysed by these transition metals cannot take place in the presence of hydrazones [8-10]. Hydrazones also act as herbicides, insecticides, nematocides, rodenticides and plant growth regulators. They show spasmolytic activity, hypotensive action and activity against leukaemia, sarcomas and other malignant neoplasms. Hydrazones are used as plasticizers and stabilizers for polymers and as polymerization initiators, antioxidants etc. Hydrazones of 2-methylphthalazone are effective sterilants for houseflies [11]. 3-N-Methyl-N-(4-chloro-1-phthalazinyl) and 3-N-methyl-N-(4-oxo-1-phthalazinyl) hydrazones possess anthelmintic activity [12].

Schiff bases from the condensation of salicylaldehyde with alkyl- and arylamines are widely used in coordination chemistry [13]. They display biological activity, play an important role in biological systems [14-19] and are considered to be suitable models for pyridoxal and in general, B₆ vitamins [20]. Adducts of non transitions, early transitions and *f*-metals with *ortho*-hydroxy Schiff bases [21] have been studied. Thiazoles are of interest because of their pharmaceutical, phytosanitary, analytical and industrial applications, e.g., as fungicides, anthelmintics and herbicides [22]. On the other hand, cyclobutane carboxylic acids were described as L-glutamate, N-methyl-D-aspartate (NMDA) antagonists and anticonvulsive drugs [23-25]. Salicylaldehyde thiazolyhydrazones are reported to be pharmacologically active and useful as ligands in coordination chemistry [26].

It is reported and patented a novel class of ligands based on 2-pyridinecarbaldehyde isonicotinoylhydrazone (HPCIH) that have shown great promise *in vitro*, demonstrating a high iron chelation efficiency [27-29]. Moreover, these chelators show very low toxicity *in vitro* in cultured cells and the compounds are simple and economical to prepare by a Schiff- base condensation reaction [30-32]. Iron metabolism in humans is characterized by limited external exchange and efficient reutilization from internal sources because of the limited ability of the body to excrete excess iron, iron overloads develops in transfusion-dependent patients, such as those with β -thalassemia, aplastic anemia or myelodysplastic syndrome. The only treatment for secondary iron overload is the administration of iron chelating agents [33, 34]. Pyridoxal isonicotinoylhydrazone (PIH) is reported to have the capacity to mobilize iron both *in vitro* [35] and *in vivo* [36], and shows promise for the treatment of secondary iron overload. More recently over 40 analogs of PIH were synthesized, some of which proved more potent in mobilizing iron from iron labeled cells [37]. These chelators significantly enhanced biliary excretion of iron in rats following intraperitoneal or oral administration [38]. A range of tridentate ONO hydrazones was evaluated as iron chelating drugs *in vivo* [39].

Hydrazones of this type also have interesting biological properties as antibacterial and antitumor activity related to the inhibition of DNA synthesis in various human and rodent cells [40,41]. In spite of the toxicity on repeated dosing, isonicotinoylhydrazone (INH) is still considered to be a first line drug for chemotherapy of tuberculosis [42]. Preparation of Mannich bases of isonicotinoylhydrazone has improved the lipid solubility and antimycobacterial activity [43].

The heterocyclic hydrazones constitute an important class of biologically active drug molecules which have attracted attention of medicinal chemists due to

their wide range of pharmacological properties including iron scavenging and antitubercular activities [44-46]. 2-Acetylpyridine benzoylhydrazone and its copper complexes were reported to have *in vitro* antimycobacterial activities against *Mycobacterium smegmatis*. 2,6-Diacetylpyridine bis(acylhydrazones) and several of their complexes with some first transition series metal ions are also reported to have significant antibacterial and antifungal properties [47].

Salicylaldehyde acetylhydrazone was demonstrated to have radioprotective properties [48] and a range of hydrazones was shown to be cytotoxic [49] again with the copper complexes showing enhanced activity. The use of benzene- and *p*-toluenesulphonylhydrazines and their hydrazones derivatives as ligands for transition metal ions has received considerable attention because of their photochromic effect [50-54]. Investigations to assess the possible use of metal chelates in the stabilization of unusual high oxidation states have been described in literature. 2-Hydroxyacetophenone-arylohydrazone derivatives are reported to use as corrosion inhibitors for copper dissolution in nitric acid solution [55]. Aromatic hydrazone molecules dispersed in a binder polymer are used as the main constituent of electrophotographic devices due to their excellent hole-transporting properties and relatively simple synthesis [56-59]. Some of the low molar mass aromatic hydrazones are reported as glass forming compounds [60-62].

A facile, rapid, selective, sensitive and reproducible spectrophotometric flow-injection method for the determination of ultra trace levels of Au(III) in aqueous medium by coupling with 3,5-dimethoxy-4-hydroxy-2-aminoacetophenone isonicotinoylhydrazone at pH 6.0 in water and pharmaceutical samples was also reported [63]. Biscyclohexanone oxalyldihydrazone was one of the earliest used hydrazones for the spectrophotometric determination of copper in paper pulp products [64], human serum [65], steel [66], plants [67], non-ferrous metals and alloys [68] and

cadmium sulphide [69]. Salicylaldehyde isonicotinoylhydrazone was used for the spectrophotometric determination of gallium and indium. 2-Hydroxy-1-naphthaldehyde isonicotinoylhydrazone has been used for the colorimetric determination of iron(II) and (III) in the presence of each other and other metals [70]. The complexes formed by vanadium with acetone isonicotinoylhydrazone and with 4-hydroxybenzaldehyde isonicotinoylhydrazone were used for the spectrophotometric determination of vanadium [71].

The fluorescence of isonicotinylhydrazones of a number of carbonyl compounds has been examined [72]. In the presence of aluminium, these hydrazones give a yellowish-green fluorescence in an acetate buffer, while under similar conditions the parent carbonyl exhibit only feeble fluorescence. Taniguchi *et al.* [73] used 2-hydroxy-1-naphthaldehyde benzoylhydrazone for the fluorimetric titration of copper(II). The bis(4-hydroxybenzoylhydrazone)s of glyoxal, methylglyoxal and dimethylglyoxal form colored chelates with several cations [74]. The chelates formed are reported to be fluorescent. *p*-Dimethylaminobenzaldehyde isonicotinoylhydrazone forms an intensely orange-yellow precipitate with mercury(I or II) in slightly acidic, neutral or slightly alkaline medium [75] and hence find application as spot test reagent. The zinc and cadmium complexes of 2,2'-bipyridyl-2-pyridylhydrazone have been proposed as indicators in acid-base titrations [76].

1.3. *Non-linear optics*

Non-linear optics is concerned with how electromagnetic field of a light wave interacts with the electromagnetic fields of matter and of other light waves. The interaction of light with a non-linear optical material will cause the materials properties to change and the next photon that arrives will “see” a different material. As light travels through a material, its electric field interacts with other electric fields

with in the material. These internal fields are function of the time dependent electron density distribution in the material and the electric fields of the other light waves, if for e.g., two or more light sources are used. In a non-linear optical (NLO) material, strong interactions can exist among the various fields. These interactions may change the frequency, phase, polarization or path of incident light. When an electric field of intensity E , interacts with a material, an instantaneous displacement (polarization) of electron density of the atoms occurs. The displacement of the electron density away from the nucleus results in a charge separation, an induced dipole with moment μ . For small fields, the displacement of charge from the equilibrium position is proportional to the strength of the applied field.

$$\text{Polarization, } p = \alpha E$$

Thus a plot of polarization as a function of the applied field is a straight line whose slope is linear polarizability, α , of the optical medium. If the field oscillates with some frequency, then the induced polarization will have the same frequency if the response is instantaneous. When light interacts with the internal electric field of the material, the light wave moves the internal electric charge of the material back and forth. This motion of charge in turn will re-emit radiation at the frequency of radiation. For linear polarization, this radiation displays same frequency as the incident light. However the polarization does change the propagation of the light wave. But actually the polarization of a material by an applied electric field E is given by the equation,

$$p_i = \sum_j \alpha_{ij} E_j + \sum_{j \leq k} \beta_{ijk} E_j E_k + \sum_{j \leq k \leq l} \gamma_{ijkl} E_j E_k E_l + \dots$$

Where p_i is the electronic polarization induced along the i^{th} molecular axis, α is the linear polarizability, β is the quadratic hyperpolarizability and γ is the cubic hyperpolarizability. α is a second rank tensor and is responsible for the linear optical behavior. β and γ relates the polarization to the square and cube of the field strength and are third and fourth rank tensors respectively. They are responsible for second order and third order non-linear optical (NLO) properties. For small fields β and γ can be neglected, so that induced polarization is proportional to the strength of the applied field. However when an intense electric field such as laser pulse is used, β and γ become significant. Among second order optics, frequency doubling (second harmonic generation), frequency mixing, and electro-optic pockel effects (linear change in the index of refraction) etc are the main types. For second order non-linear polarization, the emitted radiation displays a doubled frequency as the incident light. To combine polarization waves efficiently, conditions must be met so that the fundamental and the second harmonic light waves reinforce each other. If this requirement is met, then the second harmonic intensity will build as the light propagates throughout the crystal. If this condition is not met, a periodic oscillation of second harmonic intensity occurs as the light travels through the crystal. Therefore the refractive indices experienced by the interactive waves as they propagate through the medium must match to achieve efficient SHG.

1.4. Materials for second order non-linear optics

The quantum mechanical ‘sum over states’ and related equations provide a simple prescription for second order NLO molecular materials: the existence of a strong intramolecular charge transfer excitations in a noncentrosymmetric molecular environment. This can be satisfied by considering a polarizable molecular system (e.g., a π – conjugated pathway) having an asymmetric charge distribution (e.g., with donor and/or acceptor group substituents), such as prototypical *p*-nitroaniline

molecule. In this respect, almost all successful strategies for obtaining second order NLO dipolar organic molecules and metal complexes have been developed within a simple molecular scheme formed by a D – π – A structure, and design of new second order NLO chromophores has focused primarily on engineering the aleuronic nature of the donor and the acceptor, and the conjugation length of the bridge.

1.5. *Metal complexes and non-linear optics*

Since mid 1980s, there has been a growth of interest in the search and development of molecular second order non-linear optical (NLO) materials that possess various device applications. Beside the most traditional donor-acceptor (“push-pull”) organic chromophores, chemists have increasingly extended their field of investigations to newer generations of organic molecules of greater complexity. In recent years, coordination complexes through their unique characteristics such as various redox and magnetic properties, in addition to their great diversity of geometries, have introduced a new dimension to the area. Organometallic structures should be intriguing candidates as second order NLO chromophores by virtue of their low energy electronic charge transfer excitations. Report in 1987 that *cis*-1-ferrocenyl-2-(4-nitrophenyl)ethylene [77] exhibited an SHG efficiency 62 times that of urea has motivated many organometallic chemists to enter the field. As a result, a number of reports of organotransition metal systems with NLO properties have appeared in literature [78-81]. Until early 1990s the main strategy in the design of metal-organic NLO chromophores was to simply mimic organic molecules by using metal centers instead of organic donors. However the fact that NLO response of such chromophores was almost invariably lower than that of π – organics gave rise to an idea that copying organic NLO structures by means of organometallic substituents might not have been the best guideline towards coordination compounds with enhanced optical non-linearities. This idea becomes more relevant in the case of

inorganic complexes, where the *d*-electrons are more strongly held by the metal atom than in the case of organometallic compounds.

The first report of an NLO metal complex of the tetradentate salen [N,N'-bis(salicyleneamino)ethylene] ligand was that of Thompson *et al.* in 1991 [82]. In this system, The metal-salen core was probably not directly involved in the charge transfer process responsible for the NLO response but was rather used to enhance the NLO response of an apical substituted pyridine ligand. The report by Di Bella *et al.* [83] on various Ni(salen) derivatives with experimental sizable NLO responses opened interesting perspectives for metal complexes. In contrast with widely investigated push-pull organic chromophores, such complexes offer a large variety of structures that allows to locate the metal atom in a more strategic position at the center of the charge transfer system, making better use of the metal *d*-orbital hybridization schemes in an organic environment.

1.6. Objectives of the present work

The chemical properties of hydrazones and their complexes are widely explored in recent years, owing to their coordinative capability, pharmacological activity and their use in analytical chemistry as metal extracting agents. In particular the chelating behavior of aroylhydrazones of various aldehydes or ketones is currently being studied in our group [84-89] with the aim of investigating the influence of coordination on their conformation and/or configuration, in connection with the nature of the metal and of the counter ion. The selection of 4-diethylamino-2-hydroxybenzaldehyde, 4-methoxy-2-hydroxybenzaldehyde and 4-methoxy-2-hydroxyacetophenone as carbonyl components and 4-nitrobenzoylhydrazine as the hydrazine part was based on the idea of developing ligands having D- π -A general structure, so that they can produce metal complexes having NLO activity. Hence it is

interesting to explore the coordinating capabilities of these ligands whether in neutral form or anionic form and to study the structural variations occurring in the ligands during complexation such as change in conformation. Also to study the NLO activity of the ligands and complexes prepared in the crude form itself.

So three ligands and their metal complexes are synthesized. They were characterized by various spectroscopic techniques and crystallographic studies. Magnetic studies were also conducted. The NLO activity of ligands and complexes were also studied in the powder form.

1.7. Physical measurements

Elemental analyses were carried out at the Sophisticated Analytical Instruments Facility, Kochi using VarioEL III CHNS. The magnetic susceptibility measurements were done in polycrystalline state at room temperature on a Vibrating Sample Magnetometer at the Indian Institute of Technology, Roorkee, India. IR spectral analyses were done using KBr pellets on Thermo Nicolet AVATAR 370 DTGS FT-IR spectrophotometer in the 4000 - 400 cm^{-1} region. UVD-3500, UV-VIS Double Beam Spectrophotometer was used to record the electronic spectra in the range 200 - 900 nm. NMR spectra were recorded using Bruker AMX 400 FT-NMR Spectrometer using TMS as the internal standard at the Sophisticated Instruments Facility, Indian Institute of Science, Bangalore, India. EPR spectral measurements were carried out on a Varian E-112 X-band spectrometer using TCNE as standard at the Sophisticated Analytical Instruments Facility, Indian Institute of Technology, Bombay, India. The non-linear optical properties were studied in powder form by Hyper Rayleigh scattering technique at Indian Institute of Science, Bangalore, India. The well powdered sample was filled in capillary tube having 0.8 mm thickness. NLO responses of these samples were recorded using urea as the reference, filled in

similar capillary tube. The experimental arrangement for non-linear optical properties utilizes a Quanter A DCR II Nd /YAG laser with 9 mJ a pulse at a repetition rate of 5 Hz. The selected wavelength is 1064 nm.

1.8. Crystallographic data collection and structure analyses

Single crystal X-ray diffraction measurements were carried out on a Bruker Smart Apex CCD diffractometer equipped with fine-focused sealed tube at the Analytical Sciences Division, Central Salt & Marine Chemicals Research Institute, Gujarat. The unit cell parameters were determined and data collections were performed using a graphite-monochromated Mo K α ($\lambda = 0.71073 \text{ \AA}$) radiation. The data collected were reduced using SAINT [90] and MAXUS programs [91] correspondingly for the Bruker Smart Apex CCD diffractometer. The trial structure was obtained by direct methods [92] using SHELXS-97, which revealed the position of all non-hydrogen atoms and refined by full-matrix least squares on F₂ (SHELXL-97) [93] and the graphics tool used includes DIAMOND version 3.0 [94]. All non-hydrogen atoms are refined anisotropically, while the hydrogen atoms are treated with a mixture of independent and constrained refinements.

References

1. P.Espinet, M. A. Estreuelas, L. A. Oro, J. L. Serrano. E. Sola, *Coord. Chem. Rev.* 117 (1992) 215.
2. A. M. G. Godquin, P. M. Maitlis, *Angew. Chem. Int. Ed. Engl.* 30 (1991) 375.
3. E. N. Jacobsen, W. Zhang, A. R. Muci, J. R. Ecker, L. Deng, *J. Am. Chem. Soc.* 113 (1991) 7063.
4. H. Schmidt, M. Bashirpoor, D. Rehder, *J. Chem. Soc. Dalton Trans.* (1996) 3865.
5. Yu. P. Kitaev, B.I. Buzykin, T.V. Troepol'skaya, *Russian Chem. Rev.* (1970) 441,
6. Ng. Ph. Buu-Hoi, Ng. D. Xuong, Ng. N. Ham, F. Binson, R. Roger, *J. Chem. Soc.* (1953) 1358.
7. T.S. Ma, T.M Tien, *Antobiot. Chemother. (Washington)* 3 (1953) 491.
8. Q. Albert, *Nature* 153 (1953) 370.
9. J.M. Price, *Federation Proc.*, 20 (1961) 223.
10. J.M. Price, R.R. Brown, F.C Larson, *J. Clin. Invest.* 36 (1957) 1600.
11. B I. Buzykin, N.N Bystrykh, A.P. Bulgakova, Yu. P. Kitaev, *Otkrytitya, Izobret.,Prom. Obraztsy, Tovarnye Znaki* 54 (1977) 69; *Chem. Abstr.*, 88 (1978) 132034r.
12. Zh. V. Molodykh, B.I. Buzykin, N.N. Bystrykh, Yu. P. Kitaev, *Khim. Farm. Zh.*, 11 (1977) 37; *Chem Abstr.*, 88 (1978) 989280y.
13. A.S.N. Murthy, A.R. Reddy, *Proc. Indian Acad. Sci. Chem. Soc.* 90 (1981) 519.
14. L. Streyer, *Biochemistry*; Freeman: New York, 1995.
15. V. Razakantoanina, P.P. Nguyen Kim, G. Jaureguiberry, *Parasitol Res* 86 (2000) 665.

16. R.E. Royer, L.M. Deck, T.J.V. Jagt, F.J. Martinez, R.G. Mills, S. Young, A.D.L.V. Jagt, *J. Med. Chem.* 38 (1995) 2427.
17. M. R. Flack, R.G. Pyle, N. Mullen, M. B. Lorenzo, Y. W. Wu, R. A. Knazek, B.C. Nusule, M.M. Reidenberg, *J. Clin. Endocrinol. Metab.* 76 (1993) 1019.
18. R. Baumgrass, M. Weiwad, F.J. Edmann, *J. Chem.* 276 (2001) 47914.
19. P.J.E. Quintana, A. de Peyster, S. Klitzke, H.J. Park, *Toxicol Lett.* 117 (2000) 85.
20. T. M. Devlin, *Textbook of Biochemistry with Clinical correlations*; Wiley: New York (1997) 449.
21. J. I. Bullock, H. A. Tajmir-Riahi, *Inorg. Chim. Acta* 38 (1980) 141.
22. J.V. Metzger, A.R. Katritzky, W. Rees, K.T. Potts, *Comprehensive Heterocyclic Chemistry*; Pergamon: Oxford, 6(4b) (1984) 328.
23. R.D. Allan, J.R. Hanrahan, T.W. Hambley, G.A. Johnston, K.N. Mewett, A.D. Mitrovic, *J. Med. Chem.* 33 (1990) 2905.
24. T.H. Lanthorn, W.F. Hood, G.B. Watson, R.P. Compton, R.K. Rader, Y. Gaoni, J.B. Moanhan, *Eur. J. Pharmacol.* 182 (1990) 397.
25. Y. Gaoni, A.G. Chapman, N. Parvez, P.C. Pook, D.E. Jane, J.C. Watkins, L. *Med. Chem.* 37 (1994) 4288.
26. I. Yilmaz, A. Cukurovali, *Heteroatom Chem.* 14 (2003) 617.
27. E. Becker, D.R. Richardson, *J. Lab. Clin. Med.* 134 (1999) 510.
28. D.R. Richardson, E. Becker, P.V. Bernhardt, *Acta Crystallgr. Sect. C* 55 (1999) 2102.
29. D.R. Richardson, P.V. Bernhardt, E.M. Becker, in *PCT Int. Appl.*, University of Queensland, Australia, Heart Research Institute Ltd., 0117530 (2001) 50.
30. T.R. Richardson, C. Mouralian, P. Ponka, E. Becker, *Biochim. Biophys. Acta-Mol. Basis Dis.* 1536 (2001) 133.
31. P.V. Bernhardt, P. Chin, D.R. Richardson, *J. Biol. Inorg. Chem.* 6 (2001) 801.

32. C.M. Armstrong, P.V. Bernhardt, P. Chin, D.R. Richardson, *Eur. J. Inorg. Chem.* (2003) 1145.
33. C. Hershko, A.M. Konijn, G. Link, *Br. J. Haematol.* 101 (1998) 399.
34. N.F. Olivieri, G.M. Brittenham, *Blood* 89 (1997) 739.
35. P. Ponka, J. Borova, J. Neuwirt, O. Fuchs, *FEBS Lett.* 97 (1979) 317.
36. M. Cikrt, P. Ponka, E. Necas, J. Neuwirt, *Br. J. Haematol.* 45 (1980) 275.
37. P. Ponka, D. Richardson, E. Baker, H.M. Schulman, J.T. Edward, *Biochim. Biophys. Acta.* 967 (1988) 122.
38. K. Blaha, M. Cikrt, J. Nerudova, H. Fornuskova, H.F. Ponka, *Blood.* 91 (1998) 4368.
39. J.L. Buss, E. Arduini, P. Ponka, *Biochem. Pharmacol.* 64 (2002) 1689.
40. D. K. Johnson, T. B. Murphy, N. J. Rose, W. H. Goodwin, L. Pickart, *Inorg. Chim. Acta* 67 (1982) 159.
41. L. Pickart, W. H. Goodwin, W. Burgua, T. B. Murphy, D. K. Johnson, *Biochem. Pharmacol.* 32 (1983) 3868.
42. D. Sriram, P. Yogeewari, K. Madhu, *Bioorg. & Med. Chem. Lett.* 15 (2005) 4502.
43. C. Joshi, N. Khosla, P. Tiwari, *Bioorg. Med. Chem.* 14 (2004) 571.
44. J. R. Dilworth, *Coord. Chem. Rev.* 21 (1976) 29.
45. Q. Albert, *Nature* 9 (1953) 370.
46. S. Fuchareon, R.T.Rowley, N.W. Paul. Eds. *Thalassemia: Pathophysiology and Management, Part B*; Alan R.Liss: New York (1988).
47. M. Carcelli, P. Mazza, C. Pelizzi, G. Pelizzi, F. Zani, *J. Inorg. Biochem.* 57 (1995) 43.
48. O.V. Arapov, O.F. Alferva, E.I. Levocheskaya, I. Krasil'nikov, *Radiobiologiya* 27 (1987) 843.
49. L.L Koh, K.W. Koh, K.O Lain, Y.C. Lian, Y.C. Long, J.D. Ranford, L.C.Tan, Y.Y.Tjan, *J. Inorg, Biochem.* 72 (1998) 155.

50. L. Friedman, R.L. Litle, W.R. Rechile, *Org. Synth. Collect.* 5 (1973) 1055.
51. M.T. Bogert, A. Stull, *Org. Synth. Collect.* 1 (1941) 220.
52. E. Wertheim, *Org. Synth. Collect.* 2 (1961) 471.
53. J.L. Wang, F.N. Bruscato, *Tetrahedron Lett.* (1968) 4593.
54. E. Hadjoudis, D.G. Hadjoudis, *Chim. Chronica. New. Series* 4 (1975) 51.
55. C. Cordier, E. Vauthier, A. Adenier, Y. Lu, A. Massat, A. Cosse-Barbi, *Structural Chemistry.* 15 (2004) 295.
56. N. Mori, US Patent No. 5, 567, 557 (1996).
57. N. Tatsya, u. Minoru, Japan Patent No. 8, 101, 524 (1996).
58. Y. Suzuki, US patent No. 5, 665, 500 (1997).
59. N. Jubran, Z. Tokarski, T.P. Smith, US Patent No. 6, 340, 548 (2002).
60. S. Nomura, K. Nishimura, *Thin Solid Films* 273 (1996) 27.
61. H. Nam, D.H. Kang, J.K. Kim, S.y. Park, *Chem. Lett.* (2000) 1298.
62. P.M. Borsenberger, *Adv. Chem. Mater. Opt. Electr.* 1 (1992) 73.
63. S. Hribabu, K. Suvadhan, K. Suresh Kumar, K.M. Reddy, D. Rekha, P. Chiranjeevi, *J. Hazardous Mater. B* 120 (2005) 213.
64. C.U. Wetlesen, G. Gran, *svensk Papperstid.* 55 (1952) 212.
65. R.E. Peterson, M.E. Bollier, *Anal. Chem.* 27 (1955) 1195.
66. R. Capelle, *Chim. Anal. (Paris)* 42 (1960) 69.
67. K.R. Middleton, *Analyst* 90 (1965) 234.
68. G. Brown, R.K. Rohde, *Anal. Chem.* 38 (1966) 911,
69. F.C. Frouty, *Anal. Chim. Acta* 47 (1969) 511.
70. S. Belal, I. Chaaban, *Pharnazie* 32 (1977) 704.
71. S. Zommer, *Rocznici Chem.*, 47 (1973) 425.
72. T. Uno, H. Taniguchi, *Bunseki Kagaku* 20 (1971) 997.
73. H. Taniguchi, K. Teshima, K. Tsuge, S. Nakano, *Bunseki Kagaku* 24 (1975) 314.

74. M. Lever, *Anal. Chim. Acta* 65 (1973) 311.
75. G.S. Vasilikiotis, *Microchem. J.* 13 (1968) 526.
76. H. Alexaki-Tzivanidou, G. Kounenis, *Microchem. J.* 23 (1978) 530
77. M.L.H. Green, S.R. Marder, M.E. Thompson, J.A. Bandy, D. Bloor, P.V. Kolinsky, R.J. Jones, *Nature* 330 (1987) 360.
78. L.T. Cheng, W. Tam, G.R. Meredith, S.R. Marder, *Mol. Cryst. Liq. Cryst.* 189 (1990) 137.
79. S.R. Marder, *Inorganic Materials*. John Wiley & Sons, New York (1992) 115.
80. N.J. Long, *Angew. Chem. Int. Ed. Engl.* 34 (1995) 21.
81. I.R. Whittal, A.M. McDonagh, M.G. Humphrey, M. Samoc, *Adv. Organomet. Chem.* 42 (1998) 291.
82. W. Chiang, M.E. Thompson, D. VanEngen, J.W. Perry, *Spec. Publ. R. Soc. Chem.* 91 (1991) 210.
83. S. Di Bella, I. Fragala, I. Ledoux, M.A. Diaz-Garcia, P.G. Lacroix, T.J. Marks, *Chem. Mater.* 6 (1994) 881.
84. P. B. Sreeja, A. Sreekanth, C. R. Nayar, M. R. P. Kurup, A. Usman, I. A. Razak, S. Chantrapromma, H. -K. Fun, *J. Mol. Stru.* 645 (2003) 221.
85. P. B. Sreeja, M. R. P. Kurup, A. Kishore, C. Jasmin, *Polyhedron* 23 (2004) 575.
86. P. B. Sreeja, M. R. P. Kurup, *Spectrochim. Acta A* 61 (2005) 331.
87. M. Kuriakose, M. R. P. Kurup, E. Suresh, *Spectrochim. Acta A* 66 (2007) 353.
88. B. N. B. Raj, M. R. P. Kurup, *Spectrochim. Acta A* 66 (2007) 898.
89. B. N. B. Raj, M. R. P. Kurup, E. Suresh, *Struct. Chem.* 17 (2006) 201.
90. Siemens, SMART and SAINT, Area Detector Control and Integration Software, Siemens Analytical X-ray Instruments Inc., Madison, Wisconsin, USA, 1996.

91. S. Mackay, C. J. Gilmore, C. Edwards, N. Stewart and K. Shankland, maXus Computer Program for the Solution and Refinement of Crystal Structures. Nonius, The Netherlands, MacScience, Japan and The University of Glasgow, 1999.
92. G. M. Sheldrick, *Acta Crystallogr. A*46 (1990) 467.
93. G. M. Sheldrick, SHELXS-97 Program for the solution of Crystal Structures, University of Göttingen, Göttingen, Germany, 1997.
94. K. Bradenburg, H. Putz, DIAMOND Version 3.0, Crystal Impact, GbR, Postfach 1251, D-53002 Bonn, Germany, 2004.

CHAPTER TWO

Syntheses, spectral characterization, crystal structures and non-linear optical properties of the *N*-salicylidine- *N'*-aroylhydrazone ligands

Schiff bases derived from the condensation of salicylaldehyde and its derivatives with alkyl and aroylhydrazones play a very important role in coordination chemistry [1]. They display biological activity [2-5], play an important role in biological systems [6-11] and are considered to be suitable models for pyridoxal, and in general B₆ vitamins [12]. Adducts of nontransition, early transition, and *f* metals with *ortho* hydroxy Schiff bases [13] have been widely studied. Furthermore, abilities of aroylhydrazones to coordinate to metals either in keto (I) or enol (II) tautomeric form (Fig. 2.1) make them attractive as ligands [14-16]. As the salicylaldehyde aroylhydrazone Schiff base is concerned, it can act as a tridentate ligand both in the monoanionic and dianionic forms and hence can form very stable chelates with all metal ions.

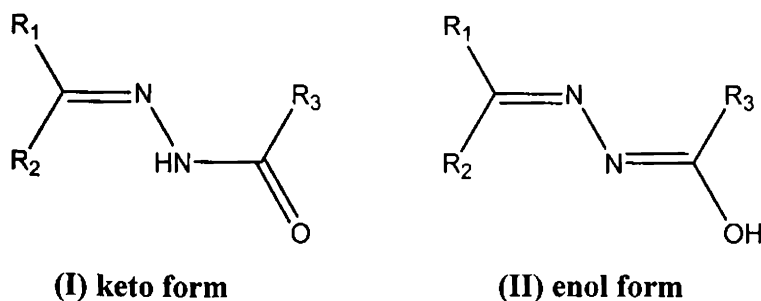


Fig. 2.1

Some metal complexes of aroylhydrazones, particularly of salicylaldehyde benzoylhydrazone and pyridine-2'-carboxaldehyde-2-pyridylhydrazone, are potential inhibitors of DNA synthesis in a variety of cultured human and rodent cells. This hydrazone also has mild bacteriostatic activity and a range of analogues has been investigated as potential oral iron chelating drugs for genetic disorders [17]. Several aroylhydrazones have wide spread applications in the field of analytical chemistry as a selective metal extracting agent as well as in spectroscopic determination of certain transition metals [18-19]. Many of aroylhydrazones have interesting electric and magnetic properties [20-22], which make research in this field even more attractive. 2-Hydroxyacetophenone aroylhydrazone derivatives are reported to act as corrosion inhibitors for copper dissolution in nitric acid solution [23].

Salen based metal complexes play an important role in the SHG efficiency also. Thompson *et al.* in 1991 reported the first salen based NLO metal complex of the tetradentate salen [*N,N'*-bis(salicylaldehydato) ethylene] ligand [24]. Compared to organic molecules, they can offer large variety of molecular structures, the possibility of high thermal and environmental stability and a diversity of electronic properties by the virtue of coordinated metal atom. Detailed study on the NLO active materials provide a simple prescription of strong intramolecular charge transfer excitations in a non-centrosymmetric molecular environment. This can be satisfied by considering a polarizable molecular system (π -conjugated pathway) having an asymmetric charge distribution (donor-acceptor group substituents) such as the prototypical *p*-nitroaniline molecule. Keeping all these findings in mind we synthesized three new aroylhydrazones of salicylaldehyde derivatives having proper donor and acceptor substituents both in the aldehyde and hydrazone parts [25-26]. The ligands were prepared by condensing 4-*N,N*-diethylamino salicylaldehyde, 4-methoxysalicylaldehyde, 4-methoxy-2-hydroxyacetophenone respectively with 4-nitrobenzoylhydrazone.

2.1. *N*-4-Diethylamino-2-hydroxybenzaldehyde-*N'*-4-nitrobenzoylhydrazone, H₂L¹

The compound *N*-4-Diethylamino-2-hydroxybenzaldehyde-*N'*-4-nitrobenzoyl hydrazone H₂L¹ (Fig. 2.2) was prepared from 4-diethylamino-2-hydroxybenzaldehyde and 4-nitrobenzoylhydrazine.

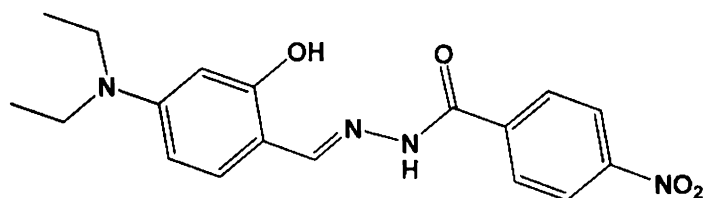


Fig. 2.2. Structure of H₂L¹.

2.1.1. Experimental

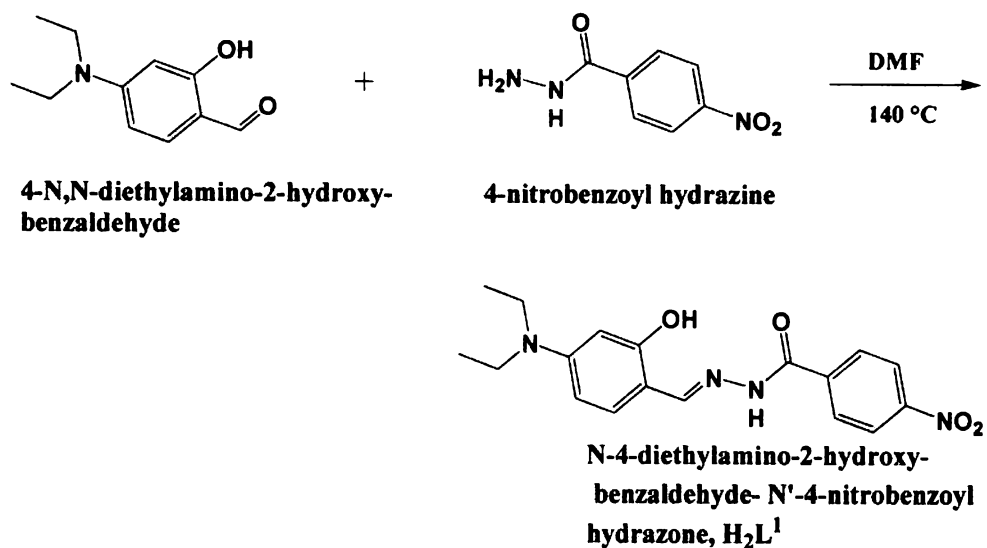
2.1.1a. Materials

4-Diethylamino-2-hydroxybenzaldehyde (Sigma Aldrich), 4-nitrobenzoylhydrazine (Sigma Aldrich) and DMF (S.D. Fine) were used as received.

2.1.1b. Synthesis

The compound was prepared by the reported procedure [27] for aroylhydrazones by the condensation reaction between 4-diethylamino-2-hydroxybenzaldehyde and 4-nitrobenzoylhydrazine using DMF as solvent. 4-Nitrobenzoylhydrazine (1.852 g, 10 mmol) and 4-diethylamino-2-hydroxybenzaldehyde (1.812 g, 10 mmol) were dissolved in 14 ml DMF. The solution was heated to boiling for 5 minutes and then is cooled to room temperature and poured into crushed ice containing a little concentrated sulphuric acid. The

Scheme 1 for the reaction is shown below. The compound separated as dark red powder, which was recrystallized from DMF. Yield: 2.88 g (77%). Elemental Anal. Found (Calcd.) (%): C, 60.93 (60.66); H, 5.76 (5.66); N, 15.83 (15.72).



Scheme 1

2.1.2. Crystal structure

The molecule crystallizes as H₂L¹·H₂O in the monoclinic crystal system with a space group of *C2/c*. The crystal structure of the compound with atom numbering scheme is shown in Fig. 2.3. The crystal data and structure refinement parameters are listed in Table 2.1 and selected bond lengths and bond angles in Table 2.3.

The bond distances C11–N2 (1.267 Å), N2–N3 (1.378 Å) and N3–C12 (1.324 Å) correspond to C=N double, N–N single and C–N single bonds and are comparable to the previously reported analogous of hydrazones [28–34]. Hence it is concluded that the ligand molecule is in the keto tautomeric form. The configuration

at N2–C11 bond is *E*. There is a completely extended conformation in the central part of the molecule C8–C11=N2–N3–C12=O2. The molecule is found to be nonplanar as a whole and the central hydrazone moiety shows a maximum deviation of 0.062(4) Å from the mean plane. There is an intramolecular hydrogen bonding interaction is seen in the molecule comprising of O1–H1...N2 (O1–H1 = 0.82 Å, H1...N2 = 1.96 Å, O1–N2 = 2.670(7) Å).

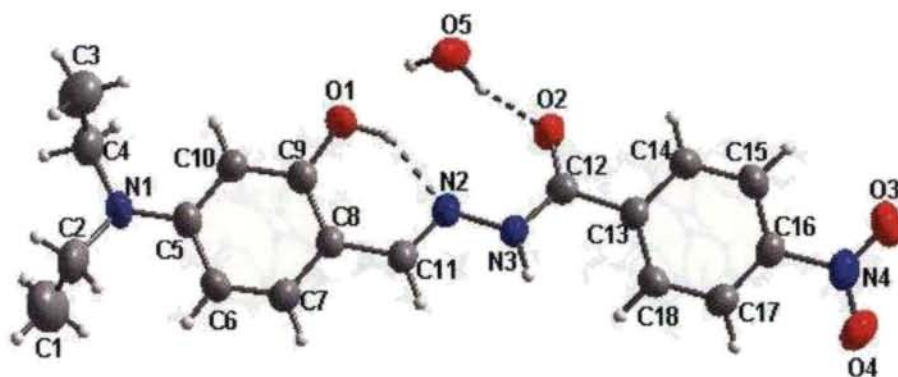


Fig. 2.3. Molecular structure of $H_2L^1 \cdot H_2O$. Intramolecular hydrogen bonds are shown as dotted lines. Ellipsoids are drawn with 50% probability.

In the crystal lattice (Fig. 2.4), two-dimensional packing is effected by the network of intermolecular hydrogen bonding interactions. The repeating unit consists of two adjacent molecules aligned in an offset fashion. Three intermolecular hydrogen bonds involving the water residue viz, N3–H3...O5ⁱ ($i = x, -y, -1/2 + z$, N3–H3 = 0.81(4) Å, H3...O5 = 2.01(4) Å, N3–O5 = 2.811(8) Å, N3–H3...O5 = 166(3)°), O5–H51...O2ⁱⁱ ($ii = 1/2 - x, 1/2 + y, 3/2 - z$, O5–H51 = 1.03(7) Å, H51...O2 = 2.03(6) Å, O5–O2 = 2.957(8) Å, O5–H51...O2 = 149(4)°) and O5–H52...O2, link the neighboring repeating units. Thus the water residue acts both as an acceptor and donor in hydrogen bonds. However the $\pi - \pi$ interactions are

observed between $Cg1$ and $Cg2$ ranging from 3.7162 \AA to 3.8400 \AA . $Cg1$ and $Cg2$ comprising of C5, C6, C7, C8, C9, C10 and C13, C14, C15, C16, C17, C18 respectively. There is a pseudo two fold axis can be observed, passing through the middle of N2–N3 bond, perpendicular to the plane described by C11, N2, N3 and C12 atom, will be responsible for the stacking of the two phenyl group along the 'b' axis. But the hydrogen bonding interactions have the key role during packing of the molecule in the unit cell.

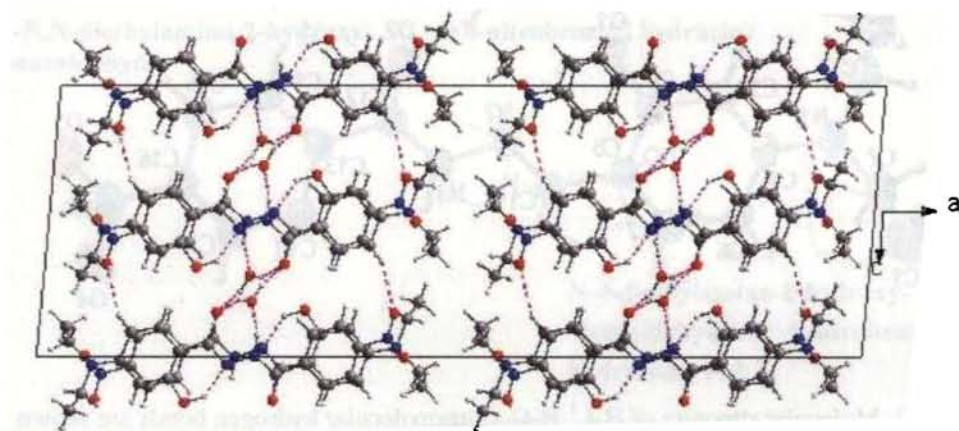


Fig. 2.4. Packing diagram of the compound $H_2L^1 \cdot H_2O$ in the crystal lattice. Intra and internuclear hydrogen bonding are shown as dotted lines.

2.1.3. Spectral studies

2.1.3a. NMR spectra

The 1H NMR spectrum of the compound H_2L^1 along with the assignment of peaks is shown in Fig. 2.5. The absorption at the δ value 1.10 ppm is seen as a triplet with an intensity ratio of 1:2:1 and an area integral of six. It is assigned to the six equivalent methyl protons at C1 and C3. The quartet in the ratio 1:3:3:1 seen at 3.36

ppm is assigned to the equivalent methylene protons at C2 and C4. The area integral of four also supports this. The protons at C6 and C10 are not equivalent but in nearly same chemical environment and so peaks due to them are very close to each other. Peak due to C10 comes in low δ value (δ 6.12 ppm singlet) because of the presence of OH *ortho* to it. C6 proton absorption appears as a doublet (δ 6.27 ppm) due to the presence of a neighboring proton at C7. Because of the same reason, C7 proton resonance peak δ (7.23 ppm) split into two in 1:1 ratio. Proton attached to C11 resonates at δ value 8.44 ppm. This high value of δ is because that proton is attached to a carbon that is double bonded to electronegative nitrogen and hence in a low electron density environment. The protons at C14 and C18 are in same chemical environment and so resonate in same δ value (8.14 ppm).

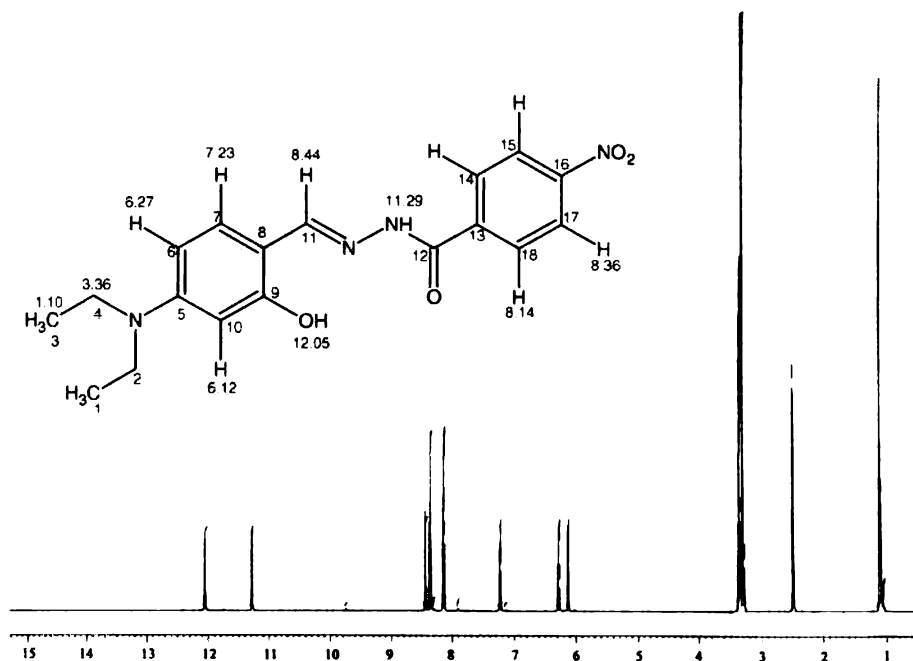


Fig. 2.5. The 1H NMR spectrum of the compound H_2L^1 in $DMSO-d_6$.

Similarly in the case of C15 and C17 (8.36 ppm). The latter group resonates in slightly downfield compared to the former one due to the presence of electron withdrawing nitro group in its *ortho* position. Two absorptions observed at the very downfield region of the spectrum, δ 11.29 and δ 12.05 ppm, and are assigned to the NH and OH protons respectively [35]. The significant loss of intensity of these peaks in deuteriated spectrum confirms this. The higher δ values of these protons are because they are attached to highly electronegative nitrogen and oxygen atoms. This fact also suggests the possibility of considerable extent of hydrogen bonding involved by them, which is confirmed by the crystal structure. Hydrogen bonding decreases the electron density around the proton and thus moves the proton absorption to lower field.

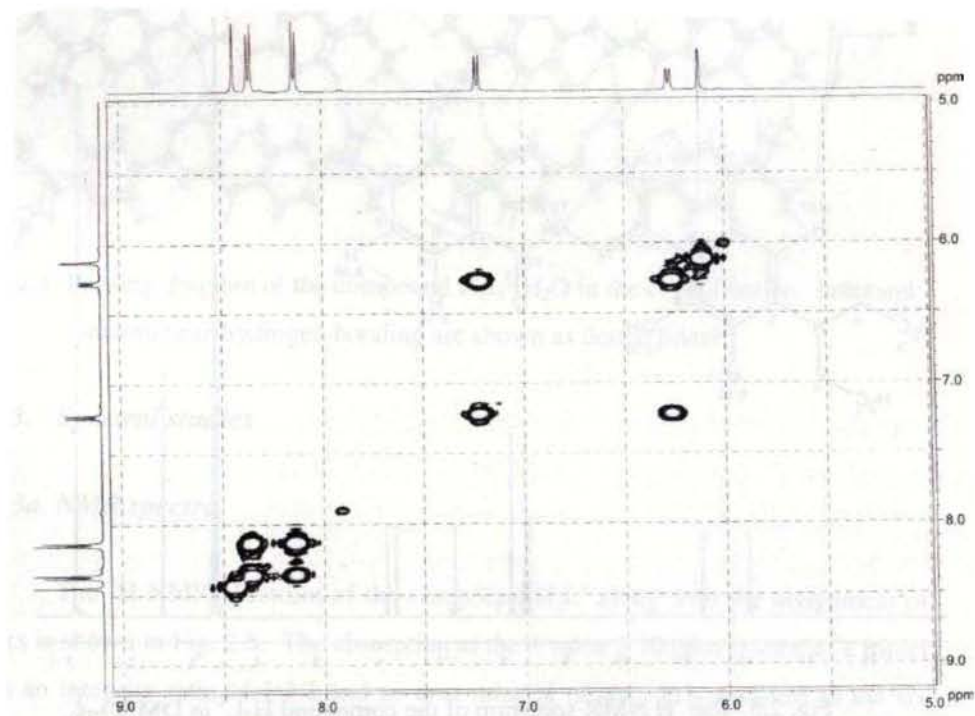


Fig. 2.6. ^1H - ^1H COSY spectrum of the compound H_2L^1 in $\text{DMSO-}d_6$.

^1H - ^1H correlation spectrum confirms the proposed structure for the compound H_2L^1 (Fig. 2.6). No correlation patterns are observed for the signals at δ 8.44, 11.29 and 12.05 ppm according to the proposed assignments. Peaks at 1.10 and 3.36 ppm show considerable correlation to each other so that they are attached to the neighboring carbons. Resonance at 6.27 ppm makes intense interaction with 7.23 absorption and small interaction with 6.12 absorption. This makes sure that proton which makes 7.23 peak (C7) is at *ortho* and that make 6.12 peak (C10) is at *meta* to the 6.27 (C6) proton. Peak at 8.14 ppm (C14 and C18) make good contours with 8.36 ppm peak (C15 and C17) and it confirms that these protons are attached to the neighboring carbon atoms.

^{13}C spectrum of the compound H_2L^1 is interpreted with the help of ^1H - ^{13}C correlative HSQC spectrum (Fig. 2.7). Absorption at ^{13}C δ values 150.70, 106.14, 159.45, 168.45, 138.78 and 149.12 ppm do not have any contours in HSQC suggesting that these absorptions are due to carbons to which no hydrogens attached. These peaks are assigned as C5 (150.70), C8 (106.14), C9 (159.45), C12 (168.45), C13 (138.78) and C16 (149.12). The peak due to the carbonyl carbon C12 at δ 168.45 ppm is very weak and is difficult to distinguish from the noise. This may be due to the following reasons. Firstly, in the solution state, there may be considerable extent of keto-enol tautomerism so that the resonance frequency of carbonyl carbon changes continuously and the peaks are difficult to locate due to the poor solubility of the compound. Secondly, the common spin-lattice relaxation mechanism for ^{13}C results from dipole-dipole interaction with directly attached protons. Thus nonprotonated carbon atoms often have longer relaxation times and give small peaks. Hence carbonyl carbon will give only small peaks and at low concentrated solutions, it may not be detected.

The remaining ^{13}C peaks, δ 12.45, 43.76, 103.79, 131.59, 97.26, 150.38, 128.93 and 123.59 ppm make interaction with ^1H peaks, δ 1.1, 3.36, 6.27, 7.23, 6.12,

8.44, 8.14 and 8.36 ppm respectively in HSQC and so those are assigned as C1 and C3 (12.45), C2 and C4 (43.76), C6 (103.79), C7 (131.59), C10 (97.26), C11 (150.38), C14 and C18 (128.93) and C15 and C17 (123.59).

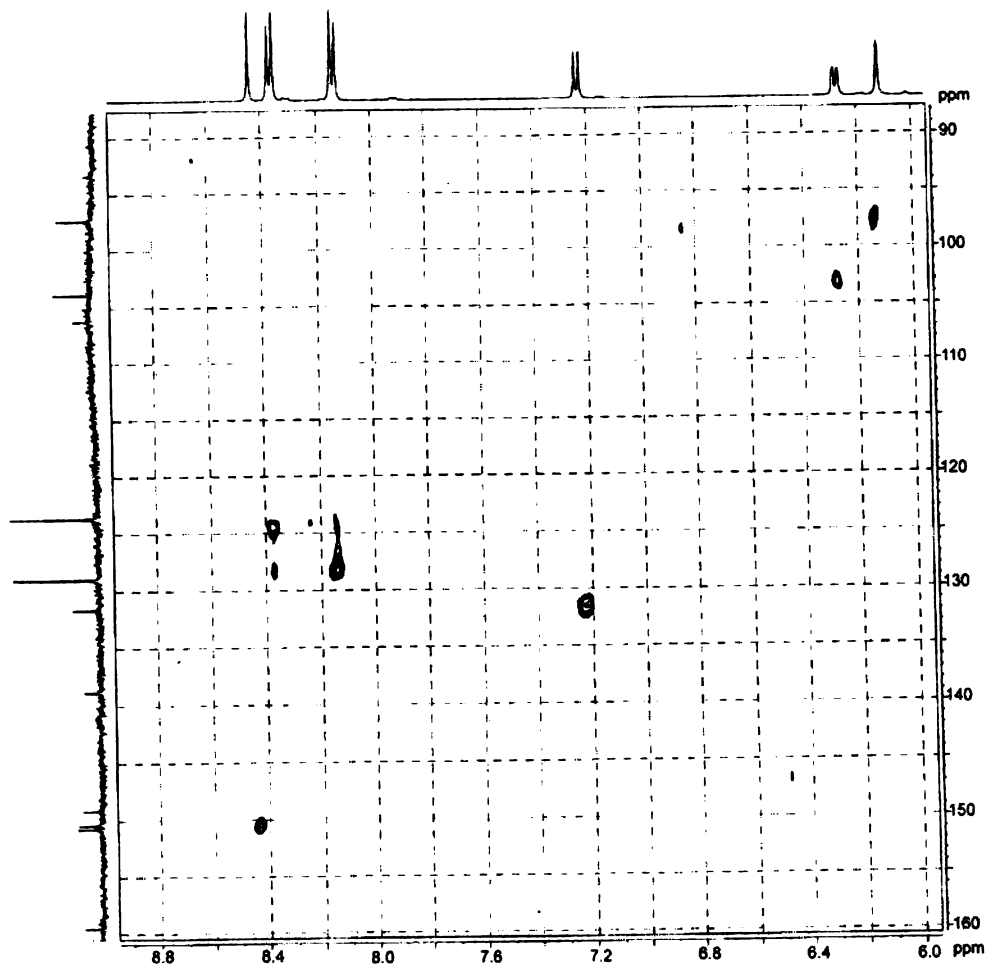


Fig. 2.7. The HSQC correlation spectrum of the compound H_2L^1 in $DMSO-d_6$.

2.1.3b. Infrared spectrum

The infrared spectrum of the compound is shown in the Fig. 2.8. The existence of the compound in the keto tautomeric form can be well confirmed by strong $\nu(\text{C}=\text{O})$ absorption at 1631 cm^{-1} and it is the amide I band. Amide II band is observed as a weak band at 1594 cm^{-1} , absorption due to NH bending vibration. These bands are shifted to the low frequency region than the theoretical value due to conjugation of the amide group with aromatic ring.

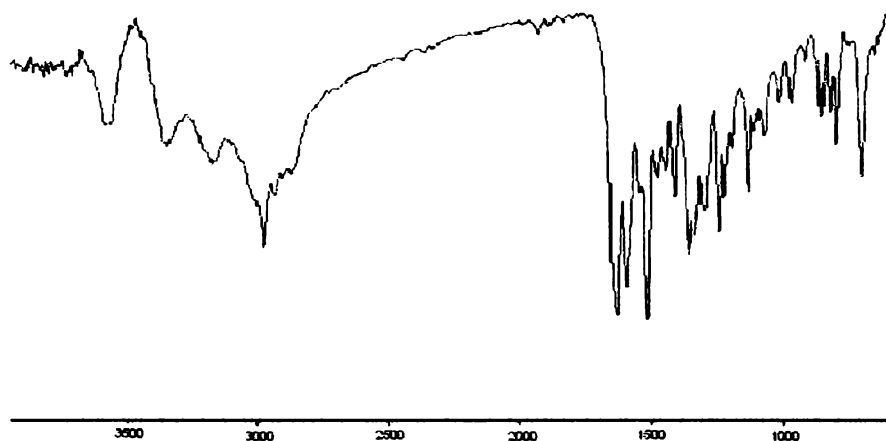


Fig. 2.8. The IR spectrum of the compound H_2L^1 .

The $\text{C}=\text{O}$ stretching absorptions of amides occur at longer wavelengths than normal carbonyl absorption due to the resonance effect. Occurrence of amide II band within the range of $1570\text{--}1515\text{ cm}^{-1}$, in the solid state shows the presence of secondary acyclic amides [35]. A broad band observed in the region $3000\text{--}3600\text{ cm}^{-1}$, comprising of the $-\text{OH}$ and $-\text{NH}$ stretching absorptions and it is very difficult to differentiate them. The very broad nature of this band is due to the large extent of hydrogen bonding. Two sharp bands observed at 1594 and 1414 cm^{-1} may be due to

aromatic carbon carbon double bond stretching vibrations, but aromatic CH stretching vibrations cannot be separately viewed because of the broad bands in the 3000-3100 cm^{-1} region. The intense band observed at 1518 cm^{-1} is assigned to the C=N stretching vibration of the Schiff base. A medium band observed at *ca.* 985 cm^{-1} may be due to the $\nu(\text{N-N})$ stretching vibration.

2.1.3c. Electronic spectrum

The UV-vis absorption spectrum of the compound H_2L^1 in DMF (10^{-5} M) is shown in Fig. 2.9. Two strong absorptions 330-370 and 375-450 nm are seen in the spectrum. The first one has more intensity than the second one and is assigned to the $\pi \rightarrow \pi^*$ transitions of the electrons in *p*-substituted benzene rings and in azomethine bond. The second absorption in the region 375-500 nm with low intensity is due to the $n \rightarrow \pi^*$ transitions of the nonbonded electrons in the carbonyl and nitro chromophores. The latter absorption is extended towards the visible region of the spectrum and hence the compound is intense red in color.

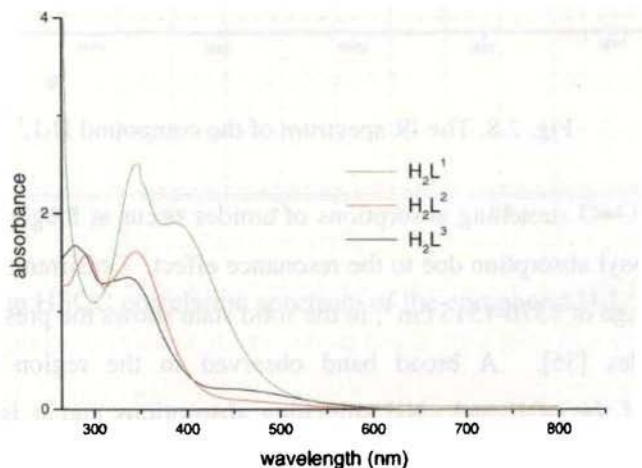


Fig. 2.9. The combined UV-Vis spectra of the ligands H_2L^1 , H_2L^2 and H_2L^3 .

2.2. *N*-2-Hydroxy-4-methoxybenzaldehyde- *N*'-4-nitrobenzoylhydrazone, H_2L^2

Similar to H_2L^1 , *N*-2-hydroxy-4-methoxybenzaldehyde- *N*'-4-nitrobenzoyl hydrazone, H_2L^2 (Fig. 2.10) was prepared by the reaction between 2-hydroxy-4-methoxybenzaldehyde and 4-nitrobenzoylhydrazine.

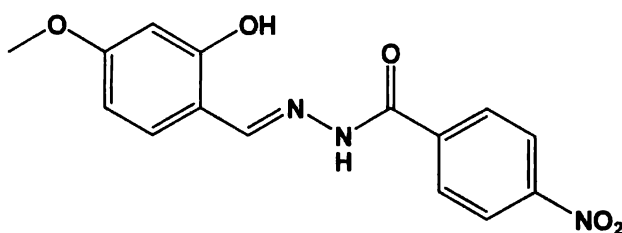


Fig. 2.10. Structure of compound H_2L^2 .

2.2.1. Experimental

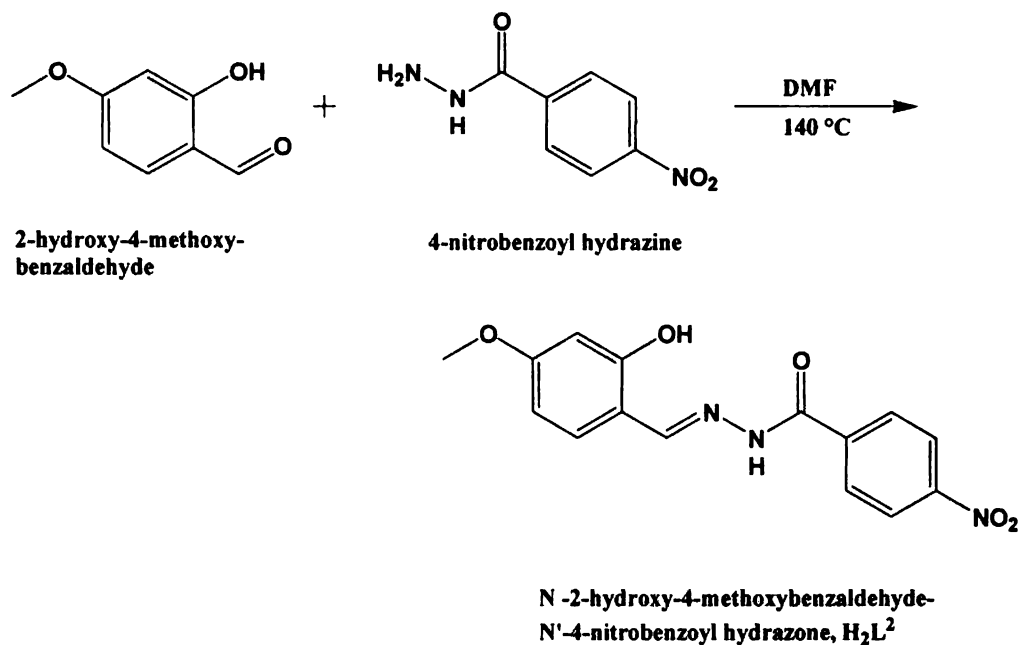
2.2.1a. Materials

2-Hydroxy-4-methoxybenzaldehyde (Sigma Aldrich), 4-nitrobenzoylhydrazine (Sigma Aldrich) and DMF (S.D. Fine) were used as received.

2.2.1b. Synthesis

4-Nitrobenzoylhydrazine (1.852 g, 10 mmol) and 2-hydroxy-4-methoxybenzaldehyde (1.521 g, 10 mmol) were dissolved in 14 ml DMF. The solution was heated to boiling for 5 minutes and then is cooled to room temperature and poured into crushed ice containing a little concentrated sulphuric acid. The Scheme 2 for the reaction is shown below. The compound separated as bright red

powder, which was recrystallized from DMF. Yield: 2.59 g (82%). Elemental Anal. Found (Calcd.) (%): C, 57.12 (57.14); H, 4.52 (4.16); N, 12.96 (13.33).



Scheme 2

2.2.2. Crystal structure

The molecule crystallizes as $\text{H}_2\text{L}^2 \cdot \text{H}_2\text{O}$ in the triclinic crystal system with a space group of *P*-1. The crystal structure of the compound with atom numbering scheme showing 50% displacement ellipsoids is shown in Fig. 2.11. The crystal data and structure refinement parameters are listed in Table 2.1 and selected bond lengths and bond angles are in Table 2.3.

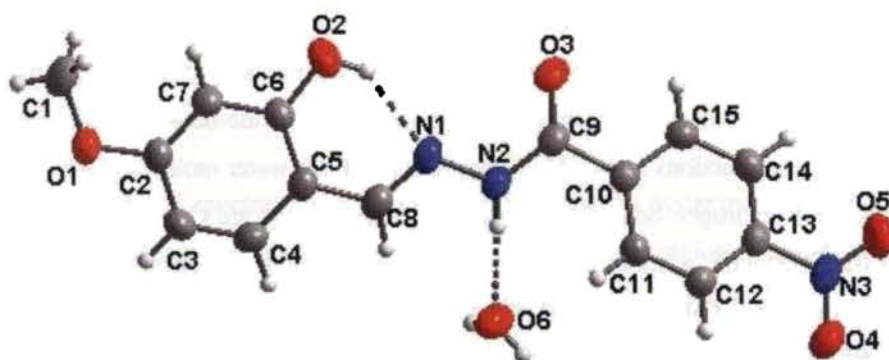


Fig. 2.11. Molecular structure of $\text{H}_2\text{L}^2 \cdot \text{H}_2\text{O}$. Intramolecular hydrogen bonds are shown as dotted lines. Ellipsoids are drawn with 50% probability.

The molecule exists in the keto tautomeric form and the configuration of C8–N1 bond is *E*. The molecule exists mainly in two planes. One plane corresponding to the phenyl ring of the nitrophenyl moiety and the other to the remaining part of the molecule. This twisting may be to relieve the steric interactions between the hydrogen atoms N2–H and C11–H. The three bond angles around C9 atom are not equal to 120° each. It is seen that the N2–C9–O3 bond angle is considerably greater than N2–C9–C10 angle. This observation is similar to the structures of hydrazones reported earlier, which is explained in order to decrease the repulsion between the lone pairs present in N2 and O3 atoms. The central part of the molecule adopts a completely extended double bonded conformation. It can be confirmed by the C9–O3 bond length (1.2324 (23) Å), which is considerably longer than the standard C=O bond length 1.21 Å and N2–C9 bond length (1.3380 (25) Å), which is shorter than standard N–C single bond length (1.47 Å). Similar observation was reported in the case of early-published crystal structures of hydrazone molecules.

The packing (Fig. 2.12) of the molecules in the crystal is effected by a wide network of intermolecular hydrogen bonds involving water. In the crystal lattice, the

molecules are arranged parallel to each other, but in a zigzag fashion such that the nitrobenzoyl fragment of one molecule is just above the methoxy phenyl fragment of second one. The molecules are thus stalked together by a wide network of hydrogen bonds, *Cg-Cg* interactions and *C-H...π* interactions. Each water molecule forms three intermolecular hydrogen bonds in the packing pattern. They are $O6 \cdots H(2A)-O2$ and $O6-H(62) \cdots O3$ with a molecule in the same plane and $O6-H(61) \cdots O1$ with a molecule of adjacent plane arranged in an opposite fashion with it. In addition to this there are two intramolecular $O2-H(2A) \cdots N1$ and $N2-H1 \cdots O6$. *Cg-Cg* interactions also have considerable influence in the packing pattern. There is a *C-H...π* is also present between *C8-H8* and *Cg1* comprising of *C2, C3, C4, C5, C6* and *C7* with an $H \cdots Cg$ distance $3.357(2) \text{ \AA}$.

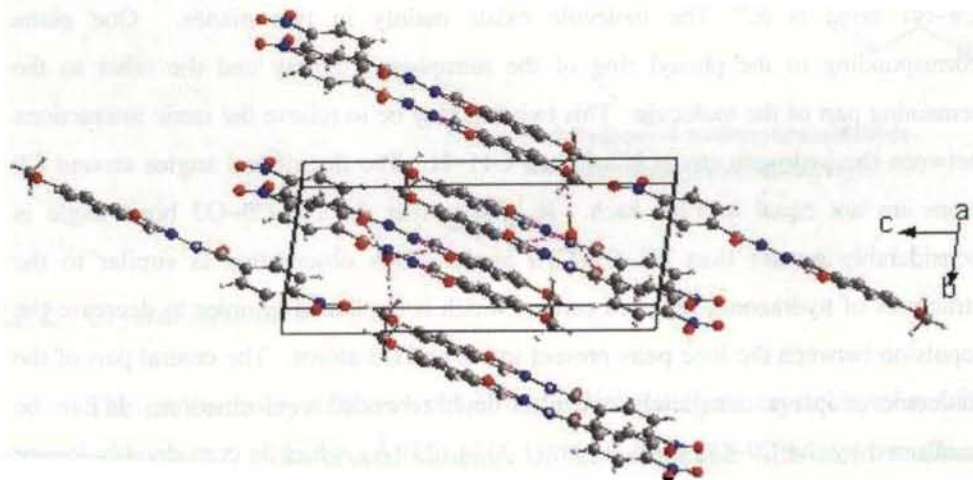


Fig. 2.12. Packing diagram of the compound $H_2L^2 \cdot H_2O$. Intra and intermolecular hydrogen bonds are shown as dotted lines.

2.2.3. Spectral studies

2.2.3a. NMR spectra

The ^1H NMR spectrum of the compound H_2L^2 and its assignments are shown in Fig. 2.13. There are two sharp singlets at the very downfield region of the spectrum i.e., at 12.24 and 11.43 ppm are assigned to OH and NH protons respectively. These hydrogen resonances are seen in the high δ values because they are attached to highly electronegative atoms oxygen and nitrogen respectively and hence in a low electron density environment. This assignment can be confirmed by the deuteriated proton spectra in which the intensity of these bands considerably decreased. Position of these peaks in the downfield region suggests the possibility of considerable extent of hydrogen bonding involved by them. Hydrogen bonding decreases the electron density around the proton and thus moves the proton absorption to lower field.

The doublets observed at 8.15 and 8.37 ppm are assigned to the equivalent protons at C11 and C15 and C12 and C14 respectively. Protons at C12 and C14 resonate at more downfield compared to those at C11 and C15 because of the presence of electron withdrawing nitro group at its *ortho* position. The singlet with an area integral of one at δ 8.57 ppm is due to the resonance of the proton at C8. The peak at δ 7.47 ppm is the C4 proton resonance, is a doublet due to the presence of a neighboring proton at C3. Peaks generated by C3 and C7 are very close to each other because of their nearly same electron environment. C7 gives a singlet at 6.49 ppm and C3 gives a doublet due to the presence of neighboring proton C4 at 6.53 ppm. The singlet at 3.77 ppm, having an area integral of three is assigned to the methoxy protons.

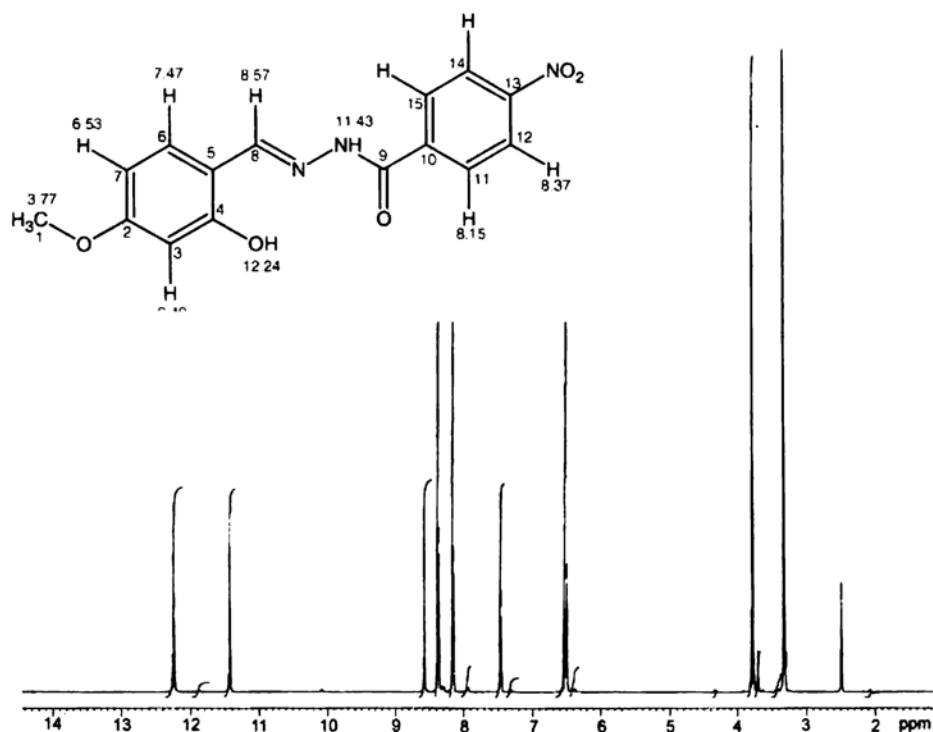


Fig. 2.13. The 1H NMR spectrum of the compound H_2L^2 in $DMSO-d_6$.

The above assignments of the proton NMR spectrum are also confirmed by 1H - 1H correlation spectroscopy. The COSY spectrum is shown in Fig. 2.14 with the possible correlation pattern in the molecule. There is no correlation for the peaks at δ 3.77, 8.57, 11.43 and 12.24 in the 1H NMR spectra, which confirms the above assignments. Correlation patterns are observed in the aromatic region only. Peaks at δ 8.15, 8.37, 6.53 and 7.47 ppm make good contours in the COSY spectrum and peak at δ 6.49 ppm makes only a small correlation. Horizontal and vertical straight lines drawn from δ 8.15 ppm in the diagonal of COSY spectrum will meet the contours at δ 8.37 ppm, confirms the correlation between C11 and C15 protons with C12 and C14 protons. Similarly lines from δ 6.53 meet at δ 7.47, confirming the aforesaid

assignments of the peaks. Small contour made by δ 6.49 peak with δ 6.53 peak suggests the small extent of correlation with the proton at the *meta* position.

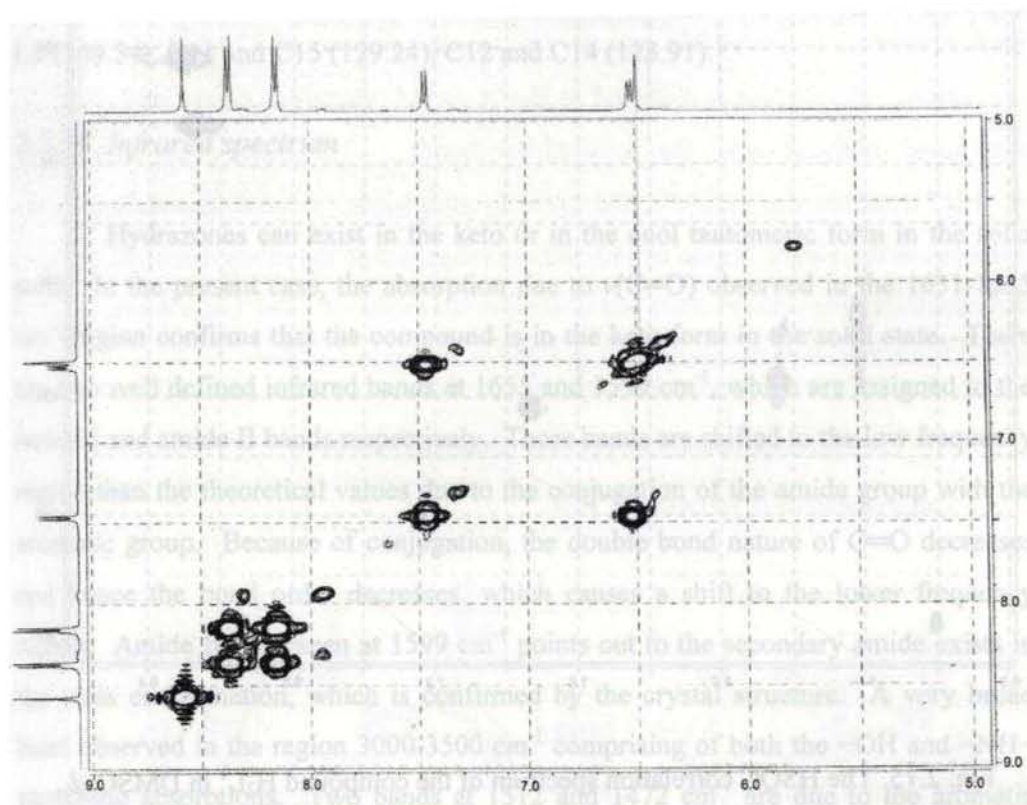


Fig. 2.14. ^1H - ^1H COSY spectrum of the compound H_2L^1 in $\text{DMSO-}d_6$.

The ^{13}C spectrum and ^{13}C - ^1H correlation HSQC spectrum (Fig. 2.15) of the compound were also recorded in $\text{DMSO-}d_6$. The correct assignment of the ^{13}C peaks can be done with the help of HSQC. The ^{13}C peaks at δ 162.6, 111.88, 159.2, 169.8, 138.8 and 149.82 do not make any correlation pattern in HSQC suggesting that these peaks are made by non-protonated carbons and are assigned as C2 (162.2), C5 (111.88), C6 (159.2), C9 (169.8) C10 (138.8) and C13 (149.82).

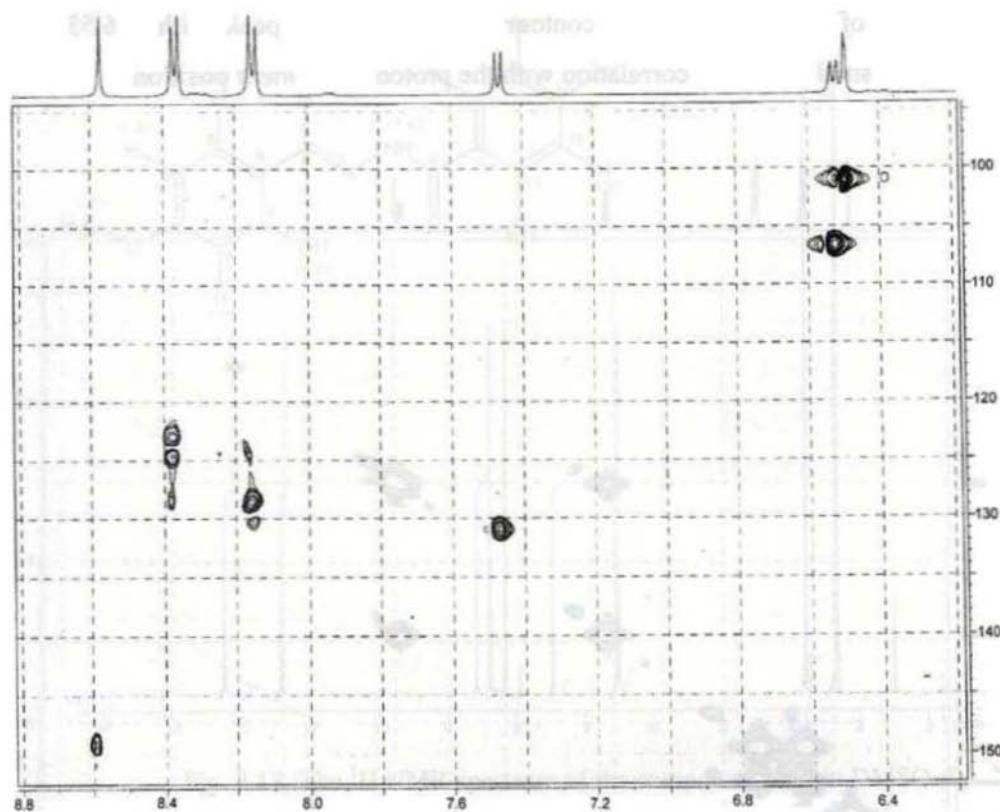


Fig. 2.15. The HSQC correlation spectrum of the compound H_2L^1 in $DMSO-d_6$.

The peak due to the carbonyl carbon C9 at δ 169.8 ppm is very weak and is difficult to distinguish from the noise. This may be due to the following reasons. Firstly, in the solution state, there may be considerable extent of keto-enol tautomerism so that the resonance frequency of carbonyl carbon changes continuously and the peaks are difficult to locate due to the poor solubility of the compound. Secondly, the common spin-lattice relaxation mechanism for ^{13}C results from dipole-dipole interaction with directly attached protons. Thus nonprotonated carbon atoms often have longer relaxation times and give small peaks. Hence carbonyl carbon will give only small peaks and at low concentrated solutions, it may not be detected.

Peaks at δ 55.58, 106.87, 131.32, 101.31, 149.54, 129.24 and 123.91 make contours at ^1H δ values corresponding to 3.77, 6.53, 7.47, 6.49, 8.57, 8.15 and 8.37 ppm respectively and are assigned as C1 (55.58), C3 (106.87), C4 (131.32), C7 (101.31), C8 (149.54), C11 and C15 (129.24), C12 and C14 (123.91).

2.2.3b. Infrared spectrum

Hydrazones can exist in the keto or in the enol tautomeric form in the solid state. In the present case, the absorption due to $\nu(\text{C}=\text{O})$ observed in the 1631-1655 cm^{-1} region confirms that the compound is in the keto form in the solid state. There are two well defined infrared bands at 1655 and 1599 cm^{-1} , which are assigned to the amide I and amide II bands respectively. These bands are shifted to the low frequency region than the theoretical values due to the conjugation of the amide group with the aromatic group. Because of conjugation, the double bond nature of $\text{C}=\text{O}$ decreases and hence the bond order decreases, which causes a shift to the lower frequency region. Amide II band seen at 1599 cm^{-1} points out to the secondary amide exists in the trans conformation, which is confirmed by the crystal structure. A very broad band observed in the region 3000-3500 cm^{-1} comprising of both the $-\text{OH}$ and $-\text{NH}-$ stretching absorptions. Two bands at 1512 and 1472 cm^{-1} are due to the aromatic $\text{C}=\text{C}$ stretching absorptions. It is very difficult to differentiate the bands in the fingerprint region, but a well-defined band at 1221 cm^{-1} may be due to phenolic $\text{C}-\text{O}$ stretching vibration. The characteristic $\nu(\text{C}=\text{N})$ bands of Schiff bases come in the region 1689 – 1471 cm^{-1} . In the present case, it appears as a shoulder to the amide II band nearly at 1550 cm^{-1} .

Electronic spectrum

The electronic spectrum shows two well-defined bands in the UV region and weak absorption in the visible region. The strong bands are at 270-319 and 320-380 nm region. The former is assigned to the $\pi \rightarrow \pi^*$ electronic transitions of the *p*-substituted benzene and the azomethine bonds. The latter one is due to $n \rightarrow \pi^*$ transitions of carbonyl and nitro chromophores. A weak absorption is also observed in the visible region at 440-580 nm range due to the much extended electron delocalization from one to other end of the overall molecule. The UV-vis spectrum of the 10^{-4} M solution of the compound in DMF is shown in Fig. 2.9.

2.3. *N*-2-Hydroxy-4-methoxyacetophenone-*N'*-4-nitrobenzoylhydrazone, H₂L³

The compound *N*-2-hydroxy-4-methoxyacetophenone-*N'*-4-nitrobenzoylhydrazone H₂L³ was prepared from *N*-2-hydroxy-4-methoxyacetophenone and 4-nitrobenzoylhydrazine.

2.1.1. Experimental

Materials

N-2-Hydroxy-4-methoxyacetophenone (Sigma Aldrich), 4-nitrobenzoylhydrazine (Sigma Aldrich) and DMF (S.D. Fine) were used as received.

Synthesis

4-Nitrobenzoylhydrazine (1.852 g, 10 mmol) and *N*-2-hydroxy-4-methoxyacetophenone (1.662 g, 10 mmol) were dissolved in 14 ml DMF. The

solution was heated to boiling for 5 minutes and then is cooled to room temperature and poured into crushed ice containing a little concentrated sulphuric acid. The compound separated as red powder, which was recrystallized from DMF. Yield: 2.45 g (74%). Elemental Anal. Found (Calcd.) (%): C, 58.70 (58.36); H, 5.10 (4.59); N, 12.03 (12.76).

Crystal structure

The molecule crystallizes in the monoclinic crystal system with a space group of $P2_1/n$. The crystal structure of the compound with atom numbering scheme is shown in Fig. 2.16. The crystal data and structure refinement parameters are listed in Table 2.2 and selected bond lengths and bond angles in Table 2.3. The crystal structure confirms the NMR data for the keto form of the compound.

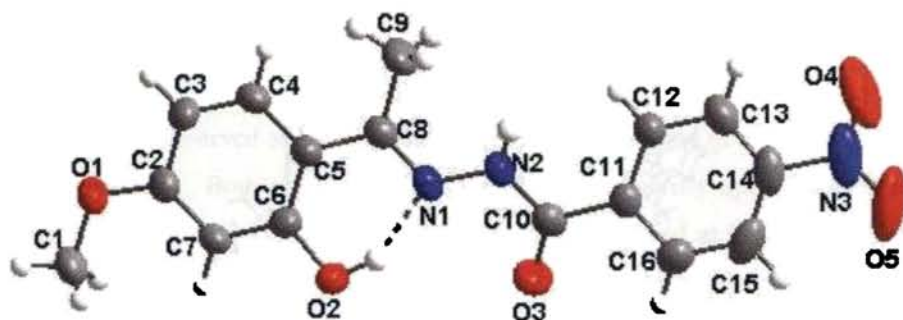


Fig. 2.16. Molecular structure of H_2L^3 . Ellipsoids are shown with 50 % probability. Intramolecular hydrogen bond is shown as dotted line.

The C10—O3 bond length (1.216(3) Å) is very close to the standard C=O double (1.21 Å) than to C—O single bond length (1.43 Å) [36] and C10—N2 bond length (1.350(3) Å) is more close to C—N single (1.47 Å) than to C—N double bond length (1.25 Å). This suggests the keto form of the hydrazone molecule. The C8—N1

bond length is (1.290(3) Å) very much comparable to the corresponding bond length 1.284 Å reported for 2-hydroxyacetophenone nicotinic acid hydrazone [37]. There is a completely extended conformation in the central part of the molecule C5—C8=N1—N2—C10=O2 with an E configuration at the double bond of the hydrazinic bridge. Similar observation was reported in the case of early published hydrazone molecules [28-34]. Contrary to the early reported examples of hydrazones, the angle N2—C10—O3 (122.4(2)°) and C11—C10—O3 (122.3(2)°) are almost equal suggesting that the repulsion between the lone pairs of electrons on N1 and O3 are negligible. An intramolecular hydrogen bonding is observed with O2—H102...N1 (O2—H102 = 0.91(3) Å, H102...N1 = 1.73(3) Å, O2—N1 = 2.546(3) Å, O2—H102...N1 = 148(3)°).

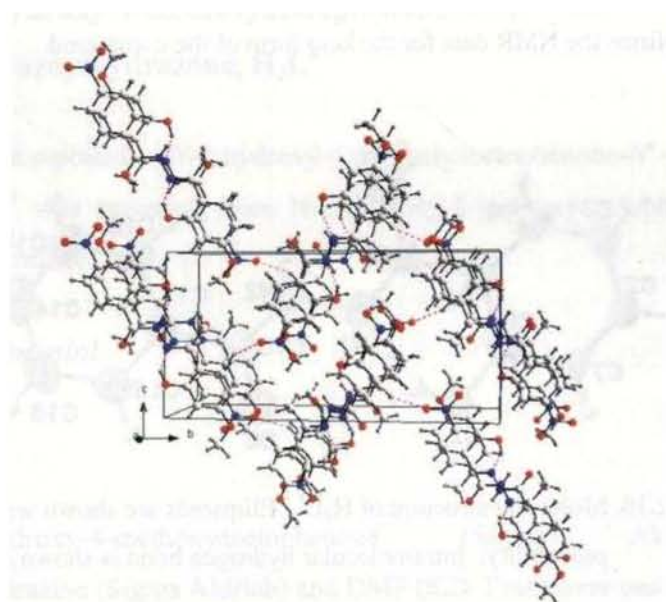


Fig. 2.17. The packing diagram of the compound H_2L^3 in the crystal lattice viewed along 'a' axis. Intramolecular hydrogen bonds and intermolecular C—H... π interactions are shown as dotted lines.

In the crystal lattice (Fig. 2.17), the packing is effected by a weak intermolecular C—H $\cdots\pi$ interaction of C16—H16 \cdots O5. It is rather weak compared to the hydrogen bonding interactions, but plays a key role in the packing pattern of the molecule in the crystal lattice. The packing is in a zigzag fashion with two molecules aligned together as head to tail. There is a pseudo two fold axis is observed, passing through the middle of N2—N3 bond, perpendicular to the plane described by C11, N2, N3 and C12 atom, will be responsible for the stacking of the two phenyl groups.

Spectral studies

NMR spectra

Both one and two dimensional NMR of the compound H_2L^3 were recorded. From this data, the characterization of the compound is possible on the basis of chemical shift, coupling constant and multiplicity and proton-proton connectivity. The 1H NMR spectrum of the compound in DMSO- d_6 is given in Fig. 2.18.

The peaks observed at δ 13.55 and 11.56 ppm are assigned to —OH and —NH protons respectively. Both show significant decrease in intensity upon addition of D_2O , confirms the proposed assignment. The singlets observed at δ 3.88 and 2.49 ppm having an area integral near to three indicate the three equivalent protons in the methoxy group and methyl group respectively. An intense peak observed at 3.55 ppm may be due to the impurity in the solvent, which undergoes a change in intensity and position upon the addition of D_2O . There are two peaks very close to each other at 6.51 and 6.56 ppm. The first one is a singlet and the second one is a doublet, which are assigned to the protons at C7 & C3 respectively. The doublet at δ 7.59 is due to the resonance of proton at C4, which splits into two due to the presence of a neighboring proton at C3. The doublet at δ 8.19 ppm is due to the equivalent protons

at C12 and C16 and that at δ 8.40 ppm is assigned to the equivalent protons at C13 and C15.

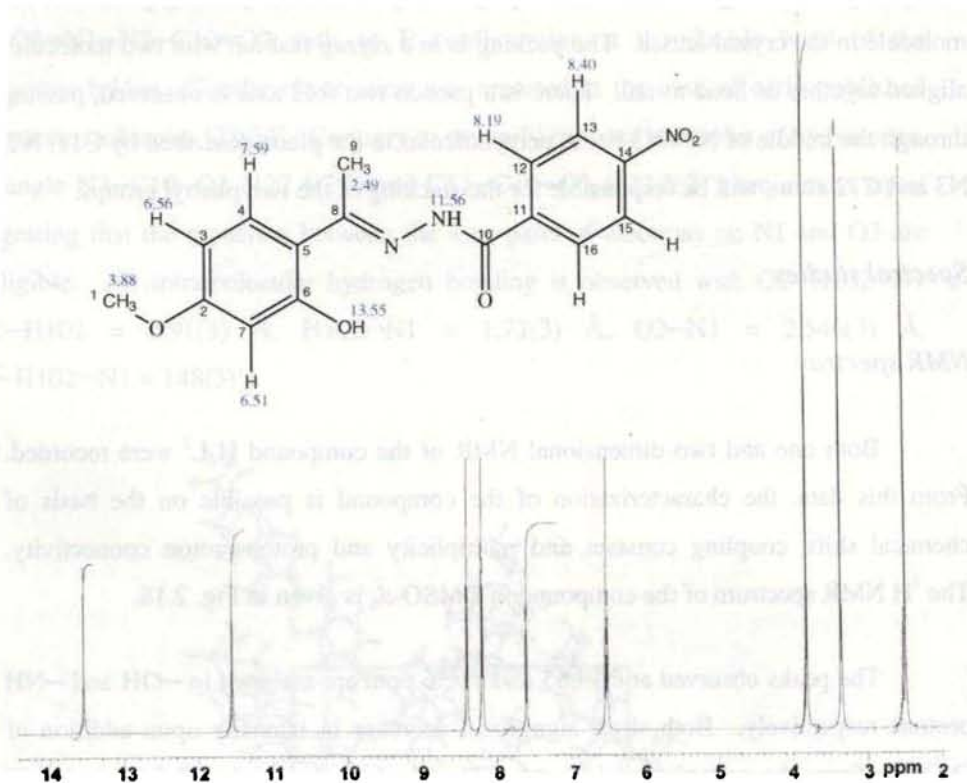


Fig. 2.18. The 1H NMR spectrum of the compound H_2L^3 in $DMSO-d_6$.

The 1H - 1H COSY spectrum and its assignments are shown in Figs. 2.19 and 2.20 respectively. The COSY spectrum confirms the above assignments. Peaks at δ values 13.55, 11.56, 3.88 and 2.49 ppm have no correlation pattern in the COSY, which indicate the absence of interaction of these protons with any other proton. Contours are observed in the aromatic region only. The doublet at δ 6.56 ppm is assigned to C3 proton. In the COSY spectrum, if horizontal and vertical lines are

drawn from δ 6.56 ppm, it will meet the off-diagonal peak at 7.59 ppm, which is assigned to the C4 proton. Similarly the lines from the peak at δ 7.59 ppm will meet the off-diagonal peak at δ 6.56 ppm. This establishes the fact that the proton at C4 splits the peak of C3 proton into two and vice versa. Similarly the peak due to C11 and C15 is split into two by the interaction of protons at C12 and C14 and vice versa.

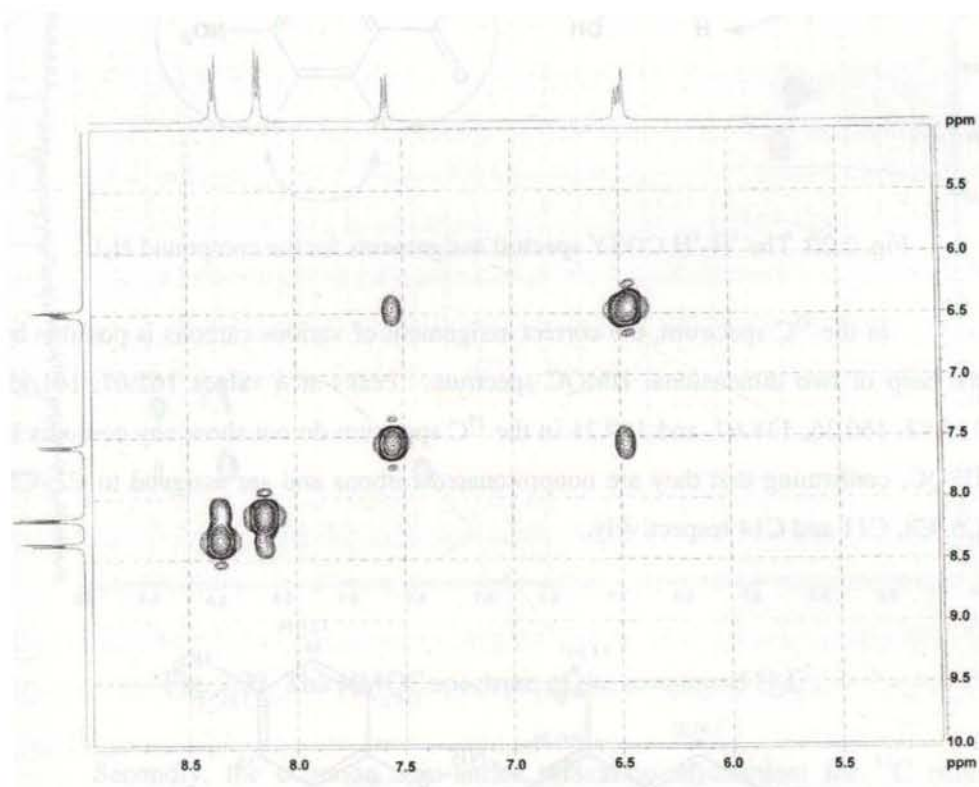


Fig. 2.19. The ^1H - ^1H COSY spectrum of the compound H_2L^3 .

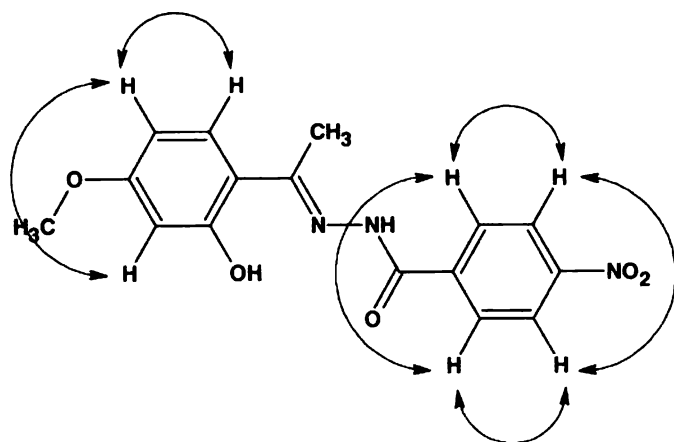


Fig. 2.20. The ^1H - ^1H COSY spectral assignments for the compound H_2L^3 .

In the ^{13}C spectrum, the correct assignment of various carbons is possible by the help of two dimensional HMQC spectrum. Peaks at δ values 162.67, 161.95, 159.93, 160.36, 138.67, and 149.21 in the ^{13}C spectrum do not show any contours in HSQC, confirming that they are nonprotonated carbons and are assigned to C2, C5, C6, C8, C11 and C14 respectively.

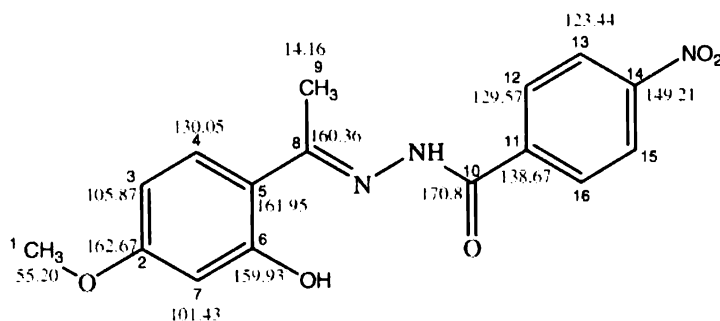


Fig. 2.21. The complete ^{13}C assignment for the compound H_2L^3 .

The peak due to the carbonyl carbon C10 at δ 170.80 ppm is very weak and is difficult to distinguish from the noise. This may be due to the following reasons.

Firstly, in the solution state, there may be considerable extent of keto-enol tautomerism so that the resonance frequency of carbonyl carbon changes continuously and the peaks are difficult to locate due to the poor solubility of the compound.

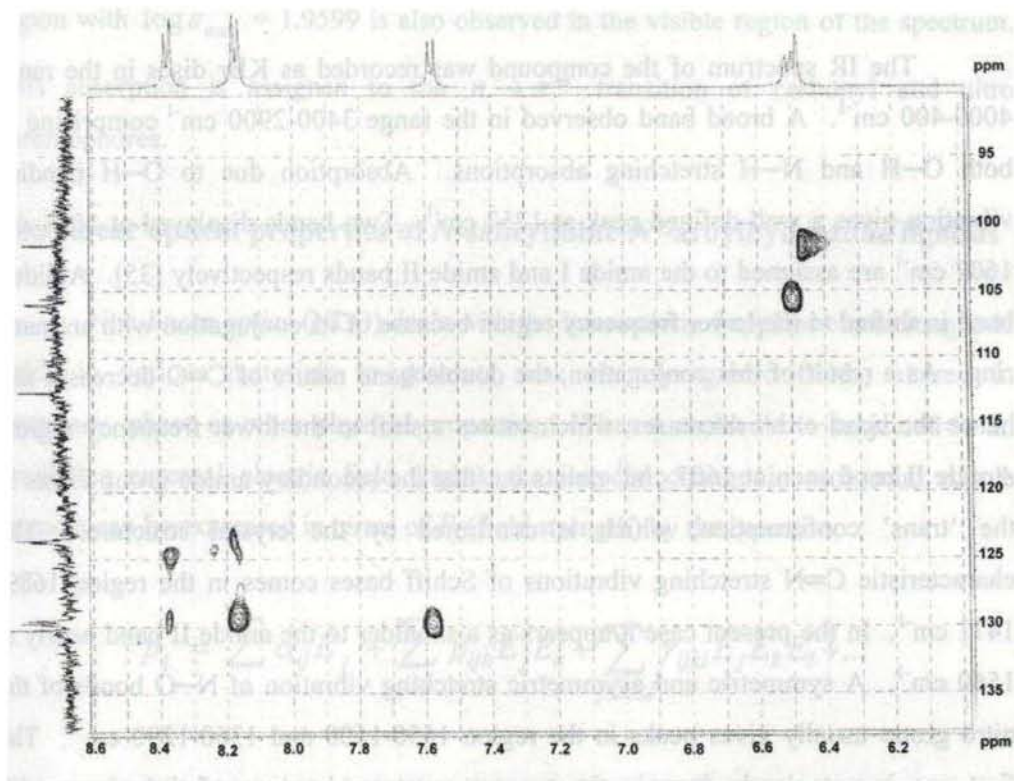


Fig. 2.22. The HMQC spectrum of the compound H_2L^3 .

Secondly, the common spin-lattice relaxation mechanism for ^{13}C results from dipole-dipole interaction with directly attached protons. Thus nonprotonated carbon atoms often have longer relaxation times and give small peaks. Hence carbonyl carbon will give only small peaks and at low concentrated solutions, it may not be detected. From the contours obtained in HMQC, the rest of the carbons are assigned as C1 (δ 55.20), C3 (δ 105.87), C4 (δ 130.05), C7 (δ 101.43), C9 (δ 14.16),

C12 (δ 129.57) and C13 (δ 123.44 ppm). The complete ^{13}C assignment and the HMQC spectrum are shown in Figs. 2.21 and 2.22 respectively

IR spectrum

The IR spectrum of the compound was recorded as KBr discs in the range 4000-400 cm^{-1} . A broad band observed in the range 3400-2900 cm^{-1} comprising of both O—H and N—H stretching absorptions. Absorption due to O—H bending vibration gives a well-defined peak at 1257 cm^{-1} . Two bands displayed at 1688 and 1607 cm^{-1} are assigned to the amide I and amide II bands respectively [35]. Amide I band is shifted to the lower frequency region because of its conjugation with aromatic ring. As a result of this conjugation, the double bond nature of C=O decreases and hence the bond order decreases, which causes a shift to the lower frequency region. Amide II band seen at 1607 cm^{-1} points out that the secondary amide group exists in the 'trans' conformation, which is confirmed by the crystal structure. The characteristic C=N stretching vibrations of Schiff bases comes in the region 1689-1471 cm^{-1} . In the present case it appears as a shoulder to the amide II band nearly at 1560 cm^{-1} . A symmetric and asymmetric stretching vibration of N—O bonds of the nitro group usually gives peaks in the region 1550-1500 and 1360-1290 cm^{-1} . The first one is not clearly seen in the present spectrum because of the presence of aromatic stretching absorptions, but the second one displays as a sharp band at 1346 cm^{-1} . The C—N stretching of aromatic nitro compound cannot be assigned in the fingerprint region due to the crowding of bands.

Electronic spectrum

The electronic spectrum of the compound was recorded in solution state by dissolving in DMF and is shown in Fig. 2.22. Two strong bands in the region 260 –

290 nm are observed with $\log \epsilon_{\max}$ values 2.7075 and 2.6135 respectively. These two bands may be due to the $\pi \rightarrow \pi^*$ absorptions of the *p*-substituted benzene rings and the azomethine bond. There is a weak and broad absorption in the 420 – 540 nm region with $\log \epsilon_{\max} = 1.9599$ is also observed in the visible region of the spectrum. This absorption is assigned to the $n \rightarrow \pi^*$ transition of carbonyl and nitro chromophores.

Non-linear optical properties of *N*-salicylidine-*N'*-aroylhydrazone ligands

Non-linear optics (NLO) deals with the interaction of applied electromagnetic fields in various materials to generate new electromagnetic fields, altered in frequency, phase or other physical properties. When a molecule is subjected to an oscillating external electric field (light), the induced change in molecular dipole moment can be expressed in terms of E_j (field strength) by the equation,

$$p_i = \sum_j \alpha_{ij} E_j + \sum_{j \leq k} \beta_{ijk} E_j E_k + \sum_{j \leq k \leq l} \gamma_{ijkl} E_j E_k E_l + \dots$$

Where p_i is the electronic polarization induced along the i^{th} molecular axis, α is the linear polarizability, β is the quadratic hyperpolarizability and γ is the cubic hyperpolarizability [38-41].

α is a second rank tensor and is responsible for the linear optical behavior. β and γ relates the polarization to the square and cube of the field strength and are third and fourth rank tensors respectively. They are responsible for second order and third order non-linear optical (NLO) properties. For small fields β and γ can be neglected, so that the induced polarization is proportional to the strength of the applied field.

However when an intense electric field such as laser pulse is used, β and γ become significant. Among second order optics, frequency doubling (second harmonic generation), frequency mixing, and electro-optic pockel effects (linear change in the index of refraction) etc are the main types.

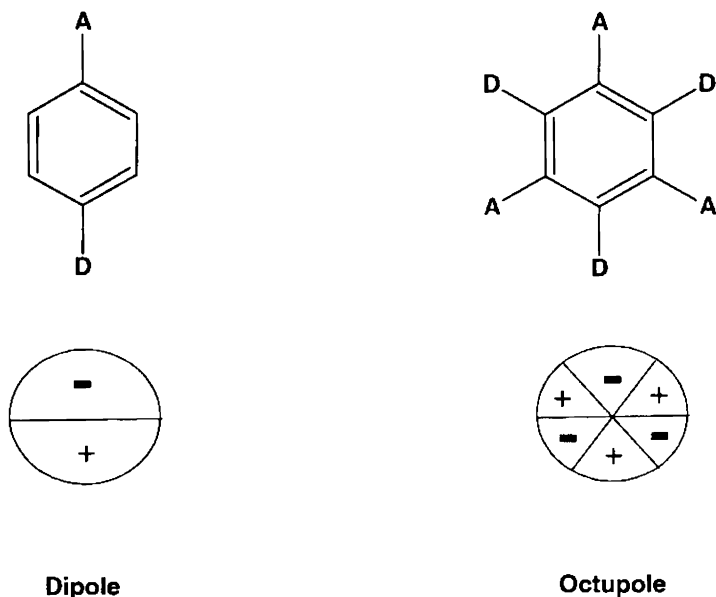
Materials for second order non-linear optics

On the basis of the quantum mechanical 'sum over states' (SOS) perturbation theory for the description of molecular polarization, it is concluded that the simple prescription for second order NLO molecular materials is 'the existence of strong intramolecular charge transfer excitations in a non centrosymmetric molecular environment'. This can be satisfied by considering a polarizable molecular system having an asymmetric charge distribution, such as the prototypical *p*-nitroaniline molecule. Almost all successful strategies for obtaining second order NLO dipolar organic molecules and metal complexes have been developed within a simple molecular scheme formed by a D- π -A structure, and the design of second order NLO chromophores has focused primarily on engineering the electronic nature of the donor and acceptor, and the conjugation length of the bridge.

In addition to these, octupolar molecules are also having NLO activity. These are non-dipolar species whose second order NLO is related to multidirectional charge transfer excitations.

Metal coordination has been used in several ways to improve the behavior of all organic push – pull chromophores for applications in second order non-linear optics. The most common approach is the use of metal coordinated fragments attached at the end of organic π conjugated systems: proper choice of the metal and its oxidation state and of the ligands allows the fragment to behave as an electron donor

or acceptor group [42]. Another possibility is using metals as conjugation bridges along a push pull organic system. In that case, the choice of metals that give planar coordination geometry may force a coplanar arrangement of the organic skeleton, so improving conjugation and possibly NLO properties [43-44].



N-Aroyl-*N*-salicylidene hydrazine metal complexes and their adducts [45-46] with monodentate neutral Lewis bases have been studied for their biological and magnetic properties. Here the organic tridentate ligands have been properly functionalized with strong electron donor-acceptor groups, making them potential interest in second order NLO. These compounds have some peculiarities with respect to this above described approaches for generating NLO active metal coordinated materials. First of all the ligands alone are not expected to show a high NLO activity because their electronic structure should be in the keto form with rather low

conjugation from the dialkyl amino or methoxy donor to the nitro acceptor group. The existence of keto tautomeric forms in the solid state has been confirmed by the single crystal X-ray diffraction studies. Upon coordination to the metal, the electronic structure of the ligand changes to the enolic form with increase in the conjugation and hence in NLO activity is expected.

The non-linear optical properties of all the three ligands were studied in powder form by Hyper Rayleigh scattering technique. The well powdered sample was filled in capillary tube having 0.8 mm thickness. The NLO responses of these samples were recorded using urea as the reference, filled in similar capillary tube. The experimental arrangement for the non-linear optical properties utilizes a Quanter A DCR II Nd /YAG laser with 9 mJ a pulse at a repetition rate of 5 Hz. The selected wavelength is 1064 nm. After the selection of the wavelength the laser beam is split in to two parts, one to generate the second harmonic signal in the sample and the other to generate second harmonic signal in the reference (urea). An output signal of 532 nm was measured in a 90° geometry using urea as the standard. The efficiency of the NLO activity of the compounds are expressed in percentage as

$$\text{Efficiency} = \frac{\text{Signal of Sample}}{\text{Signal of Urea}} \times 100\%$$

As expected from the electronic structure of the compounds, they showed a very mild SHG efficiency, when compared with the reference compound urea. Comparing the three ligands, the second one, *N*-2-hydroxy-4-methoxy benzaldehyde-*N'*-4-nitrobenzoylhydrazone, H₂L², gave considerable activity. It has about 10 % efficiency of that of urea. This may be due to the presence of a small fraction of keto tautomeric form in the ligand sample. In the case of the other two ligands, H₂L¹ and H₂L³ the activity was negligible.

References

1. A.S.N. Murthy, A.R. Reddy, Proc. Indian Acad. Sci. Chem. Sci. 90 (1981) 519.
2. D.K. Johnson, M.J. Pippard, T.B. Murphy, N.J. Rose, J. Pharmacol. Exp. Ther. 221 (1982) 399.
3. P. Ponka, J. Barova, J. Neuwirt, O. Fuchs, E. Necas, Biochim. Biophys. Acta 586 (1979) 278.
4. J.R. Dimmock, G.B. Baker, W.G. Taylor, Can. J. Pharm. Sci. 7 (1972) 100.
5. J. Patole, U. Sandbhor, S. Padhye, D.N. Deobagkar, C.E. Anson, A. Powell, Bioorg. Med. Chem. Lett. 13 (2003) 51.
6. L. Streyer, Biochemistry; Freeman: New York, (1995).
7. V. Razakantoanina, P.P. Nguyen Kim, G. Jaureguiberry, Parasitol Res. 86 (2000) 665.
8. R.E. Royer, L.M. Deck, T.J.V. Jagt, F.J. Martinez, R.G. Mills, S. Young, A.D.L.V. Jagt, J. Med. Chem. 38 (1995) 2427.
9. M.R. Flack, R.G. Pyle, N. Mullen, M.B. Lorenzo, Y.W. Wu, R.A. Knazek, B.C. Nuzule, M.M. Reidenberg, J. Clin. Endocrinol. Metab. 76 (1993) 1019.
10. R. Baumgrass, M. Weiwad, F. Edmann, J. Biol. Chem. 276 (2001) 47914.
11. P.J.E. Quintana, A. de Peyster, S. Klatzke, H.J. Park, Toxicol. Lett. 117 (2000) 85.
12. T.M. Devlin, Textbook of Biochemistry with Clinical correlations; Wiley: New York (1997) 449.
13. J.I. Bullock, H.A. Tajmir-Riahi, Inorg. Chim. Acta 38 (1980) 141.
14. P.B. Sreeja, M.R.P. Kurup, A. Kishore, C. Jasmin, Polyhedron 23 (2004) 575.
15. P.B. Sreeja, M.R.P. Kurup, Spectrochim. Acta 61A (2005) 331.
16. C. Pelizzi, G. Pelizzi, J. Chem. Soc., Dalton Trans. (1980) 1970.
17. D.K. Johnson, T.B. Murphy, N.J. Rose, W.H. Goodwin, L. Pickart, Inorg. Chim. Acta 67 (1982) 159.

18. S. Patel, A.D. Sawant, *Indian J. Chem. Technol.* 8 (2001) 88.
19. K.H. Reddy, K.B. Chandrasekhar, *Indian J. Chem.* 40A (2001) 727.
20. R. Sumita, D.D. Mishra, R.V. Maurya, N. Nageswara, *Polyhedron* 16 (1997) 1825.
21. M.F. Iskander, T.E. Khalil, R. Werner, W. Haase, I. Svoboda, H. Fuess, *Polyhedron* 19 (2000) 1181.
22. S.C. Chan, L.L. Koh, P.-H. Leung, J.D. Ranford, K.Y. Sim, *Inorg. Chim. Acta* 236 (1995) 83.
23. A.S. Fouda, M.M. Gouda, S.I.A. El-Rahman, *Bull. Korean Chem. Soc.* 21 (2000) 1085.
24. W. Chiang, M.E. Thompson, D. VanEngen, J.W. Perry, *Spec. Publ. R. Soc. Chem.* 91 (1991) 210.
25. B.N. Bessy Raj, M.R.P. Kurup, E. Suresh, *Struct. Chem.* 17 (2006) 201.
26. B.N. Bessy Raj, M.R.P. Kurup, Unpublished data.
27. F. Carati, U. Caruso, R. Centore, W. Marcolli, A. De Maria, B. Panunzi, A. Roviello, A. Tuzi, *Inorg. Chem.* 41 (2002) 6597.
28. X.-X. Xu, X.-Z. You, Z.-F. Sun, X. Wang, H.-X. Liu, *Acta Cryst. C*50 (1994) 1169.
29. Z.-L. Lu, C.-Y. Duan, Y.-P. Tian, X.-Z. You, H.-K. Fun, K. Sivakumar, *Acta Cryst. C*52 (1996) 1507.
30. S.-H. Liu, X.-F. Chen, Y.-H. Xu, X.-Z. You, W. Chen, Z. Arifin, *Acta Cryst. C*54 (1998) 1919.
31. L.-H. Huo, S. Gao, H. Zhao, J.-G. Zhao, S.M. Zain, S.W. Ng, *Acta Cryst. E*60 (2004) o1538.
32. Z.-L. Lu, B.-S. Kang, H.-K. Fun, I.B. Razak, K. Chinnakali, *Acta Cryst. C*55 (1999) 89.
33. S.S.S. Raj, H.-K. Fun, Z.-L. Lu, W. Xiao, X.Y. Gong, C.-M. Gen, *Acta Cryst. C*56 (2000) 1013.

34. J.-P. Souran, M. Quarton, *Acta Cryst.* C51 (1995) 2179.
35. R.M. Silverstein, G.C. Bassler, T.C. Morrill, *Spectrometric Identification of Organic Compounds*, fourth ed., Wiley, New York, 1981.
36. J.E. Huheey, E.A. Keiter, R.L. Keiter, *Inorganic Chemistry, Principles of Structure and Reactivity*, 4th ed., Harper Collins College Publishers, New York, 1993.
37. P.B. Sreeja, A. Sreekanth, C.R. Nayar, M.R.P. Kurup, A. Usman, I.A. Razak, S. Chandrapromma, H.-K. Fun, *J. Mol. Struct.* 645 (2003) 221.
38. N.P. Prasad, D.J. Williams, *Introduction to Non-linear Optical Effects in Molecules and Polymers*, Wiley, New York, 1991.
39. S.R. Marder, J.E. Sohn, G.D. Stucky, *Materials for Non-linear Optics, Chemical Perspectives*, ACS Symposium Series 455, American Chemical Society, Washington DC, 1991.
40. H.S. Nalwa, S. Miyata, *Non-linear Optics of Organic Molecules and Polymers*, eds. CRC Press, Boca Raton, FL, 1997.
41. R.W. Boyd, *Non-linear Optics*, Academic Press, New York, 1992.
42. I.R. Whittal, A.M. McDonagh, M.G. Humphrey, M. Samoc, *Adv. Organomet. Chem.* 42 (1998) 291.
43. J. Buey, S. Coco, L. Diez, P. Espinet, J.M. Martin Alvarez, J.A. Miguel, S. Garcia-Granda, A. Tesoro, I. Ledoux, J. Zyss, *J. Organometallics* 17 (1998) 1750.
44. R. Centore, B. Panunzi, A. Roviello, A. Tuzi, *Acta Cryst.* C58 (2002) m26.
45. M. Kato, Y. Muto, *Coord. Chem. Rev.* 92 (1988) 45.
46. S.A. Warda, P. Dahlke, S. Wocadlo, W. Massa, C. Friebel, *Inorg. Chim. Acta* 268 (1998) 117.

Table 2.1

Crystal data and structure refinement for $H_2L^1 \cdot H_2O$ and $H_2L^2 \cdot H_2O$

| Parameters | $H_2L^1 \cdot H_2O$ | $H_2L^2 \cdot H_2O$ |
|---|---|---|
| Empirical formula | $C_{18}H_{22}N_4O_5$ | $C_{15}H_{15}N_3O_6$ |
| Formula weight | 374.40 | 333.30 |
| Crystal system | Monoclinic | Triclinic |
| Space group | $C2/c$ | $P-1$ |
| Unit cell dimensions | | |
| a (Å) | 38.13(8) | 6.721(6) |
| b Å | 7.519(16) | 7.009(6) |
| c (Å) | 12.47(3) | 16.839(14) |
| α (°) | 90.00(3) | 78.103(13) |
| β (°) | 95.25(3) | 80.585(13) |
| γ (°) | 90.00(4) | 78.125(13) |
| Volume V (Å ³), Z | 3560(14), 8 | 753.5(11), 2 |
| Calculated density (ρ) (Mg m ⁻³) | 1.397 | 1.469 |
| Absorption coefficient μ (mm ⁻¹) | 0.104 | 0.116 |
| F (000) | 1584 | 348 |
| Crystal size (mm ³) | 0.30 x 0.23 x 0.05 | 0.16 x 0.10 x 0.07 |
| θ range for data collection | 2.76 - 25.00 | 1.28 - 28.48 |
| Index ranges | $-45 \leq h \leq 45, -8 \leq k \leq 8,$ $-14 \leq l \leq 14$ | $-8 \leq h \leq 8, -9 \leq k \leq 9,$ $-22 \leq l \leq 22$ |
| Reflections collected / unique | 11752 / 3125 [R(int) = 0.0807] | 6316 / 3357 [R(int) = 0.0174] |
| Refinement method | Full-matrix least-squares on F^2 | Full-matrix least-squares on F^2 |
| Data / restraints / parameters | 3125 / 0 / 259 | 3357 / 0 / 277 |
| Goodness-of-fit on F^2 | 1.033 | 1.025 |
| Final R indices [$I > 2\sigma(I)$] | $R_1 = 0.0730,$ $wR_2 = 0.1871$ | $R_1 = 0.0483,$ $wR_2 = 0.1279$ |
| R indices (all data) | $R_1 = 0.1096,$ $wR_2 = 0.2086$ | $R_1 = 0.0582,$ $wR_2 = 0.1386$ |

| Table 2.2 Crystal data and structure refinement for H_2L^3 | |
|---|---|
| Parameters | H_2L^3 |
| Empirical formula | $\text{C}_{16}\text{H}_{15}\text{N}_3\text{O}_5$ |
| Formula weight | 329.31 |
| Crystal system | Monoclinic |
| Space group | $P2_1/n$ |
| Unit cell dimensions | |
| a (Å) | 7.3343(9) |
| b Å | 20.3517(9) |
| c (Å) | 10.1375(5) |
| α (°) | 90.00 |
| β (°) | 95.735(7) |
| γ (°) | 90.00 |
| Volume V (Å ³), Z | 1505.6(2), 4 |
| Calculated density (ρ) (Mg m ⁻³) | 1.453 |
| Absorption coefficient μ (mm ⁻¹) | 0.110 |
| F (000) | 688 |
| Crystal size (mm) | 0.35 x 0.20 x 0.15 |
| θ range for data collection | 2.00 – 24.97° |
| Index ranges | $0 \leq h \leq 8, 0 \leq k \leq 24, -12 \leq l \leq 11$ |
| Reflections collected / unique | 2820 / 2615 [R(int) = 0.0165] |
| Refinement method | Full-matrix least-squares on F^2 |
| Data / restraints / parameters | 2615 / 0 / 228 |
| Goodness-of-fit on F^2 | 1.015 |
| Final R indices [$I > 2\sigma(I)$] | $R_1 = 0.0469, wR_2 = 0.1109$ |
| R indices (all data) | $R_1 = 0.1244, wR_2 = 0.1326$ |

Table. 2.3. Selected bond lengths (Å) and bond angles (°) of H₂L¹·H₂O, H₂L², H₂L³.

| Bonds | | Bonds | |
|--|----------|--|------------|
| H₂L¹·H₂O | | H₂L²·H₂O | |
| C9–O1 | 1.338(4) | C6–O2 | 1.350(2) |
| C8–C11 | 1.433(5) | C5–C8 | 1.450(2) |
| C11–N2 | 1.267(4) | C8–N1 | 1.278(2) |
| N2–N3 | 1.378(4) | N1–N2 | 1.384(1) |
| C12–N3 | 1.324(4) | C9–N2 | 1.338(2) |
| C12–O2 | 1.219(5) | C9–O3 | 1.232(2) |
| C12–C13 | 1.485(5) | C10–C9 | 1.501(2) |
| Bond angles | | Bond angles | |
| O1–C9–C8 | 121.8(3) | O2–C6–C5 | 123.21(15) |
| C8–C11–N2 | 121.9(3) | C5–C8–N1 | 122.89(16) |
| C11–N2–N3 | 115.4(3) | C8–N1–N2 | 114.95(15) |
| N2–N3–C12 | 119.1(3) | N1–N2–C9 | 120.59(15) |
| N3–C12–O2 | 122.8(3) | N2–C9–O3 | 124.66(15) |
| O2–C12–C13 | 120.3(3) | O3–C9–C10 | 120.47(15) |

| Bonds | H₂L³ |
|--------------------|-----------------------------------|
| C6–O2 | 1.355(3) |
| C5–C8 | 1.467(3) |
| C8–N1 | 1.290(3) |
| N1–N2 | 1.383(3) |
| C10–N2 | 1.350(3) |
| C10–O3 | 1.216(3) |
| C10–C11 | 1.495(3) |
| Bond angles | |
| O2–C6–C5 | 122.3(2) |
| C5–C8–N1 | 116.0(2) |
| C8–N1–N2 | 119.6(2) |
| N1–N2–C10 | 118.6(2) |
| N2–C10–O3 | 122.4(2) |
| O3–C10–C11 | 122.3(2) |

CHAPTER THREE

Syntheses, characterization and non-linear optical properties of copper(II) complexes of the aroylhydrazone ligands

Copper, the name came from the Latin word '*cuprum*' meaning '*from the island of cyprus*', is the most ancient and one of the most abundant elements in earth's crust. Compared to the other coinage metals silver and gold, copper is more reactive and its coordination chemistry has become a diverse field of interest, which intersects with many other research domains [1-10]. Copper coordination chemistry finds a wide range of applications in the field of biological activity. Schiff base Cu(II) complexes especially of thiosemicarbazones present a great variety of biological activity ranging from antitumoral [11-12], fungicide [13], bactericide [14] and anti-inflammatory [15]. Coming to aroylhydrazones, the discovery that salicylaldehyde benzoylhydrazone inhibits DNA synthesis and cell growth [16-17] led to their investigation of metal complexes. Surprisingly the Cu(II) complex was shown to be significantly more potent than the metal free chelate, leading to the suggestion that the metal complex was the biologically active species. Because of the biological interest in this type of chelate system, several structural studies have been carried out on copper with this ligand and analogues [18-22]. Acylhydrazones of salicylaldehyde subsequently attracted attention. Salicylaldehyde acetylhydrazone displays radio protective properties, and a range of acylhydrazones has been shown to be cytotoxic, the Cu complexes again showing enhanced activity.

Metal complexes of late transition metals are better choices for non-linear optical materials because they are the best to provide metal to ligand charge transfer

transitions and hence enhance the electron delocalization mechanism in the ligands [23-25]. Surely our attention went to copper(II), since it is the most extensively studied and a typical transition metal ion in respect of the formation of coordination complexes, but less typical in its reluctance to take up a regular octahedral or tetrahedral stereochemistry. Copper can form metal complexes with different stereochemistries depending on the ligand field effects. Nine new copper(II) complexes of the three aroylhydrazone ligands are synthesized and characterized by various physico-chemical techniques. The stereochemistry of these copper(II) complexes along with syntheses and characterization are covered here in detail.

3.1. Stereochemistry

The $3d^9$ outer electronic configuration of the copper(II) ion lacks cubic symmetry and hence yields distorted forms of the basic stereochemistries. The coordination numbers of four, five and six predominate [26], but variations of each structure occur through bond length or bond angle distortions. In a cubic environment, d^9 configuration is subject to distortion, called Jahn-Teller distortion, because it is an electronically degenerate state [27]. The extent of distortion may lead the stereochemistry of the resulting metal complex to structures ranging from distorted octahedron to square coplanar i.e., compressed and elongated octahedrons, square pyramidal, trigonal bipyramidal, and square planar structures. The structure of complexes also depends on the nature of ligands involved in coordination. Tridentate dibasic Schiff bases are excellent ligands in forming dinuclear species of metal ions, which prefer square planar geometry. Aroylhydrazones of *ortho*-hydroxy aldehydes used here are such species and provide a phenolic -OH, an imine -N and an amide -O as coordinating centers. In a dinuclear complex either the phenolate -O or the deprotonated amide -O can act as the bridging atom. It has been found earlier that in a

situation similar to this the most negatively charged center is preferred as the bridging atom in the dinuclear copper(II) complexes.

3.2. Experimental

3.2.1. Materials

4-Nitrobenzoyl hydrazide (Sigma Aldrich), 4-*N,N*-diethylamino-2-hydroxybenzaldehyde (Sigma Aldrich), 4-methoxy-2-hydroxybenzaldehyde (Sigma Aldrich), 4-methoxy-2-hydroxyacetophenone (Sigma Aldrich), Cu(OAc)₂·H₂O (Qualigens), pyridine, 4-picoline, DMF (S.D. Fine) were used as received. When ethyl alcohol was used as the solvent repeated distillation was carried out before use.

3.2.2. Syntheses of ligands

The ligands H₂L¹, H₂L² and H₂L³ were synthesized as described in Chapter 2.

3.2.3. Preparation of copper(II) complexes

[CuL¹]₂·H₂O (**1**): The complex was prepared by refluxing a mixture of equimolar amounts of the ligand H₂L¹ (0.355 g, 1 mmol) and Cu(OAc)₂·H₂O (0.199 g, 1 mmol) in a 1:1 mixture of absolute ethanol and DMF. The reddish brown colored product obtained on cooling the reaction mixture to room temperature was filtered, washed several times with absolute ethanol followed by diethyl ether and dried over P₄O₁₀ *in vacuo*. Yield: 0.590 g (68.9%). Elemental Anal. Found (Calcd.) (%): C, 50.36 (50.52); H, 4.29 (4.71); N, 13.06 (13.09).

[CuL¹py]·H₂O (**2**): The complex was prepared by dissolving 0.200 g (0.23 mmol) of complex **1** in 15 ml of boiling pyridine and again boiled for 5 minutes. The

solution was then added to water and the brown colored solid formed was recovered by filtration. Washed several times with absolute ethanol followed by diethyl ether and dried over P_4O_{10} *in vacuo*. Yield: 0.155 g (77.5%). Elemental Anal. Found (Calcd.) (%): C, 53.44 (53.64); H, 4.78 (4.89); N, 13.04 (13.60).

$[CuL^1pi]$ (3): 0.200 g (0.23 mmol) of the complex 1 was dissolved in 15 ml of boiling 4-picoline for 5 minutes and after cooling the solution was added to cold water. The dark red colored product obtained was filtered, washed several times with absolute ethanol followed by diethyl ether and dried over P_4O_{10} *in vacuo*. Yield: 0.148 g (74%). Elemental Anal. Found (Calcd.) (%): C, 56.42 (56.41); H, 4.47 (4.93); N, 13.39 (13.70).

$[CuL^2]_2 \cdot 3/2 H_2O$ (4): A mixture of the ligand H_2L^2 (0.315 g, 1 mmol) and $Cu(OAc)_2 \cdot H_2O$ (0.199 g, 1 mmol) was refluxed in a 1:1 mixture of absolute ethanol and DMF. The red product obtained was filtered and washed several times with absolute ethanol followed by diethyl ether and dried over P_4O_{10} *in vacuo*. Yield: 0.398 g (76.1%). Elemental Anal. Found (Calcd.) (%): C, 45.98 (46.16); H, 2.75 (3.23); N, 10.81 (10.77).

$[CuL^2py]$ (5): After dissolving 0.200 g (0.26 mmol) of complex 4 in 15 ml boiling pyridine, the solution was boiled for about 5 minutes and poured the cooled solution to cold water, so that a red colored product was obtained. It was filtered, washed several times with absolute ethanol followed by diethyl ether and dried over P_4O_{10} *in vacuo*. Yield: 0.135 g (67.5%). Elemental Anal. Found (Calcd.) (%): C, 52.70 (52.69); H, 3.28 (3.53); N, 12.19 (12.29).

$[CuL^2pi]$ (6): The complex was prepared by dissolving 0.200 g (0.26 mmol) of complex 4 in 15 ml boiling 4-picoline and refluxed for about 5 minutes. After cooling the solution was poured to cold water and the red colored product obtained

was filtered, washed several times with absolute ethanol followed by diethyl ether and dried over P_4O_{10} *in vacuo*. Yield: 0.126 g (63.2%). Elemental Anal. Found (Calcd.) (%): C, 53.66 (53.67); H, 3.73 (3.86); N, 11.87 (11.92).

$[CuL^3]_2 \cdot \frac{1}{2} H_2O$ (7): The ligand H_2L^3 (0.329 g, 1 mmol) and $Cu(OAc)_2 \cdot H_2O$ (0.199 g, 1 mmol) were dissolved in a 1:1 mixture of absolute ethanol and DMF and refluxed for about two hours. The bright red colored product obtained was filtered, washed several times with absolute ethanol followed by diethyl ether and dried over P_4O_{10} *in vacuo*. Yield: 0.324 g (61.3%). Elemental Anal. Found (Calcd.) (%): C, 48.62 (48.61); H, 3.21 (3.44); N, 10.67 (10.63).

$[CuL^3py]$ (8): 0.200 g (0.25 mmol) of the complex 7 was dissolved in 15 ml of boiling pyridine for 5 minutes and after cooling the solution was added to cold water. The red colored product obtained was filtered, washed several times with absolute ethanol followed by diethyl ether and dried over P_4O_{10} *in vacuo*. Yield: 0.114 g (56.9%). Elemental Anal. Found (Calcd.) (%): C, 53.41 (53.67); H, 3.70 (3.86); N, 11.87 (11.92).

$[CuL^3pi]$ (9): The complex was prepared by dissolving 0.200 g (0.25 mmol) of complex 7 in 15 ml of boiling 4-picoline and again boiled for 5 minutes. The solution was then added to water and the red colored solid formed was recovered by filtration. Washed several times with absolute ethanol followed by diethyl ether and dried over P_4O_{10} *in vacuo*. Yield: 0.122 g (61.2%). Elemental Anal. Found (Calcd.) (%): C, 54.65 (54.60); H, 4.11 (4.17); N, 11.52 (11.58).

3.3. Results and discussion

From the elemental analyses data of the copper complexes, it is clear that the reaction between equimolar amounts of the ligands and metal salts yield a chance of dimeric or polymeric form of the complexes, in which each copper centre is in a four coordinated environment. An attempt to incorporate the heterocyclic bases in to the complex was done by preparing the complex directly in presence of the required heterocyclic base as reported earlier [28-32], but it was not successful. So such a method was adopted to boil the dimeric precursor in excess of heterocyclic bases such as pyridine and picoline, and the attempt was successful.

The complexes prepared have different shades of red from light red to brown. All were soluble in DMF and DMSO, but only slightly soluble in other organic solvents like ethanol, methanol, chloroform etc. The magnetic susceptibility values for each copper centre of all the complexes were found to be within the range of 1.5 – 2.0 BM which was expected for a copper centre having d^9 configuration.

3.3.1 Crystal structure of complexes

3.3.1a. Crystal structure of $[\text{CuL}^1]_2$ (1)

The single crystal X-ray diffraction studies revealed a polymeric structure for the compound $[\text{CuL}^1]_2$ (1) (Fig. 3.1), in which each monomeric unit is almost symmetrical with respect to an inversion centre. The molecule crystallizes in a triclinic lattice with a space group of $P\bar{1}$. The structural refinement parameters are given in Table 3.1 and the selected bond lengths and bond angles are given in Tables 3.2 and 3.3. The tridentate dianionic ligand molecules are bonded to the copper centre through deprotonated enolic oxygen O1, azomethine nitrogen N2 and deprotonated

phenolic oxygen O2 forming a six membered Cu1–O2–C14–C9–C8–N2 and a five membered O1–C7–N1–N2–Cu1 chelate rings. The same copper centre is coordinated to the enolic oxygen O1 and phenolic oxygen O2 of two different ligand molecules. As a result, each copper atom is in a five coordinated environment. The enolization of the ligand molecule is confirmed by the increase in bond length C7–O1 (1.304(9) Å) and decrease in C7–N1 bond length (1.309(9) Å), from the corresponding bond lengths in the free ligand 1.219(5) Å and 1.324(5) Å [27]. Coordination through the azomethine nitrogen is confirmed by the increase in N1–N2 bond length to 1.392(8) Å from the corresponding bond in the ligand 1.378(4) Å.

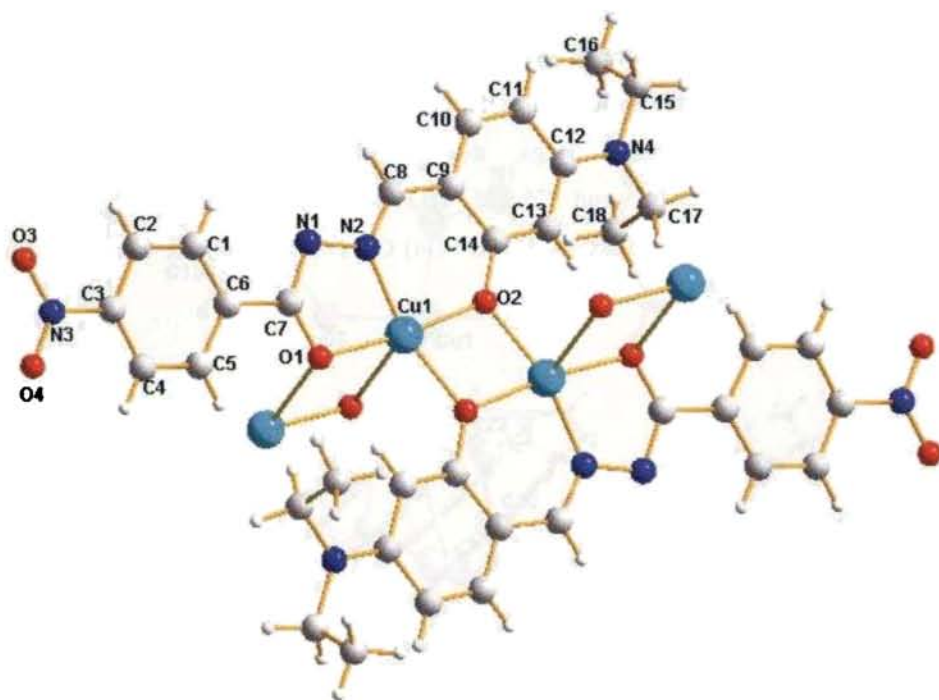


Fig. 3.1. Molecular structure of $[\text{CuL}^1]_2$ (1). The atoms are shown at 50% probability.

Similarly the coordination through the phenolic oxygen O2 is confirmed by the increase in C14–O2 bond length 1.340(9) Å from 1.338(4) Å in the ligand. From the bond angles, it can be concluded that in the crystal lattice, the coordination around the copper atom is distorted square pyramidal, in which the deprotonated enolic oxygen, deprotonated phenolic oxygen and the azomethine nitrogen of one ligand molecule and the deprotonated phenolic oxygen of a second ligand molecule develop the basal plane of the pyramid, while the deprotonated enolic oxygen of a third ligand molecule forms the apex.

In the packing diagram of the molecule (Fig. 3.2) no classic hydrogen bonds were found. In the polymeric form, since the ligand molecules are arranged in a head to tail fashion so that a centre of symmetry at the copper atom is expected in the crystal. The packing of the molecules in the unit cells were effected due to a series of *Cg–Cg* interactions between rings, π –*Cg* and C–H \cdots π interactions. Both intramolecular (C1–H1 \cdots N1 and C5–H5 \cdots O1) and intermolecular (C5–H5 \cdots O2, C10–H10 \cdots O3, C13–H13 \cdots O1, C18–H18B \cdots O4) C–H \cdots π interactions were found in the packing pattern.

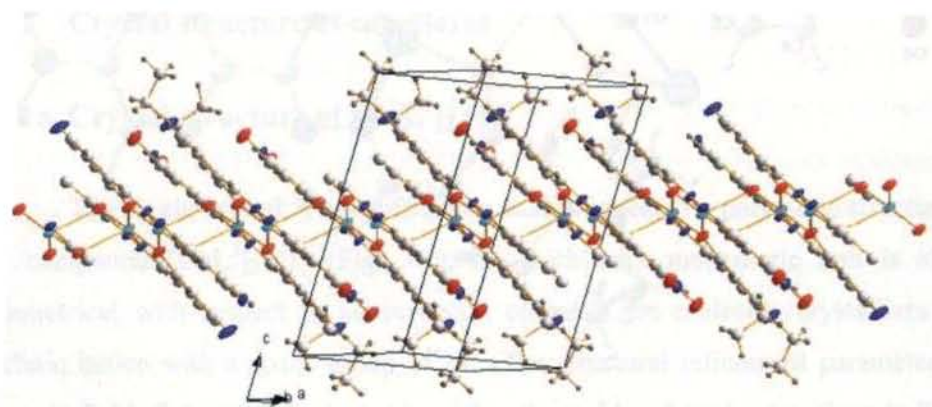


Fig. 3.2. Molecular packing diagram of [CuL¹]₂ (1).

3.3.1b. Crystal structure of [CuL¹pi] (3)

The molecule crystallizes in a triclinic lattice with a space group of $P\bar{1}$. The structural refinement parameters are given in Table 3.1 and the selected bond distances and bond angles are given in Tables 3.4 and 3.5. The structure of the molecule together with the atom numbering scheme are shown in Fig. 3.3. In this complex, The dinegative tridentate *N*-4-diethylamino-2-hydroxybenzaldehyde-*N'*-4-nitrobenzoylhydrazine is coordinated to Cu(II) through the deprotonated phenolic oxygen O2, azomethine nitrogen N2 and deprotonated enolic oxygen O1 forming respectively five and six membered chelate rings. The fourth coordination site is occupied by the pyridine nitrogen N5 of the 4-picoline molecule.

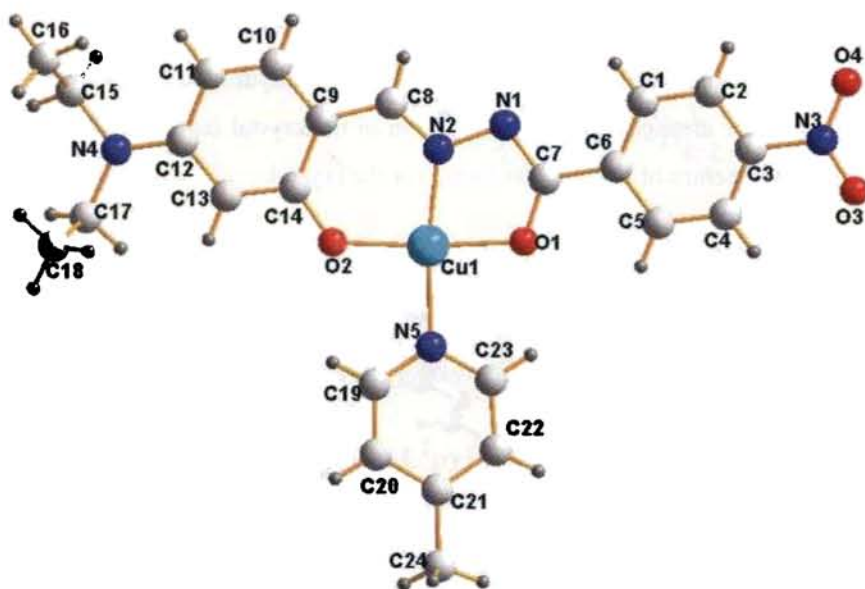


Fig. 3.3. Molecular structure of [CuL¹pi] (3). The atoms are shown at 50% probability.

The copper(II) is in a distorted square planar environment and lies approximately in the ligand plane showing a slight deviation of 0.0412 Å from the best fit least square planes through the four donor atoms and Cu(II) atom. The distortion from regular square planar is seen in the departure from 180° of the angles O2–Cu1–O1 (171.6(9)°) and N2–Cu1–N5 (172.2(1)°) and from 90° of the bite angles O2–Cu1–N2 (94.4(1)°, N2–Cu1–O1 (80.7(9)°, O2–Cu1–N5 (93.4(1)°) and O1–Cu1–N5 (91.6(9)°). This distortion may be imposed by the rigidity of the formed two chelate rings. The coordinated bond distances in the complex are more or less similar to those reported for other similar complexes [33-35]. The picoline ring is planar and lies at an angle of 7.05° to the plane of best fit through the copper coordination sphere. The bond distance between the picoline nitrogen N5 and the copper(II) atom is 1.997(3) Å which is comparable with other similar compounds [36-39].

In the packing pattern of the complex, no classic hydrogen bonds were found. The molecules are arranged in a zigzag fashion in the crystal lattice as shown in the Fig. 3.4 so that a centre of inversion is found for the crystal.

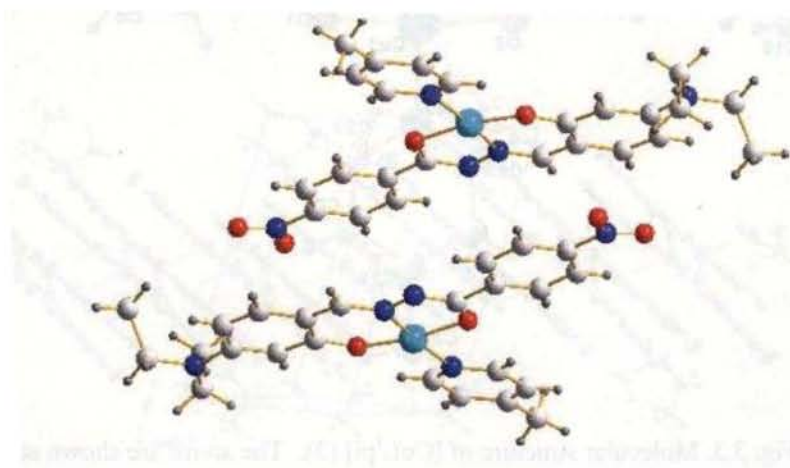


Fig. 3.4. The repeating unit of the crystal lattice, showing zigzag arrangement.

The crystal lattice Fig. 3.5 is expected to be stabilized by Cg–Cg ring interactions, ring metal interactions, C–H⋯π interactions. The C–H⋯π interactions are predominant that both intra (C5–H5⋯O1, C19–H19⋯O2 and C23–H23⋯O1) and intermolecular (C8–H8⋯O4 and C15–H15A⋯O3) interactions are found.

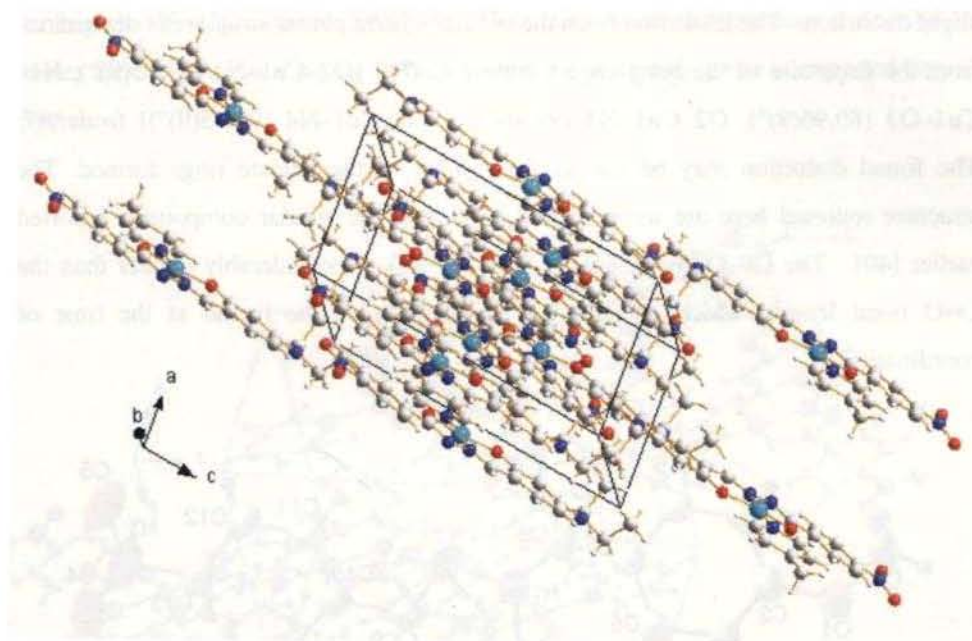


Fig. 3.5. Molecular packing diagram of the compound $[\text{CuL}^1\text{pi}]$ (3).

3.3.1c. Crystal structure of $[\text{CuL}^2\text{py}]$ (5)

The structure of the Cu(II) complex together with the atom numbering scheme is shown in Fig. 3.6. The structural refinement parameters are given in Table 3.1 and the selected bond distances and bond angles are given in Tables 3.6 and 3.7. In this complex the dinegative *N*-2-hydroxy-4-methoxybenzaldehyde-*N'*-4-nitrobenzoylhydrazone is coordinated to Cu(II) through the deprotonated phenolic

oxygen O2, azomethine nitrogen N1 and deprotonated enolate oxygen O3 forming five and six membered chelate rings. The fourth site is occupied by the pyridyl nitrogen N4. The C8–N1 and N1–N2 bonds of the ligand are found to be slightly increased and N2–C9 bond is found to be slightly decreased after coordination confirming the proposed mode of coordination. The complex is almost planar with a slight distortion. The distortion from the regular square planar structure is determined from the departure of the bond angles around Cu(II) [O2–Cu1–N1 (93.55(9)°), N1–Cu1–O3 (80.96(9)°), O2–Cu1–N4 (92.46(9)°), O3–Cu1–N4 (93.13(9)°)] from 90°. The found distortion may be due to the rigidity of the chelate rings formed. The structure reported here are more or less similar to the similar compounds reported earlier [40]. The C9–O3 bond length is 1.300(3) Å is considerably greater than the C=O bond length, which confirms the enolization of the ligand at the time of coordination.

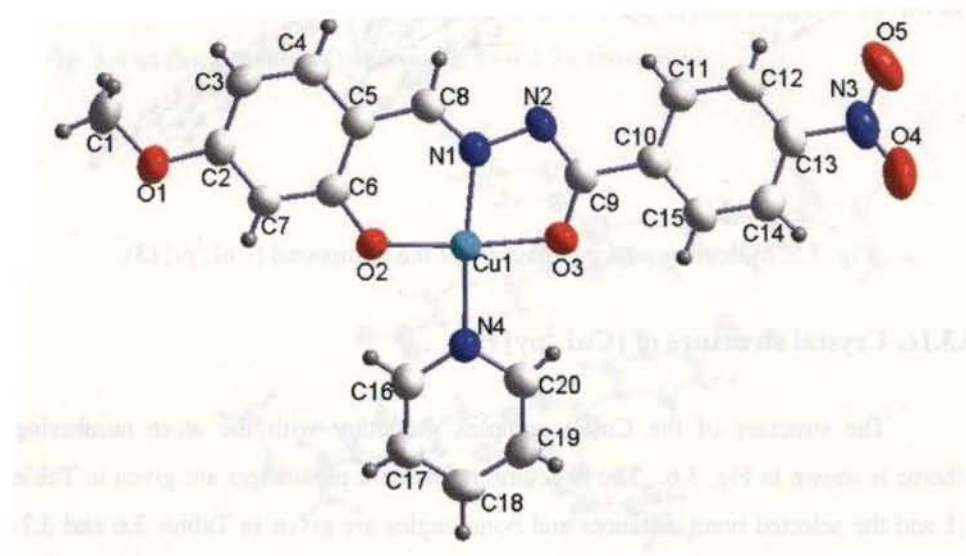


Fig. 3.6. Molecular structure of $[\text{CuL}^2\text{py}]$ (5). The atoms are shown at 50% probability.

In the crystal lattice (Fig. 3.7) the packing is effected by a wide network of π - π staking interactions. No classic hydrogen bonds are found in the lattice, but weak C-H \cdots π interactions are found between the hydrogens in the aromatic rings with the oxygen atoms of the neighboring molecules. Additional Y-X \cdots π ring interactions are found between N3-O4 and Cg1, where the centroid Cg1 consists of Cu1, O3, C9, N2, N1 having the Y \cdots Cg distance 3.585 Å. Here also as in the previous case, the molecules are arranged in a zigzag fashion so that an inversion centre is expected for the crystal.

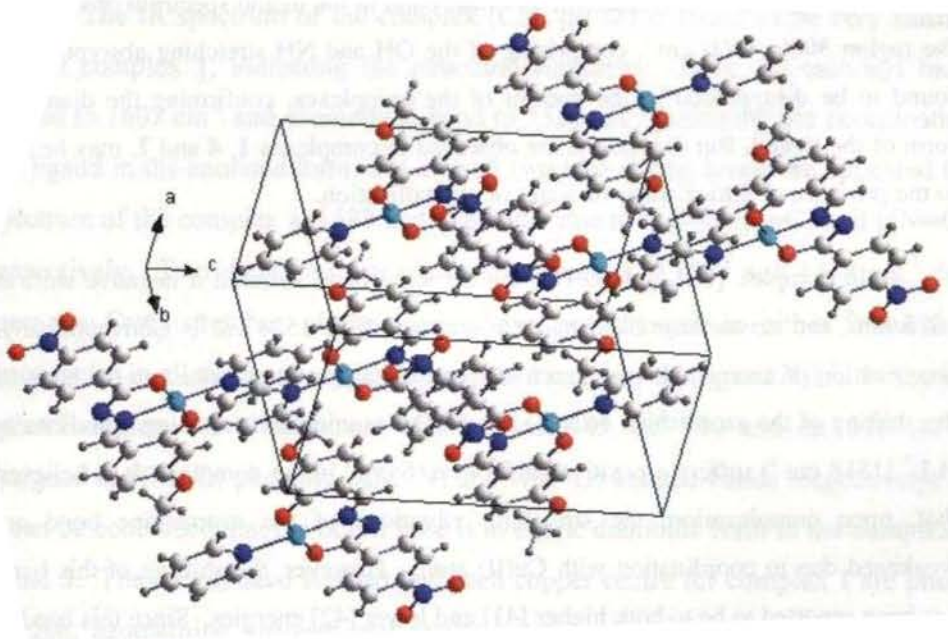


Fig. 3.7. Molecular structure of [CuL²py] (5).

3.3.2. Spectral characteristics of copper(II) complexes

3.3.2a. Infrared spectral studies

A comparison of the IR spectra of the ligands and the complexes generally gives an idea about the coordination sites of the ligands in the complexes. The infrared spectra of the copper complexes showed a considerable negative shift of the carbonyl peak from the region $1630 - 1690 \text{ cm}^{-1}$, which was present in the ligand IR spectra due to strong $\nu(\text{C}=\text{O})$ absorption. This indicates the existence of the ligand in the enolate form upon coordination. A broad band in the ligand spectrum observed in the region $3000 - 3600 \text{ cm}^{-1}$, comprising of the OH and NH stretching absorptions is found to be disappeared in the spectra of the complexes, confirming the dianionic form of the ligand. But exceptions are observed in complexes **1**, **4** and **7**, may be due to the presence of lattice water or water of crystallization.

In complex $[\text{CuL}^1]_2 \cdot \text{H}_2\text{O}$ (**1**), the carbonyl band suffered a negative shift to 1615 cm^{-1} and azomethine band had a positive shift to 1524 cm^{-1} . Conventionally, coordination of azomethine nitrogen to a metal ion has been proposed on the basis of the shifting of the azomethine $\nu(\text{C}=\text{N})$ bond. The azomethine stretching vibrations in H_2L^1 (1518 cm^{-1}) suffers a positive shift of *ca.* 6 cm^{-1} in the complex. It is believed that, upon complexation, the stretching vibrations of the azomethine bond are weakened due to coordination with Cu(II) atom. However, the shifting of this band has been reported to be to both higher [41] and lower [42] energies. Since this band is unlikely to be exclusively $\nu(\text{C}=\text{N})$, but a combination band, a shift is difficult to be predicted with accuracy. Both the types of shifts can occur due to the different mixing of the $\nu(\text{C}=\text{N})$ band with other bands [43]. The coordinated sites around each copper centre are phenolic oxygen, azomethine nitrogen and enolic oxygen of one molecule of the principal ligand and phenolic oxygen of the second molecule.

In the complex $[\text{CuL}^1\text{py}]\cdot\text{H}_2\text{O}$ (**2**), the carbonyl stretching band shifted from 1631 cm^{-1} to 1602 cm^{-1} and azomethine band, from 1518 cm^{-1} to 1525 cm^{-1} indicating the coordination through enolized carbonyl oxygen and azomethine nitrogen to the copper atom. Absence of broad band in $3000\text{-}3600\text{ cm}^{-1}$ region confirms the coordination through deprotonated phenolic oxygen. The fourth coordination site of the square planar copper atom is satisfied by the pyridine nitrogen, which is proposed on the basis of far IR spectral data. In the far IR region, the Cu-N_{py} vibration frequency was observed at 282 cm^{-1} .

The IR spectrum of the complex $[\text{CuL}^1\text{pi}]$ (**3**) is found to be very similar to that of complex **1**, indicating the structural similarity. Here the carbonyl band is shifted to 1607 cm^{-1} and azomethine band to 1522 cm^{-1} indicating the coordination of the ligand in the enolised form. As a result two new strong bands are appeared in the spectrum of the complex at 1588 and 1489 cm^{-1} due to $\nu(\text{C}=\text{N}-\text{N}=\text{C})$ and $\nu(\text{N}=\text{C}-\text{O})$ respectively. Two medium-to-strong bands observed at 1594 and 1414 cm^{-1} due to aromatic $\text{C}=\text{C}$ stretches of the ligand have not changed in either intensities or frequencies in all the three copper complexes formed by the ligand H_2L^1 . In the far IR spectral region, the predominant bands at *ca.* 445 , *ca.* 430 and *ca.* 335 cm^{-1} are assigned to $\nu(\text{M}-\text{O})$ phenolic, $\nu(\text{M}-\text{N})$ and $\nu(\text{M}-\text{O})$ ketonic bands respectively. Thus it can be concluded that the Schiff base is in enolic dianionic form in the complexes **1**, **2** and **3**. The coordinated sites around each copper centre for complex **1** are phenolic oxygen, azomethine nitrogen and enolic oxygen of one molecule of the principal ligand and phenolic oxygen of the second molecule and those for the complexes **2** and **3** are phenolic oxygen, azomethine nitrogen and enolic oxygen of the principal ligand and the pyridyl nitrogen of pyridine and picoline respectively.

Similar trend of shifting of the IR bands are observed in the copper complexes formed by the ligand H_2L^2 . In $[\text{CuL}^2]_2\cdot 3/2\text{ H}_2\text{O}$ (**4**), $\nu(\text{C}=\text{O})$ band showed a negative

shift from 1655 cm^{-1} to 1611 cm^{-1} and $\nu(\text{C}=\text{N})$ shifted to 1526 cm^{-1} from 1550 cm^{-1} confirming the coordination through enolized carbonyl oxygen and azomethine nitrogen. The intensity of the broad band observed in the ligand spectrum in the region $3000\text{-}3500\text{ cm}^{-1}$, comprising of the OH and NH stretching frequencies is found to be lowered in the spectrum of the complex, confirming the dianionic form of the ligand. The weak band in this region may be due to the presence of lattice water. So the coordination mode in complex 4 is similar to that in complex 1. In the case of complexes, $[\text{CuL}^2\text{py}]$ (5) and $[\text{CuL}^2\text{pi}]$ (6), the Cu-N_{py} vibration frequency in the far infrared region was observed at 291 and 295 cm^{-1} respectively.

Same trend is observed in the copper complexes formed by the ligand H_2L^3 . Based on the infrared spectral bands observed, the coordination pattern around the copper atom for the complex $[\text{CuL}^3]_2 \cdot \frac{1}{2}\text{H}_2\text{O}$ (7) is proposed as phenolic oxygen, azomethine nitrogen and enolic oxygen of one molecule of the principal ligand and phenolic oxygen of the second molecule of the ligand. Similarly the coordinated sites in the complexes $[\text{CuL}^3\text{py}]$ (8) and $[\text{CuL}^3\text{pi}]$ (9) are phenolic oxygen, azomethine nitrogen and enolic oxygen of the principal ligand and the pyridyl nitrogen of pyridine and picoline respectively.

3.3.2b. Electronic spectral studies

The electronic absorption spectra are often very helpful in the evaluation of results furnished by other methods of structural investigation. The electronic spectral measurements were used for assigning the stereochemistries of metal ions in the complexes based on the positions and number of *d-d* transition peaks.

The $d^9\text{ Cu}^{2+}$ ion with a 2D ground state free ion term has an electron vacancy or hole in its d level and can be regarded as the inverse of a d^1 arrangement. So in an

octahedral field, the ground state will be split into a lower 2E_g and upper ${}^2T_{2g}$ level [27]. But usually due to the lower symmetry of environments around the Cu(II) ion, the energy levels again split resulting in more transitions. Copper(II) complexes are known in a wide variety of structures. A very broad band with a peak maximum near $15,000\text{ cm}^{-1}$ is observed for most geometries [44]. Thus the electronic spectrum of Cu(II) is often of little value in structural assignment making difficult to use electronic spectroscopy alone as a definitive tool for identifying the geometry.

Tetragonal distortion is usually assumed to be the most common example of Cu^{2+} coordination. In an axially elongated octahedron the splitted energy levels 2E_g and ${}^2T_{2g}$ again undergo splitting because of the unsymmetrical electron arrangement in the orbitals. Thus 2E_g get splitted to ${}^2A_{1g}$ and ${}^2B_{1g}$ and ${}^2T_{2g}$ to ${}^2B_{1g}$ and 2E_g respectively. The ground state of Cu(II) ion in an elongated tetragonally distorted octahedral crystal field of D_{4h} symmetry may be described as a single electron in d_{z^2} orbital, or a ${}^2A_{1g}$ spectroscopic state. In the case of square planar complexes with d_{z^2} ground state, the possible transitions between energy levels are ${}^2E_g \leftarrow {}^2A_{1g} (d_{xz}, d_{yz} \leftarrow d_{z^2})$; ${}^2B_{2g} \leftarrow {}^2A_{1g} (d_{xy} \leftarrow d_{z^2})$ and ${}^2B_{1g} \leftarrow {}^2A_{1g} (d_{x^2-y^2} \leftarrow d_{z^2})$ and they occur in the ranges 830 -580, 640 - 550, 580 - 500 nm respectively. Hence the three allowed transitions are expected in the visible region, but often these theoretical expectations are overlooked in practice, and these bands usually appear overlapped due to the very small energy difference between the d levels.

However, for the complexes under study, useful information available from the electronic spectra are the energies of the transitions to anti-bonding π molecular

orbitals from the non-bonding and π -bonding molecular orbitals. Other useful bands are the charge transfer bands, which support the coordinated nature of the complexes.

In complex $[\text{CuL}^1]_2 \cdot \text{H}_2\text{O}$ (1), two very broad bands are seen in the solution state electronic spectrum in the visible range *ca.* 564 and 460 nm. The first broad band at 564 nm comprises of the three *d-d* transitions expecting for square planar transitions. Another intense absorption at 460 nm is due to the ligand to metal charge transfer transitions, similar to those reported for a copper(II) ion in square planar environments [45-46]. The spectrum in the visible region is shown in Fig. 3.8. In the UV region, two bands at *ca.* 260 and 280 nm are observed due to the intraligand absorptions. In the ligand electronic spectrum, $\pi \rightarrow \pi^*$ and $n \rightarrow \pi^*$ transitions were at 345 and 390 nm respectively.

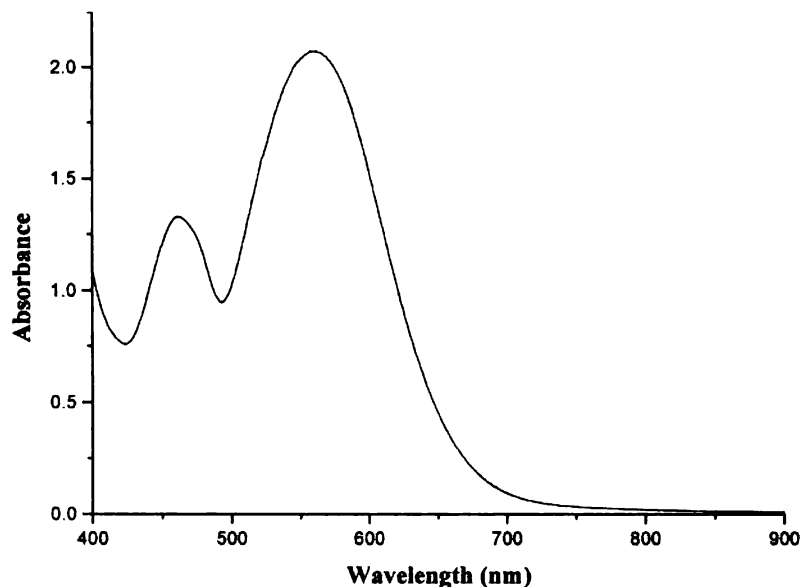


Fig. 3.8. The electronic spectrum of the compound $[\text{CuL}^1]_2 \cdot \text{H}_2\text{O}$ (1).

The electronic spectra of the complexes $[\text{CuL}^1\text{py}]\cdot\text{H}_2\text{O}$ (2) and $[\text{CuL}^1\text{pi}]$ (3) (Fig. 3.9) are found to be very similar in shape with that of $[\text{CuL}^1]_2\cdot\text{H}_2\text{O}$ (1). Here the combined $d-d$ transition bands are observed *ca.* 560 and 571 nm respectively. But the ligand to metal charge transfer bands in 2 and 3 are found at 465 and 467 nm respectively. The qualitative analysis of the electronic spectra itself reveals the similarity in structure of the three complexes 1, 2 and 3 formed by the ligand H_2L^1 .

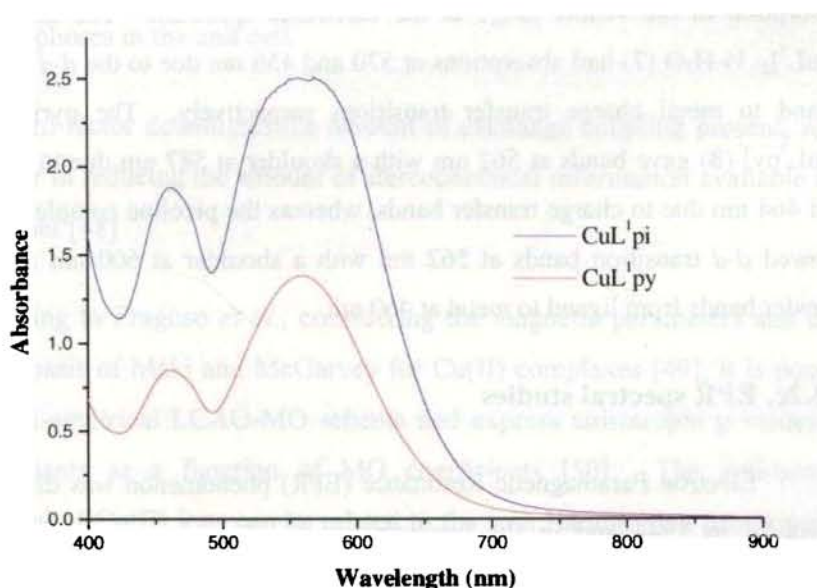


Fig. 3.9. The electronic spectrum of $[\text{CuL}^1\text{py}]\cdot\text{H}_2\text{O}$ (2) and $[\text{CuL}^1\text{pi}]$ (3).

Now about the electronic spectra of the complexes of H_2L^2 , the first one $[\text{CuL}^2]_2\cdot 3/2 \text{H}_2\text{O}$ (4) showed the absorption due to $d-d$ transitions as a broad band at *ca.* 602 nm and the ligand to metal charge transfer band at 545 nm in the visible region. But in the ultraviolet region the complexes showed a shift in the bands due to the intraligand transitions from the pure ligand electronic spectrum. Originally, the ligand bands were at 340 and 290 nm respectively, which shifted to 320 and 280 nm respectively.

As in the case of the complexes of H_2L^1 , here also the pyridine and picoline analogous of the complex $[CuL^2]_2 \cdot 3/2 H_2O$ (4), $[CuL^2py]$ (5) and $[CuL^2pi]$ (6) showed very similar appearance in the electronic spectra. Here the absorptions in the visible region were at *ca.* 613 and 550 nm respectively for the pyridine complex and 600 and 546 nm for the picoline complex respectively.

Similarly, the copper complexes formed by H_2L^3 also showed similarity in absorption in the visible range of the electronic spectrum. The dimeric complex $[CuL^3]_2 \cdot 1/2 H_2O$ (7) had absorptions at 570 and 456 nm due to the *d-d* transitions and ligand to metal charge transfer transitions respectively. The pyridine complex, $[CuL^3py]$ (8) gave bands at 562 nm with a shoulder at 587 nm due to *d-d* absorption and 464 nm due to charge transfer bands, whereas the picoline complex, $[CuL^3pi]$ (9) showed *d-d* transition bands at 562 nm with a shoulder at 600 nm and the charge transfer bands from ligand to metal at 460 nm.

3.3.2c. EPR spectral studies

Electron Paramagnetic Resonance (EPR) phenomenon was discovered by E. Zavoisky in 1944 and in the beginning it was used by physicists to study the paramagnetic metal ions in crystal lattices. It is based on the absorption of electromagnetic radiation, usually in the microwave region, which causes transitions between energy levels produced by the action of a magnetic field on an unpaired electron. In the case of a Cu(II) ion, it has an effective spin of $S = 1/2$ and is associated with a spin angular momentum $m_s = +1/2$, leading to a doubly degenerate spin state in the absence of a magnetic field. When a sufficient magnetic field is applied, this degeneracy is removed, and the energy difference between two resultant states is given by

$$E = h\nu = g\beta H$$

Where h is Planck's constant, ν is the frequency, g is the Lande splitting factor, β is the electron Bohr magneton and H is the magnetic field [47].

The factors that determine the type of EPR spectrum observed are:

- (a) the nature of the electronic ground state
- (b) the symmetry of the effective ligand field about the Cu(II) ion
- (c) the mutual orientations of the local molecular axes of the separate Cu(II) chromophores in the unit cell.

The third factor determines the amount of exchange coupling present, which is a major factor in reducing the amount of stereochemical information available from the EPR spectrum [48]

According to Frago *et al.*, considering the magnetic parameters and using the theoretical basis of Maki and McGarvey for Cu(II) complexes [49], it is possible to apply a semi-empirical LCAO-MO scheme and express anisotropic g values and hyperfine constants as a function of MO coefficients [50]. The anti-bonding molecular orbital of Cu(II) ions can be related to the spin Hamiltonian parameters by means of the following equations:

$$A_{\parallel} = P \left[-k - \frac{4\alpha^2}{7} + (g_{\parallel} - 2.0023) + \frac{3(g_{\perp} - 2.0023)}{7} \right] \quad (3.1)$$

$$A_{\perp} = P \left[-k + \frac{2\alpha^2}{7} + \frac{11(g_{\perp} - 2.0023)}{14} \right] \quad (3.2)$$

Where P is taken as 0.036 cm^{-1} and by solving the two equations, we get the values for α^2 and k . The factor α^2 arises from the dipole-dipole interaction between magnetic moments associated with the spin motion of the electron and the nucleus and its value decreases with increasing covalency [51]. The term k arises from the Fermi contact interaction that has its origin in a non vanishing probability of finding the unpaired electron at the site of the nucleus. k is assumed to be independent to the direction of the magnetic field and the maximum value is obtained at an intermediate covalence of α^2 . In other words, the stronger covalence should result in smaller hyperfine interaction.

However, Jezierska *et al.* [52] regarded α^2 as the MO index of in-plane σ bonding, which can be calculated from the expression,

$$\alpha^2 = -\frac{A_{\parallel}}{0.036} + (g_{\parallel} - 2.0023) + \frac{3(g_{\perp} - 2.0023)}{7} + 0.04 \quad (3.3)$$

Hathaway [53] investigated the evidence for out-of-plane bonding of ligands in axial copper(II) complexes to assess the out-of-plane bonding potential in a strictly square coplanar CuL_4 chromophore. He inferred that since there is no crystallographic evidence for a strictly square coplanar CuL_4 chromophore, in such complexes, some out-of-plane bonding potential still remains to be satisfied. In complexes with ligands capable of π -bonding the four ligands may satisfy the additional bonding potential of the CuL_4 chromophore by out-of-plane π -bonding. Hathaway derived the orbital reduction factors from the electronic and ESR spectral data and then related them to the MO coefficients through the following equations:

$$K_{\parallel}^2 = (g_{\parallel} - 2.0023) \frac{\Delta E(d_{xy} \rightarrow d_{x^2-y^2})}{8\lambda_0} \quad (3.4)$$

$$K_{\perp}^2 = (g_{\perp} - 2.0023) \frac{\Delta E(d_{xz}, d_{yz} \rightarrow d_{x^2-y^2})}{2\lambda_0} \quad (3.5)$$

$$K_{\parallel} = \alpha\beta \quad (3.6)$$

$$\text{and } K_{\perp} = \alpha\gamma \quad (3.7)$$

where K_{\parallel} and K_{\perp} are orbital reduction factors, α the σ bonding, β in-plane π -bonding and γ , the out-of-plane π -bonding MO coefficients. However, it should be noted that, the term α in (3.6) and the term α^2 in (3.3) are essentially the same, and hence in the present study we will consider the MO index of in-plane σ bonding as α itself.

The electron paramagnetic resonance spectra of all the nine present copper complexes were recorded both in the powder form at room temperature and in frozen state at liquid nitrogen temperature, 77 K. The first one gave the electron resonance in the polycrystalline state and the later gave information about the solution state. The polycrystalline EPR spectrum of the complex $[\text{CuL}^1]_2 \cdot \text{H}_2\text{O}$ (1) at room temperature gave an isotropic pattern with g_{iso} value 2.031. The isotropic nature of the spectrum may be due to strong dipolar and exchange interactions between the Cu(II) ions in the unit cell.

But the spectrum in DMF at 77 K showed axial behaviour (Fig. 3.10) with four well resolved copper hyperfine lines and superhyperfine lines due to the two coordinated nitrogen atoms. The spectrum is axial in nature with two g values, $g_{\parallel} = 2.207$ and $g_{\perp} = 2.037$. All the g values are less than 2.3, which indicate considerable covalent character to the M-L bonds. Since superhyperfine coupling by a second

nitrogen (azomethine nitrogen in the second ligand molecule) is observed, the molecule has a geometry with the coordination of two nitrogens in the same plane.

The f value, ($f = \frac{g_{\parallel}}{A_{\parallel}}$), which reveals the extent of tetragonal distortion, is equal to 107 cm for the complex. The f values are reported to be in the range of 105-135 cm for square planar complexes [54]. Also, the value of $g_{\perp} < g_{\parallel}$ is characteristic of square planar complexes. Based on the above observations, the Cu(II) complex $[\text{CuL}^1]_2 \cdot \text{H}_2\text{O}$ (**1**) is assigned to have a distorted square planar geometry, consistent with other spectroscopic evidences.

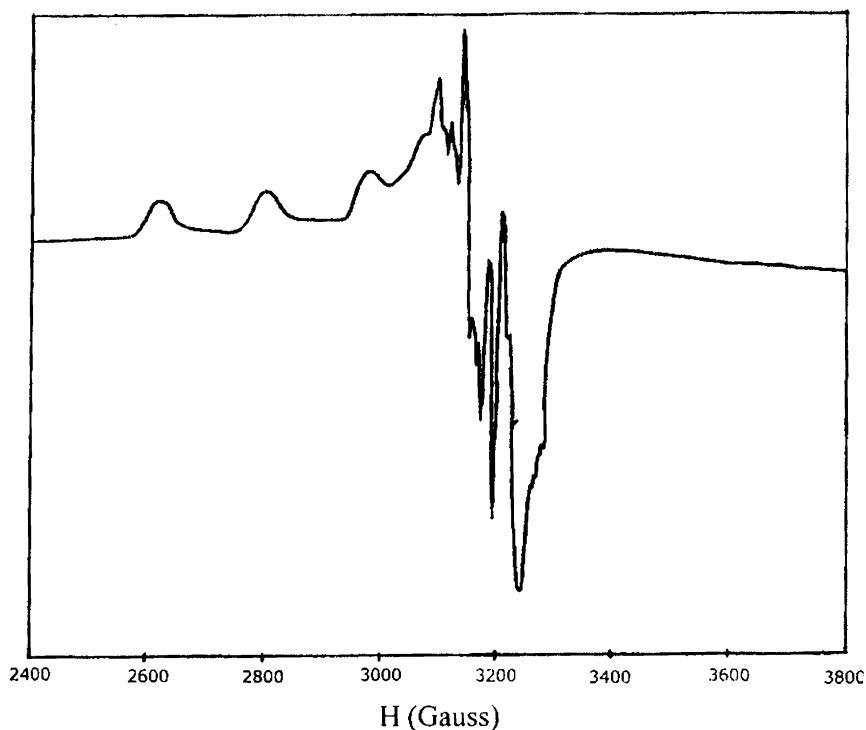


Fig. 3.10. EPR spectrum of $[\text{CuL}^1]_2 \cdot \text{H}_2\text{O}$ (**1**) at 77 K in DMF.

The room temperature spectrum of the complex $[\text{CuL}^1\text{py}]\cdot\text{H}_2\text{O}$ (**2**) also has isotropic nature (Fig.3.11) with g_{iso} value 2.067, due to the strong dipolar and exchange interactions between the Cu(II) ions in the unit cell.

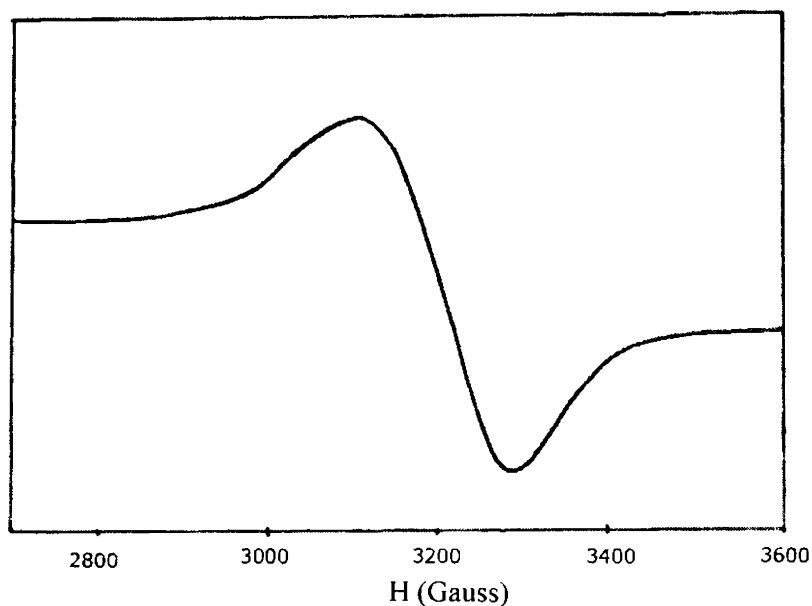


Fig. 3.11. EPR spectrum of $[\text{CuL}^1\text{py}]\cdot\text{H}_2\text{O}$ (**2**) at 298 K.

The EPR spectrum of the complex **2** in the solution state at 77 K gave an axial spectrum (Fig.3.12) having well defined copper hyperfine lines which are characteristics of monomeric copper(II) complexes. The g values are $g_{\parallel} = 2.195$ and $g_{\perp} = 2.069$.

All the g values are less than 2.3, which indicate considerable covalent character to the M-L bonds. The elemental analyses and spectroscopic data are in conformity with the four coordinate environment for the compound. The EPR spectrum also is in strong support of this four coordinate stereochemistry. The f

value, ($f = \frac{g_{\parallel}}{A_{\parallel}}$), which reveals the extent of tetragonal distortion, is equal to 108 cm for the complex. The f values are reported to be in the range of 105-135 cm for square planar complexes. Also, the value of $g_{\perp} < g_{\parallel}$ is characteristic of square planar complexes. Based on the above observations, the Cu(II) complex is assigned a four-coordinated distorted square planar geometry, consistent with other spectroscopic evidences.

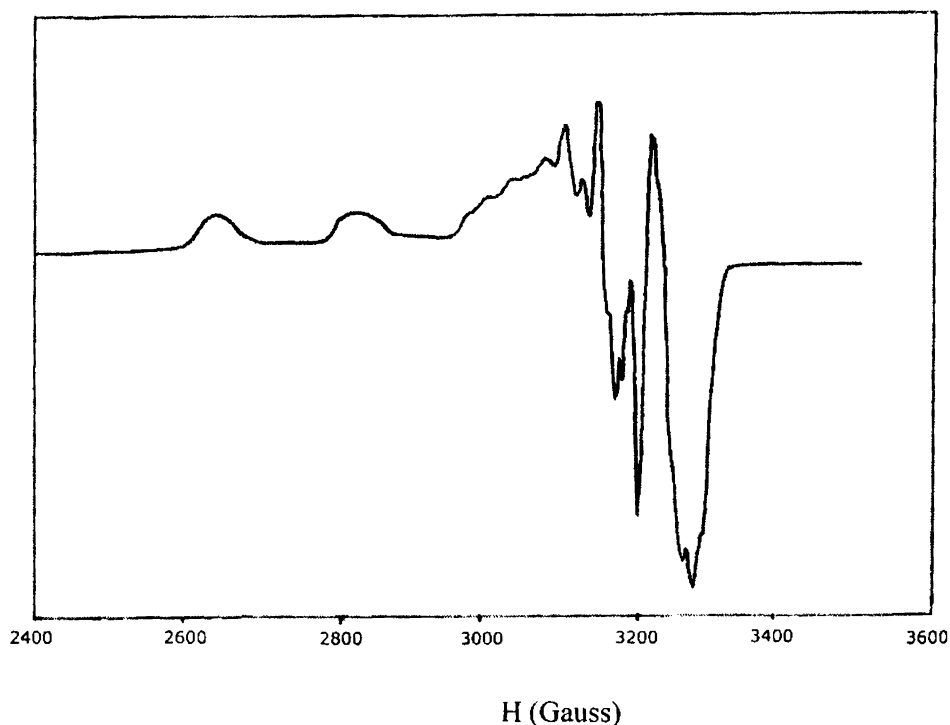


Fig. 3.12. EPR spectrum of $[\text{CuL}^1\text{py}] \cdot \text{H}_2\text{O}$ (2) at 77 K in DMF.

The EPR spectra of the complex $[\text{CuL}^1\text{pi}] \cdot \text{H}_2\text{O}$ (3) were recorded both in the powder form at room temperature and solution in DMF at liquid nitrogen temperature.

The room temperature spectrum (Fig. 3.13) itself showed an axial nature with two g values $g_{\parallel} = 2.184$ and $g_{\perp} = 2.050$. All the g values are less than 2.3, which indicate considerable covalent character to the M–L bonds and the value of $g_{\perp} < g_{\parallel}$ is characteristic of square planar complexes. The absence of hyperfine interactions at room temperature, can be attributed to strong dipolar and exchange interactions between the Cu(II) ions in the unit cell. However, the hyperfine splittings were well resolved in the frozen solution state. The solution state spectrum at 77 K (Fig. 3.14) has axial behaviour with hyperfine splittings in the g_{\parallel} region. The g values in the solution state spectra are $g_{\parallel} = 2.188$ and $g_{\perp} = 2.055$.

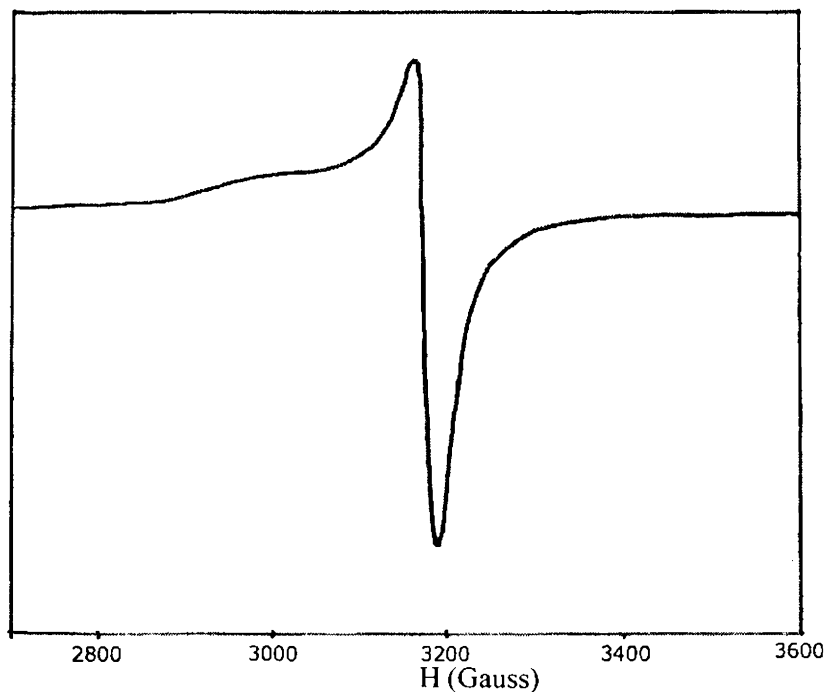


Fig. 3.13. EPR spectrum of $[\text{CuL}^1\text{pi}] \cdot \text{H}_2\text{O}$ (3) at 298 K.

In the case of the complex $[\text{CuL}^1\text{pi}]\cdot\text{H}_2\text{O}$ (**3**) the f value, ($f = \frac{g_{\parallel}}{A_{\parallel}}$), the extent of tetragonal distortion, is equal to 106 cm. The exchange interaction parameter G [$G = (g_{\parallel}-2)/(g_{\perp}-2)$] is found to be less than 4.0, suggesting considerable exchange coupling interactions [55-56] in the complex.

Based on the above observations, the Cu(II) complex $[\text{CuL}^1\text{pi}]\cdot\text{H}_2\text{O}$ (**3**) is assigned a four-coordinated distorted square planar geometry, consistent with other spectroscopic evidences.

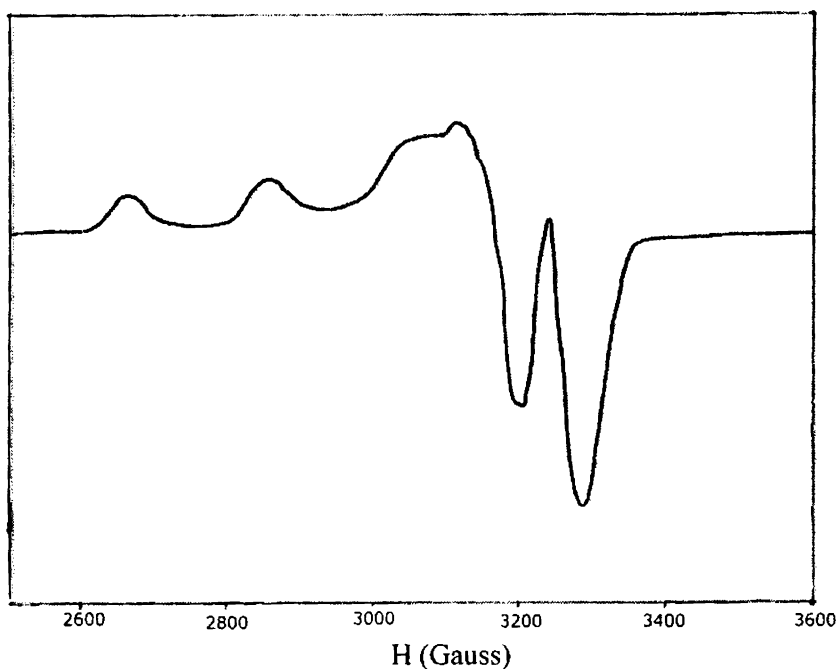


Fig. 3.14. EPR spectrum of $[\text{CuL}^1\text{pi}]$ (**3**) at 77 K in DMF.

The EPR spectra of the complex $[\text{CuL}^2]_2 \cdot 3/2 \text{H}_2\text{O}$ (4) were recorded both in the powder form at room temperature and solution in DMF at liquid nitrogen temperature.

The polycrystalline spectrum (Fig. 3.15) at room temperature is found to be axial in nature, with no splitting pattern due to the magnetically concentrated entity. The two g values are, $g_{\parallel} = 2.197$ and $g_{\perp} = 2.019$. Here also a considerable covalent character for the metal – ligand bonds is expected because all the g values are less than 2.3.

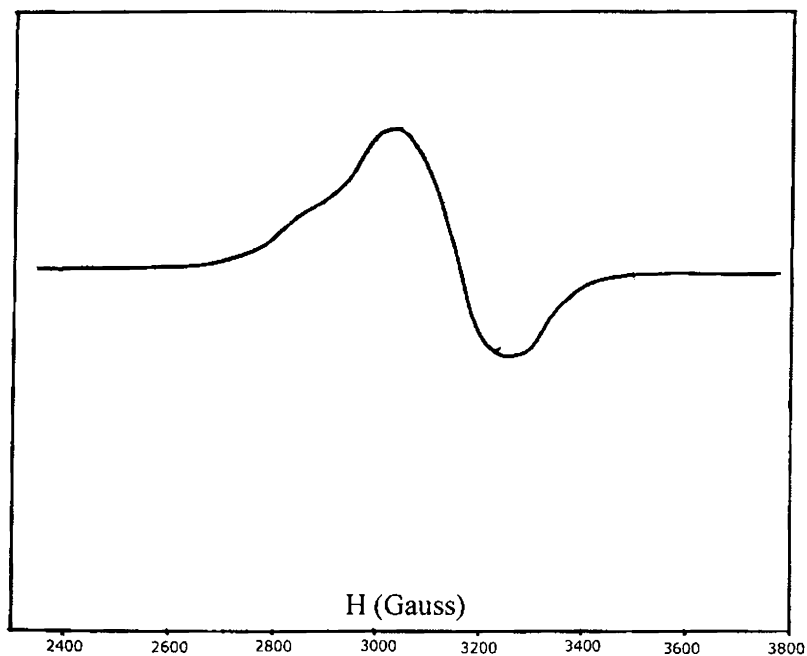


Fig. 3.15. EPR spectrum of $[\text{CuL}^2]_2 \cdot 3/2 \text{H}_2\text{O}$ (4) at 298 K.

But, the frozen state EPR spectrum (Fig. 3.16), strong hyperfine splitting pattern is seen both in the parallel and perpendicular regions. The spectrum has axial

features with the two g values $g_{\parallel} = 2.206$ and $g_{\perp} = 2.054$. Both the room temperature and the solution state spectra are strong support of the four coordinate geometry around each copper centre. The parameter for the extent of tetragonal distortion, f value, ($f = \frac{g_{\parallel}}{A_{\parallel}}$), for the complex is 108 cm shows the possibility of a distorted square planar geometry for the complex. The values $g_{\perp} < g_{\parallel}$, is also a characteristic for square planar complexes. The frozen state spectrum showed well-defined copper hyperfine lines and superhyperfine lines due to the coordinated nitrogen atoms.

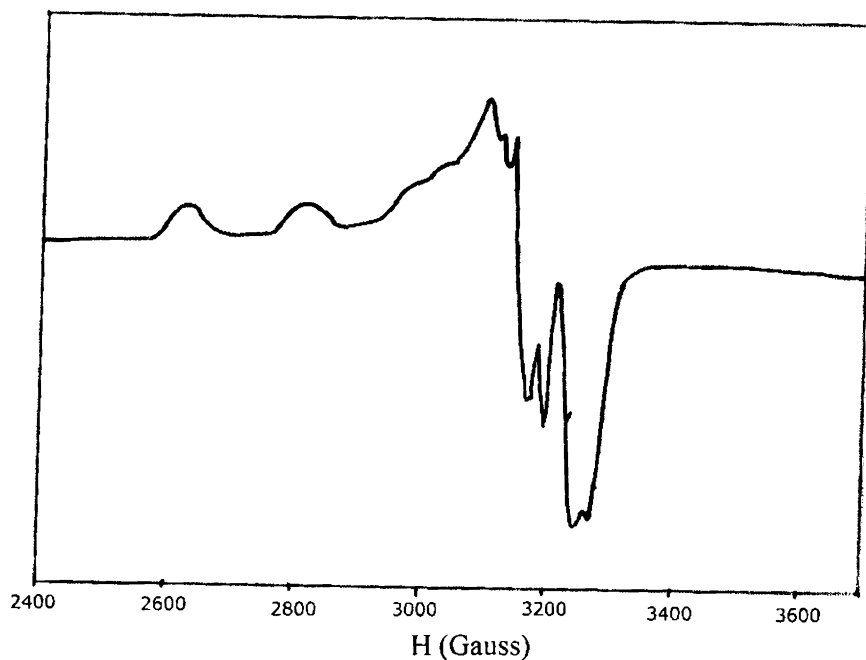


Fig. 3.16. EPR spectrum of $[\text{CuL}^2]_2 \cdot \frac{3}{2} \text{H}_2\text{O}$ (4) at 77 K in DMF.

The EPR spectra of the complex $[\text{CuL}^2\text{py}]$ (5) in polycrystalline state at 298 K and in DMF at 77 K and are shown in the Figs. 3.17 and 3.18 respectively. Both the

spectra have axial properties. The first one have $g_{\parallel} = 2.204$ and $g_{\perp} = 2.054$ and the later one with $g_{\parallel} = 2.195$ and $g_{\perp} = 2.094$. Since the lowest g value is less than 2.04, the complex may have an axial symmetry with all the principal axes aligned parallel, which supports the square planar nature of the complex. The f value, ($f = \frac{g_{\parallel}}{A_{\parallel}}$), which reveals the extent of tetragonal distortion, is equal to 107.07 for the complex. The f values are reported to be in the range of 105-135 cm for square planar complexes.

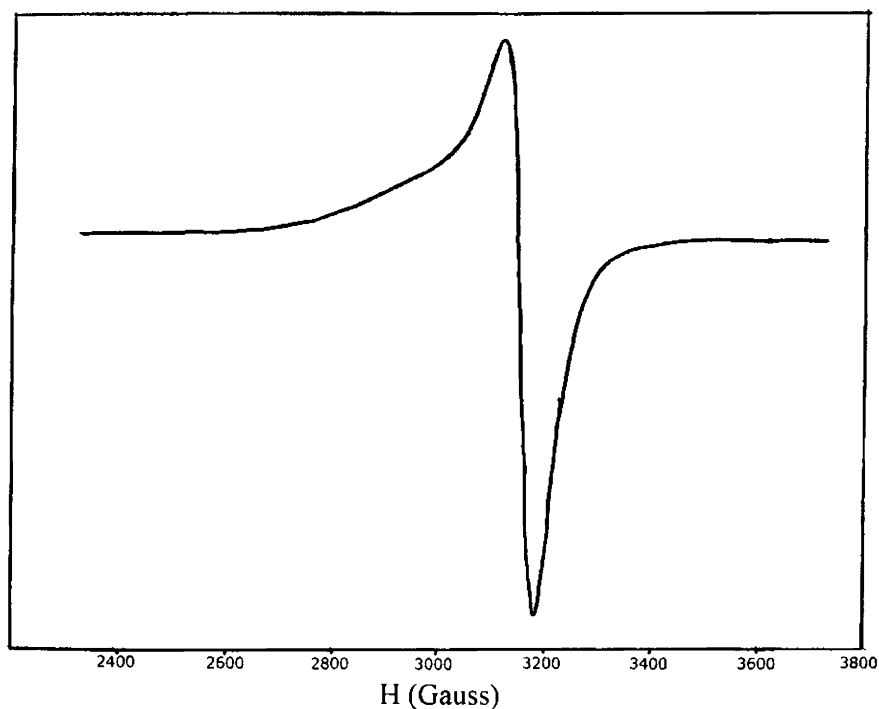


Fig. 3.17. EPR spectrum of [CuL²py] (5) at 298 K.

Also, the trend $g_e < g_{\perp} < g_{\parallel}$ observed for the complex shows that the unpaired electron is localized in the $d_{x^2-y^2}$ orbital of the copper(II) ions and the spectral features are characteristics of axial symmetry. The exchange coupling interaction between two copper centers is explained by Hathaway using the expression $G = g_{\parallel} - 2 / g_{\perp} - 2$. Since the G value is less than 4.0, significant exchange coupling is present and the misalignment is appreciable.

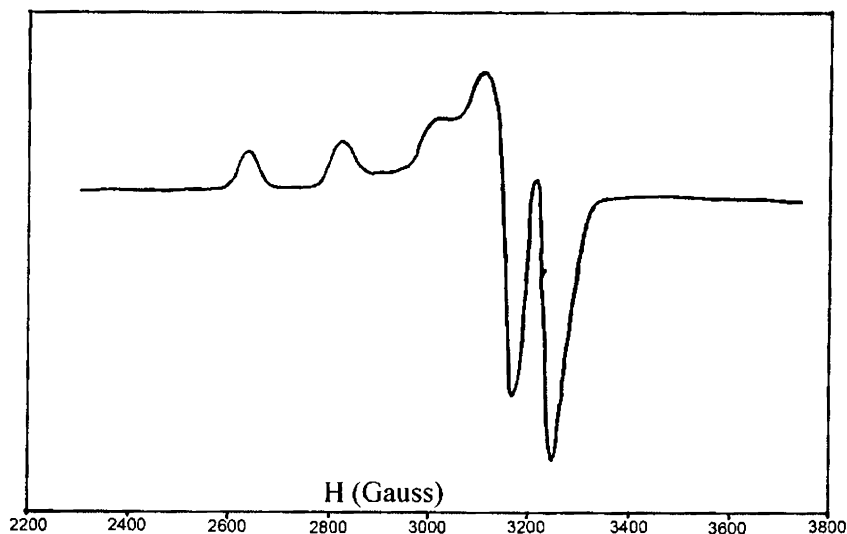


Fig. 3.18. EPR spectrum of $[\text{CuL}^2\text{py}]$ (5) at 77 K in DMF.

The powder state EPR spectrum of the complex $[\text{CuL}^2\text{pi}]$ (6) at room temperature is isotropic in nature indicating magnetically very concentrated environment. The isotropic nature may be due to the strong dipolar and exchange interactions between Cu(II) ions in the unit cell. The solution state EPR spectrum (Fig. 3.19) of the same complex is found to be very similar to that of the previous

complex **5** with axial nature and two g values $g_{\parallel} = 2.201$ and $g_{\perp} = 2.070$, indicating the similar coordination environment of the previous complex. The value of $g_{\perp} < g_{\parallel}$ is characteristic of square planar complexes. The f value, extent of tetragonal distortion, is equal to 109 cm showing distortion from the square planar geometry. The G value of the complex 2.86 suggests considerable exchange coupling interactions in the complex in the solution state.

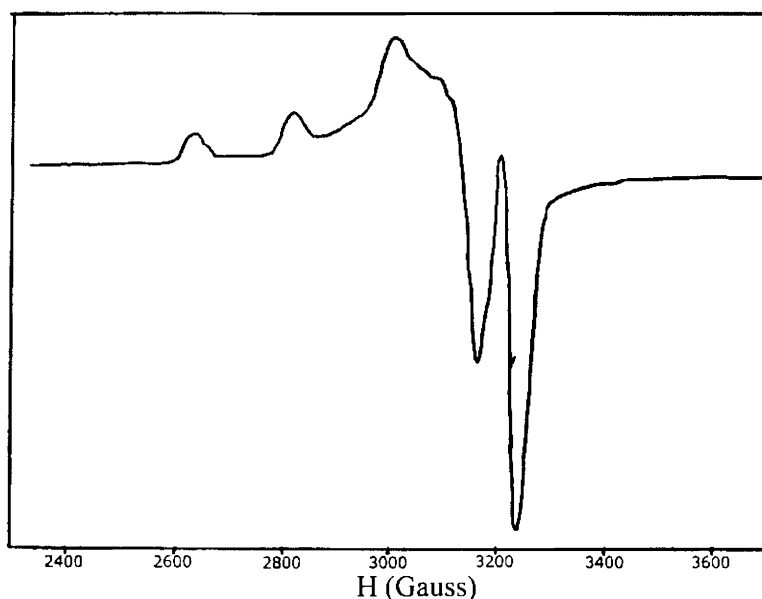


Fig. 3.19. EPR spectrum of $[\text{CuL}^2\text{pi}]$ (**6**) at 77 K in DMF.

The electron paramagnetic resonance spectra of the complex $[\text{CuL}^3]_2 \cdot \frac{1}{2} \text{H}_2\text{O}$ (**7**) were recorded both in the powder form at room temperature and in solution state at liquid nitrogen temperature. The polycrystalline state spectrum is isotropic in nature with g_{iso} value 2.073. The isotropic nature of the spectrum is explained to be due to the magnetically concentrated environment of the copper centre in the powder state.

But in the solution state spectrum (Fig. 3.20), the molecule showed an axial nature with hyperfine splittings both in the parallel and perpendicular regions. In the perpendicular region of the spectrum, both copper hyperfine splittings and nitrogen superhyperfine splittings were observed. Nine nitrogen superhyperfine lines in the spectrum indicated the dimeric nature of the complex with two nitrogen atoms coordinated, one from each ligand.

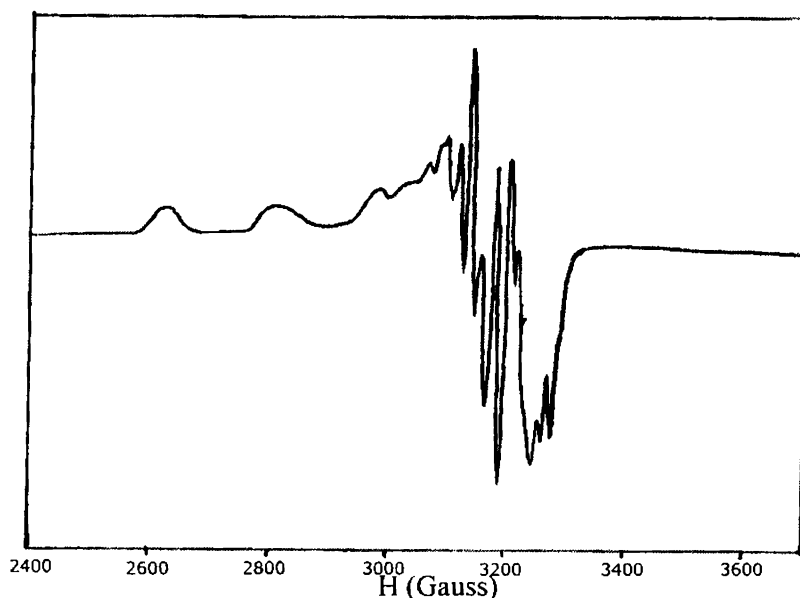


Fig. 3.20. EPR spectrum of $[\text{CuL}^3]_2 \cdot \frac{1}{2} \text{H}_2\text{O}$ (7) at 77 K in DMF.

The g values observed for the solution state EPR spectrum of the complex are $g_{\parallel} = 2.204$ and $g_{\perp} = 2.050$. The observations and g values are very similar to the complexes, $[\text{CuL}^1]_2 \cdot \text{H}_2\text{O}$ (1) and $[\text{CuL}^2]_2 \cdot \frac{3}{2} \text{H}_2\text{O}$ (4) and so similar coordination pattern is expected for the complex discussed. Here also all the g values are less than 2.3, and the f value, ($f = \frac{g_{\parallel}}{A_{\parallel}}$) 109 cm. So considerable covalent character for the

M—L bonds and tetragonal distortion for the geometry are expected. Also, the value of $g_{\perp} < g_{\parallel}$ is characteristic of square planar complexes.

The powder EPR spectrum of the complex $[\text{CuL}^3\text{py}]$ (**8**) (Fig. 3.21) is found to be axial in nature with two g values, $g_{\parallel} = 2.194$ and $g_{\perp} = 2.067$. The solution state spectrum at 77 K (Fig. 3.22), is also found to be axial in nature, having copper hyperfine splittings both in the parallel and perpendicular regions, with g values $g_{\parallel} = 2.187$ and $g_{\perp} = 2.058$. The values of $g_{\perp} < g_{\parallel}$ is characteristic of square planar complexes. All the g values are less than 2.3, giving an idea about the covalent character of the M—L bonds. The exchange interaction parameter G [$G = (g_{\parallel} - 2)/(g_{\perp} - 2)$] in the powder form (2.89) is found to be less than 4.0, suggesting considerable exchange coupling interactions in the complex.

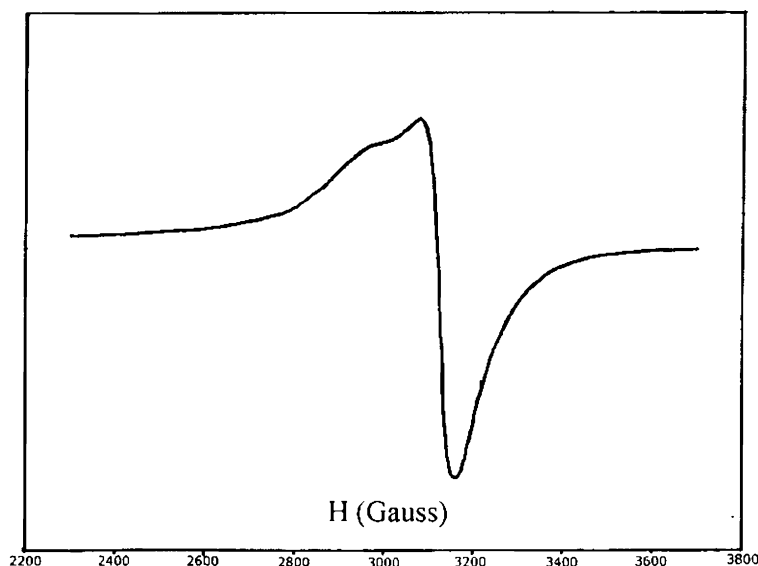


Fig. 3.21. EPR spectrum of $[\text{CuL}^3\text{py}]$ (**8**) at 298 K.

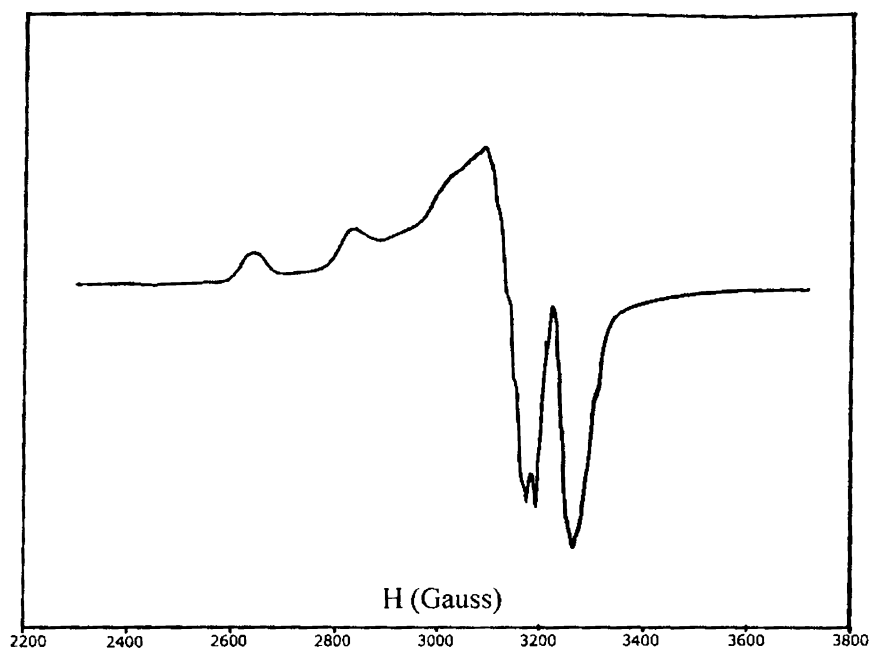


Fig. 3.22. EPR spectrum of $[\text{CuL}^3\text{py}]$ (**8**) at 77 K in DMF.

In the case of the complex $[\text{CuL}^3\text{pi}]$ (**9**) also the electron paramagnetic resonance spectra were recorded both in powder and solution states at 298 and 77 K respectively. The spectra have very similar appearance and parameters of that of the complex $[\text{CuL}^3\text{py}]$ (**8**) and so a similar structure and coordination pattern expected. Both the spectra show axial behavior with g values $g_{\parallel} = 2.164$ and $g_{\perp} = 2.061$ (powder) (Fig. 3.23) and $g_{\parallel} = 2.193$ and $g_{\perp} = 2.057$ (frozen state) (Fig. 3.24).

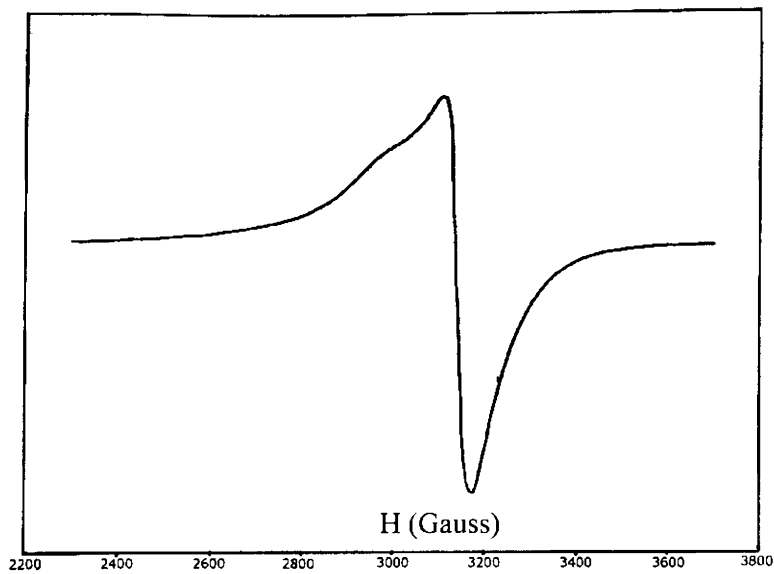


Fig. 3.23. EPR spectrum of $[\text{CuL}^3\text{pi}]$ (9) at 298 K.

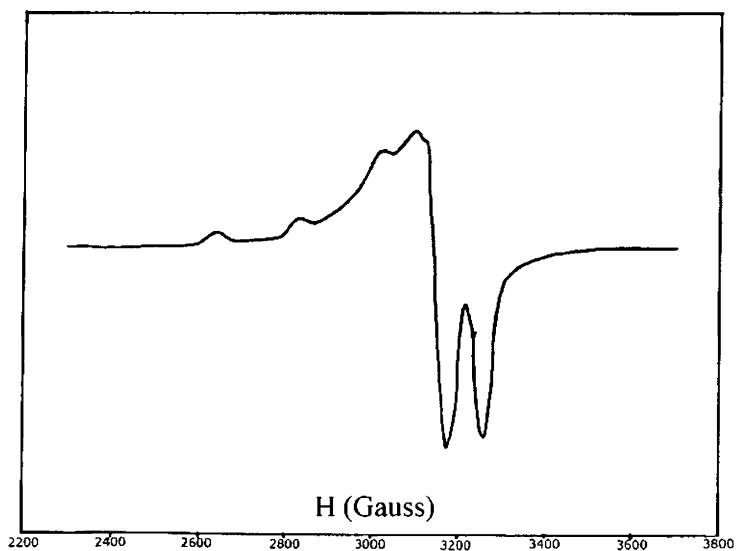
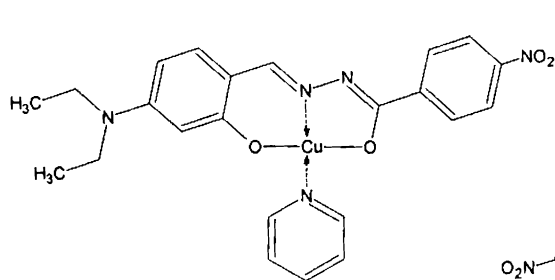
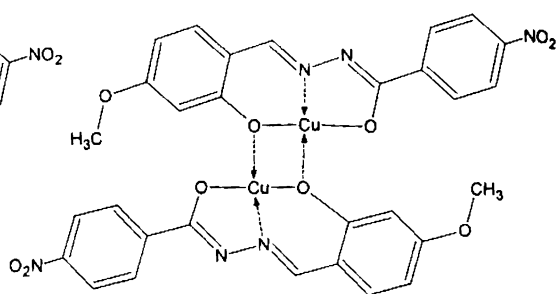


Fig. 3.24. EPR spectrum of $[\text{CuL}^3\text{pi}]$ (9) at 77 K in DMF.

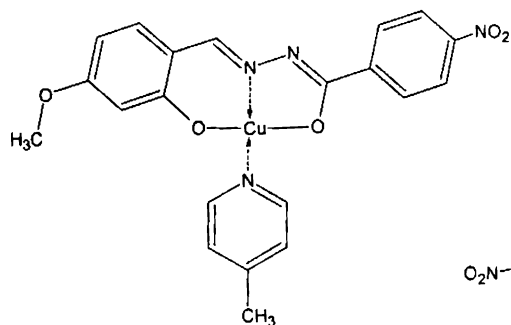
Based on the elemental analyses and spectral investigations, following tentative structures (Fig. 3.25) were assigned for the complexes for which, single crystals suitable for crystallographic studies could not be isolated.



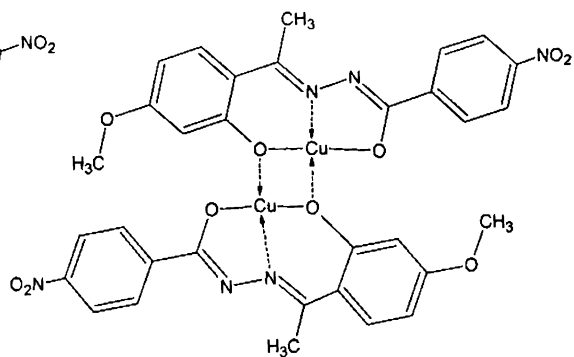
Compound 2



Compound 4



Compound 6



Compound 7

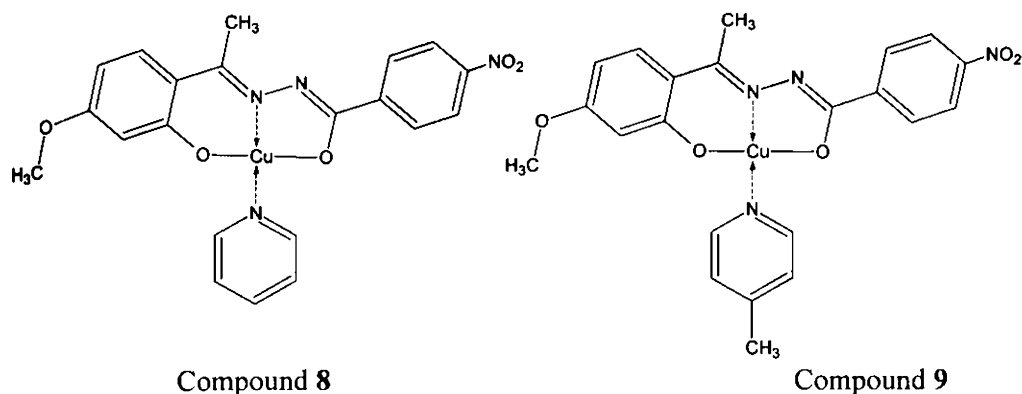


Fig. 3.25. Tentative structures of the copper complexes for which the single crystals suitable for X-ray diffraction studies are not isolated.

3.4. *Non-linear optical properties of Cu(II) complexes*

It is known that pseudo linear π -delocalized organic systems substituted by donor and acceptor groups at the two ends show significant second order NLO responses due to a reduced energy gap between ground and intramolecular charge transfer excited states, together with large oscillator strengths and a significant difference between ground and excited state dipole moments. Metal coordination has been used in several ways to improve the behavior of all organic push pull chromophores for applications in second order non-linear optics. The most common approach is the use of organometallic or metal coordinated fragments attached at the end of organic π -conjugated systems. Proper choice of the metal and its oxidation state and of the ligands allows the fragment to behave as an electron donor or acceptor group. In some cases, metals have been used as cations involved in ionic bonds with negatively charged conjugated π systems giving non-centrosymmetric crystals [57-59]. Another possibility in using metals as conjugation bridges along a push pull organic system. In that case, the choice of metals that give planar coordination

geometry may force a coplanar arrangement of the organic skeleton, so improving conjugation and possibly NLO properties [60-61].

The step toward a NLO material is based on the inclusion of the NLO active molecules within a polymer matrix; this may be performed without covalent bonding or with. In the later case NLO active fragments of the polymer chain are oriented under a strong electric field by heating a polymer above the glass transition temperature and the orientation is frozen by cooling the poled polymer below the glass transition [62].

The essential requirement for NLO activity of a sample is its noncentrosymmetric nature. In the case of the present copper(II) complexes, in the dimeric or polymeric analogous, **1**, **4** and **7**, in the molecular level itself, centre of inversion is present. So these complexes have little significance in non-linear optics. Hence the non-linear optical studies of these complexes were not done.

The non-linear optical properties of all the monomeric complexes, both the pyridine and 4-picoline derivatives were studied in the powder form by Hyper Rayleigh scattering technique. The well powdered sample was filled in capillary tube having 0.8 mm thickness. The NLO responses of these samples were recorded using urea as the reference, filled in similar capillary tube. The experimental arrangement for the non-linear optical properties utilizes a Quanter A DCR II Nd/YAG laser with a 9 mJ pulse at a repetition rate of 5 Hz. The selected wavelength is 1064 nm. After the selection of the wavelength the laser beam is split in to two parts, one to generate the second harmonic signal in the sample and the other to generate the other to generate the second harmonic signal in the reference (urea). An output signal of 532 nm was measured in a 90° geometry using urea as the standard. The efficiency of the NLO activity of the compounds are expressed in percentage as

$$\text{Efficiency} = \frac{\text{Signal of Sample}}{\text{Signal of Urea}} \times 100\%$$

For monomeric complexes **2**, **3**, **5**, **6**, **8** and **9** no centre of symmetry is there in the molecular level. But from the crystallographic pattern of the single crystal studies of **3** and **5**, it can be concluded that the molecules are packed in such a way that, there are inversion centers in the crystalline form. So a high extent of non-linear response for the copper complexes cannot be expected in the powder form of the sample. Experiments showed that only to copper complexes **3** and **8** have NLO responses in the present condition. In the case of compound **3**, a very small response of about 12% as compared to urea was obtained. But in the case of the complex **8**, a significant response of almost double of urea sample was recorded. This may be due to the absence of inversion centre in the crystal packing pattern of this complex. Since the single crystals suitable for X-rays studies were failed to be isolated, a correct structure relation of NLO response cannot be formulated.

References

1. B. Abolmaali, H.V. Taylor, U. Weser, *Struct. Bonding* 91 (1998) 91.
2. A. Messerschmidt, *Struct. Bonding* 90 (1998) 37.
3. R. Osterberg, *Coord. Chem. Rev.* 12 (1974) 309.
4. J.A. Fee, *Struct. Bonding* 23 (1975) 1.
5. H. Beinert, *Coord. Chem. Rev.* 23 (1977) 119.
6. E.L. Ulrich, J.L. Markey, *Coord. Chem. Rev.* 27 (1978) 109.
7. I. Bertini, G. Canti, R. Grassi, *Inorg. Chem.* 19 (1980) 2198.
8. H. Yokoi, A. Addison, *Inorg. Chem.* 16 (1977) 1341.
9. H. Yokoi, *Bull. Chem. Soc. Jpn.* 47 (1974) 3037.
10. I. Solomon, L.B. La Croix, D.W. Randall, *Pure Appl. Chem.* 70 (1998) 799.
11. I.H. Hall, K.G. Rajendran, D.X. West, A.E. Liberta, *Anticancer Drugs* 4 (1993) 231.
12. D.X. West, A.E. Liberta, K.G. Rajendran, I.H. Hall, *Anticancer Drugs* 4 (1993) 241.
13. S.P. Mittal, R.K. Sharma, R.V. Singh, J.P. Tandon, *Curr. Sci.* 50 (1981) 483.
14. A.S. Dobeck, D.L. Klayman, E.J. Dickson, J.P. Scovill, E.C. Tramont, *Antimicrob. Agents Chemother* 18 (1980) 27.
15. K.Raman, H.K. Singh, S.K. Salman, S.S. Parmar, *J. Pharm. Sci.* 82 (1993) 167.
16. D.K. Johnson, T.B. Murphy, N.J. Rose, W.H. Goodwin, L. Pickart, *Inorg. Chim. Acta* 67 (1982) 159.
17. L. Pickart, W.H. Goodwin, W. Burgua, T.B. Murphy, D.K. Johnson, *Biochem. Pharmacol.* 32 (1983) 3868.
18. A.A. Aruffo, T.B. Murphy, D.K. Johnson, N. J. Rose, V. Schomaker, *Acta Cryst. C* 40 (1984) 1164.
19. E.W. Ainscough, A.M. Brodie, A. Dobbs, J.D. Ranford, J.M. Waters, *Inorg. Chim. Acta* 236 (1995) 83.

20. S.C. Chan, L.L. Koh, P.H. Leung, J.D. Ranford, K.Y. Sim, *Inorg. Chim. Acta* 236 (1995) 101.
21. E.W. Ainscough, A.M. Brodie, A. Dobbs, J.D. Ranford, J.M. Waters, *Inorg. Chim. Acta* 267 (1998) 27.
22. J. Patole, U. Sandbhor, S. Padhye, D.N. Deobagkar, C.E. Anson, A. Powell, *Bioorg. Med. Chem. Lett.* 13 (2003) 51.
23. M. Kato, Y. Muto, *Coord. Chem. Rev.* 92 (1988) 45.
24. S.A. Warda, P. Dahlke, S. Wocadlo, W. Massa, C. Friebel, *Inorg. Chim. Acta.* 268 (1998) 117.
25. M.F. Iskander, T.E. Khalil, R. Werner, W. Haase, I. Svoboda, H. Fuess, *Polyhedron* 19 (2000) 1181.
26. B.J. Hathaway, G. Wilkinson, R.D. Gillard, J.A. McCleverty, In *Comprehensive Coordination Chemistry* 5 (1987) 558.
27. J.E. Huheey, E.A. Keiter, R.L. Keiter, *Inorganic Chemistry, Principles of Structure and Reactivity*, 4th ed., Harper Collins College Publishers, New York, 1993.
28. N. Nawar, N.H. Hosny, *Chem. Pharm. Bull.* 47 (1999) 944.
29. R. Gup, B. Kirkan, *Spectrochim. Acta* 62A (2005) 1188.
30. J.D. Ranford, J.J. Vittal, Y.M. Wang, *Inorg. Chem.* 37 (1998) 1226.
31. A. Syamal, K.S. Kale, *Indian J. Chem.* 16A (1978) 46.
32. P.B. Sreeja, M.R.P. Kurup, A. Kishore, C. Jasmin, *Polyhedron* 23 (2004).
33. A.A. Aruffo, T.B. Murphy, D.K. Johnson, N.J. Rose, V. Schomaker, *Inorg. Chim. Acta* 67 (1982) L25.
34. A.A. Aruffo, T.B. Murphy, D.K. Johnson, N.J. Rose, V. Schomaker, *Acta Crystallogr. Sect. C* 40 (1984) 1169.
35. E.W. Ainscough, A.M. Brodie, J.D. Ranford, J.M. Waters, *Inorg. Chim. Acta* 236 (1995) 83.

36. A.C. Bonamartini, S. Bruni, F. Cariati, L.P. Battaglia, G. Pelozzi, *Inorg. Chim. Acta* 205 (1993) 99.
37. H.-K. Fun, B.-Y. P.Z. Lu, C. Driane, Y. Tsan, -X.Z. You, *Transition Met. Chem.* 21 (1996) 193.
38. J.P. Costus, F. Dahan, M.B. Fernandez Fernandez, M.I. Fernandez Garcia, A.M. Garacia Deibe, J. Sanmartin, *Inorg. Chim. Acta* 274 (1998) 73.
39. L.L. Koh, J.O. Ranford, W.T. Robenson, J.O. Sevensson, A.L.C. Tan, D. Wu, *Inorg. Chem.* 35 (1996) 6466.
40. S. Das, G.P. Muthukumaragopal, S. Pal, S. Pal, *New J. Chem.* 27 (2003) 1102.
41. M. Mohan, P. Sharma, *Inorg. Chim. Acta* 106 (1985) 197.
42. P. Bindu, M.R.P. Kurup, *Transition Met. Chem.* 22 (1997) 578.
43. M.A. Ali, A.H. Mirza, M. Nazimuddin, H. Rahman, R.J. Butcher, *Transition Met. Chem.* 27 (2002) 268.
44. D.N. Sathyanarayana, *Electronic Absorption Spectroscopy and Related Techniques*, Universities Press Publishers, India, 2001.
45. A.B.P. Lever, *Inorganic Electronic Spectroscopy*, Elsevier, Amsterdam 1968.
46. L. Sacconi, M. Ciampolini, *J. Chem. Soc.* (1964) 276.
47. B.J. Hathaway, *Coord. Chem. Rev.* 53 (1983) 87.
48. B. J. Hathaway, D. E. Billing, *Coord. Chem. Rev.* 5 (1970) 143.
49. A.H. Maki, B.R. McGarvey, *J. Chem. Phys.* 29 (1958) 31.
50. A. Fragoso, M.C. Baratto, A. Diaz, Y. Rodriguez, R. Pogni, R. Basosi, R. Cao, *Dalton Trans.* (2004) 1456.
51. A. Rockenbauer, *J. Magn. Reson.* 35 (1979) 429.
52. J. Jezierska, B. Jezowska-Trzebiatowska, G. Petrova, *Inorg. Chim. Acta* 50 (1981) 153.
53. B.J. Hathaway, *J. Chem. Soc., Dalton Trans.* (1972) 1196.
54. R. Pogni, M.C. Baratto, A. Diaz, R. Basosi, *J. Inorg. Biochem.* 79 (2000) 333.
55. I.M. Procter, B.J. Hathaway, P. Nicholls, *J. Chem. Soc.* (1968) 1678.

56. J.F. Villa, W.E. Hatfield, *Inorg. Chem.* 11 (1972) 1331.
57. H. Minemoto, N. Sonoda, K. Miki, *Acta Crystallogr. C* 48 (1992) 737.
58. S. Brahadeeswaran, V. Venkataramanan, J.N. Sherwood, J.L. Bhat, *J. Mater. Chem.* 8 (1998) 613.
59. R. Centore, A. Tuzi, *Acta Crystallogr. C* 57 (2001) 698.
60. J. Buey, S. Coco, L. Diez, P. Espinet, J.M. Martin Alvarez, J.A. Miguel, S. Gracia-Granda, A. Tesoro, I. Ledoux, J. Zyss, *J. Organometallics* 17 (1998) 1750.
61. R. Centore, B. Panunzi, A. Roviello, A. Tuzi, *Acta Crystallogr. C* 58 (2002) m26.
62. L. Dalton, A. Harper, A. Ren, F. Wang, G. Todorova, J. Chen, C. Zhang, M. Lee, *Ind. Eng. Chem. Res.* 38 (1999) 8.

Table 3.1

Crystal data and structure refinement of [CuL]₂, [CuL⁺pi] and [CuL⁺py]

| Parameters | [CuL] ₂ | [CuL ⁺ pi] | [CuL ⁺ py] |
|--|--|--|--|
| Empirical formula | C ₃₆ H ₃₆ Cu ₂ N ₈ O ₈ | C ₂₄ H ₂₅ CuN ₅ O ₄ | C ₂₀ H ₁₆ CuN ₄ O ₅ |
| Formula weight | 835.81 | 511.03 | 455.91 |
| Crystal system | Triclinic | Triclinic | Triclinic |
| Space group | <i>P</i> -1 | <i>P</i> -1 | <i>P</i> -1 |
| Unit cell dimensions | | | |
| <i>a</i> (Å) | <i>a</i> = 5.745(6) | <i>a</i> = 8.132(9) | <i>a</i> = 6.400(4) |
| <i>b</i> (Å) | <i>b</i> = 11.591(3) | <i>b</i> = 10.040(1) | <i>b</i> = 10.082(6) |
| <i>c</i> (Å) | <i>c</i> = 13.158(4) | <i>c</i> = 14.541(7) | <i>c</i> = 15.206(9) |
| α (°) | α = 78.388(7) | α = 99.660(2) | α = 97.936(9) |
| β (°) | β = 77.624(6) | β = 99.976(2) | β = 91.940(9) |
| γ (°) | γ = 83.297(5) | γ = 100.534(2) | γ = 107.864(9) |
| Volume <i>V</i> (Å ³), <i>Z</i> | 835.8(4), 2 | 1125.0(2), 1 | 921.9(10), 2 |
| Calculated density (ρ) (Mg m ⁻³) | 1.660 | 1.509 | 1.642 |
| Absorption coefficient μ (mm ⁻¹) | 1.342 | 1.013 | 1.228 |
| <i>F</i> (000) | 430 | 530 | 466 |
| Crystal size (mm ³) | 0.35 x 0.06 x 0.03 | 0.40 x 0.25 x 0.12 | 0.22 x 0.14 x 0.10 |
| θ range for data collection (°) | 1.68 to 28.28 | 1.45 to 28.26 | 2.15 to 28.33 |
| Index ranges | -8 ≤ <i>h</i> ≤ 8, -13 ≤ <i>k</i> ≤ 13, -19 ≤ <i>l</i> ≤ 19 | -10 ≤ <i>h</i> ≤ 10, -13 ≤ <i>k</i> ≤ 13, -18 ≤ <i>l</i> ≤ 18 | -8 ≤ <i>h</i> ≤ 8, -13 ≤ <i>k</i> ≤ 13, -19 ≤ <i>l</i> ≤ 19 |
| Reflections collected / unique | 8465 / 5012 | 9600 / 5057 | 7468 / 4015 |
| Refinement method | [<i>R</i> (int) = 0.0283] Full-matrix least-squares on <i>F</i> ² | [<i>R</i> (int) = 0.0308] Full-matrix least-squares on <i>F</i> ² | [<i>R</i> (int) = 0.0239] Full-matrix least-squares on <i>F</i> ² |
| Data / restraints / parameters | 5012 / 0 / 325 | 5057 / 0 / 310 | 4015 / 0 / 335 |
| Goodness-of-fit on <i>F</i> ² | 1.098 | 1.115 | 1.065 |
| Final <i>R</i> indices [<i>I</i> > 2 σ (<i>I</i>)] | <i>R</i> ₁ = 0.0598, <i>wR</i> ₂ = 0.1265 | <i>R</i> ₁ = 0.0547, <i>wR</i> ₂ = 0.1202 | <i>R</i> ₁ = 0.0423, <i>wR</i> ₂ = 0.1022 |
| <i>R</i> indices (all data) | <i>R</i> ₁ = 0.0693, <i>wR</i> ₂ = 0.1312 | <i>R</i> ₁ = 0.0638, <i>wR</i> ₂ = 0.1243 | <i>R</i> ₁ = 0.0520, <i>wR</i> ₂ = 0.1068 |

| | |
|----------|-----------|
| Cu1 – N2 | 1.907(7) |
| Cu1 – O2 | 1.973(5) |
| Cu1 – O1 | 1.974(5) |
| Cu1 – O2 | 1.977(5) |
| O1 – C7 | 1.304(9) |
| O2 – C14 | 1.340(9) |
| N1 – C7 | 1.309(9) |
| N1 – N2 | 1.392(8) |
| N2 – Cu1 | 1.907(7) |
| C8 – C9 | 1.406(10) |
| C9 – C10 | 1.389(11) |
| N2 – C8 | 1.298(9) |

| | |
|----------------|----------|
| N2 – Cu1 – O2 | 92.4(2) |
| N2 – Cu1 – O1 | 81.0(2) |
| O2 – Cu1 – O1 | 173.4(2) |
| N2 – Cu1 – O2 | 162.0(3) |
| O2 – Cu1 – O2 | 78.0(2) |
| O1 – Cu1 – O2 | 108.5(2) |
| C7 – O1 – Cu1 | 108.1(5) |
| C14 – O2 – Cu1 | 126.9(5) |
| C14 – O2 – Cu1 | 130.7(5) |
| Cu1 – O2 – Cu1 | 102.0(2) |
| C7 – N1 – N2 | 108.1(6) |
| C8 – N2 – N1 | 116.2(7) |
| C8 – N2 – Cu1 | 127.5(6) |
| N1 – N2 – Cu1 | 116.1(5) |
| C10 – C9 – C8 | 117.7(7) |
| C10 – C9 – C14 | 117.3(7) |
| C8 – C9 – C14 | 125.0(7) |

| | |
|----------|----------|
| Cu1 – O2 | 1.895(2) |
| Cu1 – N2 | 1.911(3) |
| Cu1 – O1 | 1.936(2) |
| Cu1 – N5 | 1.997(3) |
| O1 – C7 | 1.295(4) |
| O2 – C14 | 1.312(3) |
| O3 – N3 | 1.228(3) |
| O4 – N3 | 1.231(3) |
| N2 – C8 | 1.295(4) |
| N2 – N1 | 1.404(3) |
| C6 – C7 | 1.483(4) |
| C7 – N1 | 1.317(4) |

| | |
|----------------|------------|
| O2 – Cu1 – N2 | 94.41(10) |
| O2 – Cu1 – O1 | 171.61(9) |
| N2 – Cu1 – O1 | 80.73(9) |
| O2 – Cu1 – N5 | 93.38(10) |
| N2 – Cu1 – N5 | 172.21(10) |
| O1 – Cu1 – N5 | 91.55(9) |
| C7 – O1 – Cu1 | 110.78(18) |
| C14 – O2 – Cu1 | 126.94(19) |
| C8 – N2 – N1 | 116.8(2) |
| C8 – N2 – Cu1 | 127.0(2) |
| N1 – N2 – Cu1 | 116.15(18) |
| C5 – C6 – C7 | 118.8(3) |
| C1 – C6 – C7 | 121.9(3) |
| O1 – C7 – N1 | 124.6(3) |
| O1 – C7 – C6 | 117.4(3) |
| N1 – C7 – C6 | 117.9(3) |
| C7 – N1 – N2 | 107.5(2) |
| N2 – C8 – C9 | 123.5(3) |

| | |
|-----------|----------|
| N1 – C8 | 1.287(3) |
| N1 – N2 | 1.413(3) |
| N2 – C9 | 1.312(3) |
| C11 – C12 | 1.367(4) |
| C12 – C13 | 1.369(4) |
| O3 – C9 | 1.300(3) |
| O2 – C6 | 1.318(3) |
| Cu1 – O2 | 1.892(1) |
| Cu1 – N1 | 1.921(2) |
| Cu1 – O3 | 1.932(1) |
| Cu1 – N4 | 2.000(2) |

| | |
|-----------------|-----------|
| C8 – N1 – N2 | 116.9(2) |
| C9 – N2 – N1 | 108.0(2) |
| C11 – C12 – C13 | 119.8(3) |
| O4 – N3 – C13 | 118.6(2) |
| O3 – C9 – N2 | 124.6(2) |
| O3 – C9 – C10 | 117.7(2) |
| N2 – C9 – C10 | 117.7(2) |
| C14 – C15 – C10 | 120.8(2) |
| O2 – Cu1 – N1 | 93.55(9) |
| O2 – Cu1 – O3 | 174.32(7) |
| N1 – Cu1 – O3 | 80.96(9) |
| O2 – Cu1 – N4 | 92.46(9) |
| N1 – Cu1 – N4 | 172.65(8) |
| O3 – Cu1 – N4 | 93.13(9) |

CHAPTER FOUR

Syntheses, characterization and non-linear optical properties of nickel(II) and cobalt(II) complexes of the aroylhydrazone ligands

Nickel occurs in various coordination environments of Ni(I), Ni(II) or Ni(III) in biological systems such as the active sites of certain hydrogenases and dehydrogenases [1] and hence are of great interest to inorganic biochemists. The trace presence of Ni is essential for bacteria, plants, animals and humans [2], nickel has been chosen for study, as many nickel complexes are coordinatively unsaturated, can behave as Lewis acids. The redox chemistry of nickel has received considerable attention in the last few years due to its essential role in bioinorganic chemistry and several enzymes [3-4]. Morrow and Kolasa reported the cleavage of plasmid DNA by square planar nickel-salen [bis-(salicylidene)ethylenediamine] in the presence of either magnesium monoperoxyphthalic acid (MPPA) or iodosylbenzene [5]. The observation of different oxidation states for nickel during the catalytic cycle, has spurred a great interest in the investigation of the electronic and structural factors that contribute to stabilize a particular oxidation state for the nickel center. Several factors have been recognized to be particularly important in the stabilization of the +3 and +1 oxidation states, namely coordination number, geometry, type of donor atom and electronic characteristics of the ligand.

Ni(II) complexes of aroylhydrazones have been studied extensively [6-15]. Ivanovic et al. [16] have studied the denticities of bis(acylhydrazone) with Ni(II) ion. Because of steric requirements [17] and due to a lower electron density in $d_{x^2-y^2}$ than

in d_{xy} orbital of Ni(II) ion [16], tetracoordination of bis(acylhydrazone) ligand involves the coordination of one hydrazide NH group accompanied by deprotonation. The same group reported [18] the first tridentate coordination of bis(acylhydrazone)-2,6-diacetylpyridine in which the Ni(II) metal center attained a distorted octahedral geometry. The coordination complexes of nickel are also studied for their magnetic behavior. For instance, the magnetic properties of Ni(II) complexes of diazomesocyclic ligands are carried out by Bu et al. [19], and these compounds are observed to be antiferromagnetic. Similarly, conformationally rigid molecular squares of $[\text{Ni}(\text{HL})_4]^{4+}$ are prepared from bis[phenyl(2-pyridyl)methanone]-thiocarbazone and their magnetic studies reveal antiferromagnetic characteristics [20]. However, a dinuclear nickel complex containing triethylene tetramine and tricyanomethamide is found to exhibit ferromagnetic attributes [21]. The non-linear optical properties of Ni(II) complexes are of great interest now and a number of such attempts have been reported recently both as monomeric and polymeric analogues.

The synthesis and reactivity of cobalt complexes of Schiff base ligands have played an important part in the development of coordination chemistry [22-23]. The cobalt complexes of tetradentate Schiff base ligands have been extensively used to mimic cobalamin (B_{12}) coenzymes [24-26], dioxygen carriers and oxygen activators [27-29] and enantioselective reduction [30]. Some Co(III) complexes with two amines in axial positions are also used as antimicrobial agents [31]. There have also been a large number of investigations on cobalt complexes based on the metal-radical approach for molecular magnets. The coordinational diversity and biological activities of a number of cobalt(II) metal complexes of acylhydrazones have been reported, but the investigations in the field of non-linear optical activities of this type of complexes are less studied. Hence in this chapter we are discussing the synthesis, spectral and structural characterization and non-linear optical activities of some Ni(II)

and Co(II) metal complexes of the three principal ligands discussed in Chapter 2 with pyridine and 4-picoline as auxiliary ligands.

4.1. Stereochemistry of Ni complexes

Nickel compounds occur usually in +2 oxidation state and the compounds of higher oxidation states are found to be less stable. Stereochemistry and electronic structures of Ni(II) complexes vary with the coordination numbers ranging from 3 to 6. Ni²⁺ state is a d^8 system and the main coordination environments are octahedral and square planar and is a most common example for tetragonal distortion. Some examples for trigonal bipyramidal, square pyramidal and tetrahedral nickel complexes are also reported. Here we have prepared nine Ni(II) complexes, three of each ligands. Tridentate dibasic Schiff bases are excellent ligands in forming dinuclear species of metal ions, which prefer square planar geometry. Aroylhydrazones of *o*-hydroxyaldehydes used here are such species and provide a phenolic –OH, an imine –N and an amide –O as coordinating centers. In a dinuclear complex either the phenolate –O or the deprotonated amide –O can act as the bridging atom. It has been found earlier that in a situation similar to this the most negatively charged center is preferred as the bridging atom in the dinuclear nickel(II) complexes. In the pyridine and picoline incorporated analogues, four coordinated complexes are expected, three from the principal ligand and one from pyridine or picoline.

4.2. Stereochemistry of Co complexes

Cobalt exhibits two important oxidation states as +2 and +3, and salts of Co(II) are more stable, as they are not easily oxidized to Co(III) state. However, in basic solutions, oxidation of Co²⁺ to Co³⁺ takes place relatively easily. It is usually found that when both oxidation states of an element are subject to complex formation,

the overall formation constant is greater for the higher oxidation state and thus complexation makes it difficult to be reduced. Thus, Co(III) is stabilized by complexation and Co(II) forms relatively few complexes, which are not as stable as the corresponding complexes of Co(III). However, high spin six coordinate, high/low spin five coordinate and four coordinate complexes of Co(II) are widely reported. It is observed that Co(II) forms more tetrahedral complexes than any other transition metal ion, except Zn(II), due to its d^7 configuration, which is more favorable for taking up a tetrahedral geometry than an octahedral alignment. However, the difference in the stability between the two geometries of Co(II) is small so that there exists sometimes equilibrium between the two structures.

The ground state in a Co^{2+} tetrahedral is 4A_2 and the possible transitions are ${}^4A_2 \rightarrow {}^4T_2$; ${}^4A_2 \rightarrow {}^4T_1(F)$; and ${}^4A_2 \rightarrow {}^4T_1(P)$. Usually, the ${}^4A_2 \rightarrow {}^4T_1(F)$; and ${}^4A_2 \rightarrow {}^4T_1(P)$ transitions appear as multiple absorption in the near infrared and visible regions respectively. These bands help to distinguish between tetrahedral and octahedral structures, since the latter shows less intense bands near 1000 and 500 nm corresponding to ${}^4T_{1g} \rightarrow {}^4T_{2g}$ and ${}^4T_{1g} \rightarrow {}^4T_{1g}(P)$ transitions. The electronic spectrum of four coordinate square planar complexes of Co(II) is similar to that of the low spin five coordinate Co^{2+} complexes. This gives rise to mainly two absorption bands corresponding to ${}^2A_1 \rightarrow {}^2E$ at higher and ${}^2A_1 \rightarrow {}^2B_1$ at lower energy regions. In the case of Co^{3+} , six coordinate geometry make up the majority of known Co(III) complexes. They are invariably low spin and diamagnetic with ${}^1A_{1g}$ ground state. Electronic spectra of six-coordinate low spin Co(III) complexes usually show two bands corresponding to the spin allowed transitions ${}^1A_{1g} \rightarrow {}^1T_{1g}$ and ${}^1A_{1g} \rightarrow {}^1T_{2g}$.

4.3. Experimental

4.3.1. Materials

4-Nitrobenzoyl hydrazide (Sigma Aldrich), 4-*N,N*-diethylamino-2-hydroxybenzaldehyde (Sigma Aldrich), 4-methoxy-2-hydroxybenzaldehyde (Sigma Aldrich), 4-methoxy-2-hydroxyacetophenone (Sigma Aldrich), nickel(II) acetate (CDH), cobalt(II) acetate (BDH), pyridine, 4-picoline, DMF (S.D. Fine) were used as received. When ethyl alcohol was used as the solvent repeated distillation was carried out before use.

4.3.2. Syntheses of ligands

Preparation of the ligands H_2L^1 , H_2L^2 and H_2L^3 were done as described previously in Chapter 2.

4.3.3. Preparation of nickel(II) complexes

$[NiL^1]_2 \cdot 4H_2O$ (**10**): A mixture of the ligand H_2L^1 (0.374 g, 1 mmol) and nickel(II) acetate (0.249 g, 1 mmol) was refluxed in a 1:1 mixture of absolute ethanol and DMF. The light red product obtained was filtered and washed several times with absolute ethanol followed by diethyl ether and dried over P_4O_{10} *in vacuo*. Yield: 0.832 g (70.3%). Elemental Anal. Found (Calcd.) (%): C, 48.24 (48.14); H, 4.30 (4.94); N, 12.45 (12.48).

$[NiL^1py]$ (**11**): After dissolving 0.200 g (0.22 mmol) of complex **10** in 15 ml boiling pyridine, the solution was boiled for about 5 minutes and poured the cooled solution to cold water, so that a red colored product was obtained. It was filtered, washed several times with absolute ethanol followed by diethyl ether and dried over

P₄O₁₀ *in vacuo*. Yield: 0.367 g (74.5%). Elemental Anal. Found (Calcd.) (%): C, 56.10 (56.13); H, 4.77 (4.71); N, 13.89 (14.23).

[NiL¹pi] (**12**): 0.200 g (0.22 mmol) of the complex **10** was dissolved in 15 ml of boiling 4-picoline for 5 minutes and after cooling the solution was added to cold water. The bright red colored product obtained was filtered, washed several times with absolute ethanol followed by diethyl ether and dried over P₄O₁₀ *in vacuo*. Yield: 0.320 g (63.2%). Elemental Anal. Found (Calcd.) (%): C, 57.98 (56.95); H, 4.96 (4.98); N, 13.93 (13.84).

[NiL²]₂ (**13**): The complex was prepared by refluxing a mixture of the ligand H₂L² (0.315 g, 1 mmol) and nickel(II) acetate (0.249 g, 1 mmol) in a 1:1 mixture of absolute ethanol and DMF. The orange colored product obtained on cooling the reaction mixture to room temperature was filtered, washed several times with absolute ethanol followed by diethyl ether and dried over P₄O₁₀ *in vacuo*. Yield: 0.591 g (79.5%). Elemental Anal. Found (Calcd.) (%): C, 48.48 (48.44); H, 3.09 (2.98); N, 11.16 (11.30).

[NiL²py] (**14**): After dissolving 0.200 g (0.27 mmol) of complex **13** in 15 ml boiling pyridine, the solution was boiled for about 5 minutes and poured the cooled solution to cold water, so that a red colored product was obtained. It was filtered, washed several times with absolute ethanol followed by diethyl ether and dried over P₄O₁₀ *in vacuo*. Yield: 0.291 g (64.5%). Elemental Anal. Found (Calcd.) (%): C, 53.28 (53.26); H, 3.198(3.58); N, 12.25 (12.42).

[NiL²pi] (**15**): The complex was prepared by dissolving 0.200 g (0.27 mmol) of complex **13** in 15 ml of boiling 4-picoline and again boiled for 5 minutes. The solution was then added to water and the brown colored solid formed was recovered by filtration. Washed several times with absolute ethanol followed by diethyl ether and dried over P₄O₁₀ *in vacuo*. Yield: 0.319 g (68.7%). Elemental Anal. Found (Calcd.) (%): C, 54.78 (54.23); H, 3.51 (3.90); N, 11.97 (12.05).

$[\text{NiL}^3]_2 \cdot 4\text{H}_2\text{O}$ (**16**): The ligand H_2L^3 (0.329 g, 1 mmol) and nickel(II) acetate (0.249 g, 1 mmol) were dissolved in a 1:1 mixture of absolute ethanol and DMF and refluxed for about two hours. The red colored product obtained was filtered, washed several times with absolute ethanol followed by diethyl ether and dried over P_4O_{10} *in vacuo*. Yield: 0.586 g (69.4%). Elemental Anal. Found (Calcd.) (%): C, 45.62 (45.54); H, 3.85 (4.06); N, 10.07 (9.96).

$[\text{NiL}^3\text{py}]$ (**17**): The complex was prepared by dissolving 0.200 g (0.24 mmol) of complex **16** in 15 ml of boiling pyridine and again boiled for 5 minutes. The solution was then added to water and the red colored solid formed was recovered by filtration. Washed several times with absolute ethanol followed by diethyl ether and dried over P_4O_{10} *in vacuo*. Yield: 0.293 g (63.1%). Elemental Anal. Found (Calcd.) (%): C, 54.23 (54.60); H, 3.90 (4.17); N, 12.05 (11.88).

$[\text{NiL}^3\text{pi}]$ (**18**): 0.200 g (0.24 mmol) of the complex **16** was dissolved in 15 ml of boiling 4-picoline for 5 minutes and after cooling the solution was added to cold water. The red colored product obtained was filtered, washed several times with absolute ethanol followed by diethyl ether and dried over P_4O_{10} *in vacuo*. Yield: 0.289 g (60.3%). Elemental Anal. Found (Calcd.) (%): C, 55.52 (55.15); H, 3.99 (4.21); N, 11.62 (11.69).

4.3.4. Preparation of cobalt(II) complexes

$[\text{CoL}^1]_2$ (**19**): The preparation was done by refluxing a mixture of the ligand H_2L^1 (0.374 g, 1 mmol) and cobalt(II) acetate (0.249 g, 1 mmol) in 1:1 mixture of absolute ethanol and DMF. The brown colored product obtained on cooling the reaction mixture to room temperature was filtered, washed several times with absolute ethanol followed by diethyl ether and dried over P_4O_{10} *in vacuo*. Yield: 0.492 g

(59.5%). Elemental Anal. Found (Calcd.) (%): C, 52.11 (52.31); H, 4.31 (4.39); N, 13.24 (13.56).

[CoL¹py]·4H₂O (**20**): The complex was prepared by dissolving 0.200 g (0.24 mmol) of complex **19** in 15 ml of boiling pyridine and again boiled for 5 minutes. The solution was then added to water and the dark red colored solid formed was recovered by filtration. Washed several times with absolute ethanol followed by diethyl ether and dried over P₄O₁₀ *in vacuo*. Yield: 0.387 g (68.6%). Elemental Anal. Found (Calcd.) (%): C, 48.32 (48.94); H, 4.62 (5.54); N, 12.01 (12.41).

[CoL²]₂ (**21**): A mixture of equimolar amounts of the ligand H₂L² (0.315 g, 1 mmol) and cobalt(II) acetate (0.249 g, 1 mmol) was refluxed in 1:1 mixture of absolute ethanol and DMF. The red product obtained was filtered and washed several times with absolute ethanol followed by diethyl ether and dried over P₄O₁₀ *in vacuo*. Yield: 0.489 g (65.7%). Elemental Anal. Found (Calcd.) (%): C, 49.06 (48.40); H, 3.08 (2.98); N, 11.34 (11.29).

[CoL²py] · ½ H₂O (**22**): The complex was prepared by dissolving 0.200 g (0.27 mmol) of complex **21** in 15 ml of boiling pyridine and again boiled for 5 minutes. The solution was then added to water and the red colored solid formed was recovered by filtration. Washed several times with absolute ethanol followed by diethyl ether and dried over P₄O₁₀ *in vacuo*. Yield: 0.312 g (67.8%). Elemental Anal. Found (Calcd.) (%): C, 53.23 (53.60); H, 3.57 (3.17); N, 12.41 (12.58).

[CoL³]₂ (**23**): The complex was prepared by refluxing the ligand H₂L³ (0.329 g, 1 mmol) and cobalt(II) acetate (0.249 g, 1 mmol) in 1:1 mixture of absolute ethanol and DMF. The dark red product obtained on cooling the reaction mixture to room temperature was filtered, washed several times with absolute ethanol followed by

diethyl ether and dried over P_4O_{10} *in vacuo*. Yield: 0.496 g (64.2%). Elemental Anal. Found (Calcd.) (%): C, 49.86 (49.76); H, 3.53 (3.39); N, 10.73 (10.88).

[CoL³py] (**24**): 0.200 g (0.26 mmol) of the complex **23** was dissolved in 15 ml of boiling pyridine for 5 minutes and after cooling the solution was added to cold water. The red colored product obtained was filtered, washed several times with absolute ethanol followed by diethyl ether and dried over P_4O_{10} *in vacuo*. Yield: 0.302 g (64.9%). Elemental Anal. Found (Calcd.) (%): C, 54.20 (54.67); H, 3.90 (3.86); N, 12.04 (11.92).

4.4. Results and discussion

Equimolar ratios of the ligands and nickel(II) acetate resulted in complexes of stoichiometry, [NiL₂]. The attempts to prepare heterocyclic bases, both pyridine and 4-picoline incorporated complexes by direct reaction between the ligand and metal complexes were not successful as in the case of copper complexes and the same method for copper complexes were adopted here also. All the complexes are expected to have four-coordinated environment around the metal center. The colors of the compounds were found to be light to brownish red. All the nickel complexes were diamagnetic from their magnetic susceptibility measurements and it is concluded that all of them are low spin d^8 systems. All the complexes were found to be soluble in DMF and DMSO, but only partially soluble in other organic solvents such as $CHCl_3$, ethanol, methanol etc.

The same procedure of preparation of nickel complexes was followed in the case of the cobalt complexes, but it was not successful to isolate any of the picoline substituted monomer analogues. The reactions yielded a dark brown colored liquid and none of the solid was isolated. We have prepared six cobalt complexes, three

dimers and three monomers having pyridine as heterocyclic bases. The magnetic susceptibility measurements of the cobalt complexes showed values in the range of 1.83 – 1.92 BM, which is in the range expected for low spin d^7 Co(II) complexes. The elemental analyses data also gave an idea of four-coordinated geometry for the cobalt complexes. Three cobalt complexes were found to be soluble in DMF and DMSO and only partially soluble in CHCl_3 , ethanol, methanol etc.

4.4.1. Crystal structure of complexes

4.4.1a. Crystal structure of $[\text{NiL}^1\text{py}_3]\text{py}$ (11a)

The structure of the Ni(II) complex together with the atom numbering scheme is shown in Fig. 4.1. Single crystals suitable for X-ray crystallographic studies were prepared by slow evaporation of solution of $[\text{NiL}^1\text{py}]$ in pyridine. But in contrary to the expected structure, the complex showed a six-coordinated environment by incorporating two extra pyridine molecules in axial positions. The molecule crystallizes in a triclinic lattice with a space group of $P\bar{1}$. The structural refinement parameters are given in Table 4.1 and the selected bond distances and bond angles are given in Tables 4.2 and 4.3. In this complex, the dinegative *N*-4-diethylaminosalicylidine-*N'*-4-nitrobenzoylhydrazone is coordinated to Ni(II) through the deprotonated enolate oxygen O1, deprotonated phenolic oxygen O2 and azomethine nitrogen N2 forming five and six membered chelate rings. The fourth site is occupied by the pyridyl nitrogen N6. In addition to this two extra pyridine molecules are coordinated to the metal center through N5 and N7. In the crystal lattice, the Ni(II) is in a distorted octahedral environment, but the two extra incorporated pyridine molecules are in trans positions with N5–Ni–N7 bond angle 178.25(9) Å.

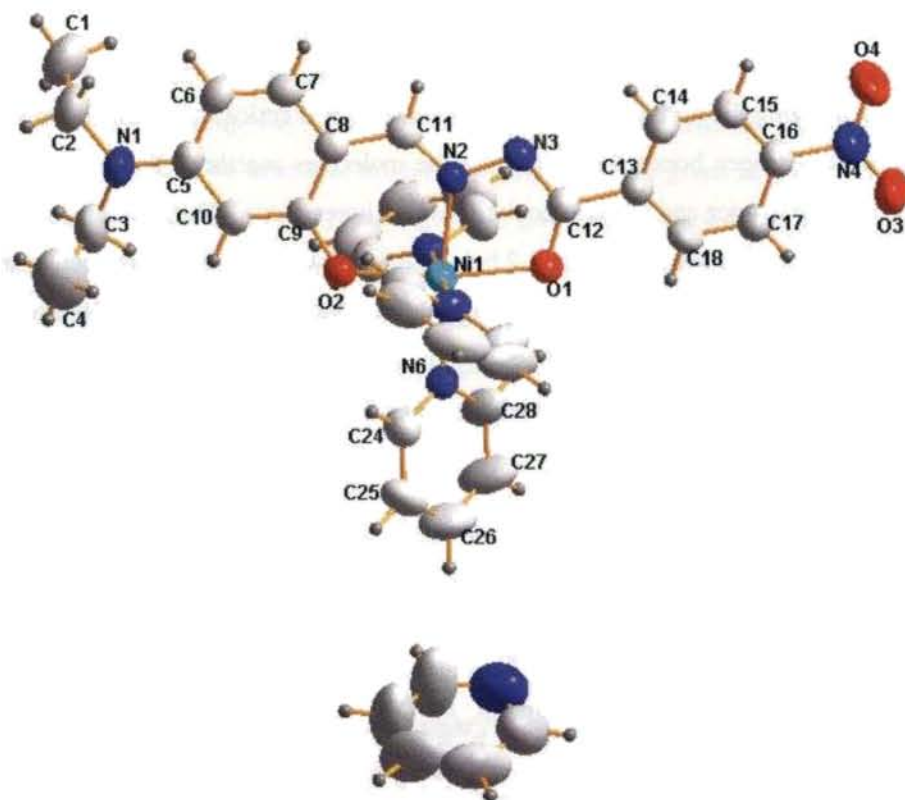


Fig. 4.1. Molecular structure of $[\text{NiL}^1\text{py}_3]\text{py}$. The atoms are shown at 50% probability.

From the crystal data, the coordination sites of ligand can be concluded by considerable change in bond lengths and bond angles from the corresponding values of the ligand. The C11–N2 bond length is increased to 1.291(4) Å from 1.267 Å and N2–N3 bond length from 1.378 Å to 1.394(3) Å in the free ligand, which confirms the coordination through azomethine nitrogen. The C9–O2 bond length is changed to 1.307(3) Å and C12–O1 to 1.280(3) from 1.338 (4) Å and 1.219 (5) Å respectively.

The first bond length increases due to coordination of phenolate oxygen and the second one decreases as a result of enolization and coordination.

Analyzing the arrangement of molecules in crystal lattice shows that there are no classical hydrogen bonds for connecting the molecules together. The packing is effected by weak inter and intramolecular C—H \cdots π interactions. The packing pattern of the molecules is shown in the Fig. 4.2 below. As we consider adjacent molecules in the lattice, they are arranged in such a way that the principal ligand molecules are in offset fashion as in the ligand lattice. This arrangement may have a stacking interaction of two phenyl groups, which plays a key role in the packing arrangement.

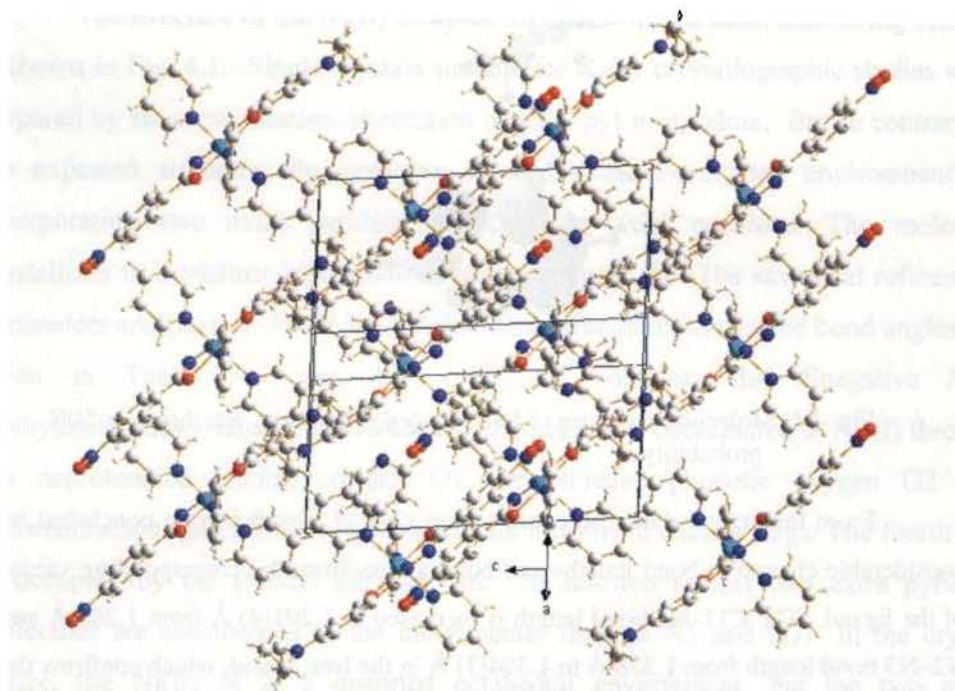


Fig. 4.2. Molecular packing diagram of $[\text{NiL}^1\text{py}_3]\text{py}$.

4.4.1b. Crystal structure of $[\text{NiL}^1\text{pi}]$ (12)

The structure of the Ni(II) complex together with the atom numbering scheme is shown in Fig. 4.3. The molecule crystallizes in a triclinic lattice with a space group of $P\bar{1}$. The structural refinement parameters are given in Table 4.1 and the selected bond distances and bond angles are given in Tables 4.4 and 4.5. In this complex the dinegative *N*-4-diethylaminosalicylidine-*N'*-4-nitrobenzoylhydrazone is coordinated to Ni(II) through the deprotonated phenolic oxygen O1, azomethine nitrogen N2 and deprotonated enolate oxygen O2 forming five and six membered chelate rings. The fourth site is occupied by the pyridyl nitrogen of 4-picoline N5.

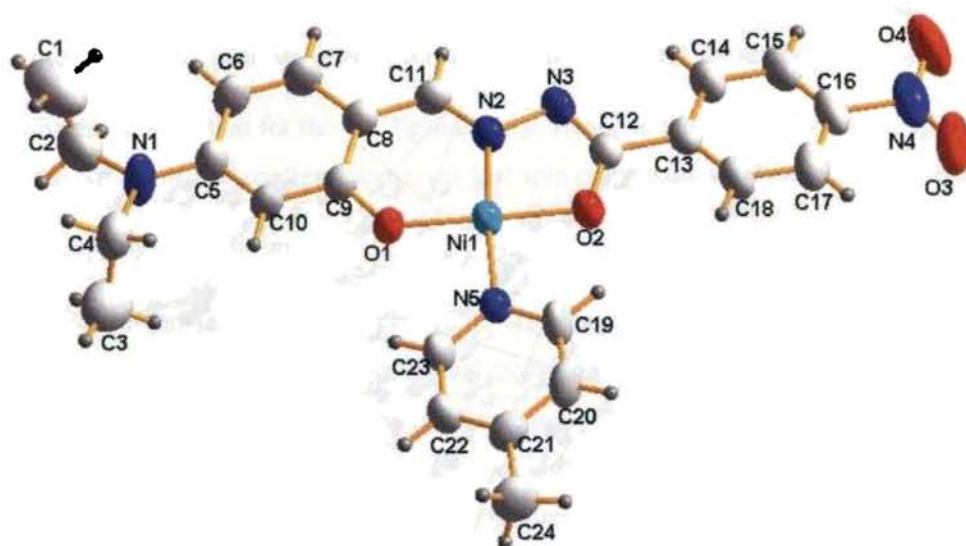


Fig. 4.3. Molecular structure of $[\text{NiL}^1\text{pi}]$. The atoms are shown at 50% probability.

The Ni(II) is in a distorted square planar arrangement and lies approximately in the plane of the ligand with a slight deviation of 0.0075 \AA with the six membered

chelate ring and 0.0046 Å with the five membered chelate ring. The 4-picoline ring makes a dihedral angle of 15° and 17° with the six and five membered chelate rings respectively. The C11–N2 and N2–N3 bonds of the ligand are found to be slightly increased and N3–C12 bond is found to be slightly decreased after coordination confirming the proposed mode of coordination. The complex is approximately planar with a distorted square planar structure with the basal plane occupied by the hydrazone ligand and the nitrogen atom of picoline. The distortion from the regular square planar structure is determined from the departure of the bond angles around Ni(II) [O1–Ni1–N2 (95.04(12), N2–Ni1–O2 (83.49(13), O1–Ni1–N5 (90.00(11), O2–Ni1–N5 (91.48(12))] from 90°. The found distortion may be due to the rigidity of the chelate rings formed. The structure reported here are more or less similar to the similar compounds reported earlier [32-34].

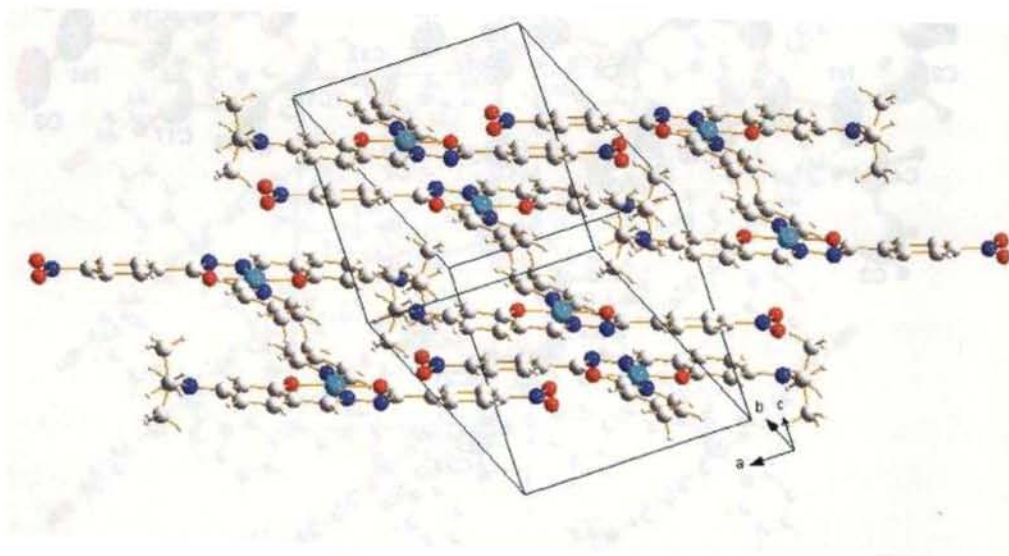


Fig. 4.4. Molecular packing diagram of [NiL¹pi].

In the crystal lattice (Fig. 4.4), the packing is effected by a wide network of π - π staking interactions involving Cg(4) and Cg(5) consisting of C5, C6, C7, C8, C9,

C10 and C13, C14, C15, C16, C17, C18, respectively. No classic hydrogen bonds are found in the lattice, but a weak one involving C20–H2···O3. Additional Y–X··· π ring interactions are found between N4–O3 and Cg1, N4–O3 and Cg2, similarly between N4–O4 and Cg2 ranging from 3.459 – 3.595 Å.

4.4.2. Spectral characteristics of nickel complexes

4.4.2a. Electronic spectral studies

Square planar situation is in fact the limit of weak field along the 'z' axis of an octahedron i.e., axial elongation. With decrease in energy of the z orbitals, the energy of $d_{x^2-y^2}$ increases, since in a real molecule, as the field along the z axis decreases, the positive charge remaining on the metal increases resulting in an increased attraction for the d_{xy} ligands [35]. Hence in the presence of a strong field, the Ni²⁺ with a d^8 configuration gives low spin complexes with the eight d electrons occupying the low-energy d_{xz} , d_{yz} , d_{z^2} and d_{xy} orbitals, while the high energy $d_{x^2-y^2}$ orbital remains unoccupied [36]. The four lower orbitals are often so close together in energy, that the individual transitions there from to the upper d level cannot be distinguished. Hence the electronic spectra of d^8 square planar complexes with strong field ligands typically show a single band in the range of 400 – 600 nm. However, there are many examples where three transitions often in the form of weak shoulders or peaks are observed on each side of the main stronger absorption band. The electronic spectral pattern of the three nickel complexes of ligand H₂L¹ is shown in the Fig. 4.5.

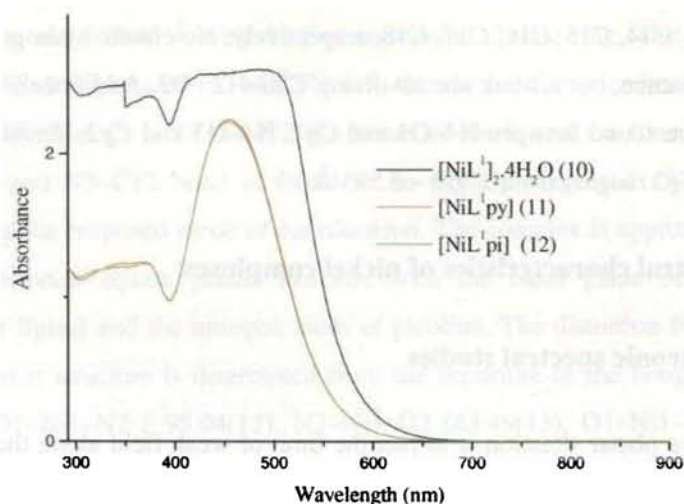


Fig. 4.5. The electronic spectra of the compounds **10**, **11** and **12** in DMF.

All the three nickel complexes have very strong and broad bands in the region 400-600 nm. The very broad band is due to the reason that all the four lower energy orbitals are so closer together in energy that the individual transitions cannot be distinguished. There are weak absorptions in 300 – 400 nm regions due to absorptions in the ligand molecule, both $\pi \rightarrow \pi^*$ and $n \rightarrow \pi^*$ transitions. In these complexes, the eight electrons being paired in the four lower lying d orbitals. The upper $d_{x^2-y^2} (b_{1g})$ remains vacant in this case. The four lower orbital are often close in energy, that individual transitions there from to the upper d level cannot be distinguished. Hence a single absorption band is observed. A second more intense band may be seen near 300-380 nm, which is often charge transfer in origin. But in this case, it may merge in the band due to $\pi \rightarrow \pi^*$ and $n \rightarrow \pi^*$ transitions. Since there is no absorption below 300 nm, the planar geometry of the complex is confirmed [37-40].

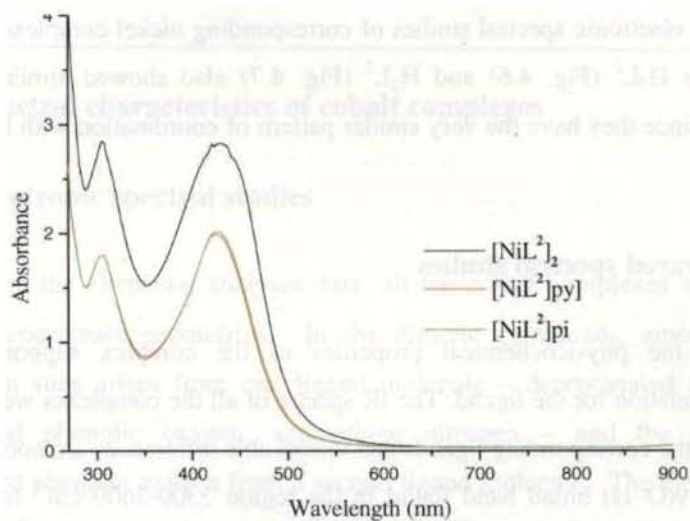


Fig. 4.6. The electronic spectra of the compounds **13**, **14** and **15** in DMF.

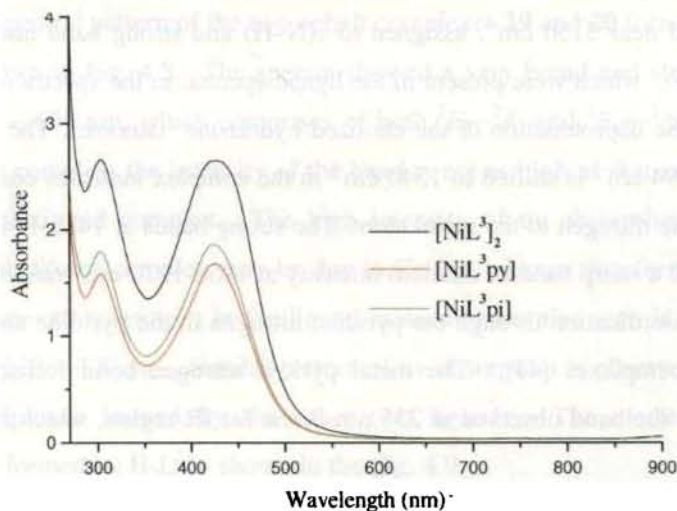


Fig. 4.7. The electronic spectra of the compounds **16**, **17** and **18** in DMF.

The electronic spectral studies of corresponding nickel complexes formed by both ligands H_2L^2 (Fig. 4.6) and H_2L^3 (Fig. 4.7) also showed similar pattern of absorption since they have the very similar pattern of coordination with the discussed complexes.

4.4.2b. Infrared spectral studies

All the physicochemical properties of the complex supports dianionic tridentate chelation for the ligand. The IR spectra of all the complexes were compared with that of the corresponding ligands and remarkable differences are noticed between them. The $\nu(O-H)$ broad band found in the region $3300-3600\text{ cm}^{-1}$ for the ligand disappears in the complexes, suggesting coordination through deprotonated phenolic oxygen. Weak absorptions observed above 3200 cm^{-1} for the complexes **10** and **16** are due to the presence of lattice water molecules. The absence of the medium intensity band near 3150 cm^{-1} , assigned to $\nu(N-H)$ and strong band near 1630 cm^{-1} due to $\nu(C=O)$, which were present in the ligand spectra, in the spectra of complexes substantiate the deprotonation of the enolized hydrazone tautomer. The band due to $\nu(C=N)$ at 1594 cm^{-1} is shifted to 1540 cm^{-1} in the complex indicates coordination of the azomethine nitrogen to the metal atom. The strong bands at $1465-1445$ and $1230-1220\text{ cm}^{-1}$ and a sharp band of medium intensity at $1050-1020\text{ cm}^{-1}$ range confirm the presence of coordination through the pyridine nitrogen in the pyridine and 4-picoline coordinated complexes [41]. The metal pyridyl nitrogen bond formation can be confirmed by the band observed at 235 nm in the far IR region, which is typical for Ni-py bond.

4.4.3. Spectral characteristics of cobalt complexes

4.4.3a. Electronic spectral studies

From the elemental analyses data, all the cobalt complexes are expected to have four coordinate geometries. In the dimeric complexes, among four, three coordination sites arises from one ligand molecule – deprotonated enolic oxygen, deprotonated phenolic oxygen, azomethine nitrogen – and the fourth one is deprotonated phenolic oxygen from a second ligand molecule. The electronic spectra of four coordinate square planar complexes of Co(II) are similar to that of the low spin five coordinate Co^{2+} complexes. This gives rise to mainly two absorption bands corresponding to ${}^2E \leftarrow {}^2A_1$ at higher and ${}^2B_1 \leftarrow {}^2A_1$ at lower energy regions. The electronic spectral pattern of the two cobalt complexes **19** and **20** formed by the ligand H_2L^1 is shown in Fig. 4.8. The spectra showed a very broad and strong band in the region 400 – 650 nm, which comprises of both ${}^2E \leftarrow {}^2A_1$ and ${}^2B_1 \leftarrow {}^2A_1$ transitions. For the dimeric complex, the intensity of the band is not as high as that in the monomeric pyridine substituted complex. The high intensity of uv absorption in the case of pyridine substituted complex may be due to $\text{Co} \rightarrow \text{py}$ charge transfer transitions. The $\pi \rightarrow \pi^*$ and $n \rightarrow \pi^*$ transitions in the ligand molecules are also seen in the spectrum in the region 320 – 400 nm. Similar pattern of uv absorption is observed in the case of cobalt complexes formed by the other two ligands. The electronic spectra of complexes formed by H_2L^3 is shown in the Fig. 4.9.

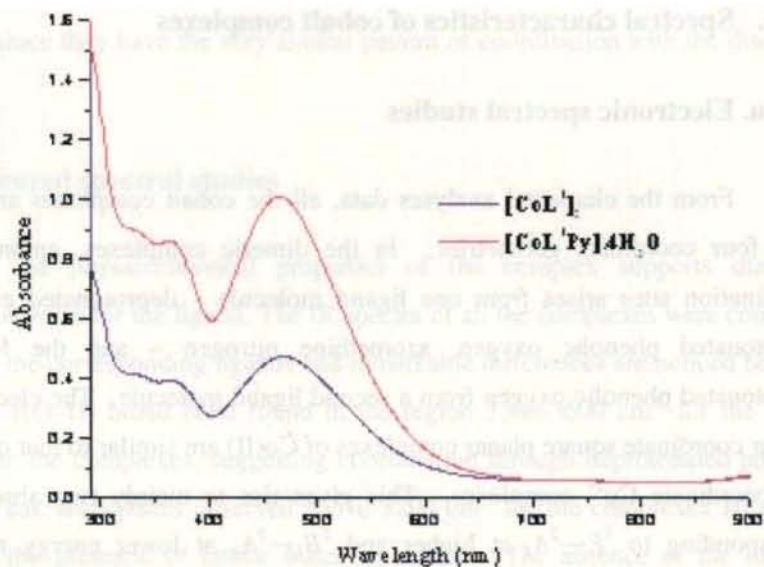


Fig. 4.8. The electronic spectra of the compounds **19** and **20** in DMF.

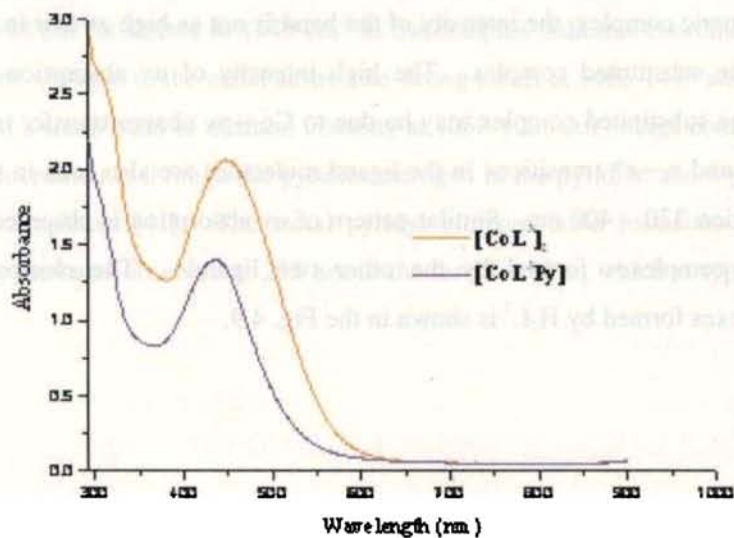


Fig. 4.9. The electronic spectra of the compounds **23** and **24** in DMF.

4.4.3b. Infrared spectral studies

The IR spectral studies of the Co(II) complexes suggest a very similar coordination pattern with the nickel complexes. All the infrared spectra were recorded in solid state as KBr pellets. Only the complexes **20** and **22** showed absorption bands above 3150 cm^{-1} , indicating the presence of water in the molecular lattice. Disappearance of broad band due to $\nu(\text{O-H})$ and medium intensity band due to $\nu(\text{N-H})$ from $3300\text{-}3600\text{ cm}^{-1}$ and 3150 cm^{-1} respectively confirms the coordination of the ligands through deprotonated phenolic and enolic oxygens. The strong band around 1630 cm^{-1} observed in the ligand spectra due to $\nu(\text{C=O})$ was also disappeared in the complex spectra because of coordination through enolic oxygen.

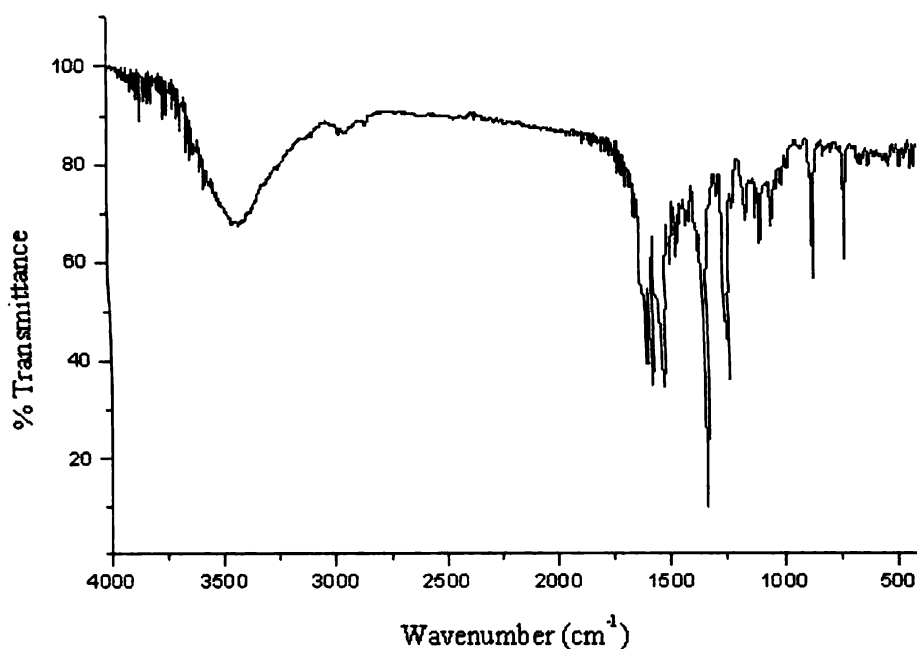


Fig. 4.10. The IR spectrum of the complex $[\text{CoL}^3]_2$ (**23**).

The bands in the ligand spectra due to $\nu(\text{C}=\text{N})$ in $1590 - 1610 \text{ cm}^{-1}$ were found to be shifted to lower frequency region in the infrared spectra of complexes. This is due to the lowering of electron density around this bond and it confirms the coordination through azomethine nitrogen atom. The phenolic oxygen in the second ligand molecule satisfies the fourth coordination sites in the dimeric complexes. The elemental analyses data of the complexes also supports this fact. In the case of pyridine and 4-picoline substituted complexes, the presence of metal-pyridyl nitrogen bond is confirmed by the spectra in far IR region. There are absorption bands around $238 - 242 \text{ cm}^{-1}$ in the far IR spectra [42] of these complexes and it confirms Co-py bond in them. The infrared absorption spectrum of the complex $[\text{CoL}^3]_2$ (**23**) is shown in Fig. 4.10.

4.4.3c. EPR spectral studies

All the cobalt complexes prepared were found to paramagnetic from the magnetic susceptibility measurements. The μ value calculated per cobalt atom in all the complexes were found to around $1.83 - 1.92 \text{ BM}$, from which it is concluded that all the complexes are low spin d^7 systems, i.e. Co(II) metal environment. So the X-band electron paramagnetic resonance studies of all the complexes were done, both in powder form at room temperature and in frozen state at liquid nitrogen temperature. But the powder state spectra were not clear to identify the electron environments. The frozen state spectra reveal axial features with g values, $g_{\parallel}=2.41$ and $g_{\perp}=2.025$ ($[\text{CoL}^2]_2$ (**21**)); $g_{\parallel}=2.34$ and $g_{\perp}=2.08$ ($[\text{CoL}^1\text{py}] \cdot 4\text{H}_2\text{O}$ (**20**)); $g_{\parallel}=2.28$ and $g_{\perp}=1.98$ ($[\text{CoL}^3]_2$ (**23**)); $g_{\parallel}=2.24$ and $g_{\perp}=2.008$ ($[\text{CoL}^1]_2$ (**19**)). The EPR spectra of other two cobalt complexes **22** and **24** were not so resolved to interpret the electron environment. The Co(II) nucleus has a nuclear spin of $7/2$ and hence eight hyperfine lines are expected in the EPR spectrum. It is interesting to note that in the

perpendicular region of the frozen state, these hyperfine splittings are clearly resolved (Figs. 4.11 – 4.14). Since it is observed that $g_{\parallel} > g_{\perp}$, considering the four-coordinate nature of the complex, a square planar geometry may be assigned to the complex.



Fig. 4.11. The EPR spectrum of $[\text{CoL}_2]_2$ (**21**) at 77 K in DMF.

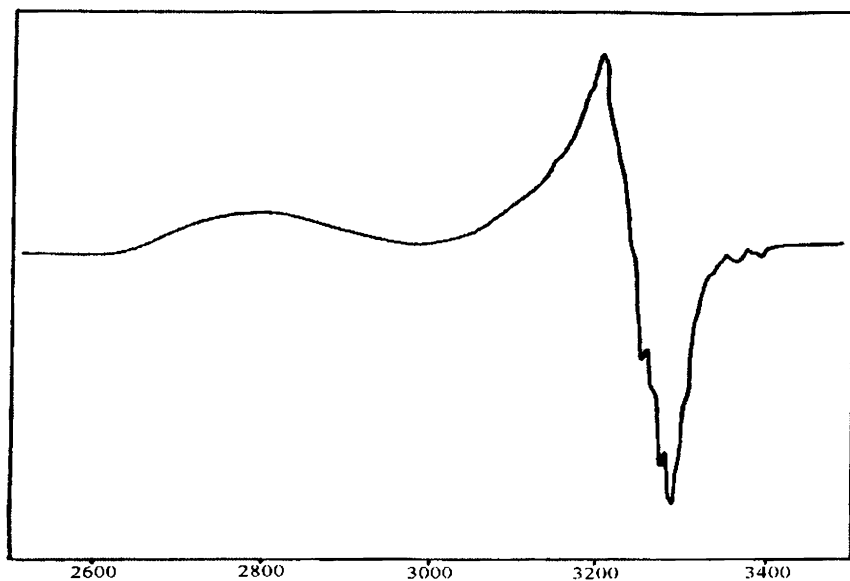


Fig. 4.12. The EPR spectrum of $[\text{CoL}^1\text{py}] \cdot 4\text{H}_2\text{O}$ (**20**) at 77 K in DMF.

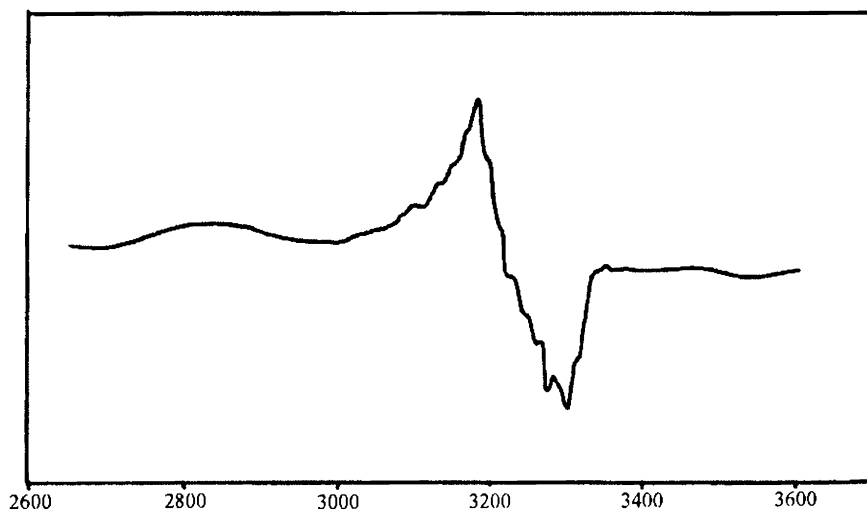


Fig. 4.13. The EPR spectrum of $[\text{CoL}^3]_2$ (**23**) at 77 K in DMF.

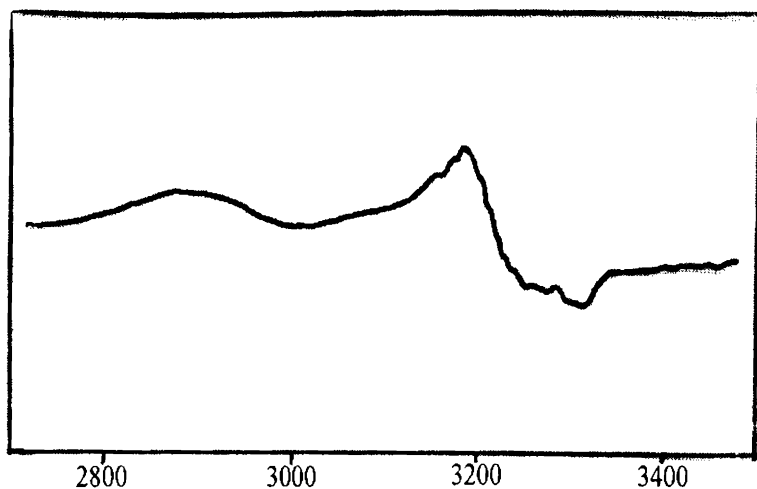
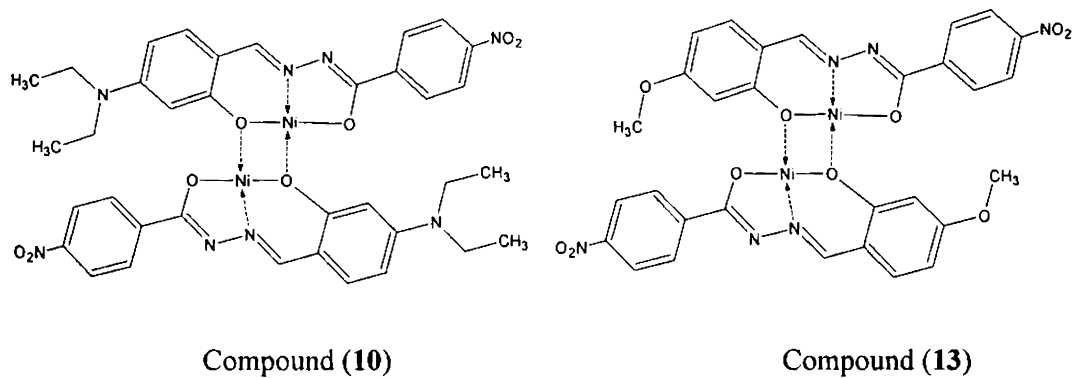
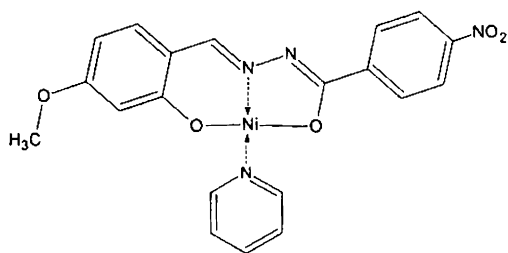


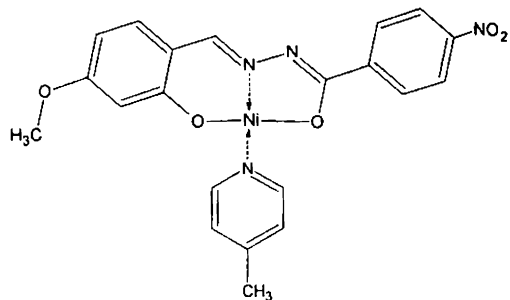
Fig. 4.14. The EPR spectrum of $[\text{CoL}^1]_2$ (19) at 77 K in DMF.

Thus the stereochemistry of the various nickel and cobalt complexes synthesized, whose single crystals were not able to isolate, can be proposed as given below (Fig. 4.15).

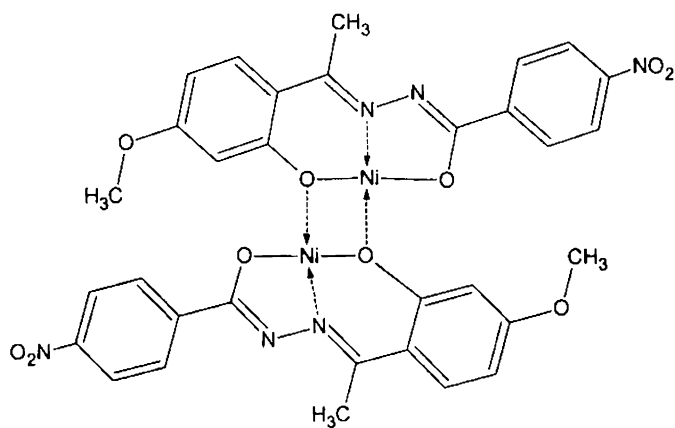




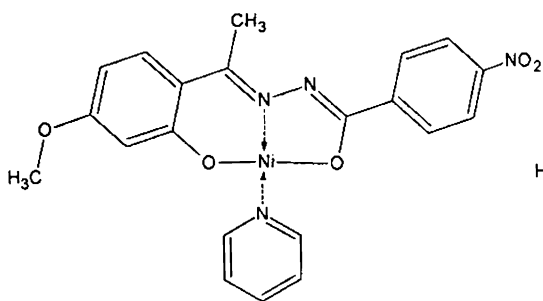
Compound (14)



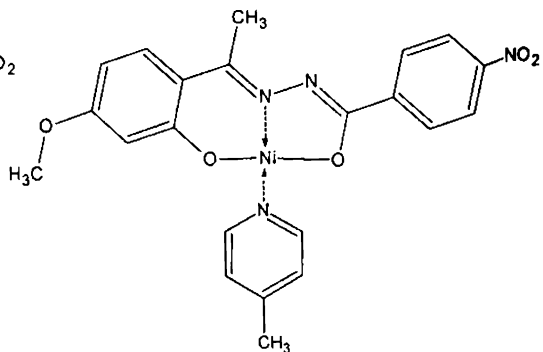
Compound (15)



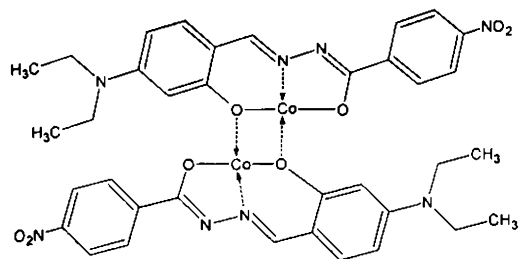
Compound (16)



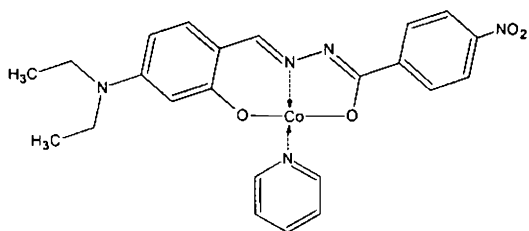
Compound (17)



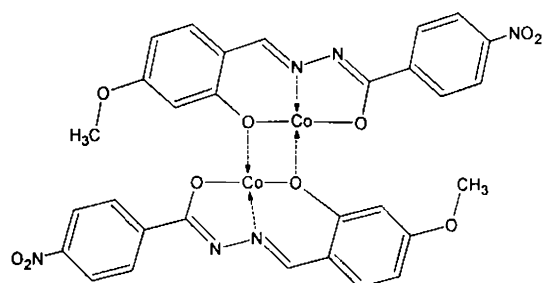
Compound (18)



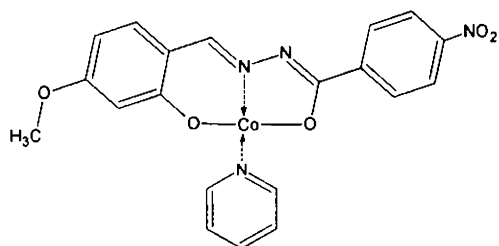
Compound (19)



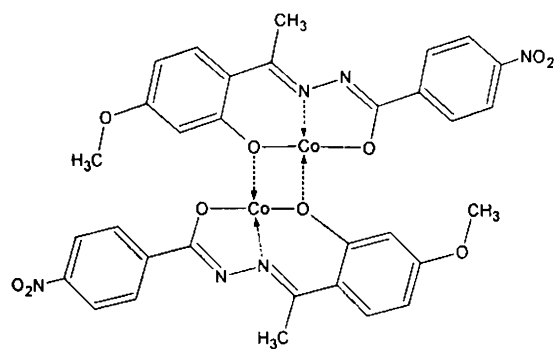
Compound (20)



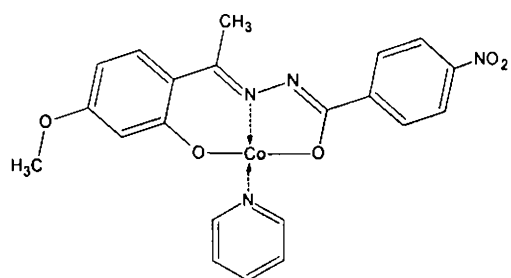
Compound (21)



Compound (22)



Compound (23)



Compound (24)

Fig. 4.15. Tentative structures of the nickel and cobalt complexes for which the single crystals suitable for X-ray diffraction studies are not isolated.

4.5. *Non-linear optical properties of Ni(II) and Co(II) complexes*

Almost all successful strategies for obtaining second order NLO dipolar organic molecules and metal complexes have been developed within a simple molecular scheme formed by a D- π -A structure, and the design of new second order NLO chromophores has focused primarily on engineering the electronic nature of the donor and the acceptor, and the conjugation length of the bridge. In the molecular D- π -A structure, the donor and/or the acceptor, or the bridge moieties are selectively replaced by a metallic or an organometallic group. This is because metal complexes possess intense, low energy metal to ligand charge transfer (MLCT), ligand to metal charge transfer (LMCT) or intraligand charge transfer (ILCT) excitations. Therefore they can effectively behave as donor and/or acceptor groups of the D- π -A system, or as constituents of the polarisable bridge. With this scheme in mind, several classes of second order NLO transition metal complexes were identified.

A series of Ni(II) and Co(II) based metal complexes exhibiting both second and third order non-linear optical properties were reported so far [43-49]. But none of acylhydrazone derivatives have been reported yet. So we decided to study the non-linear optical activities of the prepared Ni(II) and Co(II) complexes. The essential strategy for NLO activity of a sample is its nonceterosymmetric nature. In the case of the present nickel(II) and cobalt(II) complexes, in the dimeric or polymeric analogous **10**, **13**, **16**, **19**, **21** and **23**, in the molecular level itself, centre of inversion is present. So these complexes have little significance in non-linear optics. Hence the non-linear optical studies of these complexes were not done.

The non-linear optical properties of all the monomeric complexes, both the pyridine and 4-picoline derivatives were studied in the powder form by Hyper Rayleigh scattering technique. The well powdered sample was filled in capillary tube

having 0.8 mm thickness. The NLO responses of these samples were recorded using urea as the reference, filled in similar capillary tube. The experimental arrangement for the non-linear optical properties utilizes a Quanter A DCR II Nd/YAG laser with 9 mJ a pulse at a repetition rate of 5 Hz. The selected wavelength is 1064 nm. After the selection of the wavelength the laser beam is split in to two parts, one to generate the second harmonic signal in the sample and the other to generate the other to generate the second harmonic signal in the reference (urea). An output signal of 532 nm was measured in a 90° geometry using urea as the standard. The efficiency of the NLO activity of the compounds are expressed in percentage as

$$\text{Efficiency} = \frac{\text{Signal of sample}}{\text{Signal of urea}} \times 100\%$$

In the case of the complex **12**, even though there is no centre of symmetry in the molecular level, by observing the close packing pattern of the sample from the crystal data, it can be observed that there is inversion centre in the crystalline form. So a high extent of non-linear response for this complex cannot be expected in the powder form of the sample. But its pyridine substituted analogue showed a considerable 27% response with the reference compound urea. In the case of pyridine and picoline substituted complexes of the second ligand **14** and **15**, the NLO response is recordable of 20% and 14% respectively. For the nickel complex **17** also the NLO activity is considerable of 32% but for **18** is very mild of 3%. The NLO response of three cobalt complexes **20**, **22** and **24** were studied in the above specified way and only the former showed an activity of 9% of urea and the latter two were inactive, may be due to the presence of inversion centre in the crystal lattice. Since the single crystals suitable for X-rays studies could not be isolated, a correct structure relation of NLO response cannot be formulated.

References

1. V.V. Pavlishchuk, S.V. Kolotilov, A.W. Addison, R.J. Butcher, E. Sinn, J. Chem. Soc., Dalton Trans. (2000) 335.
2. M.A. Halcrow, G. Cristou, Chem. Rev. 94 (1994) 2421.
3. A.F. Kolodziej, Prog. Inorg. Chem. 41 (1994) 493.
4. D.X. West, H. Gebremedhin, R.J. Butcher, J.P. Jasinski, A.E. Liberta, Polyhedron 12 (1993) 2489.
5. J.R. Morrow, K.A. Kolasa, Inorg. Chim. Acta 195 (1992) 245.
6. N. Nawar, N.M. Hosny, Chem. Pharm. Bull. 47 (1999) 944.
7. R.C. Maurya, P. Patel, D. Sutradhar, Synth. React. Inorg. Met.-Org. Chem. 33 (2003) 1857.
8. Y.J. Jang, U. Lee, B.K. Koo, Bull. Korean Chem. Soc. 26 (2005) 925.
9. S.S. Tandon, S. Chander, L.K. Thompson, Inorg. Chim. Acta 300-302 (2000) 683.
10. M. Shakir, S. Parveen, N. Begum, Y. Azim, Transition Met. Chem. 29 (2004) 916.
11. S. Chandra, U. Kumar, Spectrochim. Acta 61A (2005) 219.
12. P.K. Singh, D.N. Kumar, Spectrochim. Acta 64A (2006) 853.
13. A. Bacchi, M. Carcelli, P. Pelagitti, C. Pelizzi, G. Pelizzi, C. Salati, P. Sgarabotto, Inorg. Chim. Acta 295 (1999) 171.
14. F.H. Urena, N.A. I. Cabeza, M.N.M. Carretero, A.L.P. Chamorro, Acta Chim. Slov. 47 (2000) 481.
15. Z.H. Chohan, H. Pervez, S. Kausar, C.T. Supuran, Synth. React. Inorg. Met. - Org. Chem. 32 (2002) 529.
16. I. Ivanovic-Burmazovic, A. Bacchi, G. Pellizzi, V.M. Leovac, K. Andjelkovic, Polyhedron 18 (1998) 119.

17. K. Andjelkovic, I. Ivanovic, S.R. Niketic, B.V. Prelesnik, V.M. Leovac, *Polyhedron* 16 (1997) 4221.
18. G. Pellizzi, A. Bacchi, I. Ivanovic-Burmazovic, M. Gruden, K. Andjelkovic, *Inorg. Chem. Comm.* 4 (2001) 311.
19. X.-H. Bu, M. Du, L. Zhang, D.-Z. Liao, J.-K. Tang, R.-H. Zhang, M. Shionoya, *J. Chem. Soc., Dalton Trans.* (2001) 593.
20. H. Cheng, D. Chun-ying, F. Chen-jie, L. Yong-jiang, M. Qing-jin, *J. Chem. Soc., Dalton Trans.* (2000) 1207.
21. R. Boca, M. Gembicky, R. Herchel, W. Haase, L. Jager, C. Wagner, H. Ehrenberg, H. Fuess, *Inorg. Chem.* 42 (2003) 6965.
22. S. Yamada, *Coord. Chem. Rev.* 190-192 (1999) 537.
23. M. Amirnasr, K.J. Schenk, A. Gorji, R. Vafazadeh, *Polyhedron* 20 (2001) 695.
24. R. Cmi, S.J. Moore, L.G. Marzilli, *Inorg. Chem.* 37 (1998) 6890.
25. S.M. Polson, R. Cini, C. Pifferi, L.G. Marzilli, *Inorg. Chem.* 36 (1997) 314.
26. S. Hirota, E. Kosugi, L.G. Marzilli, O. Yamauchi, *Inorg. Chim. Acta* 275-276 (1998) 90.
27. A.E. Martell, D.T. Sawyer, *Oxygen Complexes and Oxygen Activation by Transition Metals*, Plenum Press, New York, 1988.
28. N.J. Henson, P.J. Hay, A. Redondo, *Inorg. Chem.* 38 (1999) 1618.
29. C. Benchini, R.W. Zoeliner, *Adv. Inorg. Chem.* 44 (1997) 263.
30. T. Nagata, K. Yoruzu, T. Yamada, T. Mukaiyama, *Angew. Chem., Int. Ed. Engl.* 34 (1995) 2145.
31. A. Botterher, T. Takeuchi, K.I. Meade, H.B. Gray, D. Cwikel, M. Kapon, Z. Don, *Inorg. Chem.* 36 (1997) 2498.
32. A.A. Aruffo, T.B. Murphy, D.K. Johnson, N.J. Rose, V. Schomaker, *Inorg. Chim. Acta* 67 (1982) L25.
33. E.W. Ainscough, A.M. Brodie, J.D. Ranford, J.M. Waters, *Inorg. Chim. Acta* 236 (1995) 83.

34. S.C. Chan, L.L. Koh, P.-H. Leung, J.D. Ranford, K.Y. Sim, *Inorg. Chim. Acta* 236 (1995) 101.
35. A.B.P. Lever, *Inorganic Electronic Spectroscopy*, 2nd ed., Elsevier Science Publishers B. V., Netherlands, 1984.
36. J.E. Huheey, E.A. Keiter, R.L. Keiter, *Inorganic Chemistry, Principles of Structure and Reactivity*, 4th ed., Harper Collins College Publishers, New York, 1993.
37. B.S. Garg, M.R.P. Kurup, S.K. Jain, Y.K. Bhoon, *Transition Met. Chem.* 16 (1991) 111.
38. G.M. Mockler, G.W. Chaffey, E. Sinn, H. Wong, *Inorg. Chem.* 11 (1972) 1308.
39. V. Philip, V. Suni, M.R.P. Kurup, M. Nethaji, *Polyhedron* 23 (2004) 1225.
40. P. Bindu, M.R.P. Kurup, *Ind. J. Chem.* 36A (1997) 1094.
41. R.A. Lal, A. Kumar, J. Chakraborty, S. Bhaumik, *Transition Met. Chem.* 26 (2001) 557.
42. K. Nakamoto *in* *Infrared and Raman Spectra of Inorganic and Coordination Compounds*, 4th ed., John Wiley & Sons, United States of America, 1986.
43. M.D. Abdalla, R. Copeland, R. Sliz, P. Venkateswarlu, D.A. Manmohan, A. Williams, N. Bhat Kamala, M. Thompson James, N.B. Laxmeshwar *Proc. SPIE, Non-linear Optical Properties of Organic Materials IX*, Gustaaf R. Moehlmann; Ed. Vol. 2852, p. 12-22 (1996) 11.
44. S. Di Bella, I. Fragalà, A. Guerri, P. Dapporto, K. Nakatani *Inorg. Chim. Acta* 357 (2007) 1161.
45. S.B. Schougaard, D.R. Greve, T. Geisler, J.C. Petersen, T. Bjørnholm, *Synthetic metals* 86 (1997) 1781.
46. J.-L. Zuo, T.-M. Yao, F. You, X.-Z. You, H.-K. Fun B.-C. Yip *J. Mater. Chem.* 6 (1996) 1633.
47. Z.-M. Xue, Y.-W. Tang, J.-Y. Wu, Y.-P. Tian, M.-H. Jiang, H.-K. Fun, A. Usman *Can. J. Chem.* 82 (2004) 1700.

48. I.S. Lee, D.M. Shin, Y. Yoon, S.M. Shin, Y.K. Chung *Inorg. Chim. Acta* 343 (2003) 41.
49. V.V. Semenov, N.F. Cherepennikova, M.A. Lopatin, L.G. Klapshina, T.G. Mushtina, S.Y. Khorshev, G.A. Domrachev, W.E. Douglas, B.A. Bushuk, A.I. Rubinov, S.B. Bushuk, *Russian J. Coord. Chem.* 28 (2002) 394.

Table 4.1

Crystal data and structure refinement of [NiL^Ipy₃]py and [NiL^Ipi]

| | [NiL ^I py ₃]py | [NiL ^I pi] |
|-----------------------------------|--|--|
| Empirical formula | C ₃₈ H ₃₈ N ₈ Ni O ₄ | C ₂₄ H ₂₅ N ₅ Ni O ₄ |
| Formula weight | 729.47 | 506.20 |
| Temperature | 293(2) K | 293(2) K |
| Wavelength | 0.71073 Å | 0.71073 Å |
| Crystal system | Triclinic | Triclinic |
| Space group | <i>P</i> $\bar{1}$ | <i>P</i> $\bar{1}$ |
| Unit cell dimensions | a = 9.652(2) Å b = 12.115(3) Å c = 16.838(4) Å α = 106.016(4)° β = 98.819(4)° γ = 100.023(4)° | a = 9.6402(19) Å b = 10.498(2) Å c = 12.960(3) Å α = 73.090(4)° β = 88.942(3)° γ = 68.736(3)° |
| Volume, Z | 1820.9(7) Å ³ , 2 | 1163.9(4) Å ³ , 2 |
| Calculated density | 1.330 Mg/m ³ | 1.444 Mg/m ³ |
| Absorption coefficient | 0.584 mm ⁻¹ | 0.875 mm ⁻¹ |
| F (000) | 764 | 528 |
| Crystal size | 0.28 x 0.14 x 0.10 mm ³ | 0.30 x 0.24 x 0.18 mm ³ |
| θ range for data collection | 1.80- 28.23° | 1.65 - 28.24° |
| Index ranges | -12 ≤ h ≤ 10, -16 ≤ k ≤ 13, -19 ≤ l ≤ 21 | -12 ≤ h ≤ 12, -13 ≤ k ≤ 7, -15 ≤ l ≤ 16 |
| Reflections collected / unique | 7998 / 5613 [R (int) = 0.0196] | 6841 / 5064 [R (int) = 0.0194] |
| Completeness to 2 θ = 28.24 | 79.8% | 88.1% |
| Refinement method | Full-matrix least-squares on F ² | Full-matrix least-squares on F ² |
| Data / restraints / parameters | 7998 / 0 / 462 | 5064 / 0 / 311 |
| Goodness-of-fit on F ² | 1.028 | 0.990 |
| Final R indices [I > 2σ(I)] | R ₁ = 0.0532, wR ₂ = 0.1431 | R ₁ = 0.0612, wR ₂ = 0.1458 |
| R indices (all data) | R ₁ = 0.0750, wR ₂ = 0.1680 | R ₁ = 0.0983, wR ₂ = 0.1662 |
| Largest diff. peak and hole | 0.476 and -0.384 eÅ ⁻³ | 0.986 and -0.391 eÅ ⁻³ |

| | |
|--------|----------|
| Ni1–N2 | 1.979(2) |
| Ni1–O2 | 2.002(2) |
| Ni1–O1 | 2.056(2) |
| Ni1–N6 | 2.087(2) |
| Ni1–N7 | 2.159(2) |
| Ni1–N5 | 2.169(3) |
| O2–C9 | 1.307(3) |
| O1–C12 | 1.280(3) |
| N2–C11 | 1.291(4) |
| N2–N3 | 1.394(3) |
| N3–C12 | 1.330(4) |
| C11–C8 | 1.434(4) |

| | |
|------------|-----------|
| N2–Ni1–O2 | 91.96(8) |
| N2–Ni1–O1 | 78.73(8) |
| O2–Ni1–O1 | 170.54(7) |
| N2–Ni1–N6 | 173.26(9) |
| O2–Ni1–N6 | 94.71(8) |
| O1–Ni1–N6 | 94.57(8) |
| N2–Ni1–N7 | 91.65(9) |
| O2–Ni1–N7 | 88.94(8) |
| O1–Ni1–N7 | 92.97(9) |
| N6–Ni1–N7 | 89.47(9) |
| N2–Ni1–N5 | 89.92(9) |
| O2–Ni1–N5 | 90.23(9) |
| O1–Ni1–N5 | 88.11(1) |
| N6–Ni1–N5 | 89.07(9) |
| N7–Ni1–N5 | 178.25(9) |
| C11–N2–Ni1 | 127.01(2) |
| N3–N2–Ni1 | 116.20(2) |

| | |
|---------|----------|
| Ni1–O1 | 1.819(2) |
| Ni1–N2 | 1.823(3) |
| Ni1–O2 | 1.847(2) |
| Ni1–N5 | 1.936(3) |
| O1–C9 | 1.315(4) |
| N2–C11 | 1.304(5) |
| N2–N3 | 1.404(4) |
| C12–O2 | 1.303(4) |
| N3–C12 | 1.302(5) |
| C11–C8 | 1.405(5) |
| C12–C13 | 1.478(5) |

| | |
|------------|------------|
| O1–Ni1–N2 | 95.04(12) |
| O1–Ni1–O2 | 178.07(11) |
| N2–Ni1–O2 | 83.49(13) |
| O1–Ni1–N5 | 90.00(11) |
| N2–Ni1–N5 | 174.85(12) |
| O2–Ni1–N5 | 91.48(12) |
| C9–O1–Ni1 | 127.6(2) |
| N3–N2–Ni1 | 115.7(3) |
| C12–O2–Ni1 | 110.3(2) |
| C19–N5–Ni1 | 121.8(3) |
| C23–N5–Ni1 | 122.3(3) |
| C11–N2–Ni1 | 128.1(3) |
| C12–N3–N2 | 106.8(3) |
| C11–N2–N3 | 116.2(3) |
| O1–C9–C8 | 123.4(3) |
| N3–C12–O2 | 123.6(3) |
| O2–C12–C13 | 117.9(4) |

CHAPTER FIVE

Syntheses, characterization and non-linear optical properties of manganese(II) and iron(III) complexes of the aroylhydrazone ligands

The element manganese is relatively abundant, constituting about 0.085% of the earth's crust. Over 90% of all the manganese ores produced are used in steel manufacture, mostly in the form of ferromanganese. Manganese coordination chemistry with a diverse range of ligands has much relevance in biological systems with a number of model manganese complexes. Low nuclearity species have been studied extensively as models for the water-oxidizing complex in photosystem II, whereas nanometer-size clusters with high spin ground states are being investigated as single molecule magnets [1-3]. Manganese coordination compounds are also of growing importance as homogeneous catalysts in oxidation reactions [4-7]. The manganese porphyrins are very efficient catalysts for fractionalization of hydrocarbons in processes that involve high valent intermediates [8-9]. Manganese is identified in metalloenzymes such as oxygen evolving centre of photosystem-II, catalyses and superoxide dismutases [10-12]. Manganese complexes are also studied for their magnetic behavior. Cubane like Mn(II) complexes of di-2-pyridyl ketone in the gem-diol form are reported with single crystal X-ray structural analyses and this complex is observed to be antiferromagnetic [13]. The chemistry of manganese, in various oxidation states of the metal and in various combinations of nitrogen and oxygen donor environment, is presently witnessing intense activity [14-16]. This is because manganese plays a major key role in many biological redox processes, including water oxidation complex in photosystem II [17-18], decomposition of O₂'

radicals catalyzed by superoxide dismutases (SOD's) and disproportionation of hydrogen peroxide (catalase activity) in microorganisms, a reaction which is important for cell detoxification.

Iron (Fe) is a crucial component of a variety of metabolic pathways that are involved in DNA synthesis [19] and the production of energy. Despite the industrial and biological importance of iron containing systems, the coordination chemistry of the metal has been sadly neglected except a few examples. A considerable number of compounds were studied in earlier seventies and the relevant references may be found in the book by Sidgwick [20] and in the treatises by Gmelin [21] and Mellor [22]. This comparative lack of interest has been especially marked in the case of iron(III), largely owing to the properties of the d^5 ion. Recently, Richardson *et al.* identified a number of novel Fe-chelating agents of the pyridoxal isonicotinoylhydrazone (PIH) class that demonstrate high activity at inhibiting the growth of a range of tumor cells, including NB, leukemia, and melanoma cell lines (23-25). But only a few of examples of manganese and iron coordinated complexes were reported yet in the field of non-linear optics. This may be due to the greater chance of octahedral coordination environment among these metals and which leads to a molecular lattice having centre of symmetry.

5.1. Stereochemistry of Mn(II) complexes

The common oxidation states of manganese are +2, +3, +4, +6 and +7, though oxidation states from +1 to +7 are observed. The most common and stable oxidation state of manganese is +2. Majority of manganese complexes are high spin paramagnetic d^5 systems and are intensely colored. The manganese complexes of all the three ligands were synthesized and three of them were six coordinated and octahedral.

5.2. Stereochemistry Fe(III) complexes

The most common oxidation states of iron coordination complexes are +2 and +3. Iron(III) complexes usually exist in six coordinated and octahedral environments. Here we have synthesized three iron complexes of each of the three ligands and the studies of all of them showed the possibility of six coordinated environment around the iron centre.

5.3. Experimental

5.3.1. Materials

4-Nitrobenzoylhydrazide (Sigma Aldrich), 4-*N,N*-diethylamino-2-hydroxybenzaldehyde (Sigma Aldrich), 4-methoxy-2-hydroxybenzaldehyde (Sigma Aldrich), 4-methoxy-2-hydroxyacetophenone (Sigma Aldrich), manganese acetate (Merck), ferric chloride (Merck), DMF (S.D. Fine) were used as received. When ethyl alcohol was used as the solvent repeated distillation was carried out before use.

5.3.2. Syntheses of ligands

Preparation of the ligands H_2L^1 , H_2L^2 and H_2L^3 were done as described previously in Chapter 2.

5.3.3. Preparation of manganese(II) complexes

$[Mn(HL^1)_2] \cdot 3H_2O$ (**25**): The complex was prepared by refluxing a mixture of the ligand H_2L^1 (0.748 g, 2 mmol) and manganese acetate (0.245 g, 1 mmol) in a 1:1 mixture of absolute ethanol and DMF. The solution was then refluxed for about two hours. The dark red product obtained was filtered, washed with absolute alcohol and

finally with diethyl ether and dried over P_4O_{10} *in vacuo*. Yield: 0.537 g (65.6%). Elemental Anal. Found (Calcd.) (%): C, 52.26 (52.75); H, 5.62 (5.41); N, 13.35 (13.67).

$[Mn(HL^2)_2]$ (**26**): To a boiling solution of the ligand H_2L^2 (0.630 g, 2 mmol) in a 1:1 mixture of absolute ethanol and DMF, a solution of manganese acetate (0.245 g, 1 mmol) was added and refluxed for about two hours. The orange red product obtained by cooling the solution to room temperature was filtered, washed several times with absolute ethanol and finally with diethyl ether and dried over P_4O_{10} *in vacuo*. Yield: 0.476 g (69.9%). Elemental Anal. Found (Calcd.) (%): C, 53.38 (52.87); H, 3.74 (3.25); N, 12.36 (12.33).

$[Mn(HL^3)_2] \cdot 3H_2O$ (**27**): The complex was prepared by the same procedure described above by using solutions of the ligand H_2L^3 (0.658 g, 2 mmol) and manganese acetate (0.249 g, 1 mmol). The red colored product obtained was filtered, washed several times with ethanol, finally with diethyl ether and dried over P_4O_{10} *in vacuo*. Yield: 0.492 g (64.2%). Elemental Anal. Found (Calcd.) (%): C, 50.05 (50.20); H, 3.51 (4.48); N, 10.95 (10.98).

5.3.4. Preparation of iron(III) complexes

$[Fe(HL^1)(L^1)] \cdot H_2O$ (**28**): Ferric chloride (0.162 g, 1 mmol) dissolved in ethanol was added to a solution of the ligand H_2L^1 (0.748 g, 2 mmol) in a 1:1 ethanol and DMF, and refluxed for four hours. The black shining product formed was filtered, washed with ether and dried over P_4O_{10} *in vacuo*. Yield: 0.381 g (48.5%). Elemental Anal. Found (Calcd.) (%): C, 55.32 (55.18); H, 4.76 (5.02); N, 14.11 (14.30).

[Fe(HL²)(L²)]·3H₂O (**29**): A solution of ferric chloride (0.162 g, 1 mmol) in ethanol was added to a solution of H₂L¹ (0.630 g, 2 mmol) in a 1:1 ethanol and DMF and refluxed continuously for about five hours. Brown colored crystalline products separated out were filtered, washed with ethanol followed by ether and dried over P₄O₁₀ *in vacuo*. Yield: 0.368 g (49.8%). Elemental Anal. Found (Calcd.) (%): C, 49.45 (48.80); H, 4.62 (4.09); N, 12.07 (11.38).

[Fe(HL³)(L³)]·2H₂O (**30**): Preparation of [Fe(HL³)(L³)] was carried out by the same procedure as that of compound **29** above, except that a 1:1 ethanol/DMF solution of H₂L³ (0.658 g, 2 mmol) was used instead of H₃L². The reddish brown product formed was washed several times with ethanol and finally with ether and dried over P₄O₁₀ *in vacuo*. Yield: 0.318 g (42.5%). Elemental Anal. Found (Calcd.) (%): C, 51.68 (51.42); H, 4.39 (4.18); N, 11.02 (11.24).

5.4. Results and discussion

5.4.1. Spectral studies of manganese(II) complexes

5.4.1a. Electronic spectral studies

The ground state of high-spin octahedral Mn(II) complex is ⁶A_{1g}. As there are no other terms of sextet spin multiplicity, spin allowed *d-d* transitions are not expected. However, some forbidden transitions occur such as ⁶A_{1g} → ⁴A_{1g} (G), ⁴E_g (G), ⁶A_{1g} → ⁴E_g (D), ⁶A_{1g} → ⁴T_{1g} (G), ⁴T_{2g} (G) [26]. Thus, for a *d*⁵ octahedral complex, all transitions are not only Laporte-forbidden but also spin-forbidden. Absorptions associated with doubly forbidden transitions are extremely weak, with extinction coefficients several hundred times smaller than those for singly forbidden transitions.

The combined UV-Vis spectra of all the manganese(II) complexes have been shown in the Fig. 5.1. The intensity of electronic absorption of the complex **25** is high compared to **26** and **27**. But the pattern of absorption of all the manganese complexes is found to be very similar. The strong and broad absorption band seen in all the spectra *ca.* 400 – 550 nm is assigned to be due to the ligand to metal charge transfer the forbidden *d-d* transitions in the manganese complexes. There are weak absorptions in 280 – 380 nm regions due to absorptions in the ligand molecule, both $\pi \rightarrow \pi^*$ and $n \rightarrow \pi^*$ transitions.

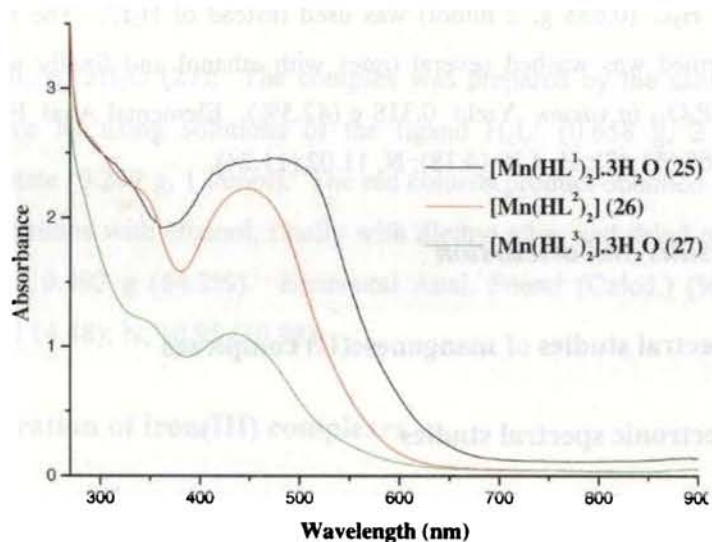


Fig. 5.1. The UV-Vis absorption spectrum of the manganese(II) complexes **25**, **26** and **27** in DMF.

5.4.1b. Infrared spectral studies

The single crystals suitable for X-ray crystallographic studies were not able to isolate in the case of manganese complexes, and so infrared spectroscopy plays an important role for assigning the coordination pattern in these complexes. A careful

comparison of the infrared spectra of the ligand and the complex reveals the mode and pattern of coordination in the complex examined. In the case of the complex, $[\text{Mn}(\text{HL}^1)_2] \cdot 3\text{H}_2\text{O}$ (**25**), the free ligand exhibit bands at $3000\text{-}3600\text{ cm}^{-1}$, comprising of the OH and NH stretching absorptions, 1631 cm^{-1} - the amide I band - and 1594 cm^{-1} - the amide II band. In the IR spectrum of **25**, there is an absorption at *ca.* 3500 cm^{-1} may be due to the presence of lattice water and a very small downward shift of amide I and amide II bands to 1628 and 1593 cm^{-1} respectively, suggesting that the ligands exist in the keto form in this complex. Whether the coordination is in enol form, both the amide I and amide II absorptions will disappear. The coordination of the azomethine nitrogen atom to the metal ion is indicated by the displacement of the bands chiefly assigned to the $\nu(\text{N-N})$ and $\nu(\text{C=N})$ stretching vibrations. The spectrum shows downward shift of $\nu(\text{N-N})$ from 1070 to 1060 cm^{-1} and $\nu(\text{C=N})$ from 1518 to 1490 cm^{-1} . Similarly the complexes **26** and **27** also showed similar shifts in the infrared spectral bands from the corresponding ligand.

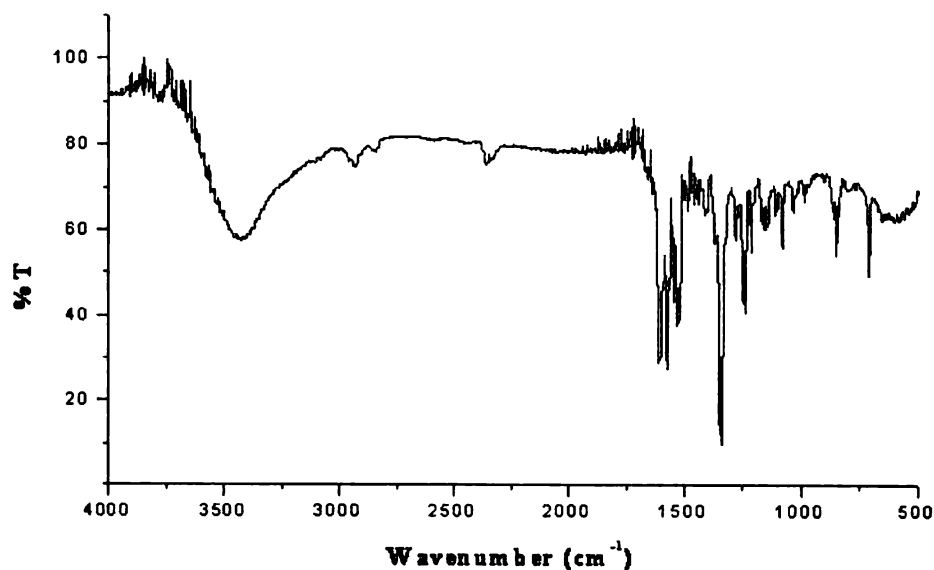


Fig. 5.2. The IR spectrum of the compound $[\text{Mn}(\text{HL}^3)_2] \cdot 3\text{H}_2\text{O}$ (**27**).

In the case of **26**, a band in the region of 3200-3600 cm^{-1} is seen, showing the presence of NH group in the keto form of the ligand. Here the coordination through azomethine nitrogen is confirmed by the downward shifting of absorptions due to $\nu(\text{N-N})$ and $\nu(\text{C=N})$ from 1013 cm^{-1} and 1549 cm^{-1} to 976 cm^{-1} and 1527 cm^{-1} respectively. In the case of the complex **27**, the bands shifted from 1032 cm^{-1} and 1560 cm^{-1} to 984 cm^{-1} and 1526 cm^{-1} respectively. So the coordination pattern around Mn(II) ion in these complexes are confirmed to be octahedral through, azomethine nitrogen, deprotonated phenolic oxygen and double bonded carbonyl oxygen of the either ligand molecules. The infrared absorption spectrum of the complex $[\text{Mn}(\text{HL}^3)_2] \cdot 3\text{H}_2\text{O}$ (**27**) is shown the Fig. 5.2. In the far-infrared region, the Mn(II) complexes exhibit bands at 440, 430 and 340 cm^{-1} , which are assigned to $\nu(\text{M-O})$ phenolic, $\nu(\text{M-N})$ and $\nu(\text{M-O})$ ketonic [27] bands respectively.

5.4.1c. EPR spectral studies

A series of examples have been reported to explain the electron paramagnetic spectral behaviour of Mn(II) complexes [28-29]. The magnetic susceptibility measurements of the manganese complexes showed that all are paramagnetic with a spin value of 5/2, having five unpaired electrons. It confirms the conclusion that all the manganese complexes are high spin d^5 systems. The μ_{eff} values of all the manganese complexes are in the range of 5.9 – 6.1 B.M, typical for high spin d^5 configuration.

The spin Hamiltonian for the high spin Mn(II) is expressed as:

$$\mathcal{H} = g\beta HS + D[S_z^2 - S(S+1)/3] + E(S_x^2 - S_y^2)$$

where H is the magnetic field vector, D is the axial zero field splitting term, E is the rhombic zero field splitting parameter. If D and E are very small compared to $g\beta HS$, five ESR transitions corresponding to $\Delta m_s = \pm 1$ are expected with a g value of 2.0. But

if D is very large, then only transition between $|+1/2\rangle \leftrightarrow |-1/2\rangle$ will be observed. However, for the case where D or E is very large, the lowest doublet has effective g values of $g_{\parallel} = 2$, $g_{\perp} = 6$ for $D \neq 0$ and $E = 0$ but for $D = 0$ and $E \neq 0$, the middle Kramers doublet has an isotropic g value of 4.29 [30-31].

The electron paramagnetic resonance spectrum of the complex $[\text{Mn}(\text{HL}^1)_2] \cdot 3\text{H}_2\text{O}$ (**25**) was recorded both in powder state at room temperature and in DMF solution at 77 K. The powder state EPR spectrum is found to be very broad and isotropic in nature without any hyperfine splitting pattern due to the magnetically concentrated environment around the metal atom.

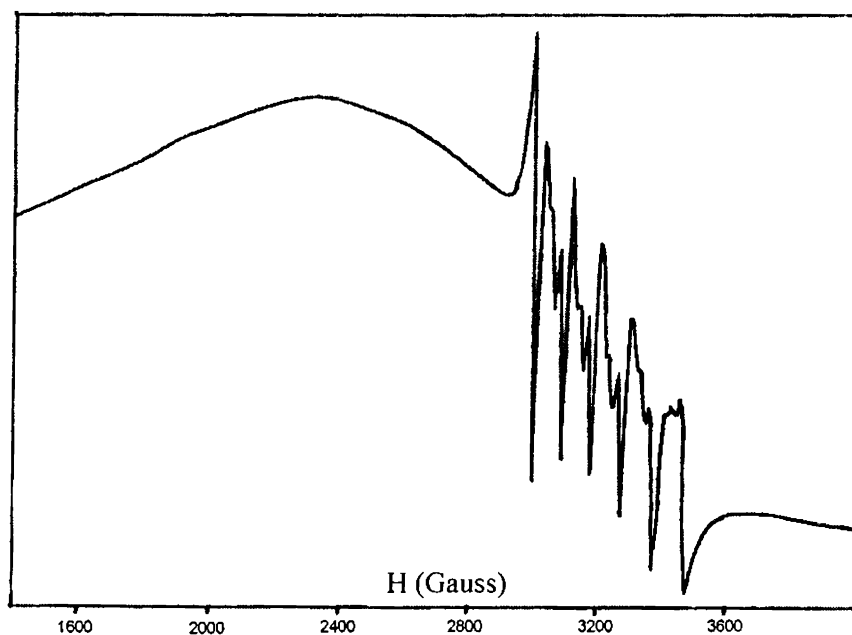


Fig. 5.3. The EPR spectrum of $[\text{Mn}(\text{HL}^1)_2] \cdot 3\text{H}_2\text{O}$ (**25**) in DMF at 77 K.

The g_{iso} value of the powder state EPR is 2.061, very close to the free electron g value. However, the solution spectrum in DMF at 77 K (Fig. 5.3), displayed a pattern having two g values, $g_1=1.991$ and $g_2=2.884$. The expected hyperfine sextet is found only for the signal in the high field region. The observance of hyperfine sextet is as expected due to the interaction of the unpaired electron with the Mn(II) nucleus of spin $I = 5/2$, resulting in $2nI+1$ lines. Thus the six lines observed corresponds to $m_s = +5/2, +1/2, \dots -5/2$ with $\Delta m_l = 0$.

A pair of low intensity lines is found in between each of the two main hyperfine lines. These are the forbidden lines corresponding to $\Delta m_l = \pm 1$, transitions arising due to the nuclear quadrupole effect as the nuclear spin quantum number I is greater than 1. Thus the general selection rule for the transition, $\Delta m_s = \pm 1, \Delta m_l = 0$ is violated. The coupling constant A_{iso} for the central sextet hyperfine lines is found to be 96 G.

The EPR spectra of the complex $[\text{Mn}(\text{HL}^2)_2]$ (**26**) were recorded both in the polycrystalline state at room temperature and solution state in DMF at 77 K. The room temperature spectrum is broad isotropic with g_{iso} value 2.05. The solution spectrum in DMF at 77 K (Fig. 5.4), displayed a central hyperfine sextet with $g_{iso} = 1.997$. The observance of hyperfine sextet is as expected due to the interaction of the unpaired electron with the Mn(II) nucleus of spin $I = 5/2$, resulting in $2nI+1$ lines. The coupling constant A_{iso} for the sextet hyperfine lines is found to be 96 G. Here also forbidden lines arising due to nuclear quadrupole effect of nuclear spin quantum number greater than 1 are observed in between the main hyperfine lines.

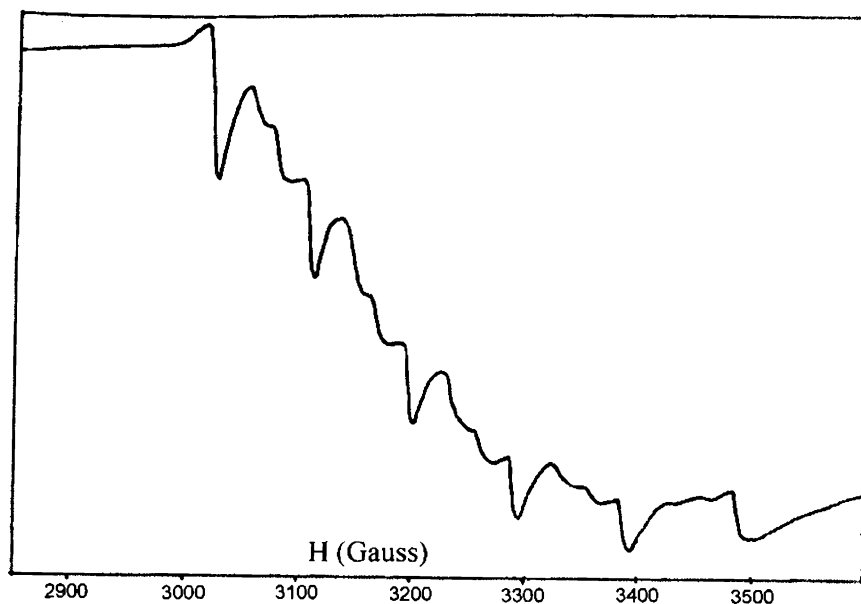


Fig. 5.4. The EPR spectrum of $[\text{Mn}(\text{HL}^2)_2]$ (**26**) in DMF at 77 K.

The electron paramagnetic resonance spectra of the complex $[\text{Mn}(\text{HL}^3)_2] \cdot 3\text{H}_2\text{O}$ (**27**) were recorded in polycrystalline state at 298 K and solution in DMF at 77 K. The powder state EPR was isotropic in nature with the $g_{iso} = 2.061$. The solution state spectrum has two g values $g_1 = 1.983$ and $g_2 = 2.744$. In the high field region, the spectrum showed clear sextet ($2nI+1$) hyperfine splitting pattern due to the interaction of unpaired electron with the nuclear spin of $I = 5/2$. The splittings due to forbidden lines of nuclear quadrupole effect is also seen in the spectrum. In this spectrum also the coupling constant A_{iso} , for the central sextet hyperfine lines is found to be 96 G. The three manganese complexes showed very similar behavior in the electron paramagnetic resonance spectroscopy, indicating similar electronic environment around the manganese centre. The EPR spectrum of **27** in solution state in DMF at 77 K is shown in the Fig. 5.5.

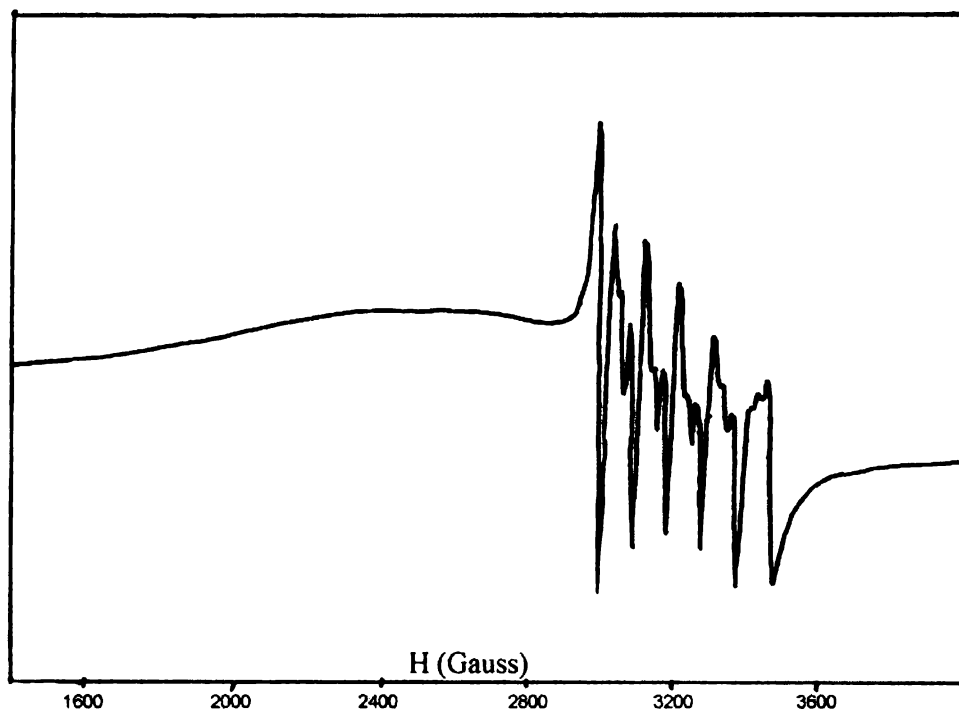


Fig. 5.5. The EPR spectrum of $[\text{Mn}(\text{HL}^3)_2] \cdot 3\text{H}_2\text{O}$ (27) in DMF at 77 K.

5.4.2. Spectral studies of iron(III) complexes

5.4.2a. Electronic spectral studies

In a cubic crystal field, the 6S free ion term transforms as 6A_1 ; no other spin sextuplet state exists, so that all the $d-d$ transitions are spin forbidden and hence rather weak. These bands are probably made possible a mixture of spin-quartet character into the ground state via spin-orbit coupling. Despite this, certain problems arise and

high spin Fe^{3+} $d-d$ spectra are generally more difficult to assign than those of the isoelectronic Mn^{2+} complexes. The main reason for this is that charge transfer absorption occurs at lower energy in the ferric complexes and often most of the $d-d$ bands are obscured.

There is a very broad absorption in the whole visible region for the complex **28**, comprising of all the charge transfer and above discussed forbidden $d-d$ transitions. The UV-Vis absorption spectra of all the three iron complexes are shown together in the Fig. 5.6 below. The bands observed in the region of 300-380 nm are assigned to the ligand $\pi \rightarrow \pi^*$ and $n \rightarrow \pi^*$ transitions.

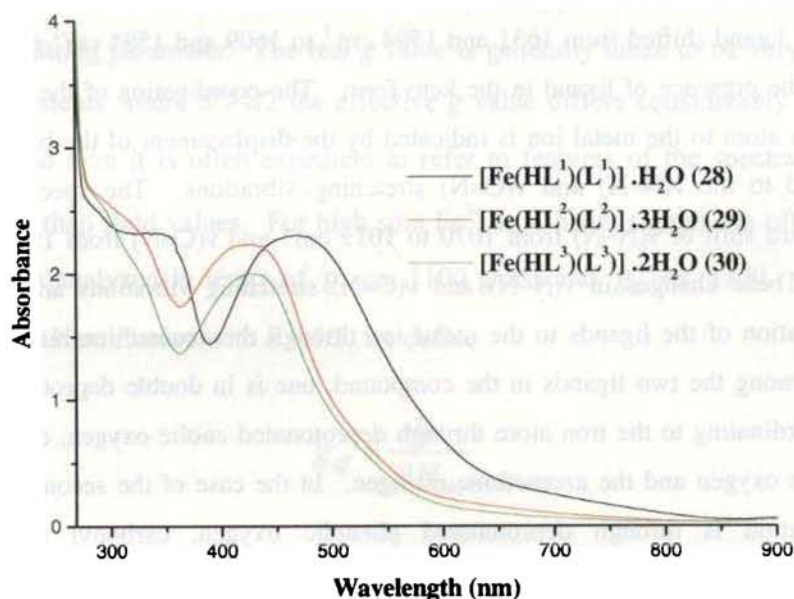


Fig. 5.6. The UV-Vis spectra of the iron(III) complexes **28**, **29** and **30** in DMF.

5.4.2b. Infrared spectral studies

The elemental analyses data shows that in all the three iron(III) complexes, the metal and ligand species are in 1:2 ratio. The assignment of infrared bands is most useful for the establishment of the mode of coordination of the aroylhydrazone ligands in the iron(III) complexes. A careful comparison of the infrared spectrum of the complex with that of the corresponding ligand reveals the mode and pattern of coordination in the complex examined. In the case of the complex **28**, the stretching absorption of NH bond remains, but not as broad as earlier, indicating the presence of non-enolized aroylhydrazone moieties in the complex sample. This also confirms the presence of lattice water in the compound. The amide I and amide II bands in the original ligand shifted from 1631 and 1594 cm^{-1} to 1609 and 1584 cm^{-1} respectively, shows the presence of ligand in the keto form. The coordination of the azomethine nitrogen atom to the metal ion is indicated by the displacement of the bands chiefly assigned to the $\nu(\text{N-N})$ and $\nu(\text{C=N})$ stretching vibrations. The spectrum shows downward shift of $\nu(\text{N-N})$ from 1070 to 1017 cm^{-1} and $\nu(\text{C=N})$ from 1518 to 1483 cm^{-1} . These changes in $\nu(\text{N-N})$ and $\nu(\text{C=N})$ stretching vibrations are typical of coordination of the ligands to the metal ion through the azomethine nitrogen atom. Thus, among the two ligands in the compound, one is in double deprotonated form and coordinating to the iron atom through deprotonated enolic oxygen, deprotonated phenolic oxygen and the azomethine nitrogen. In the case of the second ligand the coordination is through deprotonated phenolic oxygen, carbonyl oxygen and azomethine nitrogen. Thus the iron center is six coordinated and octahedral.

For the complexes, **29** and **30**, the coordination pattern is same as discussed above. In the case of **29**, the broad band *ca.* 3440 cm^{-1} , shows the presence of NH bond and thus the keto form of the compound. The coordination through azomethine nitrogen is indicated by the shifting of $\nu(\text{C=N})$ and $\nu(\text{N-N})$ to 1475 and 1027 cm^{-1}

respectively. For the compound **30**, $\nu(\text{C}=\text{N})$ and $\nu(\text{N}-\text{N})$ shifted to 1489 and 1009 cm^{-1} . Thus in all the three iron complexes, the coordination through azomethine nitrogen is confirmed.

5.4.2c. EPR spectral studies

Whilst most early EPR work on high spin systems was concerned with the elucidation of the quadratic terms in the spin Hamiltonian for virtually cubic systems [32-33], we rewrite it as

$$\mathcal{H} = g\beta HS + D[S_z^2 - S(S+1)/3] + E(S_x^2 - S_y^2)$$

Where D is the ‘out-of-plane’ zero field splitting parameter and E the in-plane zero field splitting parameter. The real g value is generally taken to be very close to 2.00. For systems where $S > 1/2$ the effective g value differs considerably from the real value and here it is often expedient to refer to features of the spectra by g_{eff} values rather than field values. For high spin Fe^{3+} at X-band, signals are often found which can be analyzed in terms of g_1 ca. 1100 gauss and g_2 ca. 3300. Taking a fictitious spin Hamiltonian with $S = 1/2$, we define

$$g_{\text{eff}} = \frac{h\nu}{\beta H_{\text{res}}}$$

So that this signal can be described in terms of the effective g values $g_1 = 6$ and $g_2 = 2$. Likewise a nearly isotropic resonance is sometimes found ca. 1500 gauss at X-band and is described as $g_{\text{eff}} = 4.3$, arising from $D > \text{ca. } 0.2 \text{ cm}^{-1}$ [34]. Because of its isotropic nature and statistical effects it generally appears much more intensely

than other transitions and usually dominates the spectrum. For near cubic systems, five transitions appear, centered on $g = 2$, these are $|5/2\rangle \rightarrow |3/2\rangle$, $|3/2\rangle \rightarrow |1/2\rangle$, $|1/2\rangle \rightarrow |-1/2\rangle$, $|-1/2\rangle \rightarrow |-3/2\rangle$, $|-3/2\rangle \rightarrow |-5/2\rangle$ transitions [35].

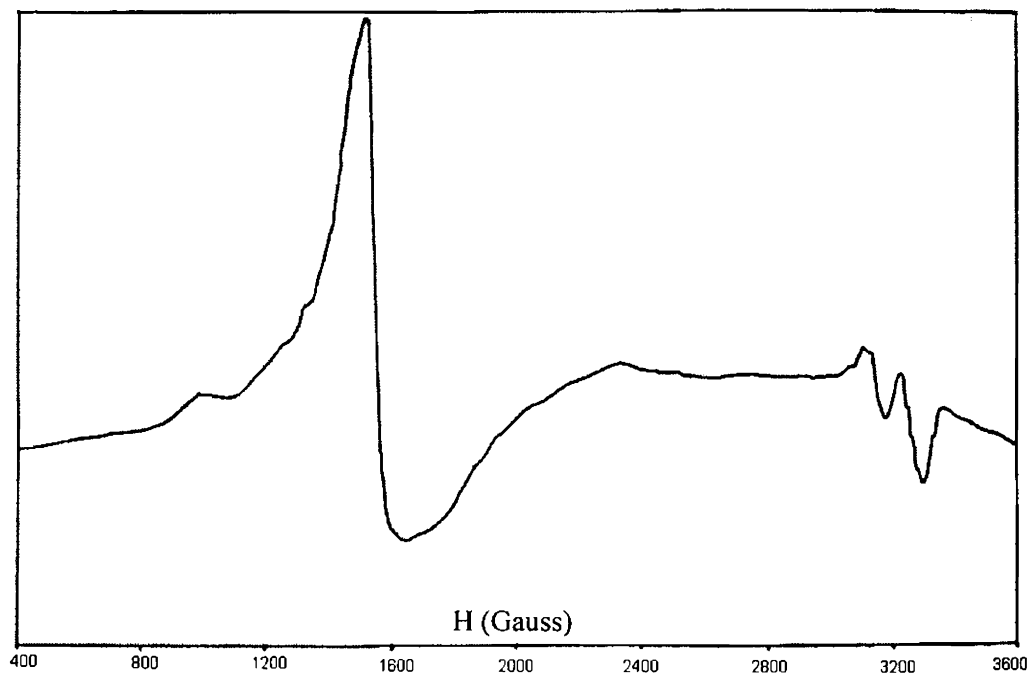


Fig. 5.7. The EPR spectrum of $[\text{Fe}(\text{HL}^1)(\text{L}^1)] \cdot \text{H}_2\text{O}$ (**28**) in DMF at 77 K.

The electron paramagnetic resonance spectra of all the iron(III) complexes were recorded in solution state in DMF at 77 K. The EPR spectrum of the compound, $[\text{Fe}(\text{HL}^1)(\text{L}^1)] \cdot \text{H}_2\text{O}$ (**28**) shown in the Fig. 5.7. The spectrum has three g values $g_1 = 6.623$, $g_2 = 4.151$ and $g_3 = 2.023$. The close verification of the pattern in the high field region shows five transitions and it can be concluded that the system is nearly symmetrical.

The electron paramagnetic resonance spectrum of the complex $[\text{Fe}(\text{HL}^2)(\text{L}^2)] \cdot 3\text{H}_2\text{O}$ (**29**) recorded in solution in DMF at 77 K is shown in the Fig. 5.8. The spectrum showed three signals corresponding to g values $g_1 = 6.581$, $g_2 = 4.208$ and $g_3 = 2.016$. The shape and g values for the spectrum are found to be very similar to that discussed earlier for the complex **28**. But in this case the five splittings observed in the high field region were not clear in this case and so it can be confirmed that this compound is not as symmetrical as the former one.

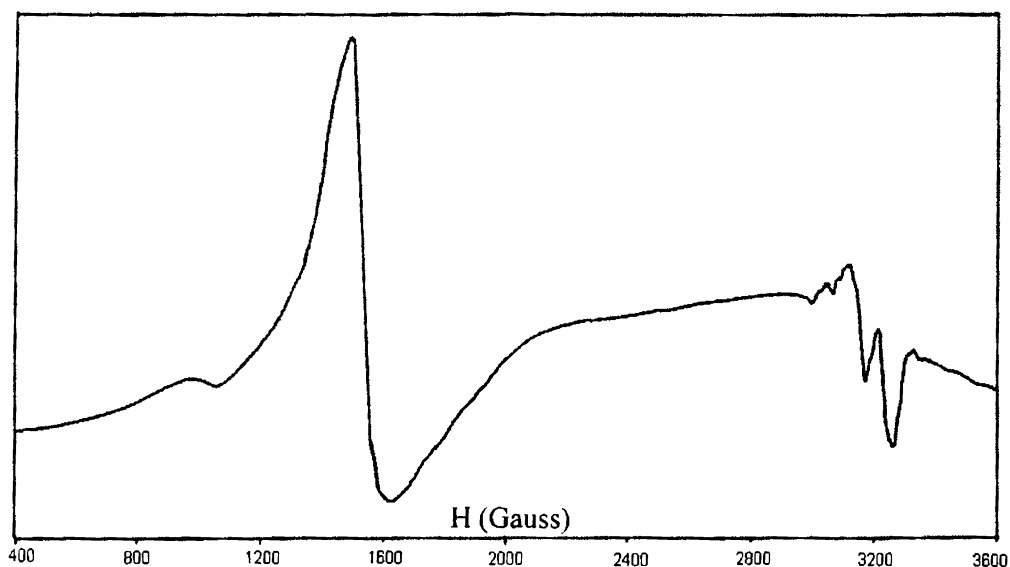


Fig. 5.8. The EPR spectrum of $[\text{Fe}(\text{HL}^2)(\text{L}^2)] \cdot 3\text{H}_2\text{O}$ (**29**) in DMF at 77 K.

The EPR spectrum of the complex $[\text{Fe}(\text{HL}^3)(\text{L}^3)] \cdot 2\text{H}_2\text{O}$ (**30**) was also recorded in solution in DMF at 77 K and is shown in the Fig. 5.9. In this case also the spectrum is very similar to the previous ones having g values $g_1 = 6.237$, $g_2 = 4.213$ and $g_3 = 1.993$. The splitting pattern of the spectrum in the high field region is

shown enlarged in the figure and it can be seen that there are five clear splittings in that region due to the symmetrical nature of the compound. In addition to that there are nine additional absorptions. This may be due to the super-hyperfine splitting pattern of two nitrogen atoms present in the molecule examined.

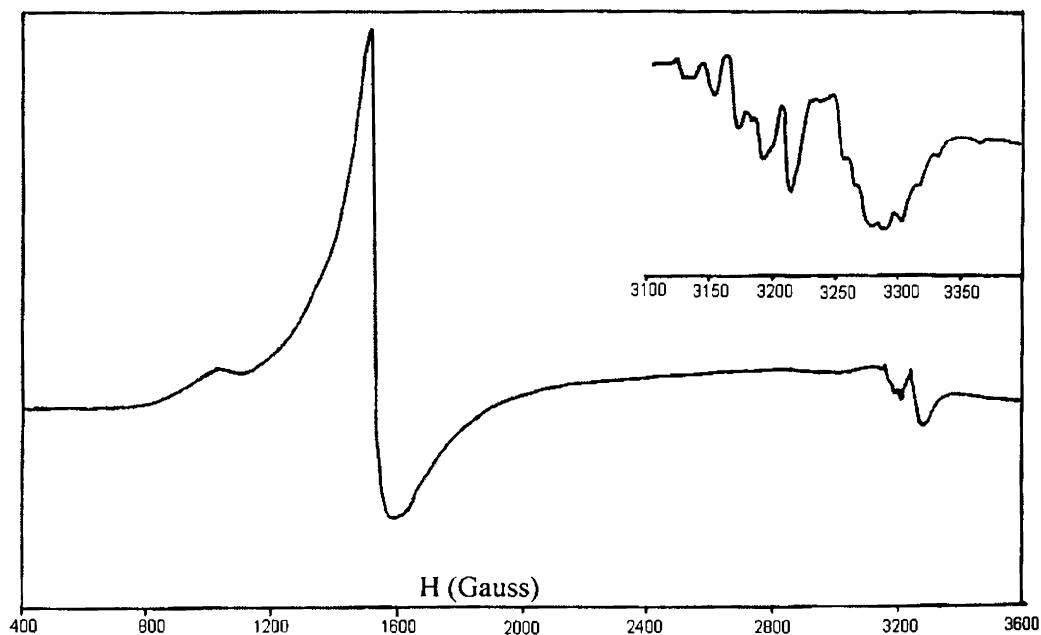


Fig. 5.9. The EPR spectrum of $[\text{Fe}(\text{HL}^3)(\text{L}^3)] \cdot 2\text{H}_2\text{O}$ (30) in DMF at 77 K.

From all the spectral data and elemental analyses, it can be concluded that all the iron(III) complexes are high spin d^5 systems, all the metal centers are six coordinate and octahedral. But the single crystals suitable for X-ray diffraction studies of none of the manganese(II) and iron(III) complexes were isolated and so based on the spectral data available, the tentative structures of these complexes can be proposed as given in the Fig. 5.10.

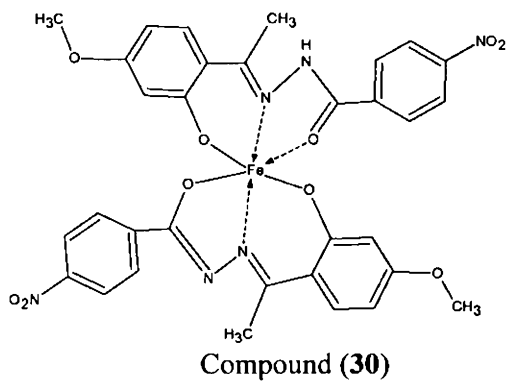
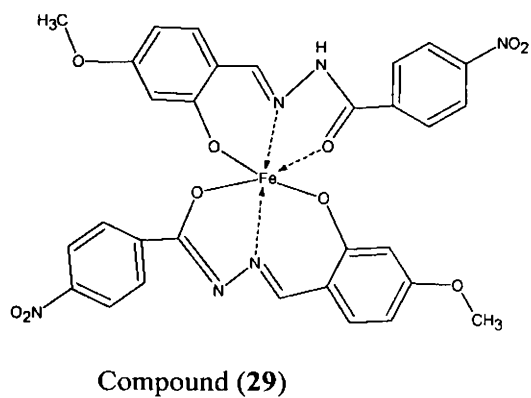
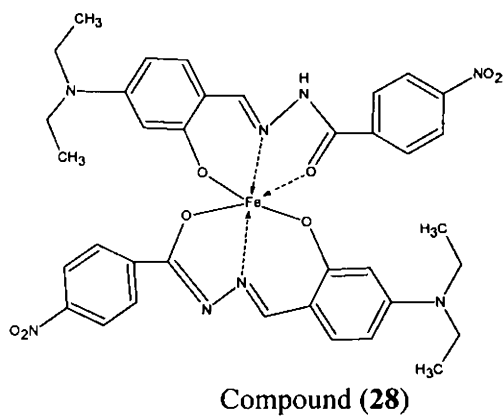
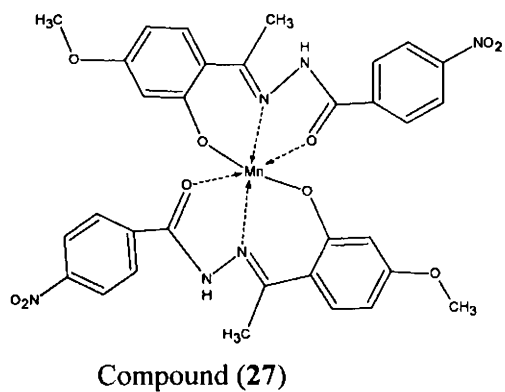
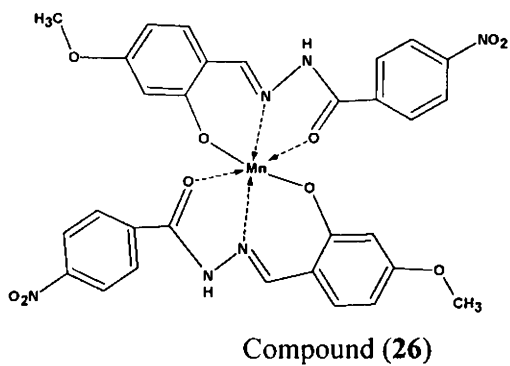
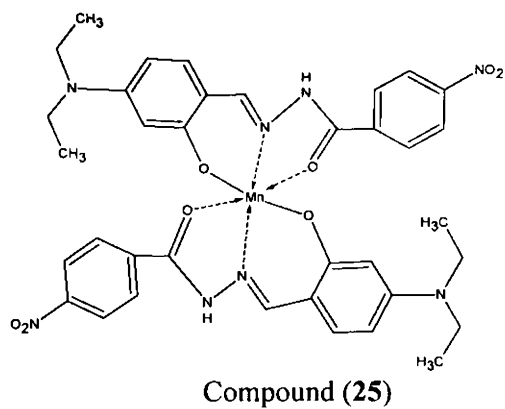


Fig. 5.10. Tentative structures of the manganese(II) and iron(III) complexes prepared.

5.5. *Non-linear optical properties of Mn(II) and Fe(III) complexes*

The essential requirement to exhibit non-linear optical properties has been proved to have a molecular structure within the general form D- π -A and the design of new second order NLO chromophores has focused primarily on engineering the electronic nature of the donor and the acceptor, and the conjugation length of the bridge. Another requirement for possessing NLO activity is that the molecule must be non centrosymmetric. Thus the existence of strong intramolecular charge transfer excitations in a noncentrosymmetric molecular environment. Even though the manganese(II) and iron(III) complexes are best examples for possessing strong metal to ligand charge transfer excitations, a very few ones have been reported [36-40] in this category yet. This may be due to the chance that majority of manganese and iron complexes are octahedral and symmetric in nature. The centrosymmetry within the molecular lattice may destroy the NLO activity in the molecule.

We also tried to establish the second harmonic generation created by the manganese(II) and iron(III) complexes prepared. From the characterization process itself it have been proved that all of them are octahedral and symmetric with the molecular centre. The conclusion was correct in the SHG efficiency also. None of them have a positive second harmonic generation efficiency, when measured by Hyper Rayleigh scattering technique.

References

1. P.D.W. Boyd, Q. Li, J.B. Vincent, K. Folting, R.H. Chang, W.E. Streib, J.B. Huffman, G. Christou, D.N. Hendrickson, *J. Am. Chem. Soc.* 110 (1988) 8537.
2. M.W. Wemple, L.H.- Tsai, W.E. Streib, D.N. Hendrickson, G. Christou, *J. Chem. Soc. Chem. Commun.* (1994) 1031.
3. K. Fegy, D. Luneau, E. Belorizky, M. Novac, J.-L. Tholence, C. Paulsen, T. Ohm, P. Rey, *Inorg. Chem.* 37 (1998) 4524.
4. J. Brinksma, R. Hage, J. Kerschner, B.L. Feringa, *Chem. Commun.* (2000) 537.
5. K.B. Jensen, E. Johansen, F.B. Larsen, C.J. McKenzie, *Inorg. Chem.* 43 (2004) 3801.
6. W. Zhang, J.L. Loebach, S.B. Wilson, E.N. Jacobsen, *J. Am. Chem. Soc.* 112 (1990) 2801.
7. R. Hage, *Recl. Trav. Chim. Pays-Bays* 115 (1996) 385.
8. B. Meunier, in *Metalloporphyrin Catalysed Oxidations*, ed. F. Montanari and L. Casella, Kluwer Academic Publishers, Dordrecht, 1994.
9. J. Bendix, H.B. Gray, G. Golubkov, Z. Gross, *Chem. Commun.* (2000) 1957.
10. D.P. Riley, *Chem. Rev.* 99 (1999) 2573.
11. V.K. Yachandra, K. Sauer, M.P. Klein, *Chem. Rev.* 94 (1996) 807.
12. J. Limburg, V.A. Szalai, G.W. Brudvig, *J. Chem. Soc. Dalton Trans.* (1999) 1351.
13. M.-L. Tong, S.-L. Zheng, J.-X. Shi, Y.-X. Tong, H.K. Lee, X.-M. Chen, *J. Chem. Soc. Dalton Trans.* (2002) 1727.
14. K. Weighardt, *Angew. Chem., Int. Ed. Engl.* 28 (1989) 1153.

15. M. Yagi, M. Kaneko, Chem. Rev. 101 (2001) 21.
16. G.C. Dismukes, Chem. Rev. 96 (1996) 2909.
17. C. Tommos, G.T. Babcock, Acc. Chem. Res. 31 (1998) 18.
18. A. Zouni, H.T. Witt, J. Kern, P. Formme, N. Kraub, W. Saenger, P. Orth, Nature 409 (2001) 739.
19. T.A. van den Berg, B.L. Feringa, G. Roelfes, Chem. Commun. (2007) 180.
20. N.V. Sidgwick, The Chemical Elements and Their Compounds, Vols. I and II, Oxford University Press, London (1950).
21. Gmelin's Handbook der Anorganischen Chemie Verlag Chemie, Weinheim (1932).
22. J.W. Meller, Comprehensive Treatise on Inorganic and Theoretical Chemistry, Longmans Green, London (1932).
23. D.R. Richardson, K. Milnes, Blood 89 (1997) 3025.
24. D.R. Richardson, P. Ponka, J. Lab. Clin. Med. 124 (1994) 660.
25. D.R. Richardson, E. Tran, P. Ponka, Blood 86 (1995) 4295.
26. A.B.P. Lever, Inorganic Electronic Spectroscopy, 2nd ed., Elsevier Science Publishers B. V., Netherlands, 1984.
27. K. Nakamoto *in* Infrared and Raman Spectra of Inorganic and Coordination Compounds, 4th ed., John Wiley & Sons, United States of America, 1986.
28. R. Luck, R. Stosser, O.G. Poluektov, O.Ya. Grinberg, S.Ya. Lebedev, G.M. Woltermann, J.R. Wasson, Inorg. Chem. 12 (1973) 2366.
29. E. Meirovitch, R. Poupko, J. Phys. Chem. 82 (1978) 1920.
30. M.R.P. Kurup *in* Stereochemical Investigations on Transition Metal Complexes of Biologically Active Substituted 2-acetylpyridine-thiosemicarbazones, Ph. D. Thesis, University of Delhi, 1988.
31. K.B. Pandeya, R. Singh, P.K. Mathur, R.P. Singh, Transition Met. Chem. 11 (1986) 347.
32. J.H. Van Vleck, W.G. Penney, Phil Mag. 17 (1934) 961.

33. A. Abragam, M.H.L. Pryce, Proc. Roy. Soc. Ser. A. 205 (1951) 135.
34. F. Rodriguez, M. Moreno, Transition. Met. Chem. 10 (1985) 351.
35. S.A. Cotton, Coord. Chem. Rev 8 (1972) 185.
36. In Su Lee, Y.K. Chung, Inorg. Chem. Commun. 10 (2007) 593.
37. H. Hou, Y. Wei, Y. Song, Y. Zhu, L. Li, Y. Fan, J. Met. Chem. 12 (2002) 838,
38. G.A. Artamkina, E.A. Shilova, M.M. Shtern, I.P. Beletskaya, Russian J. Org. Chem. 39 (2003) 1282.
39. G.A. Artamkina, I.P. Beletskaya, Mendeleev Commun., 13 (2003) 43.
40. A. Elmali, A. Karakaş, H. Ünver, Chem. Phys. 309 (2005) 251.

CHAPTER SIX

Syntheses, characterization and non-linear optical properties of zinc(II) and cadmium(II) complexes of the aroylhydrazone ligands

Zinc is a moderately reactive bluish grey metal and is an essential element, necessary for sustaining all life. It is estimated that 3,000 of the hundreds of thousands of proteins in the human body contain zinc prosthetic groups. In addition, there are over a dozen types of cells in the human body that secrete zinc ions, and the roles of these secreted zinc signals in medicine and health are now being actively studied. In the field of coordination chemistry also, zinc has its own importance. The zinc metal complexes are reported to have emerging applications in the field of medicines and as active catalysts. Zinc complexes of several ONS donor ligands are reported to possess biological applications [1]. Ghosh and Parkin have designed some N_2S and NS_2 ligands, the zinc complexes of which can serve as structural models for the related zinc enzymes [2]. Many proteins have been found to have a zinc-containing motif that serves to bind DNA embedded in their structure. In the relevance of zinc to Diabetes Mellitus (DM), zinc is known to be present in insulin, coordinated by three nitrogen atoms from histidines and three water molecules in an irregular octahedral environment, which is also believed to have a functional structure. Zinc containing carboxylate bridged complexes [3-4] have varied structural motifs in hydrolytic metalloenzymes, such as phosphatases and aminopeptidases. The catalytic role of Zn comprises Lewis acid activation of the substrate, generation of a reactive nucleophile ($Zn-OH$) and stabilization of the leaving group [5]. There are several reports in literature based on the $Zn(II)$ complexes of aroylhydrazones [6-10].

Cadmium is a soft, malleable, ductile, toxic, bluish-white bivalent metal. It is similar in many respects to zinc but reacts to form more complex compounds. Its toxicity derives from the fact that it is rapidly localized intracellularly, mainly in the liver and then bound to metallothionein forming a complex that is slowly transferred to the blood stream to be deposited in the kidneys. The most common oxidation state of cadmium is +2, though rare examples of +1 can be found. The main application of metallic cadmium is for making batteries and in pigment industry. The coordination chemistry of cadmium atom is found to be very similar to that of zinc. Considering the stereochemistry of the complexes, Zn(II) complexes are observed to be predominantly tetrahedral. Among the less common five-coordinate complexes, trigonal bipyramidal (*tbp*) geometry occurs more frequently than square-based pyramidal (*sbp*). Compared to this, Cd(II) cationic complexes are generally found in six- and four-coordination, while the five-coordinate complexes are less common and they include both *tbp* and *sbp* structures [11]. A series of examples based on the coordination complexes of cadmium with aroylhydrazone ligands have been reported. For instance, metallic salts such as Zn(OAc)₂ and Cd(OAc)₂ are known to bring about ring-chain tautomerization of thiosemicarbazones derived from β-ketoesters and β-ketoamides [12]. During the reactions of Zn(OAc)₂ with thiosemicarbazones derived from β-keto amides and esters in methanol, following the isolation of the corresponding Zn(II) thiosemicarbazones, the mother liquor afforded pyrazolonate complexes formed by the cyclization of the corresponding thiosemicarbazone [13]. It was also found that the cyclization is faster with Cd(OAc)₂ than with Zn(OAc)₂. In another report, Cd(II) complexes of the tripodal ligand, 1-(1-imidazolyl)-3,5-bis(imidazol-1-yl methyl)benzene are observed to exhibit anion-exchange properties [14].

6.1. Stereochemistry of Zn(II) complexes

The most common oxidation state of zinc is +2 and so many zinc complexes are reported in this state. It is a d^{10} system and is very stable. Zn(II) complexes are observed to be predominantly four coordinated and tetrahedral. Square planar complexes are also known. Among the less common five-coordinate complexes, trigonal bipyramidal (*tbp*) geometry occurs more frequently than square-based pyramidal (*sbp*). Aroylhydrazone complexes of zinc in six coordinated and octahedral environment were also reported.

6.2. Stereochemistry of Cd(II) complexes

The position of cadmium metal is in 12th group of the periodic table, below zinc. The oxidation state is +2, similar to zinc and the compounds formed are mainly four coordinated. Six coordinated analogues are also known and the five coordinated complexes are very rare. Cadmium complexes of aroylhydrazone ligands in octahedral environment are known.

6.3. Experimental

6.3.1. Materials

4-Nitrobenzoylhydrazide (Sigma Aldrich), 4-*N,N*-diethylamino-2-hydroxybenzaldehyde (Sigma Aldrich), 4-methoxy-2-hydroxybenzaldehyde (Sigma Aldrich), 4-methoxy-2-hydroxyacetophenone (Sigma Aldrich), zinc(II)acetate (S.D. Fine), cadmium acetate (Merck), pyridine, 4-picoline, DMF (S.D. Fine) were used as received. When ethyl alcohol was used as the solvent repeated distillation was carried out before use.

6.3.2. Syntheses of ligands

Preparation of the ligands H_2L^1 , H_2L^2 and H_2L^3 were done as described previously in Chapter 2.

6.3.3. Preparation of zinc(II) complexes

$[ZnL^1]_2 \cdot 2H_2O$ (**31**): The ligand H_2L^1 (0.374 g, 1 mmol) and $Zn(OAc)_2 \cdot 2H_2O$ (0.219 g, 1 mmol) were dissolved in a 1:1 mixture of absolute ethanol and DMF and refluxed for about two hours. The light red colored product obtained was filtered, washed several times with absolute ethanol followed by diethyl ether and dried over P_4O_{10} *in vacuo*. Yield: 0.361 g (70%). Elemental Anal. Found (Calcd.) (%): C, 48.99 (49.39); H, 4.05 (4.60); N, 12.68 (12.80).

$[ZnL^1py]$ (**32**): The complex was prepared by dissolving 0.200 g (0.23 mmol) of complex **31** in 15 ml of boiling pyridine and again boiled for 5 minutes. The solution was then added to water and the orange red colored solid formed was recovered by filtration. Washed several times with absolute ethanol followed by diethyl ether and dried over P_4O_{10} *in vacuo*. Yield: 0.186 g (81.9%). Elemental Anal. Found (Calcd.) (%): C, 55.55 (55.38); H, 4.78 (4.65); N, 13.99 (14.04).

$[ZnL^1pi]$ (**33**): The complex was prepared by dissolving 0.200 g (0.23 mmol) of complex **31** in 15 ml boiling 4-picoline and refluxed for about 5 minutes. After cooling the solution was poured to cold water and the yellowish orange colored product obtained was filtered, washed several times with absolute ethanol followed by diethyl ether and dried over P_4O_{10} *in vacuo*. Yield: 0.178 g (76%). Elemental Anal. Found (Calcd.) (%): C, 56.21 (56.20); H, 4.85 (4.91); N, 13.92 (13.66).

$[\text{ZnL}^2]_2 \cdot 2\text{H}_2\text{O}$ (**34**): The complex was prepared by refluxing a mixture of the ligand H_2L^2 (0.315 g, 1 mmol) and $\text{Zn}(\text{OAc})_2 \cdot 2\text{H}_2\text{O}$ (0.219 g, 1 mmol) in a 1:1 mixture of absolute ethanol and DMF. The reddish colored product obtained on cooling the reaction mixture to room temperature was filtered, washed several times with absolute ethanol followed by diethyl ether and dried over P_4O_{10} *in vacuo*. Yield: 0.589 g (74.2%). Elemental Anal. Found (Calcd.) (%): C, 45.80 (45.42); H, 3.14 (3.30); N, 10.70 (10.59).

$[\text{ZnL}^2\text{py}] \cdot \frac{1}{2}\text{H}_2\text{O}$ (**35**): 0.200 g (0.25 mmol) of the complex **34** was dissolved in 15 ml of boiling pyridine for 5 minutes and after cooling the solution was added to cold water. The red colored product obtained was filtered, washed several times with absolute ethanol followed by diethyl ether and dried over P_4O_{10} *in vacuo*. Yield: 0.181 g (77%). Elemental Anal. Found (Calcd.) (%): C, 51.61 (51.46); H, 3.74 (3.67); N, 11.82 (12.00).

$[\text{ZnL}^2\text{pi}] \cdot \frac{1}{2}\text{H}_2\text{O}$ (**36**): After dissolving 0.200 g (0.25 mmol) of complex **34** in 15 ml boiling 4-picoline, the solution was boiled for about 5 minutes and poured the cooled solution to cold water, so that a red colored product was obtained. It was filtered, washed several times with absolute ethanol followed by diethyl ether and dried over P_4O_{10} *in vacuo*. Yield: 0.169 g (69.8%). Elemental Anal. Found (Calcd.) (%): C, 52.60 (52.46); H, 4.00 (3.98); N, 11.41 (11.65).

$[\text{ZnL}^3]_2$ (**37**): The complex was prepared by refluxing a mixture of equimolar amounts of the ligand H_2L^3 (0.329 g, 1 mmol) and $\text{Zn}(\text{OAc})_2 \cdot 2\text{H}_2\text{O}$ (0.219 g, 1 mmol) in 1:1 mixture of absolute ethanol and DMF. The red colored product obtained on cooling the reaction mixture to room temperature was filtered, washed several times with absolute ethanol followed by diethyl ether and dried over P_4O_{10} *in vacuo*.

Yield: 0.573 g (72.9%). Elemental Anal. Found (Calcd.) (%): C, 49.35 (48.94); H, 3.44 (3.34); N, 10.72 (10.70).

[ZnL³py] (**38**): The complex was prepared by dissolving 0.200 g (0.25 mmol) of complex **37** in 15 ml of boiling pyridine and then boiled for another 5 minutes. The solution was then added to water and the yellow colored solid formed was recovered by filtration. Washed several times with absolute ethanol followed by diethyl ether and dried over P₄O₁₀ *in vacuo*. Yield: 0.173 g (72%). Elemental Anal. Found (Calcd.) (%): C, 53.39 (53.36); H, 3.52 (3.85); N, 11.69 (11.88).

[ZnL³pi] (**39**): After dissolving 0.200 g (0.25 mmol) of complex **37** in 15 ml boiling 4-picoline, the solution was boiled for about 5 minutes and poured the cooled solution to cold water, so that an orange colored product was obtained. It was filtered, washed several times with absolute ethanol followed by diethyl ether and dried over P₄O₁₀ *in vacuo*. Yield: 0.154 g (65.8%). Elemental Anal. Found (Calcd.) (%): C, 54.23 (54.39); H, 3.89 (4.15); N, 11.35 (11.53).

6.3.4. Preparation of cadmium(II) complexes

[CdL¹]₂·H₂O (**40**): To a hot 1:1 DMF/ethanol solution of ligand H₂L¹ (0.374 g, 1 mmol), Cd(OAc)₂·2H₂O (0.266 g, 1 mmol) dissolved in ethanol was added. The solution was then refluxed for about three hours. The resulting red colored solution on cooling to room temperature yielded bright orange colored solid. It was separated and washed with ether and dried over P₄O₁₀ *in vacuo*. Yield: 0.832 g (87.4%). Elemental Anal. Found (Calcd.) (%): C, 45.88 (45.44); H, 3.41 (4.03); N, 10.73 (11.08).

[CdL¹py] (**41**): 0.200 g (0.21 mmol) of the compound **40** was weighed out and dissolved in 15 ml boiling pyridine. The solution was then boiled for about 5 minutes

and poured the cooled solution to cold water, so that a yellow colored product was obtained. It was filtered, washed several times with absolute ethanol followed by diethyl ether and dried over P_4O_{10} *in vacuo*. Yield: 0.186 g (81.2%). Elemental Anal. Found (Calcd.) (%): C, 49.84 (50.61); H, 4.405 (4.25); N, 12.52 (12.83).

$[CdL^1pi] \cdot \frac{1}{2}H_2O$ (**42**): The complex was prepared by dissolving 0.200 g (0.21 mmol) of complex **40** in 15 ml of boiling 4-picoline and then boiled for another 5 minutes. The solution was then added to water and the yellow colored solid formed was filtered, washed several times with absolute ethanol followed by diethyl ether and dried over P_4O_{10} *in vacuo*. Yield: 0.173 g (72.6%). Elemental Anal. Found (Calcd.) (%): C, 52.53 (52.69); H, 4.72 (4.83); N, 13.11 (12.52).

$[CdL^2]_2$ (**43**): $Cd(OAc)_2 \cdot 2H_2O$ (0.266 g, 1 mmol) was dissolved in ethanol and added to a hot 1:1 DMF/ethanol solution of the ligand H_2L^2 (0.315 g, 1 mmol) and the solution was again refluxed for another three hours. On cooling the red solution obtained, yellowish orange product was obtained. It was then filtered, washed with ethanol followed by ether and dried over P_4O_{10} *in vacuo*. Yield: 0.719 g (84.4%). Elemental Anal. Found (Calcd.) (%): C, 43.36 (42.32); H, 2.72 (2.60); N, 10.03 (9.87).

$[CdL^2py]$ (**44**): After dissolving 0.200 g (0.23 mmol) of complex **43** in 15 ml boiling pyridine, the solution was boiled for about 5 minutes and poured the cooled solution to cold water, so that a yellow colored product was obtained. It was filtered, washed several times with absolute ethanol followed by diethyl ether and dried over P_4O_{10} *in vacuo*. Yield: 0.175 g (74.1%). Elemental Anal. Found (Calcd.) (%): C, 47.70 (47.59); H, 3.28 (3.19); N, 11.19 (11.10).

$[CdL^2pi] \cdot \frac{3}{2} H_2O$ (**45**): The complex was prepared by dissolving 0.200 g (0.23 mmol) of complex **43** in 15 ml boiling 4-picoline and refluxed for about 5 minutes. After cooling the solution was poured to cold water and the orange colored

product obtained was filtered, washed several times with absolute ethanol followed by diethyl ether and dried over P_4O_{10} *in vacuo*. Yield: 0.163 g (63.6%). Elemental Anal. Found (Calcd.) (%): C, 46.13 (46.21); H, 3.34 (3.88); N, 10.32 (10.26).

$[CdL^3]_2$ (**46**): To a solution of the ligand H_2L^3 (0.329 g, 1 mmol) in a hot 1:1 DMF/ethanol, Cd(II) acetate (0.266 g, 1 mmol) in ethanol was added and refluxed for 3 hours. The yellow solid deposited on cooling the resulting solution was separated, washed with ethanol, followed by ether and dried over P_4O_{10} *in vacuo*. Yield: 0.706 g (80.3%). Elemental Anal. Found (Calcd.) (%): C, 43.82 (43.70); H, 2.93 (2.98); N, 9.68 (9.56).

$[CdL^3py]$ (**47**): 0.200 g (0.22 mmol) of the complex **46** was dissolved in 15 ml of boiling pyridine for 5 minutes and after cooling the solution was added to cold water. The bright yellow colored product obtained was filtered, washed several times with absolute ethanol followed by diethyl ether and dried over P_4O_{10} *in vacuo*. Yield: 0.191 g (81.3%). Elemental Anal. Found (Calcd.) (%): C, 48.42 (48.62); H, 3.47 (3.50); N, 10.39 (10.80).

$[CdL^3pi] \cdot 5/2 H_2O$ (**48**): The compound **48** was prepared by dissolving 0.200 g (0.22 mmol) of complex **46** in 15 ml boiling 4-picoline and refluxed for about 5 minutes. After cooling the solution was poured to cold water and the yellow colored product obtained was filtered, washed several times with absolute ethanol followed by diethyl ether and dried over P_4O_{10} *in vacuo*. Yield: 0.183 g (69.8%). Elemental Anal. Found (Calcd.) (%): C, 45.82 (45.73); H, 3.37 (4.36); N, 9.41 (9.70).

6.4. Results and discussion

6.4.1. Spectral studies of zinc(II) complexes

6.4.1a. Electronic spectral studies

The electronic absorption spectra are often very helpful in the evaluation of results furnished by other methods of structural investigation. The electronic spectral measurements were used for assigning the stereochemistries of metal ions in the complexes based on the positions and number of *d-d* transition peaks. But in the case of Zn(II) complexes, no *d-d* transitions are expected since it is a d^{10} system and is completely filled [15].

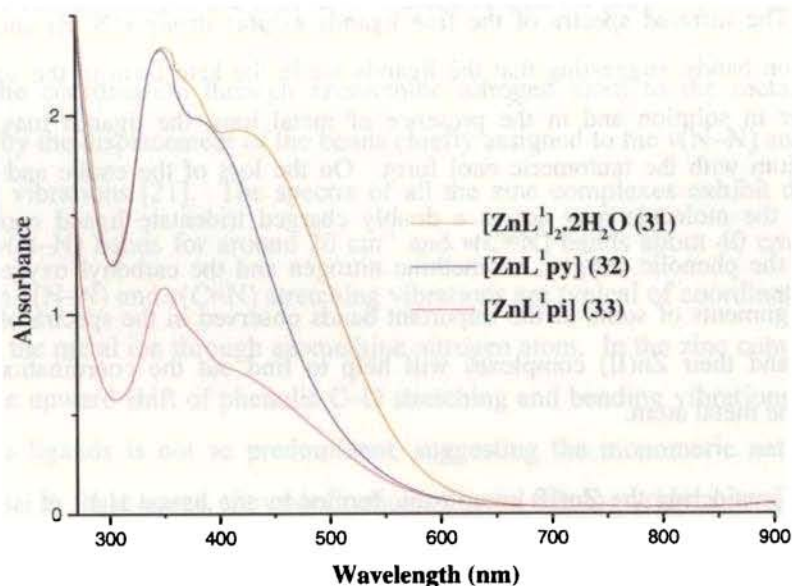


Fig. 6.1. The UV-Vis spectra of the zinc(II) complexes **31**, **32** and **33** in DMF.

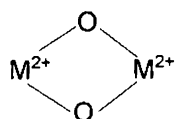
All the zinc complexes were found to be red or orange in color, which is contrary to the common nature of Zn(II) complexes. They are generally found to be colorless or very light colored. Here it may be due to the intense color of the ligands and its high intensity absorption bands in the visible region and to some extent due to the ligand to metal charge transfer transitions. The combined UV-Vis spectra of the Zn(II) complexes of the ligand H_2L^1 are shown in the Fig. 6.1. From the spectral pattern, it is clear that the shape of the absorption pattern is very similar to that of the ligand UV-Vis spectrum. The charge transfer transitions are observed as shoulder in the region 400-450 nm. The electronic spectra of other zinc complexes also showed similar trends with that of the ligand absorption.

6.4.1b. Infrared spectral studies

The infrared spectra of the free ligands exhibit strong $\nu(N-H)$ and $\nu(C=O)$ absorption bands, suggesting that the ligands are in the keto form in the solid state. However in solution and in the presence of metal ions, the ligands may exist in equilibrium with the tautomeric enol form. On the loss of the enolic and phenolic protons, the molecule may act as a doubly charged tridentate ligand coordination through the phenolic oxygen, azomethine nitrogen and the carbonyl oxygen atoms. The assignments of some of the important bands observed in the spectra of the free ligands and their Zn(II) complexes will help to find out the coordination pattern around the metal atom.

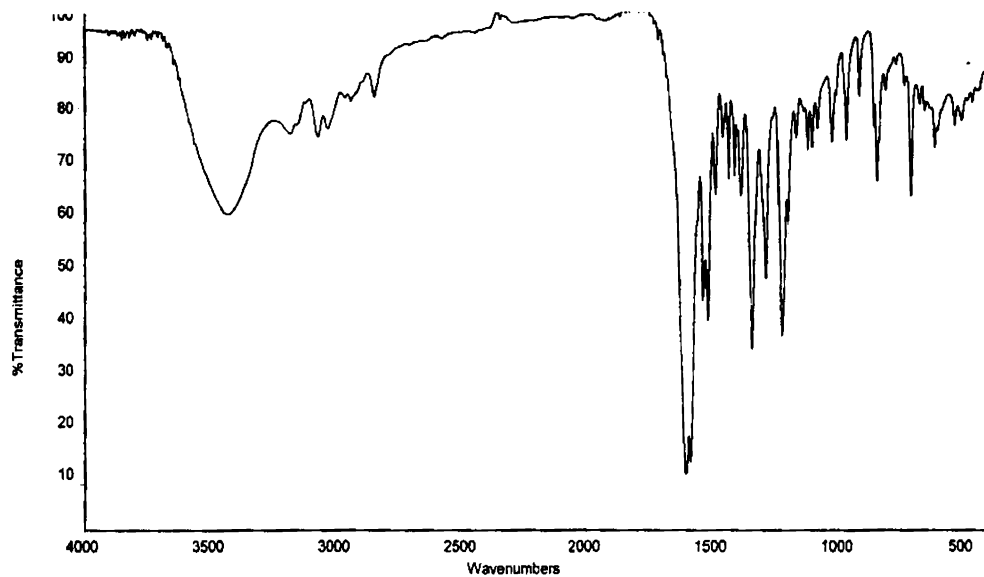
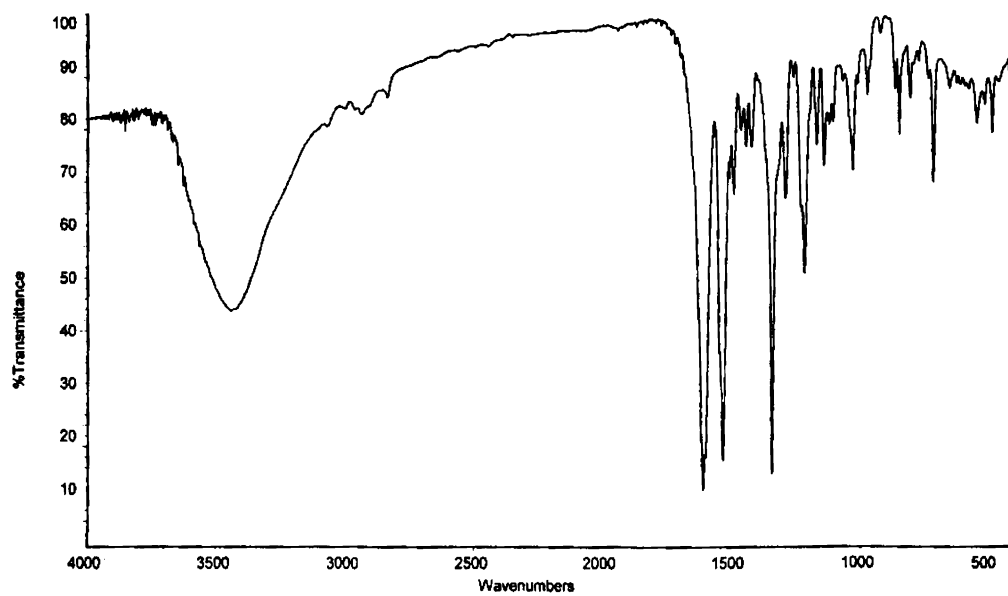
Considering the Zn(II) complexes, formed by the ligand H_2L^1 , it is seen that the broad band observed at *ca.* 3400 cm^{-1} is disappeared in all the zinc complexes except those have lattice water according to the elemental analyses data. This confirms the coordination of the ligand through phenolic oxygen. The phenolic C–O stretching and bending vibrations observed in the free ligands are displaced to higher

frequencies. The trend of these bands is a reliable criterion of the mono or polymeric nature of the complexes. The upward shift is a definite proof of the dimeric nature of the complexes, involving phenoxide bridging (16-17). The displacement to higher frequencies is probably due to the increase in C–O bond strength on extended delocalization of the π system of the azine moiety. The dimeric nature of the complexes are also supported by the appearance of new bands at 730 -740 cm^{-1} . These bands originate from,



ring vibrations [18-19]. The infrared spectra of the all the zinc complexes do not show any characteristic bands of the amide and amino groups, indicating that the ligands are coordinating in the enol form in these complexes [20].

The coordination through azomethine nitrogen atom to the metal atom is indicated by the displacement of the bands chiefly assigned to the $\nu(\text{N-N})$ and $\nu(\text{C=N})$ stretching vibrations [21]. The spectra of all the zinc complexes exhibit downward shifts of $\nu(\text{N-N})$ bands for around 20 cm^{-1} and $\nu(\text{C=N})$ bands about 40 cm^{-1} . These changes in $\nu(\text{N-N})$ and $\nu(\text{C=N})$ stretching vibrations are typical of coordination of the ligands to the metal ion through azomethine nitrogen atom. In the zinc complexes, **32** and **33**, the upward shift of phenolic C–O stretching and bending vibrations observed in the free ligands is not so predominant, suggesting the monomeric nature of the complexes. In these cases, the coordination of metal ion to pyridyl nitrogen atom is confirmed by the bands in far infrared region. The bands around 210 cm^{-1} in far infrared region is assigned to $\nu(\text{M-py})$ vibrations of Zn(II) complexes [22].

Fig. 6.2. The infrared spectrum of $[\text{ZnL}^2]_2 \cdot 2\text{H}_2\text{O}$ (34).Fig. 6.3. The infrared spectrum of $[\text{ZnL}^2\text{pi}] \cdot \frac{1}{2}\text{H}_2\text{O}$ (36).

Similar trends of shifting of the corresponding bands are observed in the case of the zinc(II) complexes formed by the other ligands H_2L^2 and H_2L^3 , suggesting similar coordination pattern. Infrared spectral data supports the dimeric nature of the zinc complexes, **31**, **34** and **37** and monomeric structure for **32**, **33**, **35**, **36**, **38** and **39**, supporting the elemental analyses studies. The IR spectra of the complexes $[ZnL^2]_2 \cdot 2H_2O$ (**34**) and $[ZnL^2pi] \cdot \frac{1}{2}H_2O$ (**36**) are shown in Fig. 6.2 and Fig. 6.3 respectively.

6.4.1c. 1H NMR spectral studies

The 1H NMR spectra of all the zinc(II) complexes were recorded in $DMSO-d_6$, but some of the spectra were very poor due to the very low solubility of the complexes in DMSO. The assignment of 1H NMR spectral peaks of the zinc complexes can confirm the mode of coordination of the ligands to the metal ion. In all the NMR spectra it was found that two sharp singlets at the very downfield region of the ligand spectrum due to $-OH$ and $-NH$ protons were disappeared upon complexation, confirming the coordination through deprotonated phenolic oxygen and deprotonated enolic oxygen [23]. It was a common trend in all the zinc complexes of all the three ligands. The remaining portion of NMR spectra of complexes **31**, **34** and **37** were very similar to the ligand NMR spectra, suggesting that proton environment is similar to those in the corresponding ligands, since the remaining are the aromatic protons, which are not disturbed. The 1H NMR spectrum of the complex, **31** is shown in Fig. 6.4.

In the case of the 1H NMR spectra of the monomeric complexes, in addition to the peaks of aromatic protons in the principal ligand, those due to pyridyl nitrogen peaks also must be there. But these were not clear, may be due to the poor solubility of the complexes in DMSO.

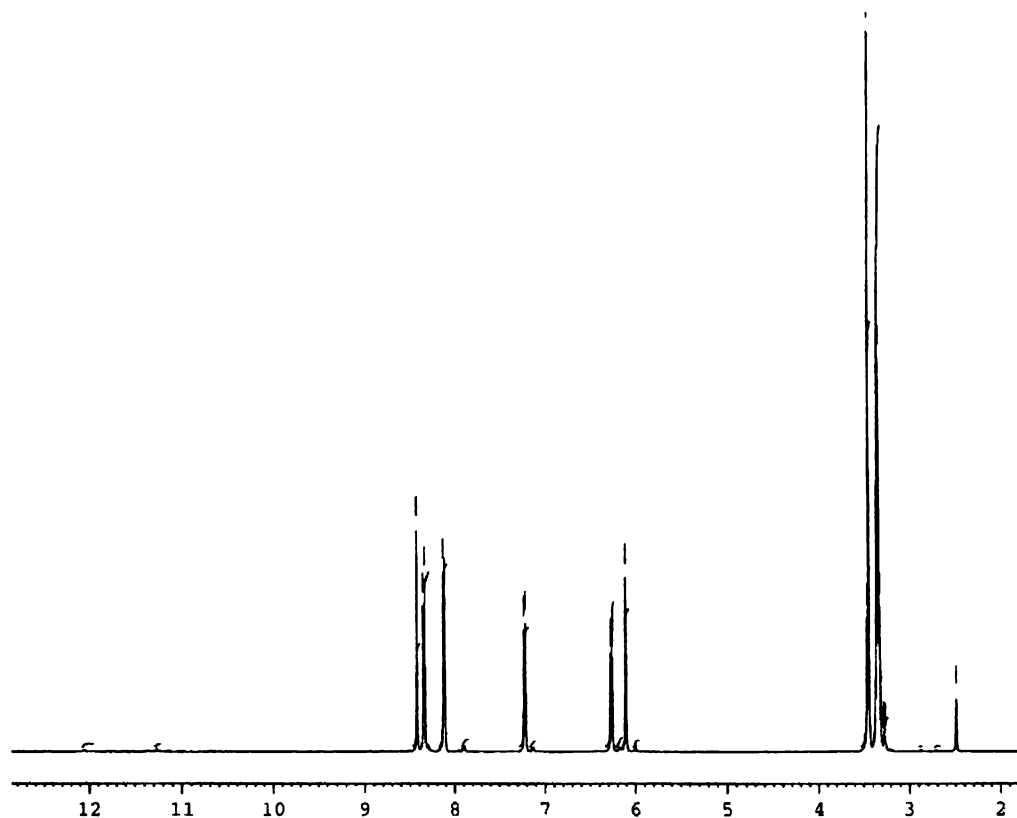


Fig. 6.4. ^1H NMR spectrum of compound $[\text{ZnL}^1]_2 \cdot 2\text{H}_2\text{O}$ (**31**) in $\text{DMSO-}d_6$.

6.4.2. Spectral studies of cadmium(II) complexes

6.4.2a. Electronic spectral studies

Since the d orbitals are completely filled in the case of Cd(II) complexes, no *d-d* transitions are expected in them. But all the presently studied nine complexes were brightly colored. This may be due to the extensively delocalized nature of the ligand molecule itself. So the bands observed in the UV-Vis spectra of Cd(II)

complexes are due to the ligand $\pi \rightarrow \pi^*$ and $n \rightarrow \pi^*$ transitions and also due to the charge transfer excitations from the filled metal orbital to the ligand orbital.

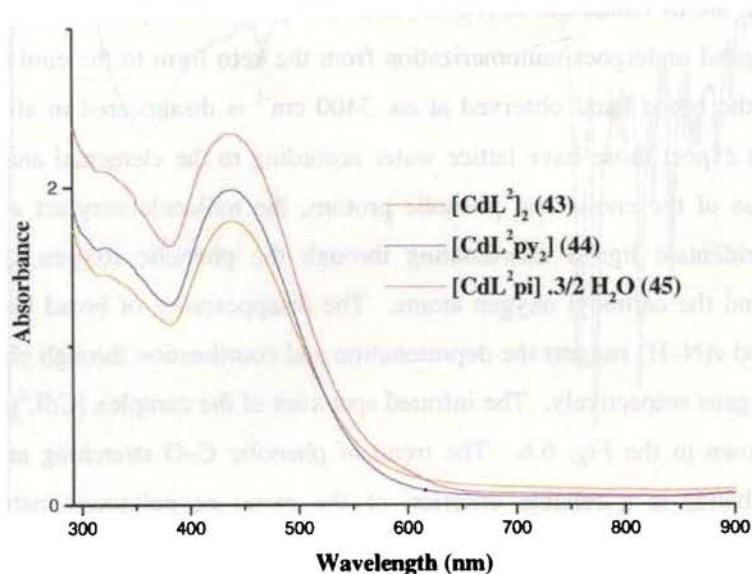


Fig. 6.5. The UV-Vis spectra of the Cd(II) complexes **43**, **44** and **45** in DMF.

The UV-Vis spectra of 10^{-4} M solution of Cd(II) complexes formed by the ligand H_2L^1 in DMF is shown in the Fig. 6.5. All of them have similar pattern of absorption at exactly same wavelengths, pointing out the similar environment in them. The ligand $\pi \rightarrow \pi^*$ transitions are observed in the region 320-380 nm and ligand $n \rightarrow \pi^*$ together with charge transfer transitions in the complex molecule are observed as a broad band in the region 400-550 nm.

6.4.2b. Infrared spectral studies

A careful comparison of the important IR frequencies of the ligand and the complexes is a way to predict the coordination nature in the metal complexes. The

infrared spectra of the free ligands exhibit strong $\nu(\text{N-H})$ and $\nu(\text{C=O})$ absorption bands, suggesting that the ligands are in the keto form in the solid state. In all the complexes, the IR bands due to $\nu(\text{C=O})$ and $\nu(\text{N-H})$ had disappeared, which indicates that the ligand undergoes tautomerization from the keto form to the enol form. It is seen that the broad band observed at *ca.* 3400 cm^{-1} is disappeared in all the cobalt complexes except those have lattice water according to the elemental analyses data. On the loss of the enolic and phenolic protons, the molecule may act as a doubly charged tridentate ligand coordinating through the phenolic oxygen, azomethine nitrogen and the carbonyl oxygen atoms. The disappearance of broad bands due to $\nu(\text{O-H})$ and $\nu(\text{N-H})$ suggest the deprotonation and coordination through phenolic and enolic oxygens respectively. The infrared spectrum of the complex $[\text{CdL}^2\text{pi}] \cdot 3/2\text{ H}_2\text{O}$ (**45**) is shown in the Fig. 6.6. The trend of phenolic C–O stretching and bending vibration bands is a reliable criterion of the mono or polymeric nature of the complexes. In the case of the cadmium complexes **40**, **43** and **46**, these bands are shifted to higher frequency region, suggesting dimeric nature of the complexes involving phenoxide bridging. The observation is found to be very similar to the corresponding zinc complexes.

The coordination through azomethine nitrogen atom to the metal atom is indicated by the displacement of the bands chiefly assigned to the $\nu(\text{N-N})$ and $\nu(\text{C=N})$ stretching vibrations. All the complexes exhibit a considerable downward shift of $\nu(\text{N-N})$ and $\nu(\text{C=N})$ bond vibrations. Among the cadmium complexes, **41**, **42**, **44**, **45**, **47** and **48**, the upward shift of phenolic C–O stretching and bending vibrations observed in the free ligands are not so predominant, suggesting the monomeric nature of the complexes. In these cases, the coordination of metal ion to pyridyl nitrogen atom is confirmed by the bands in far infrared region. The bands around 250 cm^{-1} in far infrared region is assigned to $\nu(\text{M-py})$ vibrations of Zn(II) complexes. Complexes

of all the three ligands showed similar trends in the infrared spectra, suggesting that similar molecular structure and coordination pattern exist in all of them.

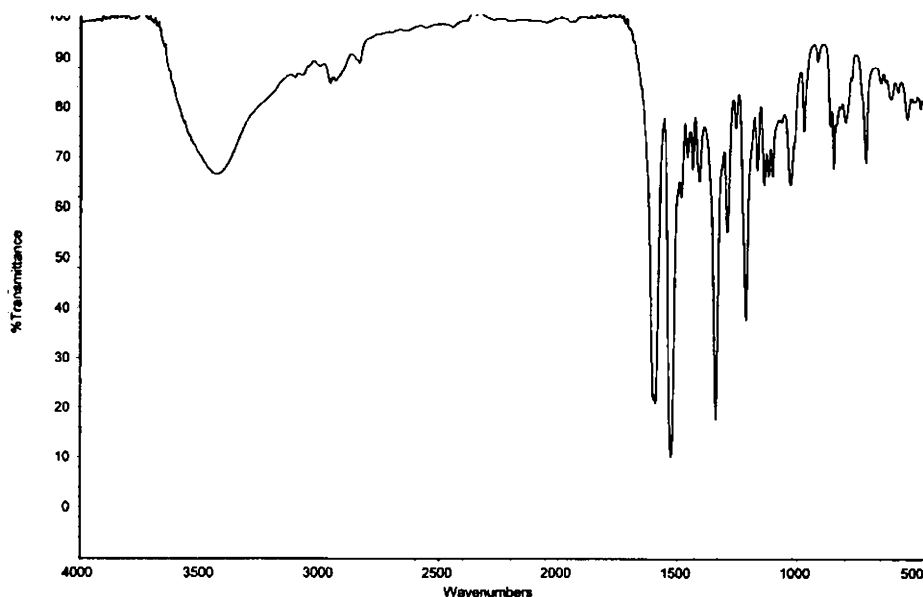
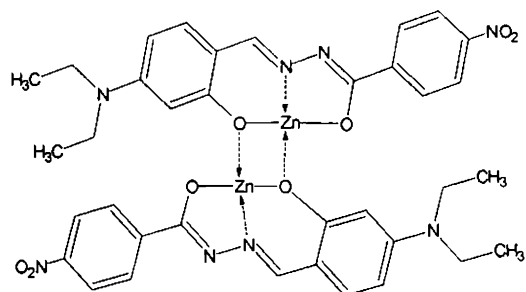


Fig. 6.6. The infrared spectrum of $[\text{CdL}^2\text{pi}] \cdot 3/2 \text{H}_2\text{O}$ (45).

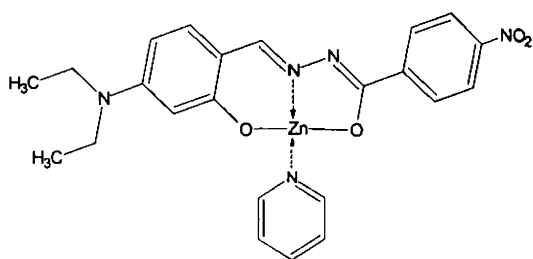
^1H NMR spectra of all the cadmium(II) metal complexes were recorded in $\text{DMSO}-d_6$, but the spectra were of very poor quality due to the very low solubility of the complexes in DMSO. They gave practically no evidence for the molecular structure of the complexes.

From all the spectral and elemental analyses data, it can be concluded that all the Zn(II) and Cd(II) complexes are d^{10} systems, all the metal centers are four coordinated and square planar. But the single crystals suitable for X-ray diffraction studies of none of the zinc(II) and cadmium(II) complexes were isolated and so based

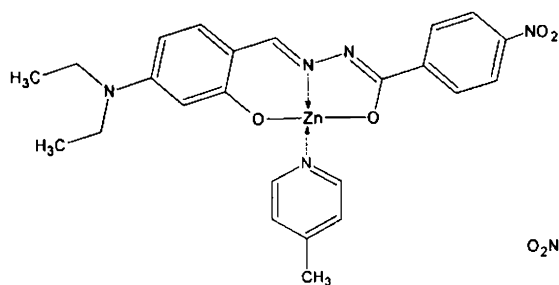
on the spectral data available, the tentative structures of these complexes can be proposed as given in the Fig. 6.7.



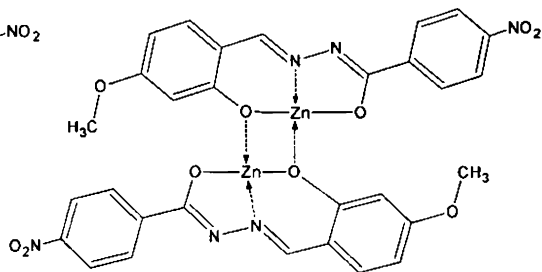
Compound (31)



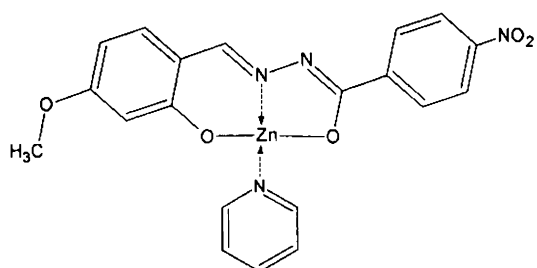
Compound (32)



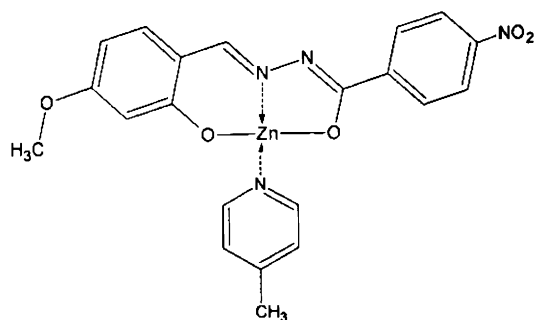
Compound (33)



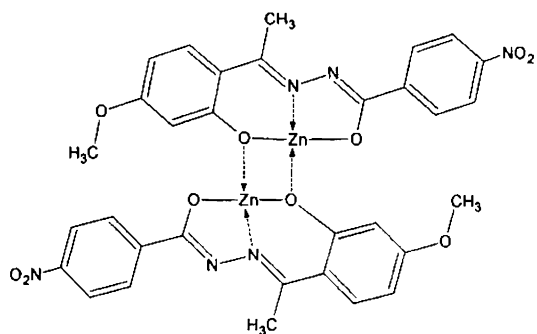
Compound (34)



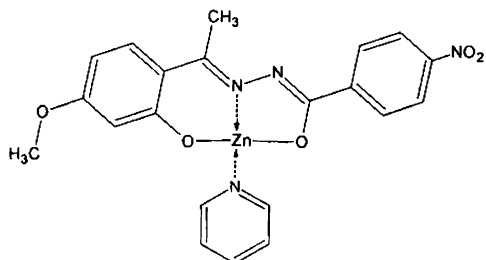
Compound (35)



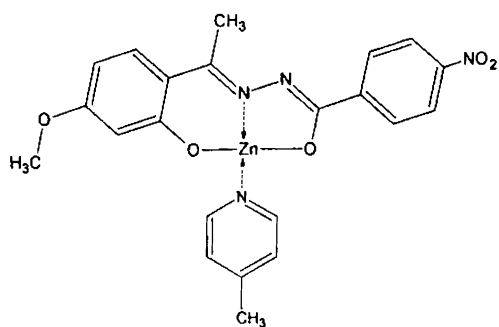
Compound (36)



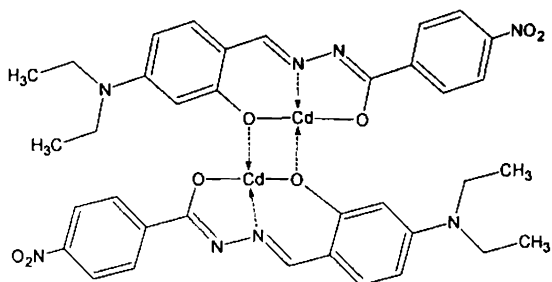
Compound (37)



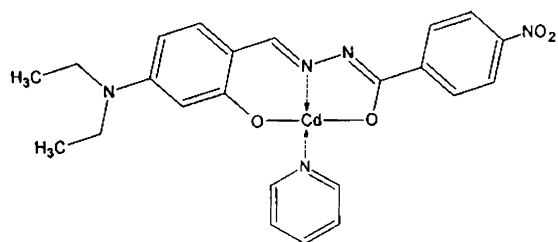
Compound (38)



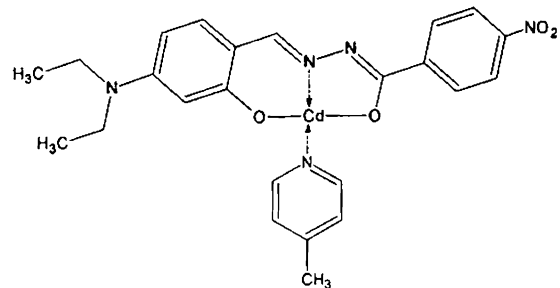
Compound (39)



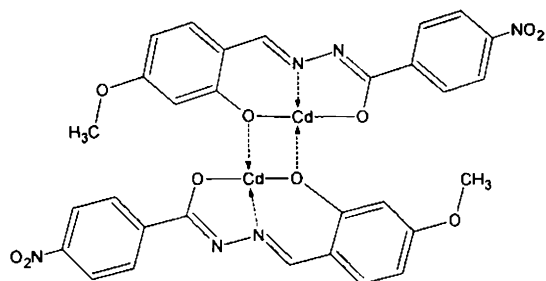
Compound (40)



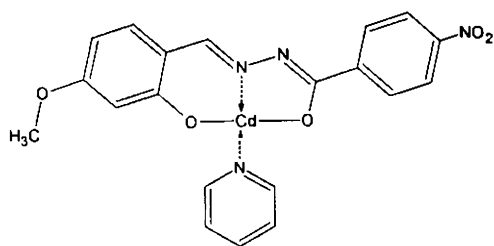
Compound (41)



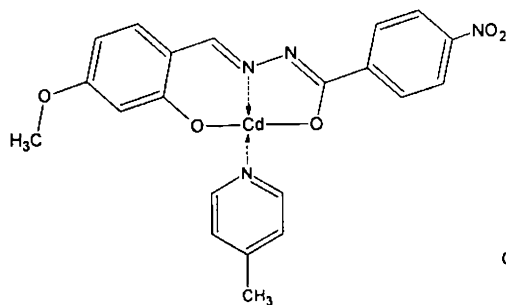
Compound (42)



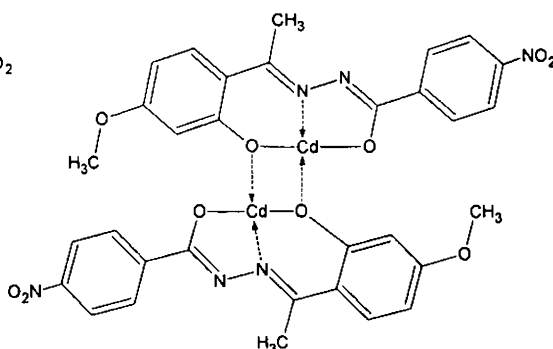
Compound (43)



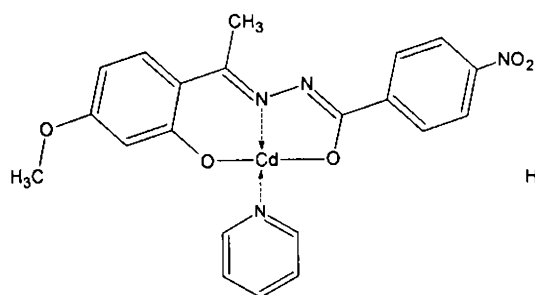
Compound (44)



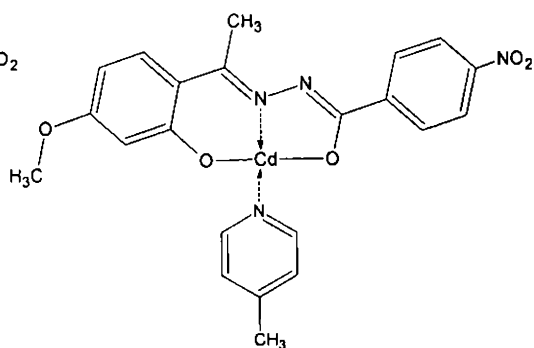
Compound (45)



Compound (46)



Compound (47)



Compound (48)

Fig. 6.7. Tentative structures of the Zn(II) and Cd(II) complexes prepared.

6.5. *Non-linear optical properties of Zn(II) and Cd(II) complexes*

In the last decade a growing number of reviews [24-26] and publications have highlighted the utility of organometallic complexes, in which organic chromophores are bound to metal centers, for second harmonic generation [27-30]. Molecular polarizabilities are frequently larger for metallic complex than for the free chromophore because of metal-to-ligand or ligand-to-metal charge transfer and because of involvement of the orbitals on the metal. Another appealing aspect for the design of non-linear optical properties is that metal centers may serve as anchors in the engineering of three dimensional geometries giving rise to octupolar molecules. Moreover, the combination of organic and inorganic elements affords materials of relatively high mechanical and thermal stability, as is also observed for organic chromophores in inorganic host matrixes.

The choice of Zn(II) and Cd(II) as metal centre is generally common in the non-linear optical chemistry of inorganic metal complexes due to transparency considerations. An important requirement for SHG applications is transparency in a large spectral region in order to avoid absorption of the generated second harmonic radiations. In this regard, Zn(II) and Cd(II) are interesting because of the lack of *d-d* transitions. Furthermore, other works has shown that, from a series of complexes with different metal centers, those with Zn(II) generally exhibit the large hyperpolarizability. The essential molecule to exhibit non-linear optical properties has been proved to have a molecular structure within the general form D- π -A and the design of new second order NLO chromophores has focused primarily on engineering the electronic nature of the donor and the acceptor, and the conjugation length of the bridge. Another requirement for possessing NLO activity is that the molecule must be non centrosymmetric. Thus the existence of strong intramolecular charge transfer excitations in a noncentrosymmetric molecular environment.

The second harmonic generation produced by all the Zn(II) and Cd(II) complexes were determined in the powder form by Hyper Rayleigh scattering technique. The well powdered sample was filled in capillary tube having 0.8 mm thickness. The NLO responses of these samples were recorded using urea as the reference, filled in similar capillary tube. The experimental arrangement for the non-linear optical properties utilizes a Quanter A DCR II Nd/YAG laser with 9 mJ a pulse at a repetition rate of 5 Hz. The selected wavelength is 1064 nm. After the selection of the wavelength the laser beam is split in to two parts, one to generate the second harmonic signal in the sample and the other to generate second harmonic signal in the reference (urea). An output signal of 532 nm was measured in a 90° geometry using urea as the standard. The efficiency of the NLO activity of the compounds are expressed in percentage as

$$\text{Efficiency} = \frac{\text{Signal of sample}}{\text{Signal of urea}} \times 100\%$$

The dimeric complexes **31**, **34**, **37**, **40**, **43** and **46** do not produce any second harmonic generation, may be due to the presence of centre of symmetry in the molecular lattice. The existence of inversion centre within the molecule may cancel the second harmonic generation produced by it. But the monomeric complexes, both the pyridine and picoline analogous produced considerable second harmonic efficiency in the crude form itself. But the capacity is not to the mark expected may be due to the lack of transparency in the molecule. All the complexes were brightly colored even though there were no *d-d* transitions in the molecule. The color is expected to be because of the extensively delocalized environment in the ligand part of the molecule. From the UV-Vis spectra of all the complexes studied, it can be concluded that all of them have considerable absorption in 532 nm region, where the second harmonic emission occurs. All the monomeric Zn(II) and Cd(II) complexes showed SHG efficiency.

References

1. S. Padhye, G.B. Kauffman, *Coord. Chem. Rev.* 63 (1985) 127.
2. P. Ghosh, G. Parkin, *J. Chem. Soc. Chem. Commun.* (1998) 413.
3. Z.-L. You, H.-L. Zhu, W.-S. Liu, *Z. Anorg. Allg. Chem.* 630 (2004) 1617.
4. Z.-L. You, H.-L. Zhu, *Z. Anorg. Allg. Chem.* 630 (2004) 2754.
5. A. Erxleben, J. Hermann, *J. Chem. Soc. Dalton Trans.* (2000) 569.
6. G. Paolucci, P.A. Vigato, G. Rosetto, U. Casellato, M. Vidali, *Inorg. Chim. Acta* 65 (1982) L71.
7. C. Pelizzi, G. Pelizzi, G. Predieri, S. Resola, *J. Chem. Soc., Dalton Trans.* (1982) 1350.
8. C. Lorenzini, C. Pelizzi, G. Pelizzi, G. Predieri, *J. Chem. Soc., Dalton Trans.* (1983) 721.
9. K.K. Narang, R.A. Lal, *Transition Met. Chem.* 2 (1977) 100.
10. K.K. Narang, R.M. Dubey, *Indian J. Chem.* 21A (1982) 830.
11. Z. Li, Z.-H. Loh, S.-W.A. Fong, Y.-K. Yan, W. Henderson, K.F. Mok, T.S. A. Hor, *J. Chem. Soc. Dalton Trans.* (2000) 1027.
12. J.S. Casas, M.V. Castano, M.S. Garcia-Tasende, E. Rodriguez-Castellon, A. Sanchez, L.M. Sanjuan, J. Sordo, *Dalton Trans.* (2004) 2019.
13. J.S. Casas, M.V. Castano, E.E. Castellano, J. Ellena, M.S. Garcia-Tasende, A. Gato, A. Sanchez, L.M. Sanjuan, J. Sordo, *Inorg. Chem.* 41 (2002) 1550.
14. W. Zhao, J. Fan, T. Okamura, W.-Y. Sun, N. Ueyama, *New. J. Chem.* 28 (2004) 1142.
15. A.B.P. Lever, *Inorganic Electronic Spectroscopy*, Elsevier, Amsterdam (1968).
16. R.J. Butcher, J. Jasinski, G.M. Mockler, E. Sinn, *J. Chem. Soc., Dalton Trans.* (1976) 1099.

17. J.O. Miners, E. Sinn, R.B. Coles, C.M. Harris, *J. Chem. Soc., Dalton Trans.* (1972) 1149.
18. D.J. Hewkin, W.P. Griffith, *J. Chem. Soc. A* (1966) 472.
19. W.P. Griffith, *J. Chem. Soc. A.* (1969) 211.
20. C.N.R. Rao, *Chemical applications of Infrared Spectroscopy*, Academic Press, New York/London, (1962).
21. M. Mohan, P. Sharma, N.K. Jha, *Inorg. Chim. Acta* 106 (1985) 117.
22. K. Nakamoto *in* *Infrared and Raman Spectra of Inorganic and Coordination Compounds*, 4th ed., John Wiley & Sons, USA, (1986).
23. R.M. Silverstein, G.C. Bassler, T.C. Morrill, *Spectrometric Identification of Organic Compounds*, 4th ed., John Wiley & Sons, New York (1981).
24. S.R. Marder, *Metal containing Materials for non-linear optics*, in *Inorganic materials*, ed. D.W. Bruce and D. O'Hare, John Wiley and Sons, Sussex, England (1992).
25. N.J. Long, *Angew. Chem. Int. Ed. Engl.* 34 (1995) 21.
26. T. Verbiest, S. Houbrechts, M. Kauranen, K. Clays, A. Persoons, *J. Mater. Chem.* 7 (1997) 2175.
27. J.C. Calabrese, W. Tam, *Chem. Phys. Lett.* 133 (1987) 244.
28. J.C. Calabrese, L.-T. Cheng, J.C. Green, S.R. Marder, W. Tam, *J. Am. Chem. Soc.* 113 (1991) 7227.
29. H.S. Nalwa, S. Kogayashi, *J. Porphyrins Phthalocyanines* 2 (1998) 21.
30. T. Thami, P. Bassoul, M.A. Petit, J. Simon, A. Gort, M. Barzoukas, A. Villaeys, *J. Am. Chem. Soc.* 114 (1992) 915.

Summary and Conclusion

Hydrazones are compounds derived from hydrazides (RNH-NH_2) as a result of condensation with an aldehyde or ketone. Again, attaching groups with potential donor sites increases the denticity of these hydrazones. One such group is the -C=O group which also makes possible an increased electron delocalization. Thus compounds with R-CO-NH-NHR are called acylhydrazones. The presence of potential donor sites in the ketone or aldehyde chosen, gives a multidentate ligand. These resultant Schiff bases can function as chelating agents complexing with transition or main group metals producing complexes with versatile stereochemistries, applications and with enhanced bioactivity compared to the parental ligands. An attractive aspect of the hydrazones is that they are capable of exhibiting tautomerism. In the solid state, the compound predominantly exists in the keto form, whereas in the solution state the enol form predominates. Upon metal complexation, the ligand can bind to the central metal ion in keto form or in enolate form depending on the reaction conditions, nature of the metal and nature of the ligand.

The chemical properties of hydrazones and their complexes are widely explored in recent years; owing to their coordinative capability their pharmacological activity and their use in analytical chemistry as metal extracting agents. In the present work, the chelating behavior of acylhydrazones of aromatic aldehydes and ketones is studied, with the aim of investigating the influence coordination exerts on their conformation and or configuration, in connection with the nature of the metal and of the counter ion and the nonlinear optical activity of the complexes synthesized. The selection of the aldehydes and ketones as well as the acylhydrazides were in such a

way that which on condensation gave acylhydrazones having a D- π -A general structure, since it is an essential requirement for a molecule to possess NLO activity. On metal coordination, these compounds may improve the electron delocalization due to proper metal-ligand, ligand-metal or intra-ligand charge transfer transitions.

Accordingly, three new acylhydrazone ligands are synthesized and characterized. The ligands synthesized are

- 1) *N*-4-*N,N*-diethylaminosalicylidine-*N'*-4-nitrobenzoylhydrazone (H_2L^1)
- 2) *N*-4-methoxysalicylidine-*N'*-4-nitrobenzoylhydrazone (H_2L^2)
- 3) *N*-2-hydroxy-4-methoxyacetophenone-*N'*-4-nitrobenzoylhydrazone (H_2L^3)

The ligands consist of two oxygens and one nitrogen capable of coordination with the metal ion. The three ligands were characterized by 1H NMR, 1H - 1H COSY, ^{13}C NMR, HSQC, IR and electronic spectral studies. We could successfully isolate the single crystals of all the three ligands. In all the three ligands, H_2L^1 , H_2L^2 and H_2L^3 the geometry is found to be *cis* in nature along the azomethine bond.

Nine Cu(II) compounds are synthesized and characterized by various spectroscopic techniques such as IR, electronic spectral studies and EPR spectra and their non-linear optical studies. The ligands are found to coordinate in the enolate form with dianionic in nature. The magnetic susceptibility measurements are also done. In the electronic spectral studies, the *d-d* transitions are found to be broad. So the three *d-d* transitions could not be assigned. The IR spectral studies revealed that the azomethine bands are found to be shifted as a result of its coordination to the metal centre. Three of the Cu(II) complexes are found to be dimeric in nature and the other six are their pyridine and 4-picoline analogues. In the pyridine and 4-picoline complexes, the coordination through pyridyl nitrogen is confirmed by the Cu-py

stretching absorption in the far IR region. The EPR spectra of all the Cu(II) complexes were recorded both in polycrystalline state at 298 K and at solution in DMF at 77 K. The g values and the various EPR spectral parameters are calculated. The g values calculated indicate that in all the complexes in the $d_{x^2-y^2}$ orbital, which is confirmed by the axial nature of the EPR spectra. We could isolate the single crystals of the three of the Cu(II) complexes, $(\text{CuL}^1)_2$, CuL^1pi and CuL^2py . In all the cases the ligand coordinates in the enolate form with ONO donor atoms. The geometry is distorted square planar. The coordination sites in the complexes are deprotonated enolic oxygen, deprotonated phenolic oxygen, azomethine nitrogen and the deprotonated enolic oxygen in the case of dimeric complexes and pyridyl nitrogen for monomeric pyridine and 4-picoline analogues. In the case of the complex, $(\text{CuL}^1)_2$, the compound is found to be polymeric in nature from the single crystal X-ray diffraction studies, with the Cu(II) centre has a fifth coordination site to the deprotonated enolic oxygen of a third ligand molecule. Some of the monomeric Cu(II) complexes are found to be NLO active.

Syntheses, characterization and non-linear optical activity studies of nine Ni(II) are also done. Elemental analyses suggested all of them have four coordinated environment around the metal centre. The Ni(II) complexes are characterized by IR and electronic spectral studies. The single crystals suitable for X-ray diffraction studies of $[\text{NiL}^1\text{pi}]$ were isolated and found to be distorted square planar in nature with the coordination sites deprotonated enolic oxygen, deprotonated phenolic oxygen, azomethine nitrogen and the pyridyl nitrogen. The single crystals suitable for X-ray diffraction studies of the compound NiL^1py were isolated from pyridine solvent and found to be six coordinated in nature with two additional pyridine molecules coordinated to the metal centre in the axial positions. Some of the monomeric Ni(II) are found to be NLO active.

Six Co(II) complexes are synthesized and characterized by IR, electronic and EPR spectra. All the Co(II) complexes are found to be paramagnetic from the magnetic measurements the susceptibility values and are close to 1.73 BM, that of one unpaired electron. Hence it is concluded that in these compounds the Co(II) centre is low spin $3d^7$ system. The EPR spectra of the all the Co(II) complexes were recorded both in powder form at room temperature and in DMF at liquid nitrogen temperature. Some of the monomeric Co(II) complexes are found to be NLO active.

Three Mn(II) and three Fe(III) complexes are synthesized. Both the types are characterized by various spectral studies. The elemental analyses data revealed that both the type of complexes are six coordinated in nature. The IR spectral data gave idea that in Mn(II) complexes the acylhydrazone ligands are coordinated in the keto form and is singly deprotonated. The coordination sites are deprotonated phenolic oxygen, azomethine nitrogen, and the carbonyl oxygen. The EPR spectra of all the Mn(II) complexes were recorded both in powder form and in the solution form. But in the case of Fe(III) complexes, the magnetic susceptibility values showed that the metal centre is high spin d^5 system. The EPR spectra of all the three Fe(III) complexes recorded in DMF at 77 K gave three g values, characteristics for high spin iron system. All the Mn(II) and Fe(III) complexes prepared are found to be NLO inactive may be due to their six coordinated nature and hence centre of symmetry.

Synthesis, characterization and non-linear optical activities of nine Zn(II) and nine Cd(II) compounds are done using various spectral studies. All the Zn(II) and Cd(II) complexes are yellowish and red in color and the ligands are found to be coordinated in the enolate and deprotonated form. The complexes are characterized by elemental analyses and spectral investigations. The elemental analyses data revealed that all the Zn(II) and Cd(II) complexes are in square planar environment.

They can be either the dimeric complexes or their pyridine or 4-picoline analogous. The coordination mode of the ligand in the complexes was confirmed by the IR and NMR spectral details. In the NMR spectra, the disappearance of peaks due to –OH and –NH protons confirmed the coordination through deprotonated phenolic and enolic oxygens. The coordination through azomethine nitrogen is confirmed by the downward shifting of C=N stretching absorption band in the IR spectrum compared with the ligand spectrum. In the pyridine and 4-picoline complexes the coordination of pyridyl nitrogen is confirmed by the metal-nitrogen stretching absorption in the far IR region. Unfortunately single crystals could not be isolated. Some of the monomeric Zn(II) and Cd(II) complexes are found to be non-linearly optically active.

Metal complexes of Cu(II), Ni(II), Co(II), Mn(II), Fe(III), Zn(II) and Cd(II) complexes are synthesized and characterized. The coordination mode of the ligands and the structural variations occurring in the ligands upon complex formation are studied. Spectral and structural studies confirm that the ligands coordinate both in keto form as well as in the enolate form with ONO donor sites. X-ray crystallographic study, which was used as major tool in the structure determination, revealed that the configuration of the ligands vary as the substituents attached and also on the nature of the ligand so as to stabilize itself with interactions such as hydrogen bonding. Except Mn(II) and Fe(III), all the complexes prepared are four coordinated and distorted square planar in geometry. In all of them the acylhydrazone ligand is coordinated in the enolate form with the coordination sites, deprotonated enolic oxygen, deprotonated phenolic oxygen and azomethine nitrogen. The Mn(II) and Fe(III) complexes are six coordinated and distorted octahedral in nature. In all the three Mn(II) complexes, the principal ligand is in the single deprotonated form and coordinated in the keto form itself. In Fe(III) complexes, the acylhydrazone ligand moiety is coordinated both in single and double deprotonated forms. Some of the monomeric complexes of Cu(II), Ni(II), Co(II), Zn(II) and Cd(II) complexes are

found to be NLO active and the inactivity of the dimeric and six coordinated complexes may be due to the presence of inversion centre within the molecular lattice.

Curriculum Vitae

BESSY RAJ. B. N

*E-mail: bessyraj@yahoo.co.in
bessyraj@gmail.com*

ACADEMIC PROFILE

Pursuing Ph.D (Inorganic Chemistry)

(2004 – present)

Topic of work: **Structural Characterization and Non-linear Optical Properties of Metal Complexes of Some Donor-Acceptor Substituted *N*-salicylidene-*N'*-aroylhydrazine Ligands.**

Supervising Guide : Dr. M.R. Prathapachandra Kurup,
Professor,

Dept. of Applied Chemistry,

Cochin University of Science & Technology, Kochi.

Master of Science (Chemistry)

I Rank, Percent – 88 (2000-2002)

Department of Chemistry, Kariavattom campus,
University of Kerala.

Bachelor of Science (Chemistry)

Percent – 93 (1997-2000)

Sree Narayana College,

Chempazhanthy, Thiruvananthapuram.

Pre-Degree

Percent – 65 (1995-1997)

Govt. Women's College, Thiruvananthapuram.

SSLC

Percent – 87 (1995)

Raja Ravi Varma Girl's High School, Kilimanoor,
Thiruvananthapuram.

ADDITIONAL QUALIFICATIONS

CSIR-UGC (NET) for Lectureship qualified
Gate Score - 82.97 (2003)

COMPUTING SKILLS

- Expertise in MS-Office
- ISIS Draw, Chems sketch, Chemdraw
- Familiar with crystallographic softwares
- Expertise in EPR simulation packages

WORK EXPERIENCE

- More than four years research experience in the field of coordination complexes of multidentate ligands such as hydrazones and thiosemicarbazones.
- Carried out a project entitled “Aminophenylpyrazolines - Emission properties”.

PERSONAL PROFILE

| | |
|-------------------|--|
| Father's name | N. Natarajan |
| Husband's name | D. Bibin |
| Date of Birth | 25 – 05 – 1980 |
| Gender | Female |
| Marital Status | Married |
| Nationality | Indian |
| Languages Known | English, Hindi, Malayalam |
| Permanent address | Bessy Raj. B. N Bessy Bhavan Porunthamon, Pulimath .P.O Thiruvananthapuram-695612 |

POSITIONS OF RESPONSIBILITY

- Member, Organizing committee, National Symposium on Current Trends in Inorganic Chemistry, CTIC-04, Cochin University of Science and Technology

RESEARCH PAPERS PUBLISHED

- A crystallographic study of 2-hydroxyacetophenone *N*(4)-cyclohexyl thiosemicarbazone, E. B. Seena, B. N. Bessy Raj, M. R. Prathapachandra Kurup, E. Suresh, J. Chem. Cryst. 36 (2006) 189.
- Synthesis, spectroscopic characterization and crystal structure of mixed ligand Ni(II) complex of *N*-4-diethylaminosalicylidine-*N'*-4-nitrobenzoyl hydrazone and 4-picoline, B. N. Bessy, Raj, M. R. Prathapachandra, Kurup, E. Suresh, Structural Chemistry, 17 (2006) 201.
- *N*-2-Hydroxy-4-methoxyacetophenone-*N'*-4-nitrobenzoyl hydrazone: Synthesis and structural characterization, Spectrochim Acta A, 66 (2007) 898.
- Synthesis, spectral characterization and crystal structure of *N*-2-hydroxy-4-methoxybenzaldehyde-*N'*-4-nitrobenzoyl hydrazone and its square planar Cu(II) complex, B.N. Bessy Raj, M.R. Prathapachandra Kurup, E. Suresh, Spectrochim Acta A, in press.